FIELD EMISSIONS OF (HYDRO)CHLOROFLUOROCARBONS AND METHANE FROM A CALIFORNIA LANDFILL

A Thesis

presented to

the Faculty of California Polytechnic State University,

San Luis Obispo

In Partial Fulfillment

of the Requirement for the Degree

Master of Science in Civil and Environmental Engineering

by

Alexander H. Sohn

December 2016

COMMITTEE MEMBERSHIP

TITLE: Field Emissions of (Hydro)Chlorofluorocarbons and Methane from a California Landfill

AUTHOR: Alexander H. Sohn

DATE SUBMITTED: December 2016

COMMITTEE CHAIR: James Hanson, Ph.D.
Professor of Civil and Environmental Engineering California Polytechnic State University, San Luis Obispo

COMMITTEE MEMBER: Nazli Yesiller, Ph.D.
Director, Global Waste Research Institute

COMMITTEE MEMBER: Yarrow Nelson, Ph.D.
Professor of Civil and Environmental Engineering, California Polytechnic State University, San Luis Obispo

ABSTRACT

Field Emissions of (Hydro)Chlorofluorocarbons and Methane

from a California Landfill

Alexander H. Sohn

A comprehensive field investigation was conducted at Potrero Hills Landfill (PHL) located in Suisun City, California to quantify emissions of twelve (hydro)chlorofluorocarbons (i.e. F-gases). The specific target constituents for this study included CFC-11, CFC-12, CFC-113, CFC-114, HCFC-21, HCFC-22, HCFC-141b, HCFC-142b, HCFC-151a, HFC-134a, HFC-152a, and HFC-245fa. The majority of the F-gas emission studies have been conducted outside of the United States and very limited field landfill emission data are available in the United States. Because of historical usage of blowing agents in insulation foams including CFC-11, HCFC-142b, HFC-134a, and HFC-245fa, models reported in literature predicted high F-gas emissions from a landfill environment, but very limited field data are available to verify such predictions.

In this investigation, the surface flux of the twelve F-gases, methane, and carbon dioxide was quantified from various landfill cover systems and in areas with different waste ages, waste heights, and cover thicknesses at Potrero Hills Landfill. In addition, destruction efficiencies for the twelve F-gases were determined based on inlet and outlet concentrations of the onsite flare system. Lastly, the surface flux

values were scaled up to a facility-wide emission value to estimate the total fugitive emissions from the landfill.

The F-gas flux values for the daily covers were in the 10^{-8} to 10^{-1} g m^{-2} day^{-1} range and 10^{-7} to 10^{-2} g m^{-2} day^{-1} range for the wet and dry season, respectively. The F-gas flux values for the intermediate covers in the -10^{-6} to 10^{-4} g m^{-2} day^{-1} range and -10^{-6} to 10^{-4} g m^{-2} day^{-1} range for the wet and dry season, respectively. The F-gas flux values for the final covers were in the 10^{-7} to 10^{-5} g m^{-2} day^{-1} range and -10^{-7} to 10^{-6} g m^{-2} day^{-1} range for the wet and dry season, respectively. F-gas fluxes for the final covers had the highest number of below detection limit cases as well as lower than R^2 threshold cases. Thest F-gas fluxes were measured from daily cover system constructed with auto shredder residue (i.e. auto fluff) for the both the wet and dry seasons. The highest fluxes were measured for CFC-11, HCFC-21, and HCFC-141b in the wet season and for CFC-11, HCFC-141b, and HFC-134a in the dry season across the seven cover locations.

Lower level of variation was observed for methane and carbon dioxide with flux values ranging over five orders of magnitude for the seven tested locations. The methane flux values for the daily covers were in the 10^{-2} to 10^{+1} g m^{-2} d^{-1} range and 1 to 10^{+1} g m^{-2} day^{-1} range for the wet and dry season, respectively. The carbon dioxide flux values for the daily covers were in the -10^{+1} to 10^{+2} g m^{-2} day^{-1} range and -10^{+1} to 10^{+1} g m^{-2} day^{-1} range for the wet and dry season, respectively. The methane flux values for the intermediate covers were in the -10^{-2} to 10^{+1} g m^{-2} d^{-1} range and -10^{-3} to 10^{+1} g m^{-2} day^{-1} range for the wet and dry season, respectively.

The carbon dioxide flux values for the intermediate covers were in the 1 to 10^{+2} g m^{-2} day^{-1} range for both seasons. The methane fluxes for the final cover were -10 $^{-3}$ g m^{-2} day^{-1} and 10^{-4} g m^{-2} day^{-1} for the wet and dry season, respectively. The carbon dioxide flux values for the final cover were in the 10^{+1} g m^{-2} d^{-1} range and 1 to 10^{+1} g m^{-2} day^{-1} range for the wet and dry season, respectively. Negative flux values were typically observed during the wet season and at the intermediate and final covers.

The destruction efficiencies for the twelve F-gases were above 99.5% for the onsite flare. Highest F-gas raw gas concentrations were measured for HFC-134a while the lowest F-gas concentration was measured for CFC-113. The F-gas concentrations in the raw gas ranged from 10^3 to 10^6 pptv. Similar to what has been reported in the literature, the landfill gas flare system was an efficient abatement device in controlling F-gas emissions.

The surface emission measurement values from the field investigation were scaled up to estimate facility-wide fugitive emission values using the relative surface areas of the daily, intermediate, and final cover distributions in the landfill. The total fugitive emissions from the landfill including twelve F-gases, methane, and carbon dioxide ranged from 6,900 to 94,000 CO_2E tonnes per year during the wet season, from 21,000 to 47,000 CO_2E tonnes per year during the dry season, and from 13,000 to 75,000 CO_2E tonnes per year during the year, prorated by the season (representing weighted average of 58% wet season emission rate and 42%

dry season emission rate in a 12-month calendar year). The total fugitive F-gas emissions ranged from 1,600 to 4,800 CO_2E tonnes per year during the wet season, from 140 to 600 CO_2E tonnes per year during the dry season, and from 1,000 to 3,000 CO_2E tonnes per year, prorated by the season. The total fugitive methane emissions ranged from 530 to 75,000 CO_2E tonnes per year during the wet season, 17,000 to 35,000 CO_2E tonnes per year during the dry season, and from 7,500 to 58,000 CO_2E tonnes per year, prorated by the season. The total fugitive carbon dioxide emissions ranged from 5,000 to 14,000 CO_2E tonnes per year during the wet season, 4,200 to 12,000 CO_2E tonnes per year during the dry season, and from 4,500 to 13,000 CO_2E tonnes per year, prorated by the season. In comparison to the total fugitive emission value derived from the first-order decay (FOD) model reported by USEPA and the total fugitive emission values calculated using waste-in-place (WIP) – landfill gas correlation equation presented in Spokas et al. (2015), the field-derived methane emission values were one to three orders of magnitude lower.

ACKNOWLEDGMENTS

This study was funded by the California Air Resources Board. Firstly, I would like to thank Dr. Jim Hanson and Dr. Nazli Yesiller for their guidance, advice, and supervision throughout the entire three years of the Master's Program. I would especially like to thank Dr. Jean Bogner, who provided continuous advice and feedback during the implementation of field tests and development of surface emission calculation methodology. I would also like to thank Dr. Donald Blake for analyzing all of our gas samples and for providing guidance in analyzing our concentration data. I would also like to thank Dr. Tracy Thatcher for assisting us during the implementation the field test program and providing guidance during various stages of the project. I would also like to thank Dr. Yarrow Nelson for serving as a mentor during the drafting of the literature review, for providing assistance during the development of surface emission calculation methodology, and for being part of thesis panel. I would also like to thank Nephi Derbidge for providing guidance in regards to geotechnical analysis of the cover materials. I would also like to thank the staff of Potrero Hills Landfill and Waste Connections for their cooperation and assistance during the field test program. I would also like to thank Dr. Amro El Badawy, Derek Manheim, Timothy Robison, Joshua Core, Ryne Mettler, Michael Onnen, Juan Alverez, Brianna Byrne, and Cameron Lane for their assistance during the field test program.

TABLE OF CONTENTS

LIST OF TABLES

LIST OF FIGURES

Chapter 1: Introduction

Chlorinated and fluorinated hydrocarbons (i.e., F-gases) including chlorofluorocarbons (CFCs), hydrochlorofluorocarbons (HCFCs), and hydrofluorocarbons (HFCs) have been historically used in insulation foams and refrigeration units due to their chemical stability and desirable physical and chemical properties since the 1930s (McCullloch et al. 2001, 2008). The use of CFCs was banned in 1993 by Montreal Protocol and was completely phased out by 1996 due to their high ozone depleting (ODP) potentials and high global warming potentials (GWP) (UNEP-TEAP 2003). The CFCs were replaced by HCFCs and HFCs. However, HCFCs and HFCs still pose threats as potent greenhouse (GHG) gases due to their relatively high GWPs.

The main sources of F-gas emissions in a landfill environment are from insulation foams due to their wide usage in domestic, commercial, and industrial refrigeration units and in buildings (Scheutz 2005). The most common F-gases used in insulation foams are CFC-11, HCFC-141b, HFC-134a, and HFC-245fa. The insulation foams used in appliances and buildings mostly end up in landfills, because from the waste management perspective, the handling of these foams as a separate waste stream is not economically viable (Caleb 2011). Based on the literature review, very limited field emissions data were available for the F-gases in the U.S. Thus, field tests are needed to quantify emission of F-gases from landfills.

A comprehensive field investigation was conducted at Potrero Hills Landfill (PHL) located in Suisun City, California to quantify emissions of fluorinated and chlorinated hydrocarbons (i.e. F-gases). Limited data is available regarding F-gas emissions from landfills in U.S. The compounds of interest in this investigation consist of chlorinated and fluorinated hydrocarbons including CFCs, HCFCs, and HFCs. These constituents are referred to as F-gases throughout this thesis. The specific target constituents for this study include CFC-11, CFC-12, CFC-113, CFC-114, HCFC-21, HCFC-22, HCFC-141b, HCFC-142b, HCFC-151a, HFC-134a, HFC-152a, and HFC-245fa. Measurements for the twelve F-gases were performed using static flux chambers at seven different locations with different waste age, waste height, cover thickness, and cover material. The tests were conducted over wet and dry seasons to account for seasonal variations. In addition, composite gas samples were obtained from inlet and outlet of the onsite flare system to determine destruction efficienpies for the twelve F-gases.

A comprehensive literature review is presented in Chapter 2. A summary of the field test program and analytical methods utilized during the investigation is presented in Chapter 3. The results obtained from the field investigation and discussions on the findings are presented in Chapter 4. Lastly, a summary of the engineering significance is presented in Chapter 5.

Chapter 2: Literature Review

2.1 Introduction

The U.S. has been generating municipal solid waste (MSW) on the order of 250 million tons annually since 2005 (USEPA 2014d). Landfilling has been the primary method of disposal with 134 million tons (54% of total generated) of MSW disposed at landfills in 2013 (USEPA 2015). California has been generating approximately 30 million tons of MSW annually since 2009 (Cal Recycle 2014). Landfilling of MSW can yield three main byproducts: landfill gas (LFG), heat, and leachate. LFG and heat are byproducts that are generated through biological decomposition and degradation occurring within the waste mass (Tchobanoglous et al. 1993). Leachate can be defined as liquid that has percolated through solid waste derived from a combination of precipitation and waste constituents and has extracted dissolved or suspended materials (Tchobanoglous et al. 1993).

Gas generation is dependent on various biological, chemical, and physical factors such as pH, moisture content, waste composition, and temperature (Tchobanoglous et al. 1993). Landfill gas generated typically consists of 45-60% (v/v) methane and 45-60% (v/v) carbon dioxide (Tchobanoglous et al. 1993). There are also other constituents such as sulfides, oxygen, ammonia, hydrogen, carbon monoxide and nitrogen that usually constitute less than 5% of LFG (Rettenberger and Stegmann 1996).

Trace gases refer to gas components that occur at fraction less than 1% in LFG. The trace gases can either be brought into a landfill with incoming waste mass or be produced through biotic or abiotic reactions (Lang et al. 1989; Tchobanoglous et al. 1993). Trace components are mostly composed of non-methane organic compounds (NMOCs) with small fraction of inorganic compounds (Tchobanoglous et al. 1993). The NMOCs in LFG are comprised of more than 200 organic compounds including alkanes, aromatics, chlorinated and fluorinated hydrocarbons, and various volatile organic compounds (VOCs) with concentrations ranging from below detection limits to 1,780 ppmV (Scheutz et al. 2008).

2.2 General Background: Chlorofluorocarbons, Hydrochlorofluorocarbons, and Hydrofluorocarbons

CFCs were first synthesized in 1928 by Thomas Midgley and have been used in a wide range of applications from refrigerants, aerosol sprays, paint strippers, and adhesives to insulation and cushioning foams due to their chemical stability and desirable physical and chemical properties (Midgeley and Henne 1930; Rettenberger and Stegmann 1996; Sturrock et al. 2002; Derwent et al. 2007; McCulloch et al. 2001, 2008). Blowing agents (BAs) are chemicals that are used in foams during the manufacturing process to improve insulation properties of the foam (IPCC-TEAP 2005). Selected F-gases are used as BAs in insulation applications. The wide use of CFCs results mainly from their low boiling points, low vapor-phase thermal conductivity, desirable solubility characteristics, and high

stability. Selected F-gases are used as BAs in insulation applications, which are ideal for domestic and commercial applications in insulation materials (McFarland 1992). The commercial production of CFCs began in 1931 by DuPont chemical company (Jacobson 2012). In 1993, the use of CFCs was banned by the Montreal Protocol and replaced by HCFCs and HFCs (UNEP-TEAP 2003). As the production of CFCs sharply decreased and was completely phased out by 1996, the “banks”, products still in use, stockpiled, or discarded in landfill, have become a significant source of projected CFC emissions (Hodson et al. 2010). According to United States Environmental Protection Agency’s (USEPA) Vintaging Model, banked foams account for roughly 60% or about 400 million metric tons CO_2 equivalent ($MMTCO_2E$) of the total potential 660 $MMTCO_2E$ banked in ozone depleting substances (ODSs) in California in 2007 (CARB 2008).

HCFCs are considered transitional compounds due to their low ozone depletion potential compared to CFCs (USEPA 2014a, 2014c). However, HCFCs still pose a threats as potent greenhouse gases due to their high global warming potential and are scheduled to be completely phased out by 2030 leaving much of the demand to be met by HFCs (Fenhann 2000; Barletta et al. 2013). The demands for HCFCs and HFCs are projected to increase in many countries, especially in Asia (Fenhann 2000). The use of HCFCs is estimated to grow to just under 50,000 tonnes by 2015 (UNEP-TEAP 2003). The emissions of HCFCs are projected to be in the 20,000-25,000 tonnes per annum range after 2015 (IPCC-TEAP 2005). The use of HFCs was projected to increase from 11,200 to 72,000 tonnes per annum

from 2002 to 2015 (IPCC 2005). Principal uses and substitutes when applicable of the target F-gases are listed in Table 1.

Foams containing the target F-gas BAs have been used in a variety of applications using their potential to create both rigid and flexible structures (IPCC 2005). Flexible foams are used in furniture cushioning, packaging, and impact management products while rigid foams are mainly used for appliances and in buildings (IPCC 2005). Historically, the most common BAs used in foams were CFC-11, HCFC-141b, HFC-134a, and HFC-245fa (IPCC 2005).

Discarded appliances are one of the main sources of F-gas emissions in landfill environments as a result of historical usage of BAs in appliances since the 1960s. Many refrigerators and freezers are shredded at the end of their use and are then either incinerated, disposed, or in rare cases, processed for reuse (Scheutz et al. 2003a). Most foams from the appliances are directly disposed in landfills and very little foam is incinerated in the United States (Scheutz et al. 2003a). Decommissioning protocol of refrigerators removes only the F-gases that are used as refrigerants. It is estimated that much of the decommissioned appliances (63% in North America) containing CFC-11 had already reached landfills prior to approval of fluorocarbon destruction and recovery law in 2003 (IPCC 2005).

Table 1 - Basic Properties and Uses of Common CFCs, HCFCs and HFCs

Name	Chemical Name	Structural Formula	Principal Use [a,b,c,d]	Principal Substitute [a]
Compounds already phased out under Montreal Protocol				
CFC-11	Trichlorofluoromethane	CCl_3F	Foam blowing agent	HCFC-141b
CFC-12	Dichlorodifluoromethane	CCl_2F_2	Refrigerant	HFC-134a
CFC-113	1,1,2-Trichlorotrifluoroethane	$C_2F_3Cl_3$	Solvent	Other technology
CFC-114	Dichlorotetrafluoroethane	CF_3CFCl_2	Propellant	Hydrocarbons
Compounds currently phasing out under Montreal Protocol				
HCFC-21	Dichlorofluoromethane	CH_2FCl_2	Refrigerant blends	HFC blends
HCFC-22	Monochlorodifluoromethane	CHF_2Cl	Refrigerant	HFC blends
HCFC-141b	Dichlorofluoroethane	CH_3CFCl_2	Foam blowing agent	HFC-365mfc
HCFC-142b	Monochlorodifluoroethane	CH_3CF_2Cl	Foam blowing agent	HFC-365mfc Formacel® TI
HCFC-151a	1,1,-Chlorofluoroethane	CH_3CHFCl	Refrigerant blends, Foams	
Alternatives controlled under Kyoto Protocol				
HFC-134a	1,1,1,2-Tetrafluoroethane	CH_2FCF_3	Refrigerant blends, foams, fire suppressant, and propellant in metered-dose inhalers	NA
HFC-152a	Difluoroethane	CH_3CHF_2	Refrigerant blends, foam blowing agent, and aerosol propellant	NA
HFC-245fa	1,1,1,3,3-Pentafluoropropane	$CF_3CH_2CHF_2$	Foam blowing agent and possible refrigerant in the future	NA

[a] McCulloch (1999); [b] USEPA (2010); [c] UNEP (2006); [d] USEPA (2014a, 2014c)
NA – Not Applicable

Kjeldsen (2010) indicated that construction and demolition (C&D) wastes are the main source of F-gases in landfills due to large quantities of BAs present in the insulation foams. It was expected that C&D waste containing CFC-11 would not reach a significant level until after 2010 (IPCC 2005). Recovery of BAs from building insulation waste is not feasible since most of the foam products were designed without taking recovery into consideration (IPCC 2005). Another challenge dealing with C&D waste is the lack of practical methods to separate foam containing waste from non-foam containing materials (Caleb 2008). The only method currently available is through manual separation, which is not economically practical (IPCC 2005).

2.3 Chemical and Physical Properties

CFCs, HCFCs, and HFCs are chlorinated and fluorinated alkanes where all the bonds around the carbon atoms are occupied either by hydrogen, fluorine, or chlorine atoms (Vollhardt et al. 1999). CFCs are alkanes with one carbon atom (methane) while HCFCs have one or two carbon atoms (methane or ethane). HFCs have two or three carbon atoms (ethane or propane). Example atomic structures of F-gases are presented in Figure 1.

a) CFC-11 (Trichlorofluoromethane) and CFC-12 (Dichlorodifluoromethane)

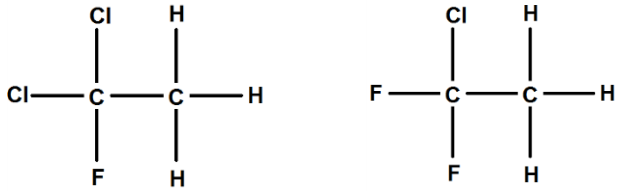

b) HCFC-141b (Dichlorofluoroethane) and HCFC-142b (Monochlorodifluoroethane)

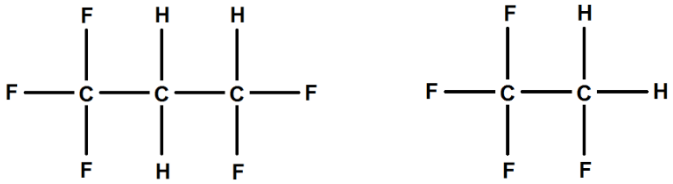

c) HFC-245fa (1,1,3,3-Pentafluoropropane) and HFC-134a (1,1,1,2-Tetrafluoroethane)

Figure 1 – Examples of Atomic Structure of F-gases (Vollhardt et al. 1999)

F-gases are classified as volatile organic compounds due to their relatively low boiling point (ranging from -40 to 53°C) existing in a gaseous state at standard temperature and pressure (USEPA 2009; NIOSH 2013). The boiling points of the F-gases are listed in Table 2. F-gases have low thermal conductivity, high latent heat, and low specific volume making them ideal as refrigerants and also as BAs (Perkins et al. 2001; Sundararajan and Malikarjuna 2015). Though CFCs have thermal properties superior compared to those of HCFCs and HFCs, the high ODP of CFCs makes them impractical for use in appliances and insulation materials when considering the potential environmental impacts (Perkins et al. 2001).

F-gases are non-flammable, non-corrosive, and are very low in toxicity (Elkins 1999; McFarland 1992). The primary concerns are due to their detrimental environmental effects as potent GHGs and as ODSs. CFCs are especially a concern since they have been historically released to the atmosphere (AGAGE 2009). A schematic of earth's atmosphere is shown in Figure 2.

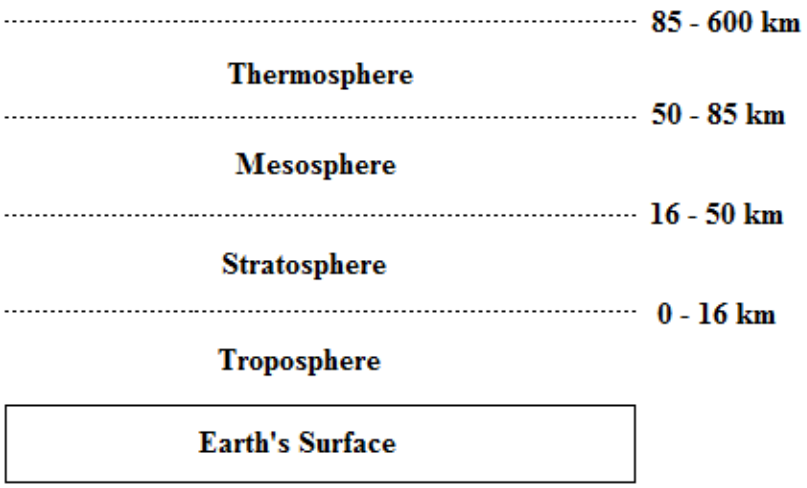

Figure 2 – Earth's Atmosphere (NASA 2014)

CFCs are highly stable and do not react with other chemicals in the troposphere (NASA 2015). HCFCs and HFCs in comparison are relatively unstable and are degraded before they can reach the stratosphere (Tang et al. 1998). The carbon-hydrogen bond in HCFCs and HFCs can react with the hydroxyl radicals in the atmosphere and become oxidized unlike the CFC molecules (NOAA 2015). Once a CFC molecule reaches the stratosphere, it is no longer shielded from ultraviolet radiation and chlorine atoms start to break off from the CFC molecule (NASA 2015). Free chlorine atoms then react with ozone forming chlorine monoxide destroying ozone molecules in the process (Payne and O'Neal 1998). Then, chlorine monoxide can react with a free oxygen in the atmosphere to release

chlorine atoms once again and this cycle repeats destroying many more ozone molecules (Payne and O'Neal 1998). A single chlorine atom is capable of destroying more than 100,000 ozone molecules in the stratosphere through this cycle (Payne and O'Neal 1998). With HCFCs and HFCs containing fewer to no chlorine atoms, they pose far less threat to the stratospheric ozone than CFCs.

2.4 Atmospheric Properties and Conditions

Understanding of atmospheric properties of the F-gases is essential to delineate their effects on the atmosphere. Atmospheric lifetime, tropospheric concentration, ODP, GWP, atmospheric concentration and radiative forcing (RF) of target F-gases and other relevant potent GHGs are listed in Table 2.

Table 2 - Summary of Atmospheric Properties and Concentration of Various GHGs

Name	Boiling Point at 1 atm (°C) [a]	Atmospheric Lifetime (years) [b,c,d]	Tropospheric Concentration (ppt) [e,f]	ODP [b,c,d]	Radiative Forcing (W/m^2) [c]	GWP – 100 years [c]
Carbon Dioxide	-78.5	100	3.98×10^8	0	1.66	1
Methane	-161.5	9.1	1.80×10^6	0	0.47	28
Nitrous Oxide	-88.5	131	3.25×10^5	0	0.16	298
CFC-11	23.8	45	233	1	0.07	4,660
CFC-12	-29.8	100	524	1	0.17	10,200
CFC-113	47.6	85	73	0.8	NA	5,820
CFC-114	3.6	190	16	1	NA	8,590
HCFC-21	8.9	1.7	NA	0.04	NA	148
HCFC-22	-40.8	11.9	226	0.055	NA	1,760
HCFC-141b	32.1	9.2	23	0.11	0.04	782
HCFC-142b	-9.1	17.2	22	0.065	0.003	1,980
HCFC-151	16	NA	6	0.004	0.003	NA
HFC-134a	-103.3	13.4	74	0	NA	1,120
HFC-152a	-24.1	1.5	NA	0	0.01	138
HFC-245fa	15.3	7.7	2	0	0.0003	858

[a] Haynes and Lide (2015); [b] WMO (2010); [c] IPCC (2013); [d] IPCC (2007); [e] AGAGE (2014); [f] NOAA (2014)

Atmospheric lifetime can be defined as the time required for 67% of a molecule to be removed from the atmosphere in absence of emissions (UNEP 2011). Lifetime controls how long the gas is retained within the atmosphere and thus affects the thermal balance between the atmosphere and land surface (IPCC 2001). The atmospheric lifetime of CFCs ranges from 45 to 190 years while atmospheric lifetime of HFCs and HCFCs range from 2 to 17 years (WMO 2010; IPCC 2007, 2013).

The atmospheric concentrations listed in Table 2 are the latest monthly mean concentrations available from NOAA (2014) and AGAGE (2014). Graphs of global monthly concentration data of methane, nitrous oxide, and target F-gases were retrieved from AGAGE (2014) and are presented in Figure 3. The monthly mean concentrations provided are global averages from various stations located throughout the world. According to the data, the tropospheric concentration of CFCs has been decreasing while concentration of HCFCs and HFCs have been increasing since the mid-1990s. This is consistent with replacement of CFCs with HCFCs and HFCs in 1996 due to Montreal Protocol (UNEP 2003).

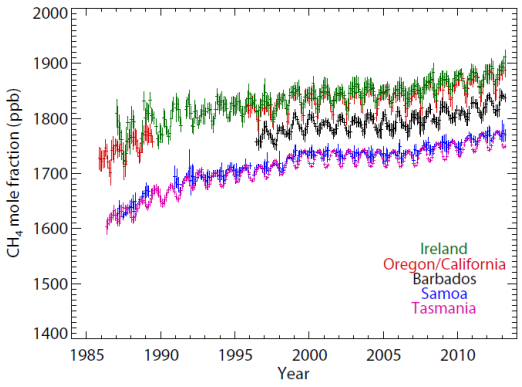

a) Methane

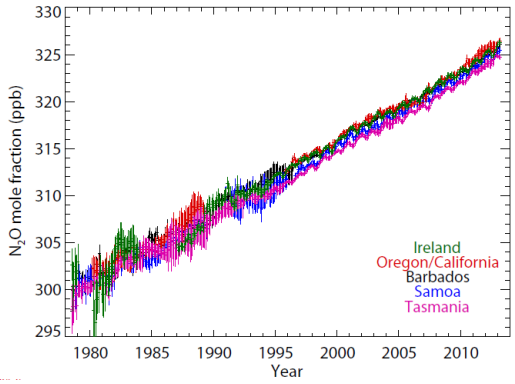

b) Nitrous Oxide

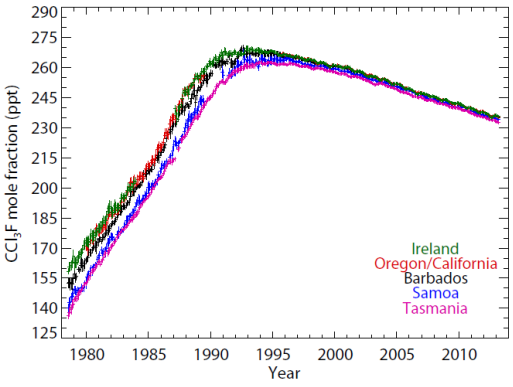

c) CFC-11

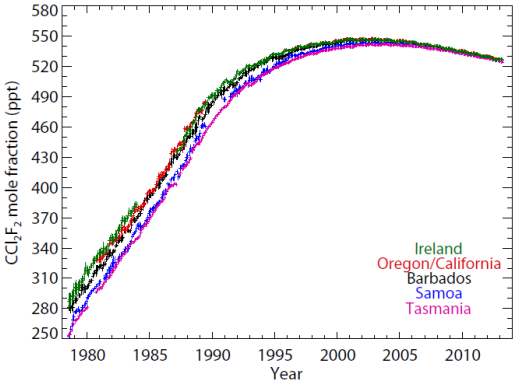

d) CFC-12

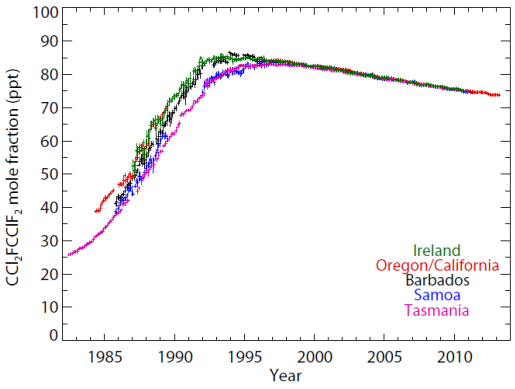

e) CFC-113

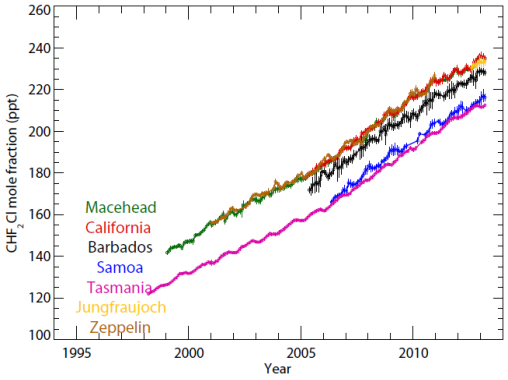

f) HCFC-22

Figure 3 - Monthly Atmospheric Concentrations of Methane, Nitrous oxide, CFC-11, CFC-12, CFC-113, HCFC-22, HCFC-141b, HCFC-142b, HFC-134a, HFC-152a, and HFC-245fa Measured at Various Stations (AGAGE 2014)

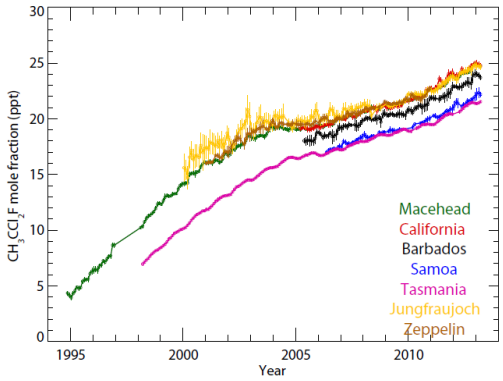

g) HCFC-141b

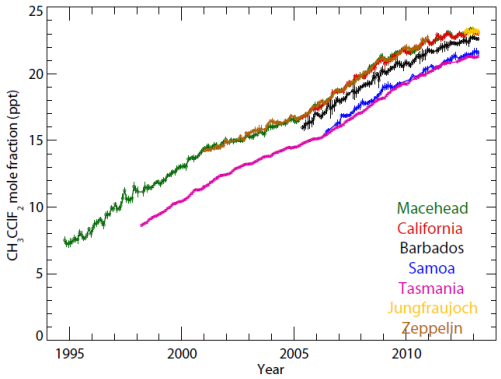

h) HCFC-142b

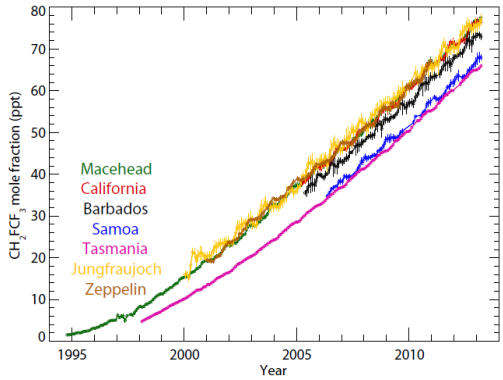

i) HFC-134a

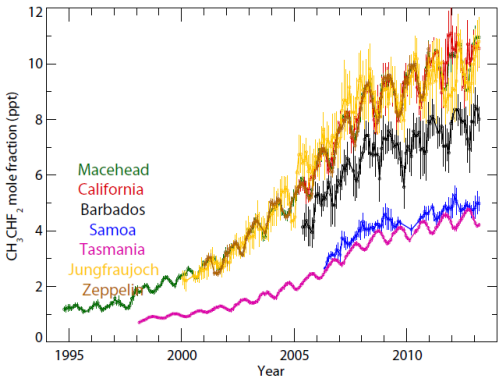

j) HFC-152a

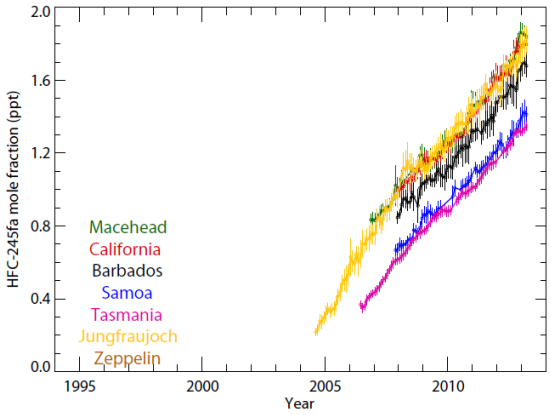

k) HFC-245fa

Figure 3 (continued) - Monthly Atmospheric Concentrations of Methane, Nitrous oxide, CFC-11, CFC-12, CFC-113, HCFC-22, HCFC-141b, HCFC-142b, HFC-134a, HFC-152a, and HFC-245fa Measured at Various Stations (AGAGE 2014)

ODP is the ratio of the ozone lost due to a certain chemical compared to ozone lost due to similar mass of CFC-11 as presented in Equation 1 (Daniel and Velders 2007; WMO 2010; UNEP 2011). Thus, the value of ODP for CFC-11 by definition is always 1. These values are calculated using computer models assuming steady-state conditions with constant emissions (Prather 1996, 2002; Daniel and Velders 2007). The stability of a molecule is important in characterizing its ozone depletion potential since this controls whether the molecule will degrade in the troposphere before reaching the stratospheric ozone.

$$ODP_i = \frac{\text{Global } O_3 \text{ loss due to unit mass emission of constituent i}}{\text{Global } O_3 \text{ loss due to unit mass emission of CFC-11}} \quad [1]$$

RF and GWP are the two main climate parameters used to quantify energy imbalance caused by an introduction of perturbation to the atmosphere (IPCC 2013). RF is the net change in planetary energy due to emission of forcing agent expressed in watts per square meter (IPCC 2013). The change in energy is usually presented using a particular time period, such as pre-industrial to present day, in order to delineate the effect of the forcing agent on climate change. There are two types of RF commonly used by the IPCC: adjusted and effective RF (IPCC 2013). Adjusted RF refers to the net change in radiative flux after only the stratosphere have adjusted to the chemical agent (Ban-Weiss et al. 2010; IPCC 2013). Effective RF refers to the net change in radiative flux after the atmosphere, water vapor, and clouds have been adjusted with surface temperature fixed (IPCC 2013). Adjusted RF and effective RF are nearly equal in many cases (IPCC 2013). Adjusted RF is referred to as RF throughout this thesis consistent with the IPCC (IPCC 2007; 2013). The RF of CFCs and HCFCs contribute approximately 11% of the overall

greenhouse gas RF (IPCC 2013). The RF of HFCs doubled from 2005 to 2013 with HFC-134a being the main contributor (IPCC 2013). The RF of CFCs has been in decline since 2005 mainly due to reduction in CFC-11 and CFC-12 concentrations in the atmosphere (IPCC 2013). The RF of HCFCs, however, is still rising mainly due to increasing HCFC-22 concentration in the atmosphere (IPCC 2013).

GWP is an index derived from radiative properties used to estimate total energy added by a greenhouse gas to the climate system relative to energy added by CO_2 (IPCC 2007, 2013). GWP is calculated by integrating RF of a chemical and carbon dioxide over a specific time horizon. Various time horizons can be used to calculate GWP but the time horizon of 100 years has been widely used since its use in the United Nations Framework Convention on Climate Change in 1997 (IPCC 2013). However, 20 and 500 years have also been used in other studies (e.g., Houghton et al. 1990). GWP is the most common metric used to convert emission of different greenhouse gases to a common scale (Shine 2009). The GWPs of CFCs are the highest among the F-gases ranging from 4660 to 10,200, while the GWPs of their substitutes, HCFCs and HFCs, range from 138 to 1,980 (IPCC 2013).

2.5 Foams

Foams are one of the main sources of F-gas emissions due to their wide use in refrigerators, freezers, and various building materials (UNEP-TEAP 2005; IPCC 2005; Vetter and Ashford 2011). These foams consist of cellular plastics or polymers and gaseous BAs that include CFCs, HCFCs, and HFCs (Landrock 1995). The polymers are created from repeated molecular structures referred to as monomers through a process termed polymerization. The most common monomers used in insulation foams include urethane and styrene, which can be polymerized to form polyurethane and polystyrene (Landrock 1995). The four main type of foams as a function of polymer type include extruded polystyrene (XPS), expanded polystyrene (EPS), polyurethane (PUR), and polyisocyanurate (PIR) foams (Figure 4).

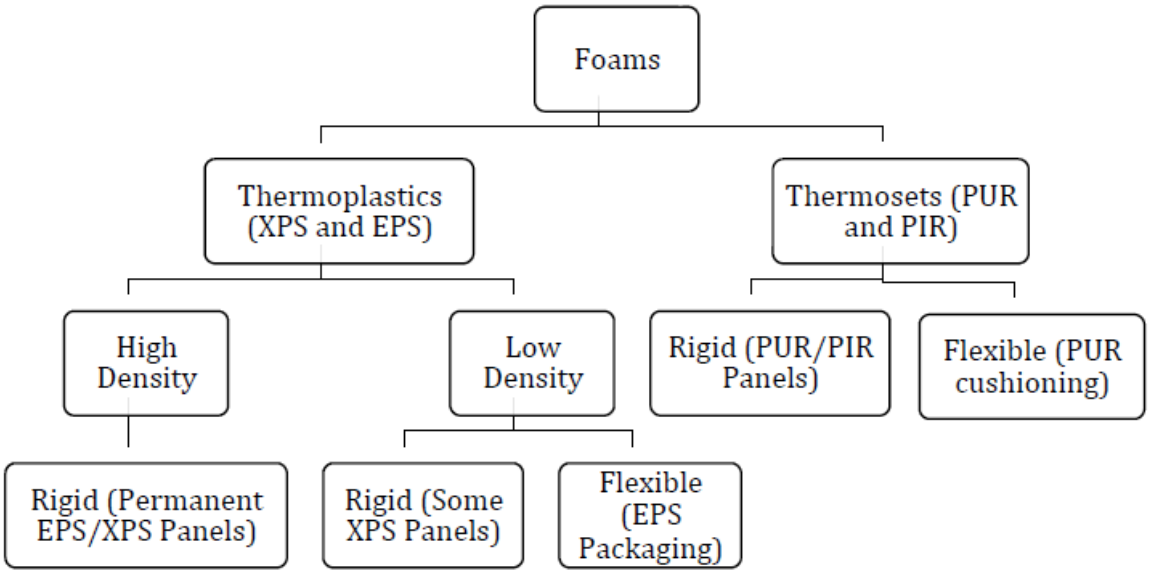

Figure 4 – Classification of Foams (Throne 2004)

Foams can be classified as a function of crystallinity (thermoset / thermoplastic), density (low / high), and stress-strain response (rigid / flexible) as presented in Figure 4. Depending on the crystallinity or degree of order in the monomer structure, foams are categorized as thermoset or thermoplastic (Crawford and Throne 2002; Throne 2004). Thermoset foams have high degree of crystallinity, resistance to solvents and chemicals, and are used in high temperature applications (BSC 2007). Thermoset foams are often used as insulation material in buildings and refrigerators due to their high resistance to physical changes (Blaga 1974; Throne 2004). However, thermoset foams cannot be melted and recycled unlike thermoplastic foams (Sivertsen 2007). Density of thermoplastic foams can be varied during their manufacturing process to suit their intended application, while density of thermoset foams is constrained to a narrow range (Throne 2004). High-density thermoplastic foams are typically used in permanent structures and appliances while low-density foams are mainly used in single use disposable products (Throne 2004).

Stress-strain response in foams is a function of crystallinity, chemical composition, and degree of crosslinkage between the polymers (Landrock 1995). High degree of crystallinity and crosslinkage leads to rigid structure, while low degree of crystallinity and crosslinkage leads to flexible structure (Landrock 1995). Rigid foams typically have close-celled structures to retain the blowing agent and have improved thermal insulation properties over flexible foams. Flexible foams are open-celled, in which the blowing agents are released during manufacturing.

Rigid foams are typically used in buildings, appliances, and transportation units (Caleb 2011). The foams used in buildings consist of insulation-based roof boards, lining boards, pipe-sections, cold store panels, and spray systems (UNEP-TEAP 2005). Foam applications in appliances include residential and commercial refrigerators/freezers, water heaters, and vending machines (UNEP-TEAP 2005). Transport refrigerated units (TRUs) and refrigerated containers (REEFERs) commonly use sandwich panel for their insulation (UNEP-TEAP 2005). Flexible foam applications include packaging, transport cushioning, and impact management (IPCC 2007).

2.5.1 Foam Bank in California

Caleb (2011) developed a comprehensive California rigid foam bank model using available literature, foam stock data, and interviews with suppliers, producers, contractors, and waste management companies that are associated with foams at various lifecycle stages. Total rigid foam consumption in 2008 in California was estimated to be 4 million m^3 with 53 million m^3 in the bank (Caleb 2011). The amount of foams that are banked were calculated by combining new foams and foams currently in use and then subtracting the foams that had been decommissioned. Over 96% of foams in California have been used in buildings and appliances with the remaining 4% of foams used in the marine sector, non-structural cold stores (N.S. Cold Store), and TRUs as presented in Figure 5 (Caleb 2011).

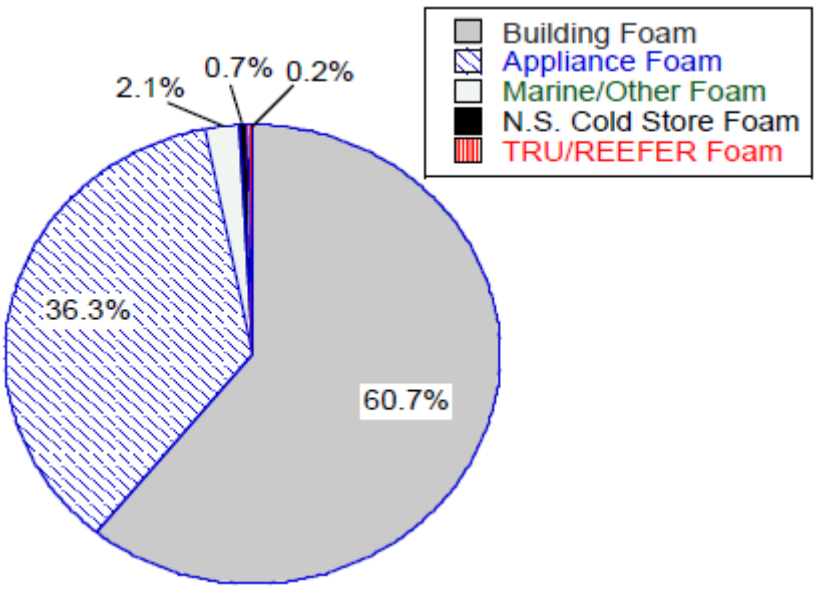

Figure 5 – Rigid Foam Consumption in California by Application in 2008 (Adapted from Caleb 2011)

Building foams in California were estimated to consist of 55% PIR panel, 29% XPS panel, 10% PUR spray and 6% PUR panel as presented in Figure 6 (Caleb 2011). The majority of foams used for appliance, marine sector, and TRU/REEFER applications were reported to consist of PUR foam (Caleb 2011). Assuming foams in these sectors are strictly PUR foams, rigid foam consumption in California by foam type (Figure 7) was calculated by multiplying foam type fractions used in buildings (Figure 6) with building foam fraction (Figure 5) and then by adding remaining appliance, marine sector, and TRU/REEFER foam fractions (Figure 5). The foam consumption consisted of 49% PUR, 33% PIR, and 18% XPS as presented in Figure 6. According to Caleb (2011), EPS foam was not considered in this model since the study was limited to foams that contained ozone depleting or high GWP BAs. The foam consumption data of California adapted from Caleb (2011) was consistent with data presented by Throne (2004) where PUR, PIR, and XPS foam composed over 70% of the foam market in the U.S. as presented in Figure 8. It is expected PIR foam consumption will increase by 10% per year in California (Singh et al. 2005). Thus, end of life management of PUR/PIR foams in the present and the future will be essential to limiting emission of F-gases from these foams.

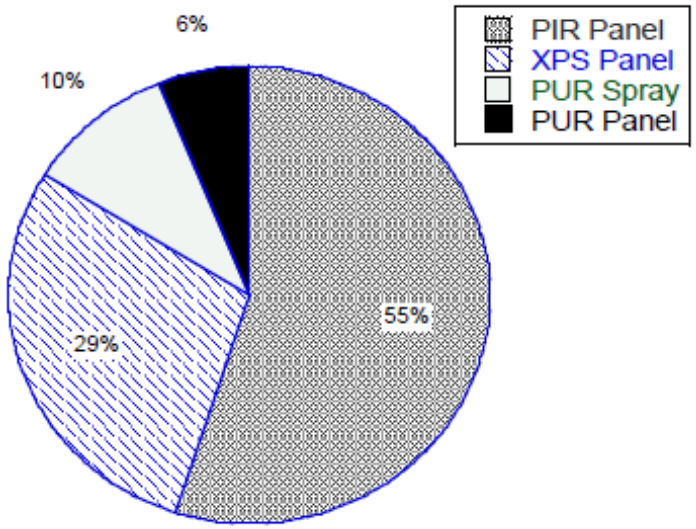

Figure 6 – Rigid Foam Consumption in Building Applications in California from 1960 to 2009 by Foam Type (Caleb 2011)

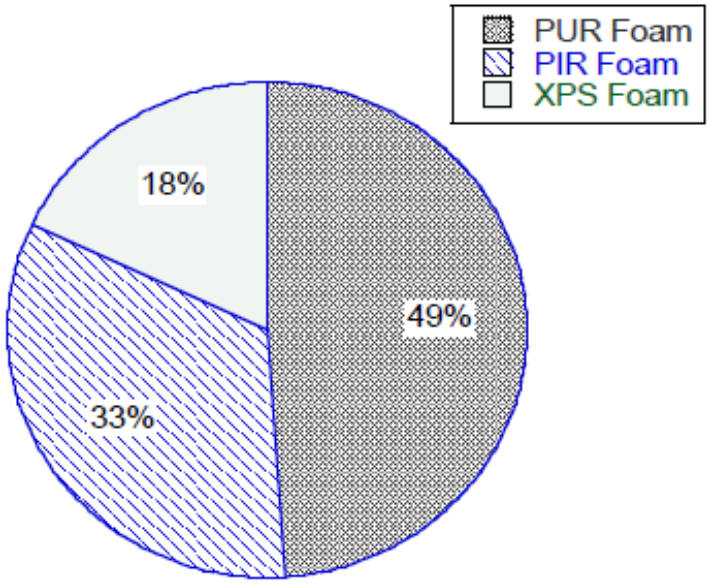

Figure 7 – Rigid Foam Consumption in California by Foam Type in 2008 (Adapted from Caleb 2011)

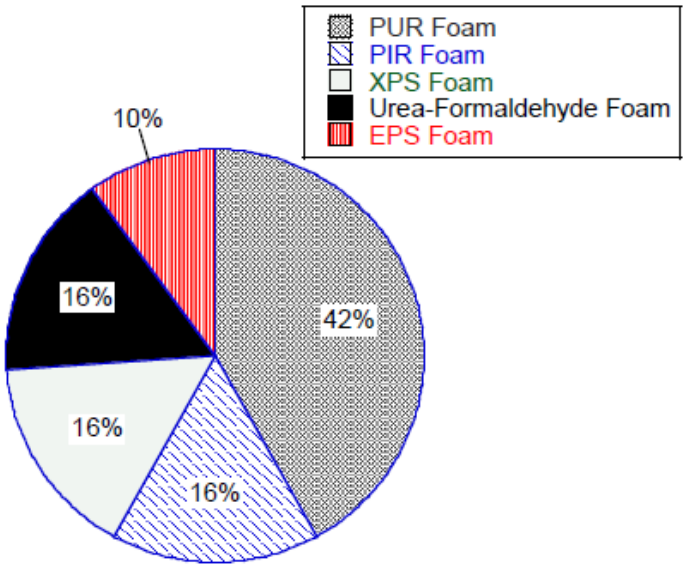

Figure 8 – Foam Consumption in United States (Adapted from Throne 2004)

2.5.2 Emissions of Blowing Agents

The release of BAs from foams depends on several factors including type of foam (rigid or flexible) and blowing agent used; partial pressure within the foam; temperature; and presence of a diffusion barrier (Scheutz and Kjeldsen 2003b). The emissions occur via diffusion which increases with increasing temperature and partial pressure and decreasing atmospheric barometric pressure. Initial release of blowing agents mainly depends on whether the foam is closed-celled (rigid) or open-celled (flexible). Open-celled foams emit all or a majority of the BAs during the manufacturing process, while closed cell foams only lose a fraction of the blowing agents during their initial manufacturing process and the remaining portion is emitted during their use and after decommissioning (Godwin et al. 2003; Caleb 2004; UNEP-TEAP 2005). The emission of BAs from foams is a concern

specifically for the banked foams since newly produced foams have converted to non-ozone depleting or hydrocarbon BAs (UNEP-TEAP 2005).

Emission of BAs from foams occur in three distinct phases: losses during production and installation, losses during use, and losses during decommissioning at end of life (Godwin et al. 2003; UNEP-TEAP 2002, 2005). The BA emission rates at distinct phases vary depending on the application. The Foams Technical Option Committee (UNEP-FTOC 1998) and Task force on Collection, Recovery and Long Term Storage (UNEP-TEAP 2002) have conducted comprehensive assessment of the status of the foams in California. Considerable field work was conducted to verify the emission studies by Japan Technical Center for Construction Materials (JTCCM) sampling over 500 buildings. Godwin et al. (2003) also conducted a study using Vintage Model developed by USEPA to simulate emission profiles for the foam end-uses. The emission factors presented in Table 3 represent averaged data since the emission factors varied depending on the assumption and methodology of the studies.

The total remaining BA in the foams at the time of decommissioning depended on the type of application, the release rate, and the loss during installation and manufacturing of the foam as indicated in Table 3. First year release could be defined as loss of BAs during manufacturing, installation, and use of the foam within the first year. Open celled foams, such as polyolefin, PE, and flexible PUR foams, had most of their blowing agent released (95 to 100 %) during

the first year of use. Closed cell rigid foams had significantly lower first year loss in comparison, with values ranging from 4 to 40 %. Overall, annual release rate of foams and total remaining percentages after decommissioning ranged from 0.25 to 2.5%/year and 0 to 90%, respectively. PIR and XPS boardstocks, the two most widely used foams in the building sector, were highly emissive having only 15 and 0% remaining, respectively, by the time of decommissioning. Emission profiles of PUR foams varied depending on the foam type. Rigid PUR foams, with the exception of PUR sandwich panels, PUR sprays, and PUR one-component foams (OCFs), typically had high percentage of BA remaining with values ranging from 44 to 92% by the time of decommissioning. The foams in appliances, especially, had high percentages remaining with BA contents ranging from 90 to 92%. In summary, the majority of the end of life bank of BAs would be present in rigid PUR foams since most of the BAs present in the rigid XPS and PIR foams would be emitted during their use.

Table 3 – Stages of BA Emissions from Foams

Foam Application	Foam Type	First Year Release (%)	Release Rate After First Year (%/year)	Time to Total Release (Years)	Lifetime of Foams (years)	Total Remaining at Decomissioning (%)
Building Insulation, Cold Store Insulation, Marine, and Other	PUR Sandwich Panels [a]	40	2	N/A	25	10
	PUR Continuous Panel [b]	5	< 0.5	190	50	70
	PUR Discontinuous Panel [b]	6	< 0.5	188	50	69
	PUR Continuous Block [b]	35	0.75	86	15	54
	PUR Discontinuous Block [b]	40	0.75	80	15	49
	Phen. Discontinuous Block [b]	40	0.75	80	15	49
	PUR Boardstock [c]	6	0.5 to 1	94	50	44
	PIR Boardstock [a]	10	1.5	N/A	50	15
	XPS Boardstock [a]	25	0.75 to 2.5	30	50	0
	Phen. Boardstock [c]	6	0.25 to 1	94	50	44
	PE Boardstock [c]	90	5	2	50	0
	PUR Spray [b]	15 to 25	0.75 to 1.5	50	50	0
	PUR OCF [a]	100	N/A	0	50	0
	PUR Pipe in Pipe a	6	0.25	376	50	81.5
	PE Pipe [a]	100	N/A	0	15	0
Appliance Insulation	PUR Appliance [b]	4	0.25	384	15	92
	PUR Com. Refrig. [b]	6	0.25	376	15	90
Cushioning, Packaging, Transportation Insulation	PUR Flexible [c]	100	0	0	0	0
	PUR Integral Skin [b]	95	2.5	2	15	0
	PUR Reefers/Trans [b]	4 to 6	0.5	188	15	86.5
	Polyolefin [a]	95	2.5	N/A	2	0

[a] Godwin et al. 2003; [b] Caleb 2004; [c] UNEP-TEAP 2002, 2005; UNEP-FTOC 1998, N/A – Not Applicable to the Study

2.5.3 Current End of Life Fate and Practice

End of life fate and practice differs depending on the application of foam during its lifetime. According to a 2008 waste characterization study conducted fover four metropolitan areas in California, a large fraction (approximately 16 %) of incoming waste was determined to be composed of C&D waste (Cal Recycle 2008). By applying C&D waste fraction to the annual waste disposal data from 2008 (approximately 35 million tons), it is estimated that 5.6 million tons of C&D waste was generated in 2008 (Cal Recycle 2009; Cal Recycle 2014). Only a small fraction (0.2%) of the C&D waste was contained insulation foams (Cal Recycle 2006). Since the quantity of disposed foams has not been reported directly, the amount of C&D waste containing insulation foam was quantified by excluding all known category of other waste (e.g. paper, glass, metal, lumber, etc.). By scaling the C&D waste foam fraction (0.2%) to the annual C&D waste disposal data from 2008 (approximately 35 milliom tons), it was estimated that 12,700 tons of C&D waste generated in 2008 contained insulation foams (Cal Recycle 2008). 12,700 tons represents the maximum foam disposal estimate for 2008. This estimate is generally consistent with the estimate of 15,130 tons, provided by Caleb (2011), which also used 2008 California waste disposal data for the study. Since no data is available regarding foam fraction for 2014, it is estimated, using the C&D waste fraction containing foam from 2008 (0.2%) and annual C&D waste disposal amount from 2014 (approximately 5 million tons), that 9,580 tons of C&D waste foams was generated in 2014. With current practices, C&D waste foams are not segregated from non-foam containing C&D waste (Caleb 2011).

It was estimated that 92% of the foams in C&D waste are directly landfilled with remaining 8% shredded prior to being landfilled (Caleb 2011). The issue with end of life management of foams from C&D waste is the weight, volume, and composition of the foam (Caleb 2011). From the waste management perspective, the handling of these foams as separate waste stream is not economically viable, since most foams do not have reuse potential and are expensive to transport (Caleb 2011). However, PUR panels are an exception as they are composed of 80% metal by weight making them more attractive for recycling (Caleb 2011). Carbon credits are offered by Climate Action Reserve (CAR) for direct incineration where F-gas reduction has been established through frequent monitoring (Caleb 2011). However, in order for this method to be economically viable, carbon credits need to be sufficiently high to cover the transport and separation cost of building demolition-derived foams (Caleb 2011).

Reduction of various NMOCs in LFG was measured through multiple studies conducted by Environment Canada with similar landfill gas collection and combustion systems as in California, achieving more than 90% reduction efficiency of CFCs and HCFCs (Environment Canada 1999, 2000a, 2000b, 2000c, 2000d, 2002, 2005). Another possible NMOC reduction measure is landfill-based natural biological attenuation. However, this method does not have any carbon credit incentives since reduction quantity cannot be measured (Caleb 2011).

In California, over 1 million freezers and refrigerators are decommissioned every year (Caleb 2011). Clean Air Act Section 608 passed in 1990 disallows any refrigerants to be vented during installation, service, or retirement of the appliances (USEPA 2013). In 1991 in California, Assembly Bill 1760 was passed making appliance recycling nearly mandatory and required that any toxic or environmentally harmful materials need to be removed and recovered prior to shredding (Cal Recycle 1991). The materials controlled under these regulations are all refrigerants (which includes CFC-, HCFC-, and HFC-based refrigerants), mercury, compressor oil, and polychlorinated biphenyls. However, the BAs contained in foams within appliances are not controlled under these regulations. Thus, most foams containing BAs are directly landfilled without any special treatment after they are removed from the appliances (DTSC 2002, 2007). The disposal pathway for domestic and commercial appliances varies. For domestic refrigerators, it is estimated that 12 to 15% of the foams are fully recycled, 39% are re-used, and the remaining 47% are processed for metal recovery and degassing and then the remaining residues are landfilled (Caleb 2011). For commercial appliances, all of the foams are processed for metal recovery and degassing and then the remaining residues are landfilled (Caleb 2011).

TRUs are treated similar to vehicles in accordance with US Clean Air Act Regulation Sections 608 and 609 meaning all refrigerants (which includes CFC-, HCFC-, and HFC-based refrigerants) are removed prior to any recycling. It is estimated that 25% of the foams in TRUs and REEFERs are reused with a small

fraction being diverted for exports. The remaining 75% are processed for metal recovery and degassing and then the remaining residues are shredded and then landfilled (Caleb 2011). For foams used in marine sector, 95 to 100% of the foams are shredded then landfilled (Caleb 2011). The TRUs, REEFERs, and marine foams have no mandated end of life measures due to the relative small quantity of foam disposed compared to foam used in appliance and building sectors.

An additional category of foam that contains F-gas blowing agents is auto fluff, commonly referred to as auto shredder residue (ASR), which is a mixture of shredded foam residues from automobiles. These foams are residual waste products from auto shredder facilities and are highly heterogeneous both in size and composition depending on the year and manufacturer of the cars processed at the facility (Moakley et al. 2010). The auto fluff is a mixture typically composed of plastics (30 to 48%), fibers (4 to 26%), glass/ceramics (3 to 19%) metal (3%), elastomers/rubbers (10 to 32%), and minerals/residues (10 to 43%) (Moakley et al. 2010). According to Duranceau and Spangenberger (2011), auto shredder foam residues contain polystyrene (4% w/w) and PUR (2 to 3% w/w) polymers indicating the presence of rigid insulation foam and possibly F-gas blowing agents in the shredded foam products.

In a comprehensive study conducted by Scheutz et al. (2007b, 2011a, 2011b), the BA and PUR contents in auto shredder residue were quantified. The waste samples for the tests were obtained from a cell located in AV Miljø Landfill,

Denmark used to dispose auto shredder residues from 1990 to 2000 (Scheutz et al. 2007c). The waste materials were sampled from a depth between 1 and 1.5 m that were in anaerobic conditions. Large sample sizes (75 to 188 kg) were taken to reduce sampling error. PUR contents of the foam ranged from 2 to 12% (w/w) (Scheutz et al. 2007b, 2011a). It was indicated that PUR foam was most likely from rigid foam panels used in cars and caravans (Scheutz et al. 2007c). CFC-11, HCFC-141b, and HFC-134a contents in the foams were determined to be 0.70, 0.080, and 0.115 g/kg foam, respectively (Scheutz et al. 2007c). The presence of F-gases was confirmed through gas probe measurements from the landfill (Scheutz et al. 2011b). The results from these studies indicated that the presence of BAs in auto fluff at disposal is likely and that these BAs may contribute to emission of BAs in a landfill environment.

2.6 The Landfill Environment

A landfill can be conceptualized as a biochemical reactor with solid waste and water as the principal inputs and leachate, LFG, and heat as the principal outputs (Tchobanoglous et al. 1993; Yesiller et al. 2005). Landfills are engineered waste containment systems that consist of composite liner and cover systems, and leachate and gas collection and removal systems. LFG is mostly composed of methane (45 to 60 %) and carbon dioxide (45 to 60 %) and the remaining fraction is composed of nitrogen (2 to 5 %), oxygen (0.1 to 1 %), sulfides (0 to 1 %), ammonia (0.1 to 1 %), hydrogen (0 to 0.2 %), carbon monoxide (0 to 0.2 %) and other trace constituents (0.01 to 0.6 %) (Tchobanoglous et al. 1993). Landfill

methane emissions are estimated to contribute 1.3% (0.6 Gt CO_2eq per year) of the global anthropogenic GHG emissions (49 Gt CO_2eq per year) (Bogner and Spokas 2010). Methane is a potent greenhouse gas with thermal absorption efficiency 28 times greater than that of carbon dioxide (IPCC 2013). Thus, landfill gas emission reduction measures are necessary to mitigate the effects of climate change. The methane produced in landfills is either recovered by LFG collection system, oxidized by the methanotrophs in cover soils, or directly released to the atmosphere. A schematic of this process is presented in Figure 9. CFCs, HCFCs, and HFCs can also be oxidized in cover soils similar to methane (Scheutz 2004; Scheutz et al. 2003a, 2003b, 2004, 2007). Thus, F-gases are likely to have similar fate as methane in a landfill environment.

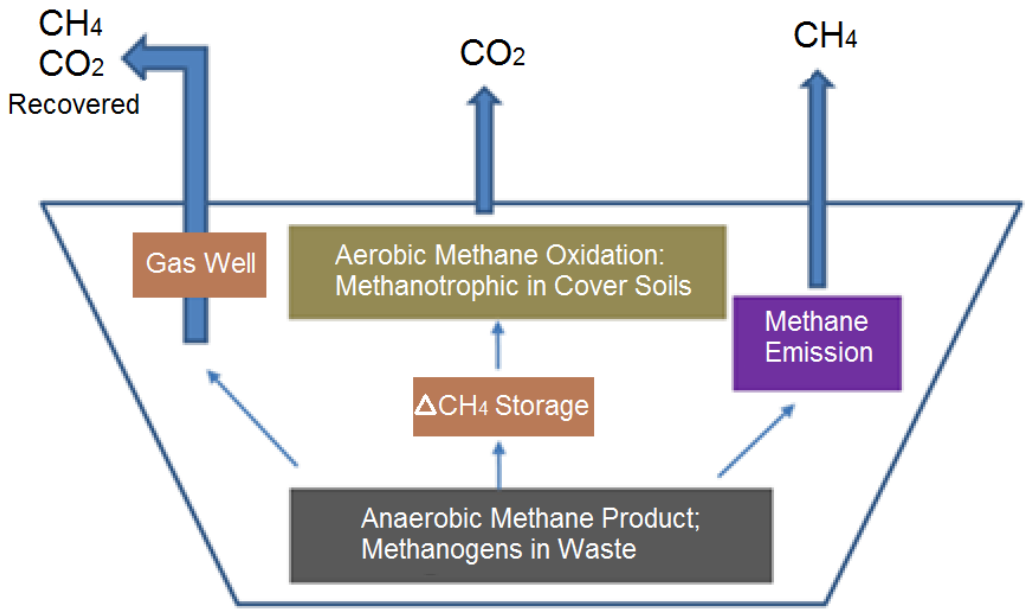

Figure 9 – Methane Mass Balance in a Landfill Environment
(Modified from IPCC 2007)

2.6.1 Physical Factors

Physical factors such as composition and organic content of MSW, compaction and compression processes, and types of cover, liner, leachate, and gas collection system used at a landfill are all variables that can affect the production and emission of LFG. For example, compaction and presence of geomembrane liners control moisture content and hydraulic conductivity in cover systems (Tchobanoglous et al. 1993; Qian et al. 2002). The presence of a liner and cover system, on the other hand, can limit the vertical and lateral diffusion or migration of LFG. The physical factors controlling the waste conversion processes are associated with the design and operation of the landfill.

The composition of MSW affects all processes in landfills including anaerobic decomposition and fugitive emissions. Comprehensive waste characterization was conducted by Cascadia Consulting group, where C&D waste foam fraction was determined. It was estimated, using the C&D waste foam fraction (0.2%) from 2008 and annual C&D waste generated from 2014 (approximately 5 million tons), that 9,580 tons of C&D waste foams was landfilled in 2014 (Cal Recycle 2006, 2008; Caleb 2011; Cal Recycle 2014). The details regarding the assumptions used for the calculation are provided in Section 2.5.3.

Cover systems are essential to operation and management of landfills for various reasons. Cover systems do not only eliminate source of disease vectors and reduce moisture infiltration, but also reduce fugitive emissions by limiting

vertical diffusion and promoting methane oxidation. There are three types of cover systems: daily, intermediate, and final. Daily and intermediate covers refer to temporary covers that are placed prior to installation of a final cover system. Daily covers range from 150 to 300 mm in thickness and various materials are used including soil, wood, geosynthetics, spray foams, shredded C&D waste, shredded auto fluff, and other wastes (USEPA 1993). By regulation, daily covers are required to have minimum thickness of 150 mm to provide equivalent performance to 150 mm of soil (USEPA 2012). Intermediate covers are placed over completed lifts that have reached their final elevation and are typically used for an extended period of time (typically over 1 year) (USEPA 1993). By regulation, intermediate covers are required to have minimum thickness of 300 mm using soil or alternate cover material with equivalent performance to 300 mm of soil (USEPA 2014b). The thickness can range from 60 to 100 cm and number of materials can be used for intermediate cover including soil and green waste, shredded C&D waste, shredded auto fluff, shredded C&D waste, and other wastes (CARB 2011). However, use of materials other than soils is highly limited in California landfills (CARB 2011).

Final cover systems are placed when the waste heights reach final levels. The main objective of the final cover systems is to minimize water infiltration to the underlying waste mass as well as to reduce emission of LFG. A general schematic of a final cover system is presented in Figure 10 (Yesiller and Shackelford 2011). Conventional final cover systems consist of vegetative soil and protective soil layer, filter/drainage layer, and a barrier system. The vegetative soil layer prevents

erosion along the surface and acts as a barrier to burrowing animals. The protective soil layer is mainly present to prevent plant roots from intruding to the underlying layers and minimum thickness of 150 mm is required. The filter/drainage layer collects water from precipitation or surface runoff infiltrating from surrounding areas. The barrier system is typically a composite barrier system used to isolate the waste from surrounding environment and to limit LFG transport to the surface. The barrier system is constructed using combination of compacted clayey soil and/or geosynthetic clay liners (GCLs), and geomembranes. The secondary filter/drainage layer is used to collect and remove LFG. Typical final cover thicknesses are at least 1000 mm and extend up to 1500 mm.

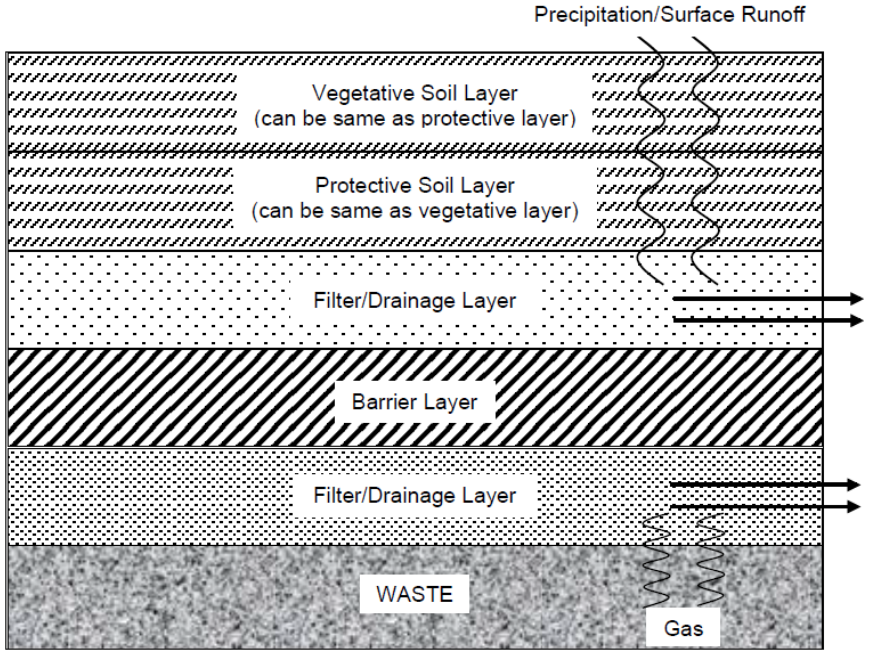

Figure 10 – The Conventional Final Cover System
(Yesiller and Shackelford 2011)

The primary design consideration for barrier systems is low hydraulic conductivity and gas conductivity. Gas conductivity typically decreases with decreases in hydraulic conductivity. Moon et al. (2008) determined that gas conductivity was about 2 to 3 orders higher than hydraulic conductivity. The difference between and gas and hydraulic conductivity was attributed to gas slippage, which makes gas more permeable, and clay-water interaction, which impedes water flow and make water less permeable (Moon et al. 2008). The flow velocity of the permeating gas at bounding solid walls (i.e. soil) is assumed to be non-zero whereas the velocity is at the bounding walls is assumed to be zero for permeating liquid. This phenomenon is referred to as gas slippage. whereas Moon et al. (2008) also indicated that compacted clay alone would not be sufficient to control landfill gas emissions. Yesiller and Shackelford (2011) indicated that compacted clay wet of optimum moisture contents dramatically decreased in both hydraulic and gas conductivity. Thus, variation in moisture content in the cover system can have significant effect on emissions of LFG from landfills.

2.6.2 Biochemical Factors

LFG is produced through multiphase conversion processes that involves biological and chemical conversion and transformation processes. Two primary biological processes that occur in the landfill environment are anaerobic degradation and aerobic oxidation. The degradation of organic fraction of waste produces carbon dioxide and methane, whereas aerobic oxidation converts the methane to carbon dioxide as it travels through the cover soil. Chemical processes

are mostly associated with the migration and sequestration of the chemicals in the landfill environment (Tchobanologus et al. 1993). The chemicals can volatilize, evaporate, or sorb onto waste materials or undergo chemical transformation through dissolution, condensation, or microbially mediated decomposition (Tchobanologus et al. 1993). The combination of these biological and chemical processes ultimately controls generation and emission of LFG.

Generation of landfill gas is known to occur in five phases as presented in Figure 11 (Tchobanologus et al. 1993). Phase I is the initial adjustment phase which occurs as soon as MSW is placed in a landfill (Tchobanologus et al. 1993). The organic biodegradable components of the MSW undergo biological decomposition due to presence of anaerobic and aerobic organisms in the cover soil. Phase II is the transition phase where oxygen is depleted and anaerobic condition starts to develop (Tchobanologus et al. 1993). This conversion from aerobic to anaerobic environment develops within weeks to several months subsequent to placement of waste (Hanson et al. 2005).

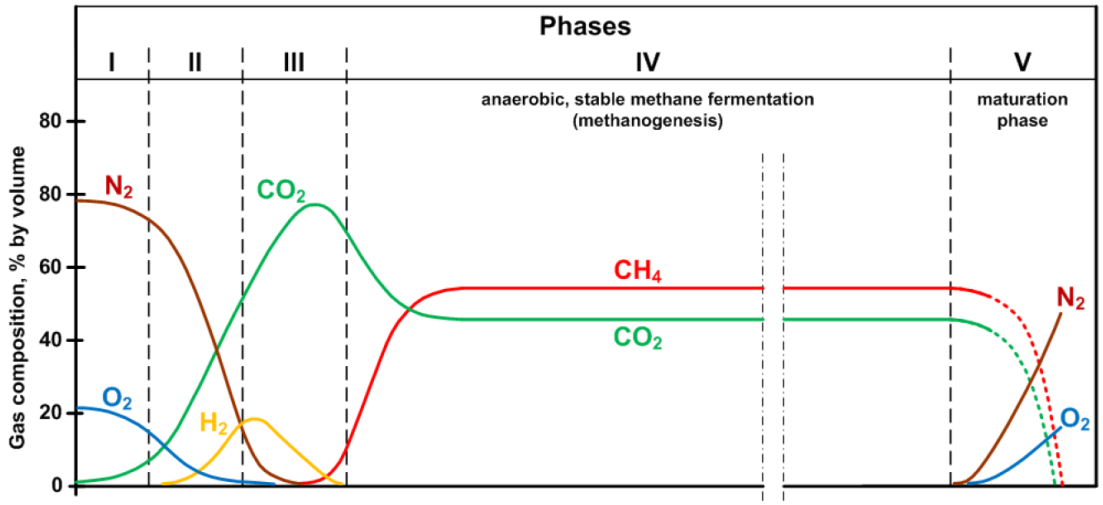

Figure 11 – Generalized Phases in the Generation of Landfill Gases (Hofstetter 2014)

In Phase III, complex organic materials are converted into organic acids with production of carbon dioxide. Phase III occurs in two steps via hydrolysis and acidogenesis (Rettenberger and Stegmann 1996). Phase IV is the methane fermentation phase or also known as methanogenesis, where organic acids produced from acidogenesis are converted to methane and carbon dioxide by methanogenic anaerobes (Tchobanologus et al. 1993). Acidogenesis and acid conversion occur simultaneously during this phase. The reactions in Phase III and IV depend on multiple factors including oxygen, hydrogen, and sulfate concentration, pH, alkalinity, presence of nutrients or inhibitors, temperature, and moisture content of waste (Rettenberger and Stegmann 1996). The specifics regarding the ideal condition for anaerobic decomposition can be found in existing literature (e.g. Merz 1964; Ramaswamy 1970; Hartz et al. 1982; Mata-Alvarez and Martinez-Viturtia 1986; Cecchi et al. 1993; Tchobanogolous et al. 1993). Phase V occurs after all the available biodegradable organic materials are depleted. The

rate of landfill gas generation greatly diminishes during this phase due to lack of nutrients and substrates (Tchobanologus et al. 1993). The duration of individual phases varies depending on multiple factors including distribution of organic components in the landfill, availability of nutrients, moisture content and routing of water in the waste, and degree of initial waste compaction (Tchobanologus et al. 1993). The peak time of LFG generation can vary depending on the climate, where the peak may be reached within the initial two-year period in a temperate climate whereas it may take up to decades in low temperature or arid conditions (Hanson et al. 2006).

Changes in moisture content and temperature in wastes influence aerobic and anaerobic degradation, which ultimately affect LFG production in a landfill environment (Stern et al. 2007). Larger LFG fluxes were reported during the summer months compared to that of winter and spring months (Chriophersen et al. 2001; Park and Shin 2001). High and low methane oxidation rates were observed during the summer and winter months, respectively. Jones and Nedwell (1993) indicated that the methane emissions were higher in the winter than in the summer due to saturation of the soil pores from higher precipitation leading to reduction in methane oxidation from lower methane transport through the soil. According to Whalen et al. (1990), gas-phase diffusion is about 10^4 times greater than aqueous diffusion. Thus, this leads to high methane emissions when soil pores are saturated.

During the summer months, considerably higher oxidation rates were observed resulting in high carbon dioxide fraction with an increase in LFG flux (Christophersen et al. 2001). Methane transport increased during the summer months with decrease in water saturated pores and increase in vertical extent of the oxidized zone allowing greater methane oxidation to occur (Christophersen et al. 2001). Thus, this lead to lower methane emissions with higher methane oxidation rate in the summer.

Aerobic oxidation in landfill covers occurs due to microorganisms present in landfill covers (Tchobanologus et al. 1993). Oxidation in landfill environment refers to conversion of methane, organic compounds, nutrients, and oxygen to new bacterial cells, carbon dioxide, water, ammonia, sulfate, and organic products by aerobic methanotrophs (Scheutz 2005). Optimal condition for aerobic oxidation includes stable pH, warm temperatures, presence of oxygen, absence of carbon dioxide and inhibitory metals, sufficient residence of LFG in the cover, and optimum moisture content (SCS Engineers 2008). Typically, maximum oxidation activity occurs within the top 15 to 20 cm beneath the surface of landfill covers (Jones and Nedwell 1993; Czepiel et al. 1996).

The optimal temperature for aerobic oxidation ranged from 20 to 30°C with 30°C being identified as the optimal temperature in multiple studies (Whalen et al. 1990; Figueroa 1993; Bender and Conrad 1994; Boeckx et al. 1996; Boeckx and Van Cleemput 1996; Stein and Hettiaratchi 2001; Scheutz and Kjeldsen 2004;

Scheutz et al. 2004; Streese-Kleeberg and Stegmann 2008; Spokas and Bogner 2011; Spokas et al. 2011). Optimum moisture content ranged from as low as 10% to over 30% (Whalen et al. 1990; Figueroa 1993; Bender and Conrad 1994; Czepiel et al. 1996a; Boeckx and Van Cleemput 1996; Boeckx et al. 1996; Börjesson 1997; Stein and Hettiaratchi 2001; Scheutz and Kjeldsen 2004; Scheutz et al. 2004; Streese-Kleeberg and Stegmann 2008). SCS Engineers (2008) reported an average oxidation rate of 35% with sandy soils having high oxidation rate of 55% and clayey soils having low oxidation rate of 22%. Methane oxidation rate ranged from 1 to over several hundred μg CH_4/ g soil-day depending on the type of cover present (Bogner et al. 2011).

Heat is a byproduct generated by various biochemical processes occurring within the landfill environment (Tchobanologus et al. 1993). The elevated temperature caused by the heat not only affects anaerobic decomposition and chemical transformation occurring within the landfill, but also affects the engineering properties of wastes, liners, covers and surrounding subgrade soils (Yesiller et al. 2005). The heat generated can influence the anaerobic decomposition in two ways: short-term effects on the reaction rate and long-term effects on the microbial population balance (Hartz et al. 1982). Optimum temperature for growth of mesophilic and thermophilic bacteria ranged from 30 to 40°C and 50 to 60°C, respectively (Cecchi et al. 1993; Tchobanogolous et al. 1993). Optimum temperature for maximum gas production from anaerobic

decomposition ranged from 34 to 41°C in laboratory studies (Merz 1964; Ramaswamy 1970; Hartz et al. 1982; Mata-Alvarez and Martinez-Viturtia 1986).

2.6.3 Environmental Factors

Common environment factors that influence LFG emissions are variations in seasonal and climatic conditions. Seasonal weather variations cause fluctuation in moisture content and temperature in incoming wastes and landfill covers. Variations in moisture content and temperature not only affect various chemical transport processes that control migration and sequestration of LFG, but can also influence the coupled biochemical processes including anaerobic degradation, aerobic oxidation, and heat generation in wastes.

Moisture content within a landfill changes with annual precipitation, fluctuation of moisture level in the incoming waste, and landfill cover configuration (e.g. daily, intermediate, and final). Hanson et al. (2010) indicated that incoming MSW moisture content varied between summer (31% w/w dry basis) and winter (53% w/w dry basis) at a landfill located in a humid temperate climate. According to Tchobanoglous et al. (1993), the moisture content of individual MSW components varied over a wide range with organic wastes in the high range (approximately 80% w/w wet basis) and inorganic components such as glass and metal in the low range (approximately 1 to 2% w/w wet basis. Optimum moisture contents for gas production ranged from 50 to 60% (w/w wet basis) (Tchobanoglous et al. 1993). Rees (1980a, 1980b) indicated that high water

content and an approximate density of 1 tonne/m^3 were necessary for optimum gas production in temperate climates, but also reported that excessive water infiltration can obstruct methanogenesis and cool down waste mass decreasing gas production.

The temperature of incoming wastes and landfill covers changes with fluctuation of ambient temperature. Initial waste placement temperature affects heat generation in landfills with higher initial waste placement temperature resulting in higher long-term waste temperature (Houi et al. 1997; Hanson et al. 2005; Yesiller et al. 2005). Farquhar and Rovers (1973) reported that the high waste placement temperature was directly correlated with the short-term temperature increase. Yesiller et al. (2008) investigated temperature variations in the landfill covers at test sites in four climatic regions. The surface temperature of the covers underwent seasonal fluctuation similar to air temperature. Typically, with increasing cover system depth, the maximum temperature decreased and the minimum temperature increased resulting in decrease in range of measured temperature (Yesiller et al. 2008). However, average temperature generally increased with depth.

Barometric pressure can affect emission and transport of LFG in a landfill environment. Methane and carbon dioxide emission were shown to be inversely related to barometric pressure (Young 1992; Czepiel et al. 1996; Christophersen et al. 2001; Czepiel et al. 2003; Xu et al. 2013). Emission quantities were strongly

associated with change in barometric pressure, where rising barometric pressure decreased the emissions and falling barometric pressure increased the emissions of LFG.

2.7 CFCs, HCFCs, and HFCs in Landfills

2.7.1 CFCs, HCFCs, and HFCs in Bank and Entering Landfills

Caleb (2011) conducted a comprehensive study using an emission model to estimate the amount of CFCs, HCFCs, and HFCs contained in foams in California. The model took various factors into account including market growth rate, average foam lifetime, foam density, blowing agent content respective to application (buildings, appliances, TRUs, and marine sector), average reuse rate for appliances and TRUs, building demotion rate, and building refurbishment rate (Caleb 2011). The end of life practices respective to applications were also taken into account to estimate amount of rigid foam entering California landfills. The model estimated the volume of F-gas containing foam waste generated, which was then converted to $MMTCO_2EQ$ using GWP and foam blowing agent content to achieve consistency with other Air Resource Board gas inventory and reduction analyses (Caleb 2011). The specifics regarding the assumptions of the model can be found in Section 3.7 of Caleb (2011).

The total amount of rigid foam generated containing high GWP BAs in 2008 was estimated to be approximately 930,000 m^3 (Caleb 2011). The two categories that generated the most foam were C&D insulations (34%) and appliance foam (34%) as presented in Figure 12. The foams containing F-gases are typically used

on average on the order of 30 years in buildings and 15 years in appliances (Caleb 2011). Bank of high-GWP gases had accumulated significantly by 1996 due to wide use of CFCs, reaching a peak of 286 $MTCO_2EQ$ as indicated in Table 4 (Caleb 2011). The bank has reduced by 90 $MMTCO_2EQ$ since then and is projected to decrease by another 40 $MMTCO_2EQ$ by 2020 as high-GWP CFCs are substituted with low-GWP hydrocarbons, HCFCs, and HFCs in various sectors (Caleb 2011).

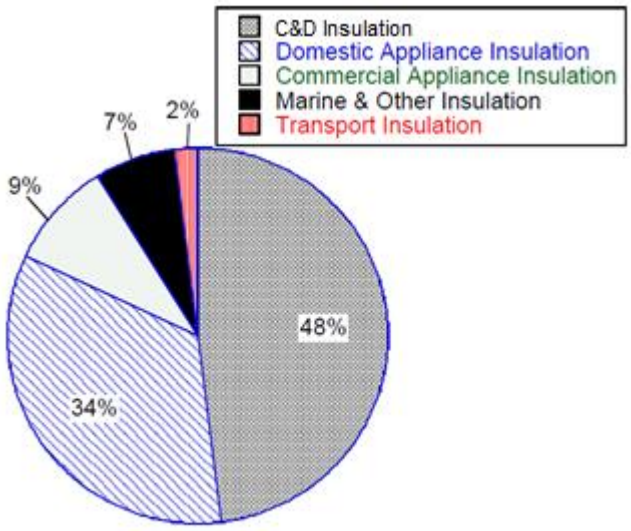

Figure 12 – Sources of Foam Waste Generated in California in 2008 (Caleb 2011)

Table 4 – Summary of All Blowing Agent Banks ($MTCO_2$-eq)

Year	Buildings	Appliances	Other Refrigeration	TRUs	Marine and Other	Total
1996	286.31	41.28	6.08	15.01	15.01	363.69
2005	267.72	28.89	2.82	7.81	7.81	315.05
2010	244.97	25.15	1.59	3.65	3.65	279.01
2015	216.49	33.00	1.81	2.84	2.84	256.98
2020	182.73	27.92	2.01	2.49	2.49	217.64

Caleb (2011) provided the amount of foam generated and the composition of F-gas BAs in California respective to their applications and usage over time. These data were used to estimate the 2008 and later conditions for foam wastes reaching end of life and foam wastes entering landfills as presented in Figure 13 and 14, respectively. For current conditions, CFC-11 represented the highest fraction of BA materials to reach end of life management processes and to enter landfills for disposal. However, for future conditions, HFC-245fa represented the highest fraction of BA materials to reach end of life management processes and to enter landfills for disposal. Overall, CFCs reaching end of life and entering landfill significantly decreased from present to future conditions due to their substitution by low-GWP alternatives.

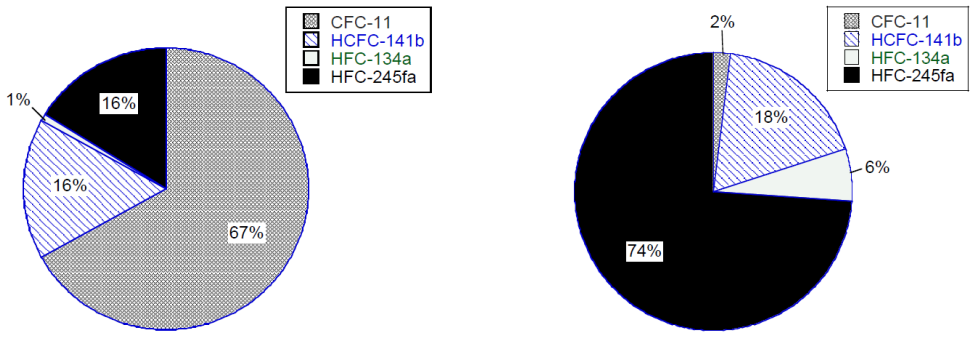

a) Current (2,705 tons BA / year) b) Future (3,418 tons BA/year)

Figure 13 – Foam Waste Entering End of Life Management in California (Caleb 2011)

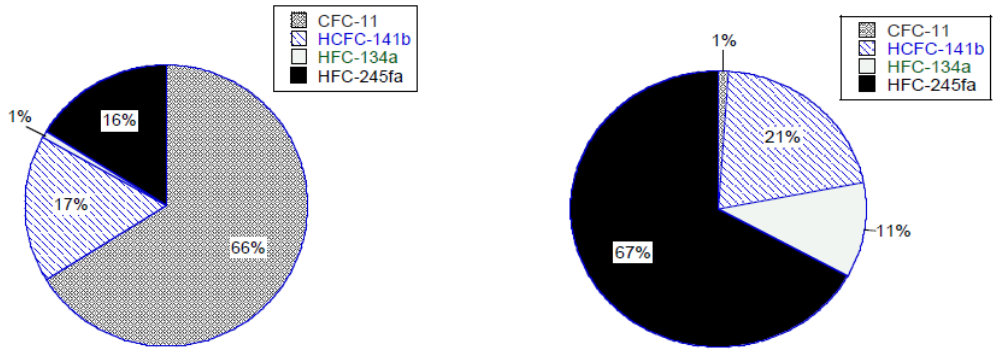

a) Current (1,784 tons BA/year) b) Future (1,655 tons BA/year)

Figure 14 – Foam Waste Insulation Materials Entering Landfills in California (Caleb 2011)

The composition of BAs banked in California landfills is presented in Figure 16. Though HFC-245fa, HCFC-141b, and HFC-134a will be entering landfills in considerably higher amounts in comparison to CFC-11 on a mass basis (Figure 16), CFC-11 will still be of utmost concern in relation to landfill emissions due to their historical usage and high GWP leading to high MMTCO_2EQ fraction in BAs banked in landfills as presented in Figure 15. As indicated in Table 5, the blowing agent banks in landfills rapidly increase from 1996 to 2020 primarily due to decommissioning of buildings with insulation foams containing CFC-11, which were extensively used prior to complete phase out of CFCs in 1996 (Caleb 2011).

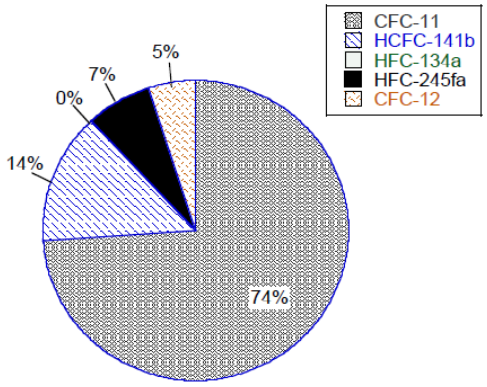

Figure 15 – Composition of BAs Banked in California Landfills in $MMTCO_2EQ$, Future (Caleb 2011)

Table 5 – Summary of Blowing Agent Banks in Landfills in $MMTCO_2EQ$ (Caleb 2011)

Year	Buildings	Appliances	Other Refrigeration	TRUs	Marine and Other	Total
1996	14.69	10.21	1.80	1.91	9.07	37.68
2005	40.40	24.60	3.99	3.19	13.40	85.58
2010	58.74	29.77	4.43	3.91	15.28	112.13
2015	80.61	29.33	4.14	3.77	14.09	131.94
2020	109.70	32.45	3.96	3.77	13.25	163.13

2.7.2 Fate of CFCs, HCFCs, and HFCs in Landfills

The two primary processes in landfills that control the fate of F-gas BAs are anaerobic degradation and aerobic oxidation. These processes govern the amount of BAs in the landfill environment as well as amount and rate of emissions from landfills. Degradation of CFCs and HCFCs occurs in anaerobic conditions. HCFC-21 and HCFC-22 are anaerobic degradation products of CFC-11 and CFC-12, respectively as presented in multiple studies (Scheutz 2005; Scheutz et al. 2007a, 2007b, 2011a, 2011b). In a batch experiment, CFC-11 was degraded to HCFC-21, HCFC-31, and HFC-41 within 5 to 10 days (Scheutz et al. 2007b). No further

degradation occurred after CFC-11, HCFC-21 and HCFC-31 was degraded to HFC-41. The degradation products did not correlate with the stoichiometric removal of CFC-11 indicating that other degradation products were also produced (Scheutz et al. 2007b). In addition, the study indicated that the degradation reactions occurred simultaneously and not sequentially. The degradation rate was directly proportional to number of chloride atoms attached to the carbon, where CFC-11 had the highest rate and the lowest rate observed for HCFC-31 (Scheutz et al. 2007b). Degradation of CFC-12 and HCFC-22 was relatively low compared to that of CFC-11 and HCFC-21. HCFC-22 was degraded to HFC-32 and was not degraded any further. HCFC-141b was also degraded at a similar rate to that of HCFC-22 and HFC-31, but the degradation pathway of the HCFC-141b was not identified in the study (Scheutz et al. 2007b).

CFCs, HCFCs and HFCs can be oxidized similar to methane in cover soils. Compounds such as HCFC-21, HCFC-22, HCFC-31, HCFC-32, and HFC-41 were oxidized with maximum oxidation rates ranging from 0.003 to 0.067 μg/g soil-day whereas highly substituted compounds such as CFC-11, CFC-12, HFC-141b, and HFC-134a were not oxidized under any aerobic conditions (Scheutz et al. 2007b). Scheutz et al. (2003b) conducted an experiment, where CFC-11, CFC-12, HCFC-21, and HCFC-22 gases were injected into a soil column containing a landfill cover sample. The injected HCFC-21 and HCFC-22 rapidly degraded in the aerobic part of the soil column (61% and 41%, respectively on mass basis). However, highly substituted compounds such as CFC-11 and CFC-12 only degraded under the

anaerobic part of the soil column. The degradation of F-gases in both aerobic and anaerobic zones indicates that both anaerobic and aerobic bacteria may be an important factor in reducing the emission of F-gases in landfill environments.

2.8 Gas Sampling Techniques

Grab sampling provides measurement of gas concentration at a single point in time. This method is used as a screening technique to identify contaminants and determine approximate concentrations in a given test area (USEPA 2005). The main advantage of grab sampling is the low sampling cost and simple testing requirements. The disadvantages include obtaining only a concentration at a single point in time, low sample volume, and potential diffusion of gases in or out of samplers. Common devices used for grab sampling in landfill emissions analysis are specially-treated canisters, glass sampling bulbs, Tedlar bags, or solid sorbent tubes (USEPA 2005).

Canisters are used commonly due to their ruggedness and ease of cleaning for reuse (Pellizari et al. 1984). For collection of trace gases from landfills or cover/surrounding soils, USEPA established method TO-14/TO-15 that requires specially-treated canisters to be used (USEPA 2005). The most common type of canister used for grab sampling is the Summa canister. Summa canisters refer to steel canisters that have internal surfaces deactivated using the Summa process (USEPA 2011). Tedlar bags also have been utilized as they provide simple, cost-effective means of collecting gas samples (Pellizari et al. 1984). The bags are used

only for short-term sampling as the reliable storage time is limited to 24 hours or less unless bags are protected from potential contamination or leakage (Pellizari et al. 1984).

Glass bulbs are another type of collection medium used for grab sampling. Glass bulbs have higher long-term storage stability than Tedlar bags, yet are fragile, which limit their practical use (Pellizari et al. 1984). Solid sorbent tubes refer to a sampling medium that utilizes the principle of adsorption to extract contaminants from gas samples (Peach and Carr 1986). The advantages are ease of sample management in the field and ease of transportation to the laboratory (Peach and Carr 1986).

2.8.1 Real-Time Sampling Techniques

Real-time sampling is a technique that provides instantaneous concentration values (USEPA 2005). Multiple measurements can be made over a short period of time, which allows for analysis and reporting of data nearly instantaneously. An advantage of this technique is that most portable real-time sampling devices are nonselective, meaning that entire class of compounds can be measured at one time. One disadvantage of real-time sampling is that the analytical system required for measurement is expensive. Also, the portable systems used are complex requiring highly trained field personnel, rigorous calibration procedures, and independent performance audits of routine monitoring and data handling operations (USEPA 2005).

Flame ionization detection (FID) is one of the most commonly used portable gas sampling techniques utilized for real-time monitoring (USEPA 2005). As a pollutant enters the ionization detector, the entering gas is mixed and then burned in a hydrogen flame to produce both ions and electrons (Liptak 2003). The electrons produced then enter an electrode gap, with decreasing gap resistance, to create a current. The flow of current then can be used to determine the pollutant concentration (USEPA 2005). A specific advantage of using FID is that it does not detect oxygen or water in the measurement process, which eliminates possible disturbance from these compounds during measurement (Liptak 2003). A main disadvantage is that a mixture varying in composition can be difficult to calibrate due to different detector responses and lower explosive limits of concentration between components in the mixture (Liptak 2003). Typical detection limits for FID are approximately 100 ppbv (USEPA 2005).

2.8.2 Time-Integrated Sampling Techniques

Time-integrated sampling includes measurement of gas concentration over a time period to provide a single, integrated value (USEPA 2005). The sampling period can vary from minutes to days to weeks. This technique is often used to detect very low concentrations since the sampling period can be varied to provide the analytical system sufficiently large samples to meet the detection limit (USEPA 2005). Various time-integrated sampling methods are available to collect compounds ranging from volatiles, semi-volatiles, inorganics, organics, to particulate matter (USEPA 2005). Time integrated sampling can be conducted

either using continuously or discontinuously operating devices. Continuous devices provide high time resolution but lack the sensitivity or selectivity to detect presence of specific classes or families of pollutants (USEPA 2004). Discontinuous techniques are favored due to the ability to detect low pollutant concentrations (USEPA 2004).

Time-integrated sampling can be conducted using active or passive sampling techniques (USEPA 2005). Active sampling utilizes pumps to allow the gas of interest to accumulate in the collection medium such as specially-treated canisters, sorbent tubes, impingers, or treated filters containing liquid media. Passive sampling method, utilizes physical processes such as diffusion to collect samples in contrast to active sampling, which requires an active moving medium (USEPA 2005). Overall, time-integrated sampling has several advantages. The technique can be cost-effective and allow for detection of chemicals present at low concentrations. The main disadvantage of the technique is the lack of real-time data (i.e. instantaneous feedback measurements), which may be significant in cases with potential issues with acute exposure. In addition, sample integrity problems may occur during transport of sampled media to another location for analysis (USEPA 2005).

2.8.3 Stationary Enclosure Measurement Techniques

A commonly used time-integrated sampling technique includes the measurement of trace gas emissions through stationary enclosure methods. Use of stationary enclosure methods has been the most common approach employed in the studies conducted to analyze emissions of chlorinated and fluorinated hydrocarbons from landfills and is detailed in this section.

Two types of stationary enclosure measurement methods exist: static and dynamic chamber methods (Hartman 2003). Static chamber methods differ from dynamic chamber methods in that no continuous inflow or outflow of gases occur to the chamber. Thus, emanating gas from the surface is accumulated in a chamber over time (Hartman 2003). The operation of static flux chambers is simpler and more cost-effective than dynamic chambers with no requirement for active equipment. (Heinemeyer et al. 2011). The disadvantage of static chamber methods is that surface emission flux rate may decrease, if a sufficiently high concentration gradient accumulates within the flux chamber (Hartman 2003) Therefore, static flux chambers may underestimate emission rates (Martin and Kerfoot 1988).

For dynamic chamber methods, a constant flow rate of clean air is introduced into the flux chamber, which mixes and transports the emitted gas from the surface (Reinhart et al. 1992). Next, continuous gas concentration measurements are made through the exit port (Reinhart et al. 1992). One

significant advantage of using the continuous flow method is that it is unlikely to have any concentration buildup that may impede emissions (Hartman 2003). One disadvantage is that, due to active measurement process, operating procedures and calibration is more complex (Hartman 2003). Also, dynamic chambers require an analysis method with lower detection limits due to dilution of gases to be measured from inlet flows (Hartman 2003). Equipment associated with dynamic chamber methods is considerably more expensive compared to flux chambers due to equipment required for the continuous flow system (Heinemeyer et al. 2011).

The primary enclosure measurement technique that has been used for analysis of trace gas concentrations is the static flux chamber. Static chamber methods have been used extensively to quantify various constituents including methane and F-gases (Bogner et al. 1997a, 1997b, 2003, 2004, 2007, 2010, Scheutz et al. 2003a, 2007b, 2008, 2011b). The principle behind a static chamber technique is to establish a sealed volume above a surface where gas is transported. As the gas cannot escape, the accumulation or depletion of the gas in the volume can be monitored (Abichou et al. 2006a, 2006b, 2006c). The gas samples are taken from the chamber at set intervals to determine change in concentration over time. Based on the change in concentration over time, surface flux is determined for the corresponding area of the chamber. A rigid frame (i.e., a collar) is inserted and sealed into the surface of the landfill to a depth of 5 to 20 cm. A cover is placed over the frame and secured in place to form a tight seal. The chamber is equipped

with ports for collection of gas from the headspace above the landfill surface. A photograph of a static flux chamber is provided in Figure 16.

Figure 16- Static Flux Chamber Installed at a California Landfill
(Photo by Dr. Jean Bogner)

The dimensions of the chamber typically are on the order of several tens of cm in diameter (circular frame) or along the sides (rectilinear frame) and a few tens of cm in height. The areas of the chambers vary between 0.1 and 1 m^2 (Bogner et al.1997b, Börjesson et al. 1998; Abichou et al. 2006a, 2006b; Spokas et al. 2006; Scheutz et al. 2003a, 2008; Stern et al. 2007). Use of smaller chambers also has been reported (Mosher et al. 1996; Czepiel et al. 1996; Börjesson et al. 2001). Chambers with large volume-to-area ratios and short deployment times are recommended for areas with high amounts of emissions, whereas chambers with low volume to area ratios are recommended for locations with low emissions (Livingston and Hutchinson 1995). Large static flux chambers with areas on the order of 1 m^2 and with low volume to area ratio are well suited for methane and trace NMOC surface flux quantification (Bogner et al. 1997a; 1997b; Barlaz et al. 2004). Increasing the accumulation area provides a high number of sampling

opportunities during a given time period, thereby allowing for improved time series analysis (Bogner et al. 1997a, 1997b; Barlaz et al. 2004).

A fan is used in the chamber to circulate the gas collected to ensure uniform distribution. The gas is sampled using gas-tight syringes or stainless steel canisters and stored (Mosher et al. 1996; Bogner et al. 1997b; Börjesson et al. 1997; Abichou et al. 2006b, 2006c; Stern et al. 2007). The gas samples are then analyzed using analytical techniques such as gas chromatography in the field or in the laboratory for determination of concentrations. An alternative method is provided by Spokas et al. (2006), where a pump is used to circulate the gas in the headspace to an outside loop. Gas concentrations are then measured using a portable gas chromatograph on site or in the laboratory if samples are collected.

In the static flux chamber method, methane or trace gas concentrations and surface flux are measured using the gas collected from the headspace of the chamber. A single sampling event provides concentration values, whereas repeated measurements over time allow for determination of flux. Concentrations are measured at intervals such as 5 minutes over total test durations of approximately 20 to over 60 minutes. Concentration (C in ppmv) is plotted against time (t in minutes) and the surface flux is determined using concentration versus elapsed time data. The gas concentration within the chamber generally increases linearly and dC/dt represents the slope of the trend (typically a linear regression fit

to the data). The change in volumetric concentration (*dC/dt*) is converted to a mass flux using the ideal gas law. The surface flux, F (g m^2-d), is calculated as follows.

$$F = \frac{(P)(V)(M)(U)(\frac{dC}{dt})}{(A)(T)(R)} \quad [2]$$

where *P* is pressure (atm), *V* is chamber volume (L), *M* is the molar mass of gas analyzed (g/mol), *U* is the unit conversion factor (0.00144 min / µL-d), *dC/dt* is the change in concentration over time expressed in µL/min, *A* is the surface area covered by the chamber (m^2), *T* is chamber temperature (K), and R is the ideal gas constant (0.08205 L-atm/(K-mol)).

2.9 Emissions of BAs from Landfills

2.9.1 Definition of BA Release Periods

The release of BA from insulation foams is known to occur over three distinct phases in landfills: instantaneous release (on the order of minutes to hours), short-term release (on the order of hours of days), and long term release (on the order of weeks to years) (Scheutz and Kjeldsen 2003b). Instantaneous release refers to release of BAs due to permanent damage to the cells from mechanical processes, such as shredding or compaction, resulting in a large release of BAs from the foams (Scheutz and Kjeldsen 2003b). Short-term release refers to release of BAs from small cracks in slightly damaged foams while long-term release refers to release of BAs over cell walls through diffusion (Scheutz and Kjeldsen 2003b). Short-term releases were observed to be strongly dependent on particle size distribution of the shredded foam (Scheutz et al. 2007c; Scheutz and Kjeldsen 2003b). Short and long-term releases were observed to be strongly dependent on

existing anaerobic conditions and diffusion coefficient of BAs (Scheutz and Kjeldsen 2003b; Scheutz et al. 2007c).

2.9.2 Modeling and Laboratory Based BA Release Studies

Summaries of instantaneous and short-term releases based on laboratory and field studies are presented in Table 6 and 7 (Kjeldsen and Jensen 2001; BRE 2002; Scheutz and Kjeldsen 2003b; Scheutz et al. 2007c). A summary of long-term release modeling studies is presented in Table 8 (Khalil and Rasmussen 1986, 1987; Kjeldsen and Jensen 2001; Scheutz and Kjeldsen 2003b; Fredenslund et al. 2005; Scheutz et al. 2007c). The majority of instantaneous and short-term release studies were conducted in laboratory environments and did not investigate these release mechanisms in landfill environments (e.g., BRE 2002; Scheutz and Kjeldsen 2003b; Scheutz et al. 2007c). However, long-term studies did take landfill environment into consideration.

Instantaneous and short-term releases from foams were quantified through direct measurement, batch release, and infinite bath testing methods (Kjeldsen and Jensen 2001; BRE 2002; Scheutz and Kjeldsen 2003b; Scheutz et al. 2007c). The results from instantaneous release studies indicated that the release varied with BA type as indicated in Table 6. Initial BA content is defined as the ratio between BA present in the foam prior to any release and the initial foam mass expressed in percentage. Total BA release is defined as the ratio between BA released and the initial BA content expressed in percentage. The releases of

HCFC-141b and HFC-245fa typically were less than the releases of CFC-11 (Scheutz and Kjeldsen 2003b; Scheutz et al. 2007c). Instantaneous release was strongly dependent on particle size, where smaller particle size generally resulted in higher releases from shredded foams. Cutting the foams instead of shredding released significantly smaller weight fraction of CFC-11 as indicated in Table 6. This was attributed to higher fraction of smaller particles in the shredded foam.

In similarity to the instantaneous release studies, the results from short-term release studies also varied with BA type as presented in Table 7. The releases of CFC-11 and HFC-134a were typically less than the releases of HCFC-141b and HFC-245fa. The total BA release was defined as the percentage of total BA released relative to the initial BA content present in the foam prior to the test. The total BA releases of CFC-11 ranged from 9 to 23% (w/w); the releases of HCFC-141b ranged from 1 to 28% (w/w); the releases of HFC-134a ranged from 3 to 15% (w/w); the releases of HFC-245fa ranged from 8 to 30% (w/w). Short-term releases were not a function of particle size unlike instantaneous release as indicated in Table 7.

Table 6 – Summary of Instantaneous BA Release Studies

Reference	BA Type	Experiment Type	Size Fraction	Initial BA Content (% w/w)	Total BA Release (% w/w)	Average Total Release (% w/w)
BRE (2002)	CFC-11	Laboratory Cutting	Refrigerator Panel	13.3	3	2.8
			Freezer Panel		3.9	
			13.3		1.4	
Scheutz and Kjeldsen (2003b)	CFC-11	Laboratory Shredding	16 to 32	13.3	9.4	24.9
			8 to 16		17.6	
			4 to 8		33.8	
			2 to 4		38.7	
	HCFC-141b	Laboratory Shredding	16 to 32	11.62	8.8	8.8
			8 to 16		-	
			4 to 8		-	
			2 to 4		-	
	HFC-245fa	Laboratory Shredding	16 to 32	11.62	11.1	11.1
			8 to 16		-	
			4 to 8		-	
			2 to 4		-	
Scheutz et al. (2007c)	CFC-11	Field Shredding	< 32	15.4	16.0 ± 8.7	24.2 ± 7.5
			16 to 32		26.3 ± 8.1	
			8 to 16		31.9 ± 8.1	
			< 8		7.2 ± 3.7	

Total BA release = [(Initial BA Content - BA Content Remaining after the Test)/Initial BA content] × 100%
- : Omitted in the study.

Table 7 – Summary of Short-Term BA Release Studies

Reference	BA Type	Experiment Type	Duration of Experiment (Weeks)	Shredded	Size Fraction of Particles (mm)	Initial BA Content (% w/w)	Total BA Release (% w/w)	Total Mass of the Foam Sample (g)
Kjeldsen and Jensen (2001)	CFC-11	Laboratory [3]	3 to 8	Yes	20	12	10	-
					10		20	
	CFC-11	Laboratory [4]	7	No [8]	N/A	11.4	23	0.036 [10]
Scheutz and Kjeldsen (2003)	CFC-11	Laboratory [1]	6	No [8]	N/A	-	20	13.6
	CFC-11	Field	6	Yes	4 to 8	10.1	6.8	-
					6 to 16		8.1	
	CFC-11	Laboratory [2]	6	Yes	16 to 32	13	12.5	-
					8 to 16		8.5	
					4 to 8		10.9	
	CFC-11	Laboratory [3]	6	No [9]	N/A	11.4	17	0.019 [10]
	CFC-11	Laboratory [5]	17	No [9]	N/A	13.3	10	0.019 [10]
	CFC-11	Laboratory [4]	17	No [9]	N/A	13.3	17	0.019 [10]
	HFC-141b	Laboratory [3]	6	No [9]	N/A	11.6	20	0.025 [10]
	HFC-141b	Laboratory [5]	17	No [9]	N/A	11.6	< 1	0.025 [10]
	HFC-141b	Laboratory [4]	17	No [9]	N/A	11.6	20	0.025 [10]
	HFC-141b	Laboratory [1]	6	No [9]	N/A	-	28	16.2
	HFC-245fa	Laboratory [3]	6	No [9]	N/A	11.6	22	0.024 [10]
	HFC-245fa	Laboratory [4]	17	No [9]	N/A	11.6	20	0.024 [10]
	HFC-245fa	Laboratory [5]	17	No [9]	N/A	11.6	15	0.024 [10]
	HFC-245fa	Laboratory [6]	6	No [8]	N/A	11.7	28 to 30	15.3
					N/A	13.7	7.6	
					N/A	18.2	9.5	
	HFC-134a	Laboratory [5]	17	No [9]	N/A	7	3	0.031 [10]
	HFC-134a	Laboratory [3]	6	No [9]	N/A	7	10	0.031 [10]

Total BA release = [(Initial BA Content – BA Content Remaining after Test)/Initial BA content] × 100%

[1] Measured BA emissions with flux chambers; [2] Artificial shredding of foam in a glove box container; [3] Batch release experiment (Scheutz and Kjeldsen 2003); [4] Infinite bath experiment, chemical extraction technique (Scheutz and Kjeldsen 2003); [5] Infinite bath experiment, gravimetric extraction technique (Scheutz and Kjeldsen 2003); [6] BA emissions measured with flux chambers on foam from different manufacturers; [7] Batch microcosm experiment with foam with organic waste and microbial inoculum (Scheutz et al. 2003); [8] Foam speciements cut into foam cubes
[9] Foam specimens cut into foam cylinders; [10] Calculated value based on 1-cm-diameter, 1-cm-height cylinder with a foam density of 24.6 g/L
N/A : Not applicable to the study;
- : Omitted in the study

Table 7 – Summary of Short-Term BA Release Studies (cont'd)

	BA Type	Experiment Type	Duration of Experiment (Weeks)	Shredded	Size Fraction of Particles (mm)	Initial BA Content (% w/w)	Total BA Release (% w/w)	Total Mass of the Foam Sample (g)
Scheutz and Kjeldsen (2003)	HFC-134a	Laboratory [4]	17	No [9]	N/A	7	10	0.031 [10]
	HFC-134a	Laboratory [6]	6	No [8]	N/A	7	15	-
Scheutz et al. (2007c)	CFC-11	Laboratory [7]	14	No [9]	N/A	13.3	9	0.019 [10]
	HCFC-141b	Laboratory [7]	14	No [9]	N/A	11.6	16	0.025 [10]
	HFC-134a	Laboratory [7]	14	No [9]	N/A	7	9	0.031 [10]
	HFC-245fa	Laboratory [7]	14	No [9]	N/A	12	19	0.024 [10]
	CFC-11	Laboratory [7]	3	Yes	-	-	1	41,600

Total BA release = [(Initial BA Content – BA Content Remaining after Test)/Initial BA content] × 100%
[1] Measured BA emissions with flux chambers; [2] Artificial shredding of foam in a glove box container; [3] Batch release experiment (Scheutz and Kjeldsen 2003); [4] Infinite bath experiment, chemical extraction technique (Scheutz and Kjeldsen 2003); [5] Infinite bath experiment, gravimetric extraction technique (Scheutz and Kjeldsen 2003); [6] BA emissions measured with flux chambers on foam from different manufacturers; [7] Batch microcosm experiment with foam with organic waste and microbial inoculum (Scheutz et al. 2003); [8] Foam speciements cut into foam cubes
[9] Foam specimens cut into foam cylinders; [10] Calculated value based on 1-cm-diameter, 1-cm-height cylinder with a foam density of 24.6 g/L
N/A : Not applicable to the study;
- : Omitted in the study

Long-term release from foams was evaluated using a model referred to as Model for Organic Chemicals in Landfills FOAM (MOCLA FOAM) (Fredenslund et al. 2005; Scheutz et al. 2007c). Unlike instantaneous and short-term release studies, the model included effects of adsorption processes occurring throughout the soil covers as well as in the waste masses, and aerobic and anaerobic degradation. Fredenslund et al. (2005) investigated two different waste foam management scenarios in landfills with the MOCLA FOAM model to evaluate the long term emissions of CFC-11 and HCFC-141b from shredded insulation foams. Typical foam waste disposal procedure in a landfill was assumed for the two scenarios, which included stockpiling of foam for a short period of time followed by a compaction process during placement.

Scenario 1 took the instantaneous BA release mechanism from the compaction into account as part of the model and did not assume that anaerobic conditions were already present in the landfill. Scenario 2 was modeled with reduced instantaneous BA emissions (5% BA release compared to Scenario 1 of 15% BA release). The simulation with the ten times higher diffusion coefficient and ten times higher degradation coefficient had the lowest total BA release (Fredenslund et al. 2005). During the 20 year simulation, release of CFC-11 and HCFC-141b ranged from 0 to 3% and 1 to 4%, respectively.

Scheutz et al. (2007a) also presented similar results with the MOCLA FOAM model evaluating long-term emissions of CFC-11, HCFC-141b, CFC-12, and

HCFC-12 from foam cubes (50 mm), which were considerably larger than shredder foams (4 to 41 mm). The foam cubes had considerably higher long-term emissions (0.5% to 57% total BA release) in comparison to emissions of shredder foams (0% to 4% total BA release) (Fredenslund et al. 2005; Scheutz et al. 2007a). For both studies, the largest fraction of BA was degraded with high diffusion and high degradation (Fredenslund et al. 2005; Scheutz et al. 2007a).

Even though modeling results indicated a large potential for anaerobic degradation of F-gas BAs, uncertainty exists whether anaerobic degradation occurs at sufficiently high rate to mitigate the release of BAs during initial compaction and short-term compression processes. The lack of field data on initial and short-term releases representing compaction process and early aerobic conditions in landfills introduces another level of uncertainty in these models, which will need further investigation in order to accurately quantify F-gas emissions from landfill environments using the MOCLA FOAM model.

Table 8 – Summary of Long-Term BA Release Studies

Reference	Type of BA	Duration of Simulation (Years)	Initial BA Content (% w/w)	Density (g/L)	Shape	Particle Size Range (mm)	Diffusion Coeff. Used (D) [2]	Degradation Coeff. Used (K_1) [3]	Predicted Total BA Release (%)
Fredenslund et al. (2005)[1]	CFC-11	20	14.9	25	Shredded Particles	41 (>32)	D	K_1	1
						24 (16 to 32)	D	K_1/10	3
						12 (8 to 16)	10D	K_1	0
						4 (<8)	10D	K_1/10	2
	HCFC-141b	20	14.9	25		41 (>32)	D	K_1	1
						24 (16 to 32)	D	K_1/10	3
						12 (8 to 16)	10D	K_1	1
						4 (<8)	10D	K_1/10	4
Scheutz et al. (2007a)[1]	CFC-11	20	14.9	25	Cubes	50	D	K_1	0.5
								K_1/10	5
							10D	K_1	0.5
								K_1/10	5
	HCFC-141b	20	14.9	32	Cubes	50	D	K_1	6
								K_1/10	29
							10D	K_1	6
								K_1/10	29
	CFC-12	20	14.9	Unknown	Cubes	50	D	K_1	6
								K_1/10	40
							10D	K_1	6
								K_1/10	40
	HCFC-22	20	14.9	25	Cubes	50	D	K_1	12
								K_1/10	57
							10D	K_1	12
								K_1/10	57

[1] Long-term modeling study using the MOCLA-FOAM model. Model inputs and scenarios described in text.
[2] Assuming D ranges from 2.0×10^{-14} to 5.1x10-14 m^2/sec depending on the BA used (laboratory determined coefficients)
[3] Assuming K_1 ranges from 0.4/day to 0.015/day depending on the BA used (laboratory determined rates)
N/A: Not applicable to study
-: Omitted by study

2.9.3 Field Based BA Emissions Studies

The two primary driving forces of landfill gas emissions are pressure differences (advection) and concentration differences (diffusion) between a landfill and the environment. Migration of LFG within a landfill can occur in vertical or lateral directions depending on local concentration and pressure gradients within the waste mass, available pore space, moisture content, and temperature (Rettenberger and Stegmann 1996). The factors that influence gas emission are divided into meteorological factors (barometric pressure, precipitation, temperature, and wind), waste factors (gas production rate, VOC release, presence and type of internal barriers or gas vents, the lengths of lateral or vertical migration pathways, and the tortuosity of the migration pathways), and geologic factors (crack and fissures, permeability, diffusivity, porosity, organic content, and water content of cover and waste materials) (Rettenberger and Stegmann 1996).

Emissions of LFG components typically occur in the vertical direction due to presence of liner and cover systems limiting lateral migration in modern landfills (Tchobanoglous et al. 1993). LFG generation and emission rates vary as a function of cover conditions (daily, intermediate, final), heterogeneity of wastes, site-specific operational conditions (compaction technique utilized, waste filling sequence, waste placement density, cover materials), and site specific climatic conditions (precipitation, temperature, humidity, atmospheric pressure) (Rettenberger and Stegmann 1996). The emissions of LFG typically decrease with the order daily, intermediate and final covers (Abichou et al. 2006b).

Rettenberger and Stegmann (1996) provided a summary comparison of seven studies from the 1980s to 1990s that included CFC and HCFC concentration measurements in LFG. The studies were conducted in Germany and the United Kingdom and did not include surface emission measurements. LFG were sampled using adsorbent tubes, which were then analyzed using gas chromatography and mass spectrometry for all studies (Rettenberger and Stegmann 1996). The areas where grab sampling measurements took place in the German studies were fairly limited (Rettenberger 1986). However, the studies conducted in the United Kingdom had the gas samples taken from the intermediate cover after the waste was placed and were taken from periods ranging from 6 months to 3 years (Brookes and Young 1983; Young and Heasman 1985; Dent et al. 1986; Allen et al. 1997). The concentrations were in the range of ppmV to ppbV for most of the CFCs and HCFCs measured as presented in Table 9.

The studies conducted from the 1980s to 1990s (e.g., Brooks and Young 1983; Rettenberger 1986; Dent et al. 1986; Deipser and Stegmann 1994; Allen et al. 1997) may not contain highly relevant information due to changing waste composition and introduction and use of new blowing agents. As a result, HCFC-141b, HFC-134a, or HFC-245fa were not provided in these studies. A review of the studies from the last two decades are expected to be more relevant with regard to current waste and BA compositions.

Table 9 – Concentrations of Selected F-Gases from LFG Samples from Landfilling of Waste (in ppmV)

Reference	CFC-11	CFC-12	CFC-13	CFC-113	CFC-114	HCFC-21	HCFC-22	HCFC-31	HCFC-142b
Brooks and Young (1983)	3.5	2	0 to 2.3	-	-	1.17	-	-	-
Young and Heasman (1985)	0.1 to 32.4	1.2 to 120	-	-	-	-	0.6 to 77	0.035 to 39	-
Rettenberger (1986)	0.2 to 15	0.8 to 24	0 to 2.3	-	-	1.17	-	-	-
Dent et al. (1986)	<0.02 to 33	<0.02 to 90.1	-	-	-	0.02 to 143	<0.03 to 78.1	-	-
Deipser and Stegmann (1994)	0.05 to 6.13	2.1 to 22.1	-	0.01 to 0.218	0.32 to 1.25	0.16 to 6.5	0.53 to 8.5	-	-
Allen et al. (1997)	<0.02 to 13	<0.1 to 23	-	<0.1 to 0.8	-	<0.1 to 55	<0.1 to 114	<0.2 to 34	<0.1 to 8

Conversion mg/m3 to ppmV: ppmV = (mg/m^3) (273.15 + °C) / (12.187 mol K/atm/L) (Molecular Weight)
-: Omitted in the study

Bogner et al. (2004) and Schuetz et al. (2008) evaluated emissions of methane and NMOCs at a landfill in Grand'Landes, France (Table 10 and 11). Tests were conducted in two cells with different gas collection systems. The first cell (Cell A) had a conventional vertical gas collection system and cover design. The cover system for Cell A from top to bottom included a 30-cm vegetated topsoil layer and a 70-cm compacted clay layer. The second cell (Cell B) had two horizontal perforated pipes within a 30-cm gravel gas collection layer for drainage installed beneath the cover system. The cover system from top to bottom included a 30-cm vegetated top soil layer, a 70-cm compacted clay layer, a geotextile layer, a 1.5-mm HDPE geomembrane, a protective geotextile, a geogrid layer, and a 30-cm drainage layer (Scheutz et al. 2008). Field measurements included surface emission and gas profile measurements followed by source gas and soil sampling (Scheutz et al. 2008). Source gas was sampled from gas collection headers in both cells. Surface emission rates were determined using the static flux chamber method. The control surface emission measurements were done in a grassy field area not underlain by waste, which was adjacent to recently filled areas. The LFG concentration measurement results and surface emission measurement results are presented in Table 9 and 10, respectively.

Landfill gas composition measurements indicated that a large intrusion of -atmospheric air into the soil covers for both cells with nitrogen and oxygen concentrations of 32% and 7%, respectively for Cell A, and 42% and 5%, respectively for Cell B (Scheutz et al. 2008). The air intrusion was deemed to occur

due to actively operating gas collection systems drawing atmospheric air into the cover soil (Scheutz et al. 2008). A total of 47 trace NMOCs were detected in the LFG and the concentrations between Cells A and B were relatively similar (Table 10). F-gases were present at relatively high concentration ranging between 2 and 841 ppmV with the exception of HCFC-141b measured at concentrations of 4,354 ppmV and 11,625 ppmV in Cell A and B, respectively (Table 10).

Changes in isotopic composition of methane and carbon dioxide between samples from the header of the gas collection system and from deep within the soil cover of both Cells A and B indicated methane oxidation was taking place in both cells (Scheutz et al. 2008). For Cell A, negative fluxes of methane were obtained in 6 out of 12 chambers as indicated in Table 10 (Bogner et al. 2004; Scheutz et al. 2008). Average fractional methane oxidation ranged from 0% to 54% and 7% to 68% for Cells A and B, respectively (Table 10). NMOC fluxes were both positive and ranging negative ranging from the order of -10^{-8} to 10^{-5} g/m^2-day and -10^{-8} to 10^{-6} g/m^2-day for Cells A and B, respectively. The highest fluxes of NMOCs occurred at local hotspots (areas with significantly higher emissions), where CFC-11 and HCFC-141b demonstrated larger positive fluxes as indicated in Table 11.

Scheutz et al. (2003a,b) and Bogner et al. (2003) investigated emissions of methane and NMOCs at a second landfill in Lapouyade, France. Waste placement at the landfill occurred over two phases. During Phase 1, 310,000 tons of MSW (household waste, industrial waste, and bulky waste) was placed between 1996

and 1998 (Scheutz et al. 2003b, 2003d). Phase 2 represented active operation phase at the landfill, which included waste placement since 1998. Active gas collection systems were present at the landfill. The Phase 1 cell had a final cover consisting from top to bottom, an 80-cm loam with vegetated surface and a 40-cm coarse sand layer. The Phase 2 cell had a 40-cm coarse sand intermediate cover layer. The methods used for LFG sampling and flux measurements were identical to the method used in Scheutz et al. (2008). The surface emissions were measured in multiple locations in the area with the final cover and in the area with the intermediate cover. The LFG samples were taken at a header of the final cover system. The results of surface emission and LFG concentration measurements are presented in Table 12.

In the LFG, elevated concentrations of oxygen and nitrogen (3% and 15% v/v, respectively) were measured indicating possibility of air intrusion occurring through the cover soil (Scheutz et al. 2003b,c; Bogner et al. 2003). The concentrations of CFC-11, CFC-12, and HCFC-22 were 373, 1,177 and 236 ppmV, respectively. Methane emissions from final cover ranged from -0.01 to 10 g/m^2-day with an average of 1.97 ± 0.88 g/m^2-day.

Results indicated a high spatial variability in methane emissions from final cover locations. Average methane oxidation rates of 40% and 3.8% were measured in the final and intermediate cover locations, respectively. Negative fluxes suggested that methane oxidation was taking place within the covers. The

intermediate cover measurement had a higher average methane flux (49.9 ± 14.4 g/m^2-day) than the final cover measurements. Final cover fluxes of NMOCs were minimal ranging from order of 10^{-7} to 10^{-5} g/m^2-day with both positive and negative fluxes (Table 12). Fluxes of NMOCs similar to methane fluxes exhibited high spatial variability. Larger fluxes of NMOCs were observed from the intermediate cover location and were mostly positive on the order of 10^{-5} g/m^2-day (Bogner et al. 2003; Scheutz et al. 2003b,c).

Scheutz et al. (2011b) evaluated LFG concentration and surface emissions from a shredder residue cell at a landfill in Denmark. The F-gases studied included CFC-11, CFC-12, HCFC-141b, HCFC-21, HCFC-22, HCFC-31, HFC-32, HFC-41, HFC-134a, and HFC-245fa. The LFG concentration measurement results are presented in Table 13. Elevated nitrogen concentrations indicated a large amount of air intrusion into the waste mass. The concentrations listed in Table 13 are corrected for dilution with atmospheric air based on the nitrogen content measured in the LFG (Scheutz et al. 2011b). Both HCFC-21 and HCFC-31 were measured at relatively high concentrations (7 to 16 ppmV), which was attributed to sequential dechlorination of CFC-11 (Scheutz et al. 2011b). CFC-11, CFC-12, and HCFC-141b were detected in considerably lower concentrations of 0.4 to 1.0 ppmV in comparison to HCFC-21 and HCFC-31. HFC-134a was measured at relatively high concentrations of 2 to 6 ppmV. A laboratory investigation (Scheutz et al. 2011a) detected significant amount of HCFC-141b and HFC-134a released during lysimeter tests. The concentrations measured in the field (Scheutz et al. 2011b)

were not as high, indicating release of BAs is slower in the field than when under laboratory conditions.

The results from surface emission measurements reported by Schuetz et al. (2011b) are presented in Table 14. Emissions of CFC-11, HCFC-22, and HCFC-31 were detected in Location 1 ranging from 0.002 to 0.006 g/m^2-day. Low surface emissions were likely a product of the oxidation in the upper layers of the landfill and anaerobic degradation occurring at the bottom of the landfill. At the bottom of the landfill, anaerobic degradation of CFC-11 and CFC-12 contributed to higher production of HCFC-21 and HCFC-31, which were accumulated and oxidized in the oxidative zone in the upper layer (Scheutz et al. 2011b). High oxidation rate could be a result of high air-filled porosity of the shredder waste providing sufficient oxygen for aerobic attenuation and oxidation to take place (Scheutz et al. 2011b). The emissions of other F-gases analyzed in this study were below detection level (less than 0.001 g/m^2-day).

Maione et al. (2005) studied the emissions and concentrations of F-gases from two landfills in Italy. The first landfill (Landfill 1) was operated from 1976 to 2000 with an active gas collection system. The second landfill (Landfill 2) was currently in operation with an active gas collection system and had areas with intermediate and active, daily covers. The gas samples were collected using adsorption collection tubes and passive steel canisters, which were analyzed using

gas chromatography. Carbon dioxide was the only gas component measured using static flux chamber.

The measured concentrations of F-gases were several orders of magnitude higher than background concentrations (Maione et al. 2005). High variability was observed in measured F-gas concentrations between the landfills with old and new wastes as well as within the same landfill (Maione et al. 2005). The LFG from older wastes had almost twice the concentration of F-gases as newer wastes for each active collection header sampled (Table 15). In both landfills, CFC-12 was detected in higher quantities than other F-gases measured, indicating that more domestic appliance foams blown with CFC-12 was banked in both landfills (Maione et al. 2005). Newer BAs, such as HFC-134a and HCFC-142b, were measured in relatively high quantities in test areas with newly placed waste suggesting that waste age is an essential factor to surface emissions of BAs (Maione et al. 2005). Surface emission of F-gases were estimated using measured concentrations and carbon dioxide flux by assuming it represents 50% of the total LFG.

Barlaz et al. (2004) quantified CFC emissions from a landfill in the United States while evaluating the effectiveness of a biocover system. The site had an active gas collection system and a final clay cover that was 1 m thick. The waste age was relatively young (3 to 5 years). The waste was actively producing LFG. Surface emissions were measured over a period of one year and experimental design included equivalent number of slopes and flat areas within the landfill. The

variability of CFC emissions was large ranging from -1.2 which may imply that CFC emissions may vary significantly depending on the measurement location and time of the year (Barlaz et al. 2004).

A report by ARCADIS (2012) evaluated LFG concentrations and surface emissions of trace NMOCs present in landfills using measurements from three MSW landfills in the United States. The first landfill site was operated from 1997 to 2006 with an active gas collection system and intermediate soil cover (mixed soil). The second site accepted waste from 2000 to 2010 and had final cover along with a gas collection system installed on the site. The description of the cover installed on site was not included in the report. The third site operated from 1972 to 2006 and had a final cover system (GCL under soil cover) along with an active gas collection system. NMOC measurements were made from the main gas collection header at each site. NMOC fluxes were estimated using the fraction of methane released and not measured directly in the study (ARCADIS 2012).

The range of ODS concentrations was small in comparison to other studies as indicated in Table 10. The concentrations of the measured constituents ranged in the ppbV range possibly indicating dilution of the LFG due to air intrusion (ARCADIS 2012). Seasonal variations in surface emission measurements were observed, where CFC-11 and CFC-113 were higher in concentration in spring, whereas CFC-12 and CFC-114 were higher in concentration in fall than in other

seasons. Fluxes were estimated based on the average concentrations of the trace components measured (ARCADIS 2012).

The Environment Canada studies evaluated the destruction efficiency of LFG combustion systems (microturbine and reciprocating engines) operating at different power outputs (26 KWe and 1 MWe) (Cianciarelli and Bourgeau 2002; Greer and Cianciarelli 2005). Cianciarelli and Bourgeau (2002) determined the destruction efficiencies of selected VOCs including F-gases by measuring the concentration and mass of inlet and outlet of VOCs during the combustion process. Concentrations of CFCs and HCFCs measured at the inlet of each combustion system are provided in Table 10. For reciprocating engine, destruction efficiencies of 94% and 96% were observed for CFC-11, CFC-12, CFC-113, CFC-114, and HCFC-22 (Cianciarelli and Bourgeau 2002). The total ODS destruction efficiency for all of the compounds above was 94% (Cianciarelli and Bourgeau 2002). For microturbine combustion system, total ODS destruction efficiency of 99% was measured (Greer and Cianciarelli 2005).

Emissions data across all studies are summarized and presented in Table 14. Surface emissions of F-gases varied considerably across landfills studied (Table 14). CFC-11 and CFC-12 flux ranged from -7.92×10^{-5} to 7.63×10^{-5} g/m^2-day and from -2.13×10^{-8} to 2.60×10^{-4}, respectively. CFC-113 and CFC-114 flux ranged from -9.98×10^{-9} to 1.98×10^{-5} g/m^2-day and from -0.50×10^{-4} to 3.10×10^{-4}, respectively. For HCFC-141b and HFC-134a, measured surface flux from several

landfills ranged from 3.63×10^{-6} to 1.0×10^{-7} and from -2.40×10^{-8} to 2.05×10^{-4}, respectively.

Limited data are available on emissions of majority of CFCs, HCFCs and HFCs (with an exception of CFC-11 and CFC-12). Variations in emissions of F-gas constituents between studies may be due to meteorological conditions, different operational practices, and geographical location in each study. A degree of uncertainty is present when comparing emission data between studies because the studies did not address all the relevant factors that can affect surface emissions. The investigation presented in this thesis provides results that have not been previously reported. Specifically, the effects of seasonal variations and operational and design practices of landfills on field-measured emissions of 12 different fluorinated and chlorinated hydrocarbons from a landfill environment are presented. In addition, all of the data were collected using the static flux chamber measurement technique.

Table 10 – Concentrations of Trace Components in LFG (in ppmV)

Gas Component	Cianciarelli and Bourgeau 2002 [1]	Bogner et al. 2004, Scheutz et al. 2008 [2]	Bogner et al. 2003; Scheutz et al. 2003a,b	Greer and Cianciarelli 2005 [3]	Maione et al. (2005) [4]	Scheutz et al. (2011a,b) [5]	ARCADIS (2012)
CFC-11	0.1	31 and 596	372	0.3	7.3 to 20.9	0.14 to 0.57	0.02 to 0.03
CFC-12	0.6	114 and 841	1,178	1.5	148 to 231	0.14 to 0.34	0.06 to 0.50
CFC-113	0.02	2	-	0.006	0.2 to 1.55	-	0.003 to 0.010
CFC-114	0.06	-	-	0.11	12.4 to 12.8	-	0.040 to 0.060
HCFC-141b	-	4,354 and 11,625	-	-	-	0.31 to 0.52	-
HCFC-21	-	-	-	-	-	4.1 to 8,7	-
HCFC-22	0.4	340 and 503	236	4.2	135 to 237	0.45 to 0.67	-
HCFC-31	-	-	-	-	-	4 to 10	-
HFC-142b	-	-	-	-	27 to 371	-	-
HFC-134a	-	369 and 626	-	-	200 to 453	1.2 to 3.6	-
HFC-245fa	-	-	-	-	-	-	-

[1] Calculated as the average of 2 concentrations measured at the inlet to the combustion system
[2] This study reported ranges from two landfill cells with different gas collection/combustion systems
[3] Calculated using the inlet VOC mass flow and the average inlet flow of LFG to the combustion system
[4] This study used an average of 3 measurements per landfill and reported as a range for two different landfill sites
[5] This study provided a range based on an average 14 samples over a one-year period at a landfill receiving shredder residue waste only
[6] This study reported ranges of values based on an average of three landfill sites for fall and spring seasons
-: Omitted in the study

Table 11 – Trace Gas Concentration and Surface Emission from Grand'Landes Landfill at Different Areas (Bogner et al. 2004; Scheutz et al. 2008)

Gas Constituents	Cell A Header	Cell B Header	Cell A Surface Emissions (g/m^2-day)						Cell B Surface Emissions (g/m^2-day)	Control Surface Emissions (g/m^2-day)
	LFG Conc. (ppmV)	LFG Conc. (ppmV)	Area 1	Area 2	Area 3	Area 4 (Hotspot)	Area 5 (Hotspot)	Area 6 (Hotspot)	Area 1	Area 1
CH_4	$3.70x10^5$	$2.90x10^5$	0	$-1.11x10^{-3}$	$1.00x10^{-4}$	29.03	24.04	1.45	$-2.0x10^{-3}$	4.78
CFC-11	596	317	$3.73x10^{-5}$	$1.33x10^{-6}$	$7.86x10^{-7}$	$4.36x10^{-7}$	$7.94x10^{-8}$	$4.11x10^{-7}$	$6.54x10^{-7}$	$2.66x10^{-6}$
CFC-12	114	841	$-2.27x10^{-7}$	$5.39x10^{-7}$	$6.02x10^{-7}$	$-2.13x10^{-7}$	$-1.11x10^{-6}$	$1.21x10^{-7}$	$-2.16x10^{-7}$	$-1.56x10^{-7}$
CFC-113	2	2	$-4.74x10^{-8}$	$1.01x10^{-7}$	$-7.81x10^{-8}$	$4.26x10^{-8}$	$-9.98x10^{-9}$	$2.19x10^{-8}$	$-2.06x10^{-8}$	$4.16x10^{-8}$
HCFC-141b	4,354	11,625	$4.75x10^{-6}$	$6.66x10^{-5}$	$7.98x10^{-6}$	$1.01x10^{-5}$	$1.02x10^{-5}$	$3.63x10^{-6}$	$4.38x10^{-6}$	$3.23x10^{-5}$
HCFC-22	503	340	$-6.10x10^{-8}$	$1.85x10^{-7}$	$-2.39x10^{-8}$	$4.64x10^{-6}$	$9.07x10^{-6}$	$-3.14x10^{-8}$	$-1.54x10^{-7}$	$-5.20x10^{-8}$
HFC-134a	626	369	$2.40x10^{-8}$	$2.75x10^{-7}$	$4.14x10^{-7}$	$5.41x10^{-6}$	$5.49x10^{-6}$	$-2.50x10^{-7}$	$-2.59x10^{-6}$	$1.75x10^{-8}$

Table 12 – Concentrations of LFG Components and Surface Emissions at Lapouyade Landfill in Different Areas (Scheutz et al. 2003b, 2003c; Bogner et al. 2003)

Gas Constituents	LFG Concentration (ppbV)	Final Cover Surface Emissions (g/m^2-day)				Intermediate Cover Surface Emissions (g/m^2-day)	Control Surface Emissions (g/m^2-day)
		Area 1	Area 2	Area 3	Area 4	Area 1	Area 1
CFC-11	372	-7.92×10^{-5}	5.18×10^{-6}	2.24×10^{-6}	7.63×10^{-5}	2.08×10^{-5}	5.21×10^{-7}
CFC-12	1,177	-1.68×10^{-5}	2.17×10^{-6}	1.84×10^{-7}	1.04×10^{-5}	2.56×10^{-5}	-7.86×10^{-8}
HCFC-22	236	-4.89×10^{-6}	5.03×10^{-7}	-4.06×10^{-6}	2.26×10^{-5}	5.74×10^{-5}	-7.86×10^{-8}
Methane	4.85×10^{5}	8.4×10^{-3}	-9.5×10^{-3}	-1.04×10^{-3}	10	49.9	-3.3×10^{-3}
Carbon Dioxide	3.37×10^{5}	8.0	13.1	15.6	77.3	107.4	19.3

Table 13 – Average Concentrations of Selected Landfill Gas Components in Waste Cells Receiving Shredder Waste (Scheutz et al. 2011b)

Landfill Gas Constituent	Corrected Measured Gas Concentration (% v/v)	Corrected Measured Gas Concentration ($\mu g/L^{-1}$)	Corrected Measured Gas Concentration (ppmV)
Methane	49.8 to 52.2	-	-
Carbon Dioxide	-0.3 to 0.3	-	-
Oxygen	1.8 to 2.2	-	-
Nitrogen	6 to 8	-	-
CFC-11	-	2 to 5	0.36 to 0.89
CFC-12	-	1.1 to 2.9	0.22 to 0.59
HCFC-141b	-	3.2 to 4.8	0.61 to 1
HCFC-21	-	28.5 to 61.5	6.8 to 14.6
HCFC-22	-	2.4 to 3.6	0.68 to 1
HCFC-31	-	20.3 to 45.7	7.3 to 16.3
HFC-134a	-	8.2 to 25.8	1.97 to 6.2
HFC-32	-	-0.2 to 0.2	-0.09 to 0.09
HFC-41	-	1.5 to 2.5	1.1 to 1.8

- : The constituent was below detection limit

Table 14 – Surface Emissions of Trace Components

	Reference / Gas Component	Bogner et al. 2004, Scheutz et al. 2007a [a]	Scheutz et al. 2003b, 2003c [b]	Barlaz et al. 2004	Maione et al. 2005 [c]	Scheutz et al. 2011a,b [d]	ARCADIS [e]
Surface Flux (g/m^2-day)	CFC-11	$7.94x10^{-8}$ to $3.72x10^{-8}$	$-7.92x10^{-5}$ to $7.63x10^{-5}$	$-8.8x10^{-5}$ to $4.2x10^{-5}$	$6.85x10^{-6}$ to $3.24x10^{-5}$	$2.0x10^{-3}$	$1.97x10^{-7}$ to $1.20x10^{-6}$
	CFC-12	$-2.13x10^{-8}$ to $6.02x10^{-7}$	$-1.68x10^{-5}$ to $2.56x10^{-5}$	$-1.2x10^{-4}$ to $2.6x10^{-4}$	$3.72x10^{-5}$ to $1.01x10^{-4}$	-	$9.84x10^{-6}$ to $2.95x10^{-5}$
	CFC-113	$-9.98x10^{-9}$ to $1.01x10^{-7}$	-	-	$1.28x10^{-7}$ to $1.66x10^{-5}$	-	$9.84x10^{-6}$ to $1.98x10^{-5}$
	CFC-114	-	-	$-0.5x10^{-4}$ to $3.1x10^{-4}$	$5.14x10^{-6}$ to $6.85x10^{-5}$	-	$1.28x10^{-6}$ to $1.78x10^{-4}$
	HCFC-141b	$3.63x10^{-6}$ to $1.01x10^{-7}$	-	-	-	-	-
	HCFC-21	-	-	-	-	-	-
	HCFC-22	$-6.10x10^{-8}$ to $9.07x10^{-6}$	$-4.89x10^{-6}$ to $5.74x10^{-5}$	-	$2.87x10^{-5}$ to $9.37x10^{-5}$	$5.0x10^{-3}$	-
	HCFC-31	-	-	-	-	$6.0x10^{-3}$	-
	HFC-142b	-	-	-	$6.58x10^{-6}$ to $1.46x10^{-4}$	-	-
	HFC-134a	$-2.40x10^{-8}$ to $5.49x10^{-6}$	-	-	$1.71x10^{-6}$ to $2.05x10^{-4}$	-	-
	HFC-245fa	-	-	-	-	-	-

[a] This study reported ranges from two landfill cells with different landfill gas collection and combustion system.
[b] The range provided encompasses both the final cover and intermediate cover areas.
[c] Data were obtained from 16 landfill sites located in both the U.S. and U.K.
[d] The study provided maximum emissions at a landfill receiving shredder residue waste only.
[e] The surface flux was calculated using the given total surface emissions and area of the landfill or cell.

Chapter 3: Testing Program and Analytical Methods

3.1 Introduction

A field investigation coupled with laboratory analysis was conducted to assess emissions of chlorinated and fluorinated hydrocarbons (i.e., F-gases) from a landfill in California. A total of 12 F-gases were investigated. In addition, emissions of methane and carbon dioxide were measured. The test program was conducted at Potrero Hills Landfill (PHL) in Suisun City, California, United States. Static flux chamber tests were conducted to measure the surface flux of the target F-gases. The tests were conducted at 7 different locations to take account of different waste ages and cover types present at the landfill. In addition, samples from each location were collected for laboratory analysis to establish characteristics of the cover materials. Samples from the inlet and outlet of the gas combustion system were also collected in order to calculate destruction efficiency of the F-gases.

The gas samples obtained from the flux chamber testing were analyzed at the Rowland-Blake Laboratory at the University of California - Irvine. The gas concentration data were then used to calculate the surface flux and the destruction efficiency of the high-temperature flare system for the 12 F-gas constituents. Details of the test program and methodology for data analysis are presented in this chapter.

3.2 Field Test Program

The field investigation was conducted to determine the surface emissions from landfill covers and the destruction efficiency of the LFG collection and combustion system for F-gases. To determine surface flux, static flux chamber tests were conducted at multiple locations throughout the site to take account of different waste ages and cover types present on site. The locations tested had daily, intermediate, and final covers. The covers were constructed using a wide range of materials including various soils, auto fluff, green waste, and geosynthetics. The static flux chamber tests were conducted twice at each location over the course of a 6-month period to capture the effect of seasonal variations. Cover samples, subsurface gas samples, and cover temperature data were also obtained at each testing location to supplement interpretation of surface flux data.

Additional gas samples were obtained from a LFG collection and control system to determine the destruction efficiency of the F-gases at the site. Vertical gas extraction wells and a high-temperature flare system are installed on site in accordance with CCR 95463. The LFG collected throughout the perimeter of the landfill is combusted by the flare system to oxidize the combustible components such as methane and VOCs to carbon dioxide and water. Raw LFG samples were obtained from a sampling port located 10 m from the inlet of the open flare system. Post-combustion gas samples were obtained from a sampling port located near the outlet of the flare system.

3.2.1 Test Site

PHL is located in Suisun City, California which is located approximately 60 km northeast of San Francisco, CA and 60 km southwest of Sacramento, CA (Figure 17). The landfill is located in a temperate climate zone that has hot and dry summer (Peel et al. 2007). The site has an average daily high temperature, average daily low temperature, and an average daily temperature of 23.6, 9.2, and 16.4°C, respectively, during 2013 and 2014 (Wunderground 2015). The landfill had an average daily precipitation of 1.0 and 1.54 mm for 2013 and 2014, respectively (Wunderground 2015).

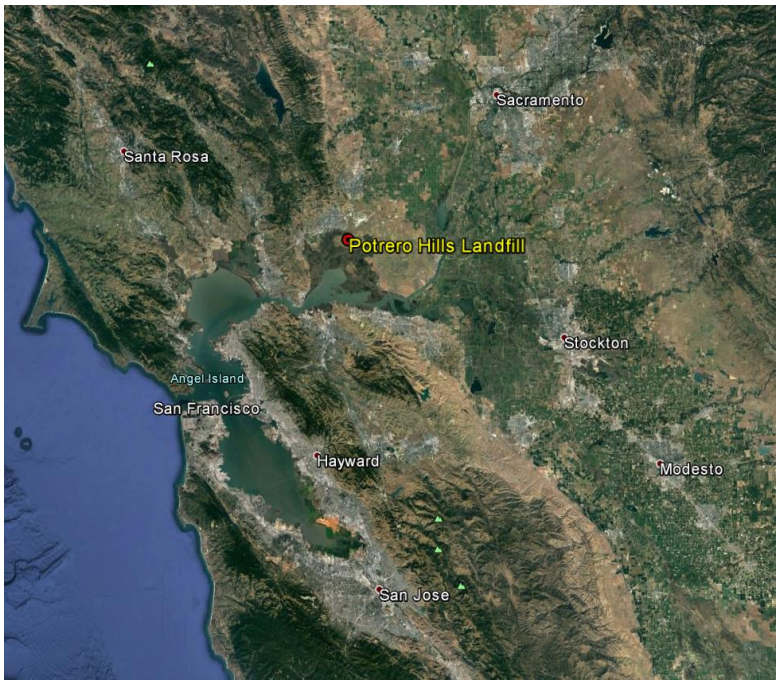

Figure 17 - Location of PHL (Google Earth 2015)

PHL has been in operation since 1987 and is classified as a Class III disposal facility. The site is permitted to accept nonhazardous solid wastes in accordance with waste classification regulations in 27 CCR, Sections 20220 and

20230 (Marshack 2012). PHL accepts residential, commercial, C&D, industrial, and agricultural wastes as part of the MSW operations. The landfill also accepts materials that follow special waste handling procedures, which include ash, sewage sludge, contaminated soils, tires, appliances, and electronic wastes.

The site consists of 210 ha total area and the current permitted disposal area is 140 ha. The facility has design capacity of 63 million m^3 (83 million yd^3) with maximum elevation limit of 105 m and maximum depth limit of 39 m. As of April 2014, the remaining air space available for disposal was 26 million m^3 (34 million yd^3) (Cal Recycle 2014). The estimated closure date for the facility is 2045. The maximum permitted throughput is 3,900 tonnes per day. The site has an average daily tonnage of 3,080 tonnes per day. In 2013, the PHL received approximately 920,000 tonnes of waste and the details regarding the type of materials received are provided in Table 15.

Table 15 – PHL Tonnage Report for 2013 by Materials

Material Category	Material	Waste Received (Tonnes)	% by Material Category	% Total
Disposal	C&D Waste	41,227	9	5
	Soil	22,771	5	2
	Sewage Sludge	16	0	0
	Auto Fluff	0	0	0
	Green Waste	5,170	1	1
	MSW	364,575	83	40
	Miscellaneous	4,750	1	1
	Total - (Disposal Only)	438,509	100	48
Cover	C&D Waste	107,030	22	12
	Soil	253,817	53	28
	Sewage Sludge	58,901	12	6
	Auto Fluff	43,974	9	5
	Green Waste	13,379	3	1
	Total - (Cover Only)	477,101	100	52
	Total Waste Received	915,610		100

3.2.2 Static Flux Chamber Testing

Experimental Design - A total of seven different testing locations with varying waste ages and cover types were selected for the field testing program. The cover types selected for the static flux chamber tests included three daily cover locations with green waste (GW), auto fluff (AF), and extended daily (ED) covers in Cell 12; three intermediate cover locations in Cell 1 (IC-1), Cell 10 (IC-10) and Cell 15 (IC-15); and one final cover location in Cell 1 (FC). The test locations selected had relatively flat areas in order to ensure proper installation of the static flux chambers. A detailed description of each cell where the tests were conducted is provided in Table 16. Waste age distribution of the underlying waste at each testing location is presented in Table 17. The tests for wet season were

conducted in February, March, and April, 2014, whereas the tests for dry season were completed in August, 2014. The relative locations of the cells where test were conducted are indicated in Figure 18. In addition, the specific date and weather conditions during the field test program are provided in Table 18.

Table 16 – Description of the Testing Cells at PHL

Cell Number	Area in Hectares and (Acre)	Waste Height (m)	Range of Waste Age (year)	Average Waste Age (year) [e]	Description
1	1.9 (4.6)	17.7[a] / 18.1[b]	17 to 29	22.0	• Constructed prior to implementation of Subtitle D. • Low permeability soil liner and leachate and collection system. • Cell completed on September 1985 and was last filled in 1997.
10	3.6 (8.8)	16.5	3 to 19	13.6	• Constructed after implementation of Subtitle D • Cell completed on July 1995 and was last filled in 2006. • Cell 10 is lined with a compacted clay liner and has a gas collection system.
12-North	2.4 (6.0)	49.4[c] / 53.7[d]	0 to 15[c] / 0 to 16[d]	9.5 [c] / 7.9 [d]	• Constructed after implementation of Subtitle D • Cell completed on October 1998 and is currently active. • Cell 12 is lined with a compacted clay liner and has a gas collection system.
15	4.5 (11.3)	32.9	3 to 10	7.2	• Constructed after implementation of Subtitle D • Cell completed on January 2005 and was last filled in 2011. • Cell 15 is lined with a compacted clay liner and has a gas collection system.

a - The waste height and age for the intermediate cover location in Cell 1.
b - The waste height and age for the final cover location in Cell 1.
c - The waste height and age where GW cover was tested during wet season in Cell 12.
d - The waste height and waste age where AF and ED covers were tested during wet season and AF, GW, and ED during dry season.
e - The waste age at each location was estimated using historic topographic survey files provided by PHL

Table 17 – Age Distribution of the Waste at the Test Locations

Locations	Waste Age (years)	Waste Height (m)	%	Total Waste Height (m)
AF	0 to 3.5	14.6	27.3	53.7
	6 to 15	39.0	72.7	
	16.4 to 21.5	0.0	0.0	
GW (Wet Season)	0 to 3.5	11.3	22.8	49.4
	6 to 15	29.6	59.9	
	16.4 to 21.5	8.5	17.3	
GW (Dry Season)	0 to 3.5	14.6	27.3	53.7
	6 to 15	39.0	72.7	
	16.4 to 21.5	0.0	0.0	
ED	0 to 3.5	14.6	27.3	53.7
	6 to 15	39.0	72.7	
	16.4 to 21.5	0.0	0.0	
IC-1	0 to 3.5	0.0	0.0	17.7
	6 to 15	0.0	0.0	
	16.4 to 21.5	17.7	100.0	
IC-10	0 to 3.5	0.9	5.6	16.5
	6 to 15	5.5	33.3	
	16.4 to 21.5	10.1	61.1	
IC-15	0 to 3.5	2.4	7.4	32.9
	6 to 15	30.5	92.6	
	16.4 to 21.5	0.0	0.0	
FC	0 to 3.5	0.0	0.0	18.1
	6 to 15	0.0	0.0	
	16.4 to 21.5	18.1	100.0	

Figure 18 – Site Plan of PHL (Google Earth 2015)

Table 18 - PHL Field Test Dates and Weather Conditions during Testing (Wunderground 2015)

Date	Season	Cover Type Tested	Barometric Pressure (hPa)	Min/Max Temperatures (℃)	Average Temperature (℃)	Precipitation (mm)	Total Precipitation within Previous 7 days (mm)	Average Wind Speed (kph) and Direction
February 7th, 2014	Wet	GW	1017	7.8 / 11.7	10.0	19.3	37.6	19.3 (SE)
March 28th, 2014	Wet	IC-10, IC-15	1020	10.0 / 16.7	13.3	0	19.3	14.5 (SW)
March 29th, 2014	Wet	IC-1	1017	9.4 / 14.4	13.3	11.7	31.0	16.1 (SSW)
March 30th, 2014	Wet	FC	1019	6.1 / 16.7	11.1	0	31.0	17.7 (SW)
April 18th, 2014	Wet	AF,ED	1012	10.6 / 23.3	16.7	0	0	19.3 (SW)
Aug 8th, 2014	Dry	AF, GW, ED	1012	14.4 / 32.2	22.8	0	0.25	32.2 (SW)
Aug 9th, 2014	Dry	IC-10, IC-15	1012	13.9 / 26.7	20.6	0	0.25	38.6 (SW)
Aug 10th, 2014	Dry	IC-1, FC	1013	13.9 / 27.8	20.6	0	0.25	35.4 (WSW)

Two different sampling intervals were used during the field investigation as presented in Tables 19 and 20. Sampling intervals outlined in Table 19 were used for the first two field visits (February and March, 2014). Based on the concentration data from February and March, the sampling intervals were modified to the sampling intervals presented in Table 20 for the remainder of the field test program. The modification yielded two additional flux values, since the data from Chamber C and D were previously constrained to two point curves. At each test location, a total of 20 gas samples were taken from the static flux chamber (including the subsurface samples), consisting of 16 static flux chamber gas samples and 4 subsurface gas samples. A total of 280 gas samples were taken over the 6-month period of the field investigation.

Table 19 – Time at which Samples Were Taken for Chamber A, B, C, and D during Wet Season (Exception of AF and ED covers)

	Elapsed Time (min)							
Chamber A	0	7	15	30	60	-	120	-
Chamber B	0	-	-	30	60	90	120	150
Chamber C	0	-	-	-	60	-	-	-
Chamber D	0	-	-	-	-	-	120	-

- : No sample was taken at this time.

Table 20 – Time at which Samples Were Taken for Chamber A, B, C, and D during Dry Season and AF and ED during Wet Season

	Elapsed Time (min)						
Chamber A	0	7	15	30	60	-	-
Chamber B	0	-	-	30	60	90	120
Chamber C	0	-	-	30	60	-	-
Chamber D	0	-	-	-	60	-	120

- : No sample was taken at this time.

Static Flux Chamber Specifications and Testing Protocols - The static flux chamber consisted of a 1 m^2 square stainless steel collar and a lid. The lid was the top section of the chamber that included a fan, temperature probe (Omega TJ36-CPSS-18G-12) and a pressure probe (Omega PX 654-2.5BD5V). The collar was the bottom section of the chamber that was embedded into the landfill cover. The lid and collar interface was sealed using the four clasps on the collar. The ability of the fan to completely mix the chamber contents of 1 m^2 stainless steel static flux chamber in less than 30 seconds was verified in Barlaz et al. (2004).

For the deployment of the flux chamber, the collar was embedded into the landfill cover to an approximate depth of 0.05 m by applying force to the edge of the collar perimeter using lumber sections and a sledgehammer (Figure 19a). Subsequently, bentonite and water was applied to the perimeter of the chamber to seal the soil-chamber interface to prevent any leakage during the test (Figure 19b). A generator that was used to power the chamber was placed 30 m downwind from the chambers. The lid of the chamber was rotated prior to placement in order to prevent any gas accumulation in the chamber prior to the zero-minute sample. As soon as the lid was placed and clipped into place with clasps, a zero-minute sample was taken. A stopwatch was used to measure the sampling intervals. Additional gas samples were taken at time intervals indicated in Tables 19 and 20.

a) Embedment Process of the the Collar

b) Remaining Bentonite Seal after the Collar Removal

Figure 19 – Photographs of Static Flux Chamber Placement Procedure

The samples were taken using an evacuated 2-L stainless steel canister equipped with a bellow valve as presented in Figure 20a. The sampling port was located at the top surface of the lid which was composed of ball valve, stainless steel tube, and Ultra-Torr vacuum fitting as presented in Figure 20b. For the sampling of the gas, an evacuated 2-L stainless steel canister was attached to the Swagelok sampling port. The valves were opened in following order: the ball valve then the bellow valve. The valves were left open for approximately 10 seconds until the canister was full. The valves were then closed in the reverse order they were opened. The valves were opened and closed in the aforementioned manner to minimize contamination of the gas sample. The canister was then removed from the Swagelok sampling port and was stored in a weather-proof box. Tests were conducted with four collars in place while the two lids were transferred to different collars at each test location.

a) Gas being Sampled using 2-L Canister

b) Swagelok Gas Sampling Port

Figure 20 – Photographs of the Flux Chamber Gas Sampling Process

After the last scheduled sample was retrieved from a given chamber, the lid was removed. Then, a 6 mm outer-diameter stainless steel tube of approximate length of 30 cm was embedded to an approximate depth of 10 cm within the perimeter of the chamber in preparation for obtaining a subsurface gas sample. The tube was secured using a vice-grip and a rubber sheath and then the assembly was lightly tamped into the ground using a hammer. The perimeter of the soil-stainless steel tube interface was sealed using moist bentonite to prevent leakage. A single subsurface sample was taken from each chamber (total of 4 at each location). The collar heights were also measured at midpoint of each side to calculate the chamber volume. In addition, the temperature of the landfill cover was measured at three different points within perimeter of the chamber using a handheld digital thermometer (Omega HH-25) and a rigid thermocouple probe that was inserted into the cover material. In addition, sand cone tests in accordance

with ASTM D1556 were performed at each location (Figure 21). Lastly, cover samples were obtained from each chamber for laboratory analysis with the mass of samples ranging from 100 to 2000 g depending on the cover material.

Figure 21 – Photograph of Sand Cone Test being Conducted within the Tested Chamber Perimeter

The cover thickness was determined at each cover location using a shovel, power auger, and measurement tape. The shovel and power auger were used to reach the waste layer below the cover material. Multiple passes with the power auger were typically necessary to reach the waste layer and to remove the accumulated soils from the auger after each pass. When the waste layer was reached, the measurement tape was used to determine the cover thickness at the cover location. The degrees of compaction of the cover materials also were evaluated visually and physically using a hand trowel.

3.2.3 Landfill Gas Collection and Combustion System Sampling

PHL has a LFG collection and combustion system installed on the site in accordance with 17 CCR, Sections 95463, 95464, and 95465. LFG generated from the waste mass is collected by vertical LFG extraction wells installed throughout the site. The LFG collected is then transported to a high-temperature flare system where the gas is combusted. The flare system operates at a temperature of approximately 1700°F and combusts LFG with methane content ranging from 42 to 57% (% v/v) throughout the year. The flare system had a height and diameter of 12 and 3 m, respectively.

Post-combustion (i.e., outflow) and raw gas (i.e., inflow) samples were taken from the flare system to determine the destruction efficiency of the F-gases. The post-combustion gas samples were taken from a sampling port located at a height of 10.5 m (1.5-m downstream from the exit). The sampling port was accessed using a boom lift as presented in Figure 22. The gas was sampled from a point 0.65 m radially inward from the outer wall using 1.5 mm inner-diameter stainless steel tubing. The tubing was coiled then run through an ice bath to decrease the volume of the gas. The tubing coiled through the ice bath is presented in Figure 23a.

The stainless steel tube exiting the ice bath was connected to a 30-cm stainless tube with a Ultra-Torr Tee Tube. A 2-L stainless steel canister was attached to one end while the other end was connected to the 30-cm stainless

steel tube with a flexible polyvinyl chloride (PVC) pipe extension and a 60-mL syringe. The fully assembled sampling connection is presented in Figure 23b. The syringe was used to remove any ambient air present in the stainless steel coil prior to the sampling. Two full draws of 60-mL syringe were applied to the coil prior to beginning of sampling. After all the connections on the Ultra-Torr Tee Tube were secured, the bellow valve on the canister was left opened for 20 to 30 seconds until the canister was full. The valve on the canister was then closed and the canister was removed from the Ultra-Torr Tee Tube connection. A total of three post-combustion gas samples were taken.

Figure 22 – Photograph of the Flare System and Boom Lift at PHL

a) Stainless Steel Coil with Ice Bath

b) Tee Tube Sampling Connection

Figure 23 – Photographs of the Sampling Process of the Post-Combustion Gas from the Open Flare System

Raw LFG samples were taken from a flare header that was located 10 m from the inlet of the flare system. An Ultra-Torr Tee Tube with a 30-cm stainless steel tube and a PVC extension were used to connect the stainless steel canister to the sampling port as presented in Figure 24. The sampling port attached to the header consisted of a ball valve and a flexible PVC tube. The PVC extension from the Swagelok Tee Tube was attached to the PVC tube prior to opening of the bellow valve on the stainless steel canister. When all the connections were secured, the ball valve on the sampling port was opened to purge any ambient air present in the sampling connection. Subsequently, the bellow valve on the canister was opened for approximately 10 seconds until the canister was full. A total of six raw LFG samples was taken over the during the entire field investigation.

Figure 24 – Photograph of the Sampling Process of the Raw LFG from the Open Flare System

3.3 Laboratory Investigation

A laboratory investigation was conducted to determine the F-gas concentrations of the gas samples and to characterize the cover materials that were represented in the field investigation. The gas samples were analyzed using VOC analytical systems in the Rowland-Blake Laboratory at the University of California – Irvine (Figure 25). In addition, a number of geotechnical tests were also conducted on the landfill cover samples to determine the moisture content, particle size distribution, and the specific gravity of the cover materials to supplement the interpretation of the surface flux data.

3.3.1 Determination of CFC, HCFC, and HFC Concentrations

The gas samples obtained during the field tests were analyzed (Figure 25) using two identical VOC analytical systems that consisted of 3 Agilent 6890 gas chromatographs containing 2 electron capture detectors, 3 flame ionization

detectors, and a quadrupole mass spectrometer. The two analytical systems are capable of identifying and quantifying hundreds of NMOCS in the parts per million to parts per quadrillion range (Colman et al. 2001; Blake et al. 2003; Zhang et al. 2006; Barletta et al. 2006, 2011).

Figure 25 - Rowland-Blake Laboratory at University of California – Irvine

For the sample analysis, an aliquot of 50 to 1100 cm^3 is cryogenically preconcentrated and injected into the multi-column/detector chromatographic system. The injected sample flow is chromatographically separated in the columns then the sample flow is injected either to electron-capture detectors (sensitive to halocarbons and alkyl nitrates), FIDs (sensitive to hydrocarbons), or quadrupole mass spectrometers (for unambiguous compound identification and selected ion monitoring) (Colman et al. 2001). The output signals from the detectors are transmitted to Dionex software, which converts the output signals into a

chromatogram (Colman et al. 2001). Each resulting chromatogram is individually checked and manually modified by a trained analyst, since slight changes in retention time or peak shape can cause problems for automated quantification (Colman et al. 2001). The details regarding the gas chromatographic parameters, calibration standards, column configurations, and the analytical methods are provided in Colman et al. (2001). The chromatograms are used to calculate concentration for the 12 F-gases, methane, and carbon dioxide.

3.3.2 Determination of Landfill Cover Properties

A number of tests were conducted to determine the baseline characteristics of the landfill cover samples collected during the field investigation. A total of 56 cover samples were collected during the field test, which consisted of daily cover samples (AF, GW, ED), intermediate cover samples (IC-1, IC-10, IC-15), and final cover sample (FC). A single sample was collected from each chamber (Chamber A, B, C, D) from the seven locations for both wet and dry season. The specific gravity and moisture content were determined for all of the cover samples. However, the particle size analysis was only performed for the soil cover samples. The other materials (auto fluff and green waste) were not conducive to grain size distribution analysis. For these cases, observational description was used.

Determination of Specific Gravity - The specific gravity of the landfill cover samples was determined using ASTM Standard D854 – “Standard Test Methods for Specific Gravity of Soil Solids by Water Pycnometer” for the soil specimens and

a modified version of ASTM Standard D854 adapted to auto fluff and green waste specimens.

For the soil specimens, the procedures outlined in ASTM D854 were performed. The pycnometer setup used for the soil sample is presented in Figure 26. For the auto fluff and green waste, a modified procedure of the method outlined in Yesiller et al. (2014) was generally followed. During the addition of the specimen to the 2000-mL Erlyenmeyer Flask, a screen was placed on top of the specimen to ensure full submersion of all of the materials, as presented in Figure 27. The Erlenmeyer flask was calibrated with the screen to ensure proper measurements. In addition, the specimen was placed under vacuum for 3 hours with routine taps to the bottom of the Erlenmeyer flask at 10-minute intervals to ensure deairing of the specimen. After the mixture was fully deaired, the remaining headspace was filled with deaired, deionized water to the calibration line and was placed into a temperature controlled container and allowed to equilibriate for 24 hours. The weight of the volumetric flask and the temperature of the water inside were recorded after reaching equilibrium, which was used to determine the specific gravity using the formulas provided in ASTM D854.

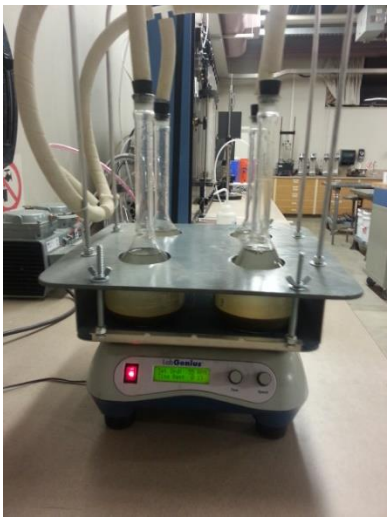

Figure 26 – Four Pycnometers on Shake Table for Specific Gravity Tests

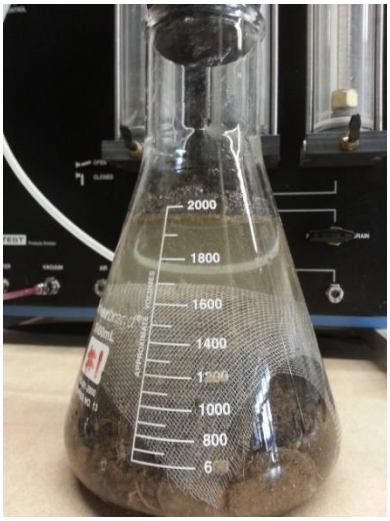

Figure 27 – Specific Gravity Test Setup for AF and GW

Particle Size Analysis - A dry sieve analysis was performed to determine the particle size distribution of the soil specimens using ASTM D422 – “Standard Test Method for Particle-Size Analysis of Soils”. A hydrometer test was also performed to determine the fine grained soil fraction using ASTM D422. The particle size distributions of the soil cover specimens obtained from five test locations (ED, IC-1, IC-10, IC-15, FC-1) were determined and used to identify the soil type of the samples based on the Unified Soil Classification System (USCS).

3.4 Data Analysis Methodology

Data analysis methodology for the static flux chamber and the flare data are described in this section. Data analysis on the concentration dataset obtained from Rowland-Blake Laboratory was performed to determine the surface flux of the F-gases and the destruction efficiency of the LFG control systems. The criteria used to determine surface flux were developed in collaboration with Dr. Jean Bogner (University of Illinois – Chicago), a leading expert in surface emission measurements from landfills.

3.4.1 Determination of Surface Flux of the F-gases

In order to quantify gas emissions from various landfill surfaces, surface flux specific to each location and constituent was determined. The surface flux was determined by converting concentration datasets obtained from the field investigation to surface flux using Equation 2.

$$F = \frac{dC}{dt}\left(\frac{V}{A}\right) \qquad [3]$$

F is the surface flux (expressed in units of mass per area-time), dC/dt is the concentration gradient (the rate of change of concentration over time within the flux chamber), V is the volume of the static flux chamber, and A is the area of the landfill surface covered by the chamber. To determine the concentration gradient, plots of the concentration versus sampling time respective to each location, constituent, and chamber (Chamber A, B, C, D) were constructed. Prior to calculation of the surface flux, a linear regression analysis was performed to evaluate the quality of fit for each concentration versus time dataset.

The fit of each linear regression model was evaluated using coefficient of determination (R^2), which indicates how well the regression models the data (Devore 2008). R^2 acceptance and rejection criterion was developed in collaboration with Dr. Jean Bogner and was used to determine the number of concentration data points were removed to reach a R^2 desired threshold for some of the datasets. If needed point removals were performed from later to earlier points in order to give higher weights on the earlier points to address the decrease in the concentration gradient in the points from later sampling. The chemical accumulation that occurs after extended run time of the chamber can cause a decrease in the concentration gradient.

The maximum number of points that can be removed for datasets with 6 and 5 concentration points was established as 3 and 2 points, respectively, as linear regression loses its statistical significance for fewer than 3 data points. The

point removal methodology for an example 6-point dataset is presented in Figure 28. If the R^2 is greater than the threshold, the dataset is accepted for surface flux calculation. An example of an accepted dataset is presented in Figure 29. If the R^2 is less than the threshold throughout the entire point removal process, the dataset is rejected and surface flux is not calculated.

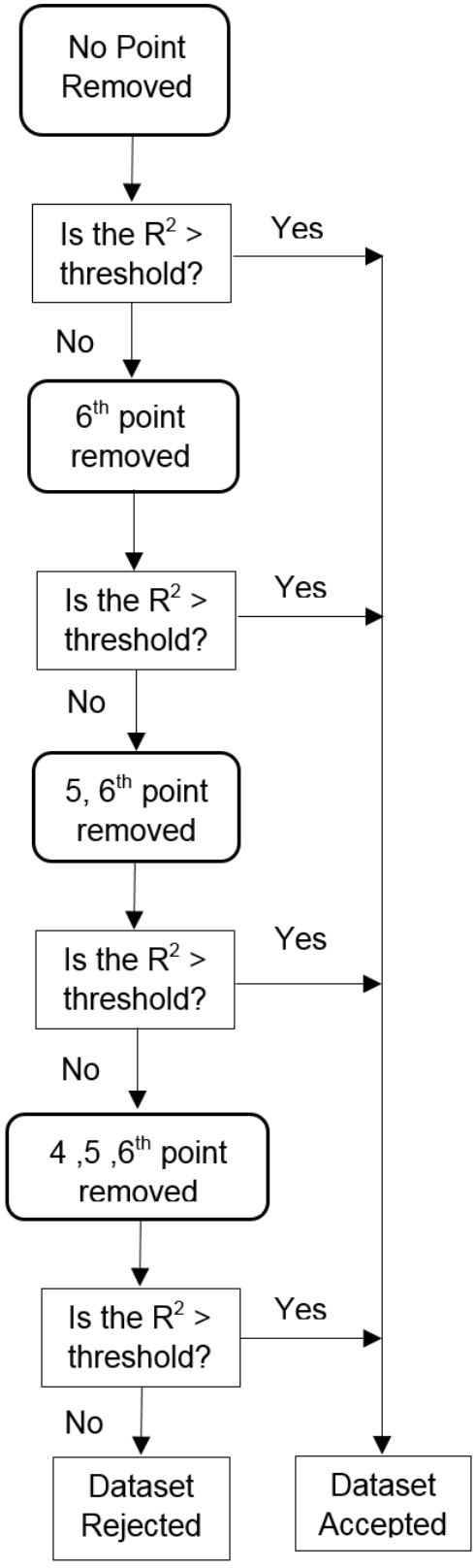

Figure 28 – Point Removal Scheme for Dataset with 6 Points

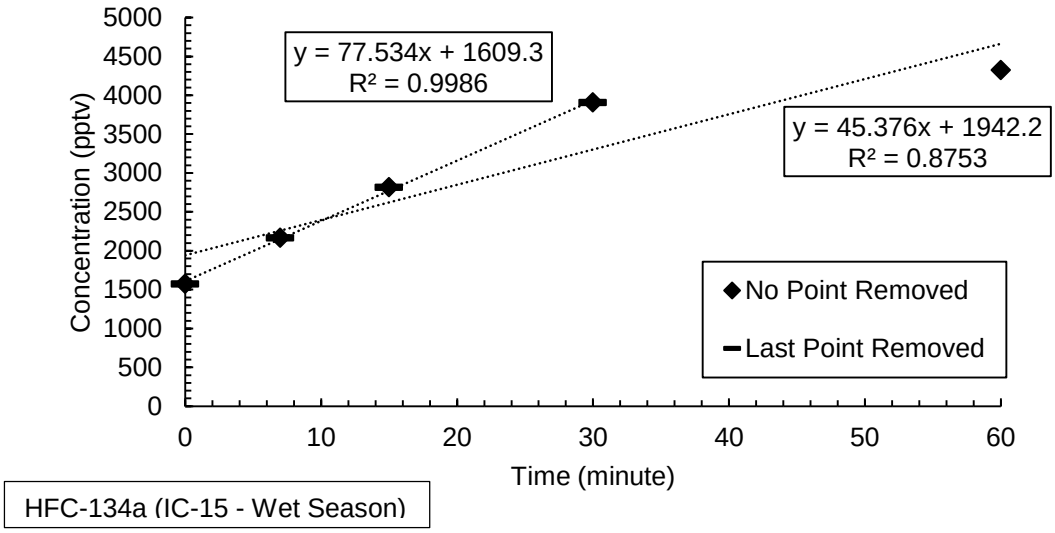

Figure 29 – Example of the Linear Regression Process

The point removal process was automated using a macro in Excel for the 12 F-gases, methane, and carbon dioxide. In order to determine appropriate R^2 threshold, the point removal process was repeated with varying R^2 threshold values ranging from 0.90 to 0.65 in 0.05 increments. Subsequently, the percentages of accepted datasets respective to number of points removed were calculated at each R^2 threshold. After analyzing the results at various R^2 values, R^2 of 0.9 was selected as the acceptance threshold. At R^2 of 0.9, a balance between having sufficient number of data points and obtaining statistically valid datasets was achieved. The distribution of the percentage accepted respective to number of points removed for wet and dry seasons at varying R^2 threhold is presented in Appendix B.

The accepted datasets were used to determine the concentration gradients. Since the concentration gradients were in units of parts-per-volume notation, the

concentration gradients were converted to mass basis using the Ideal Gas Law (Equation 4) where:

$$\left(\frac{dC_{mass}}{dt}\right) = \frac{\left(\frac{dC_{pptv}}{dt}\right) P\,MW}{R\,T} \quad [4]$$

C_{mass} is mass concentration (g/L), C_{pptv} is volumetric concentration (pptv), P is pressure (atm), MW is the molecular weight of the constituent (g/mole), R is the ideal gas constant (0.8206 L-atm / mole-K), and T (K) is the soil cover temperature. With all the necessary parameters determined, the surface flux was calculated for each location, constituent, and chamber.

3.4.2 Determination of Destruction Efficiencies of the F-gases

Destruction efficiencies of the 12 F-gases in the open flare system were determined using the raw and post-combustion concentration data collected during the field investigation. Since outlet concentration was diluted from addition of air during the combustion process, dilution factor was determined to calculate the concentrations of the post-combustion gas prior to dilution using Equation 5. In this equation methane, carbon dioxide, and carbon monoxide have concentrations in units of parts-per notation. The numerator is the sum of the concentrations of methane, carbon dioxide, and carbon monoxide from the inlet of the flare while the denominator is the sum of the concentrations of methane, carbon dioxide, and carbon monoxide from the outlet of the flare. Use of the equation assumes that the carbon in the LFG primarily consisted of methane, carbon dioxide, and carbon monoxide. The correction on the outlet concentration is necessary since the flare

is mixed with ambient air during the combustion process. By conducting mass balance over carbon with methane, carbon dioxide, and carbon monoxide, the dilution factor can be determined, since air only adds oxygen and nitrogen to the combustion process.

$$\text{Dilution Factor} = \frac{(C_{CH4} + C_{CO2} + C_{CO})_{in}}{(C_{CH4} + C_{CO2} + C_{CO})_{out}} \quad [5]$$

Using the dilution factor, corrected post-combustion concentration (i.e. concentration level without air dilution prior to dilution) can be determined using Equation 6.

$$(C_{out})_{Corrected} = C_{out}\ (\text{Dilution Factor}) \quad [6]$$

With the corrected post-combustion gas concentration, the destruction efficiencies of the flare system for the 12 F-gases were determined using Equation 7:

$$\text{Destruction Efficiency (\%)} = \frac{C_{in} - (C_{out})_{Corrected}}{C_{in}} \times 100\% \quad [7]$$

where C is chemical concentration of a chemical constituent expressed in parts-per notation. This calculation was made for 12 F-gases, methane, and carbon dioxide.

Chapter 4: Results and Discussion

4.1 Summary

Results and discussion from the field and laboratory investigations are presented in this chapter. First, the results from the field and laboratory analysis of the various landfill covers are summarized. The results from specific gravity, moisture content, particle size distribution, and sand cone tests are presented. Full depth profiles of the subsurface waste and the cover systems are also presented in this section. Second, the surface flux data of the twelve F-gases, methane, and carbon dioxide obtained from the static flux chamber tests are summarized. The surface flux data respective to the seven locations and two seasons (summer and dry season) are presented in detail. Lastly, the F-gas destruction efficiency analysis for the high-temperature flare system is presented.

4.2 Landfill Cover Properties

Geotechnical properties including specific gravity, moisture content, particle size distribution, and density were determined for the cover materials to aid the interpretation of the surface flux data through laboratory and field investigation. The geotechnical properties of the cover materials for the seven locations are presented in Tables 21 - 23. In addition, details regarding the cover material types and ages of underlying wastes at the test locations are presented in Figure 30 and 31, respectively.

The daily covers (AF, GW, and ED) had cover thicknesses ranging from 26 to 45 cm (Table 21). The intermediate covers (IC-1, IC-10, and IC-15) had cover thicknesses ranging from 80 to 82 cm whereas the final cover location (FC) had cover thickness of greater than 120 cm. The cover thicknesses for the seven locations are summarized in Table 21.

The soil samples obtained at the five soil cover locations (ED, IC-1, IC-10, IC-15, FC) had varying soil classification and soil composition (Table 22 and 23). The soil samples were classified using the USCS. The classification and composition of the soils for the seven locations are summarized in Table 21 and 23.

The geotechnical properties of the cover materials varied highly between the non-soil and soil cover materials. The specific gravity values of auto fluff and green waste were 1.48 and 1.42, respectively. The specific gravity values of the soil covers ranged from 2.62 to 2.77. The dry density values of the cover materials ranged from 266 to 1893 kg/m^3 for the seven locations. A sand cone test was not conducted at the green waste cover location in the wet season due to heavy precipitation. The dry density values of the auto fluff and green waste covers were significantly lower than the soil covers and ranged from 266 to 519 kg/m^3. The specific gravity and density values of the cover materials are summarized in Table 22.

The porosity of the soil samples varied over a wide range depending on the composition of the material. The porosities of the soil samples ranged from 0.29 to 0.65 for the five soil cover locations. The porosity generally increased as the fine soil fraction increased for the soil covers. The porosities of the auto fluff were 0.65 and 0.69 for the wet and dry season, respectively. The porosity of the green waste material was not determined for the wet season and was 0.81 for the dry season. The porosity and void ratio values are summarized in Table 22.

The moisture contents of the cover materials were significantly higher for the wet season with an average of 34% in comparison to an average value of 6% for the dry season. The degrees of saturation were also significantly higher with an average of 35% for the wet season in comparison to the average of 14% for the dry season. Higher moisture content was expected based on observed weather conditions during the field investigation. The moisture contents and degrees of saturation for the seven test locations are summarized in Table 22.

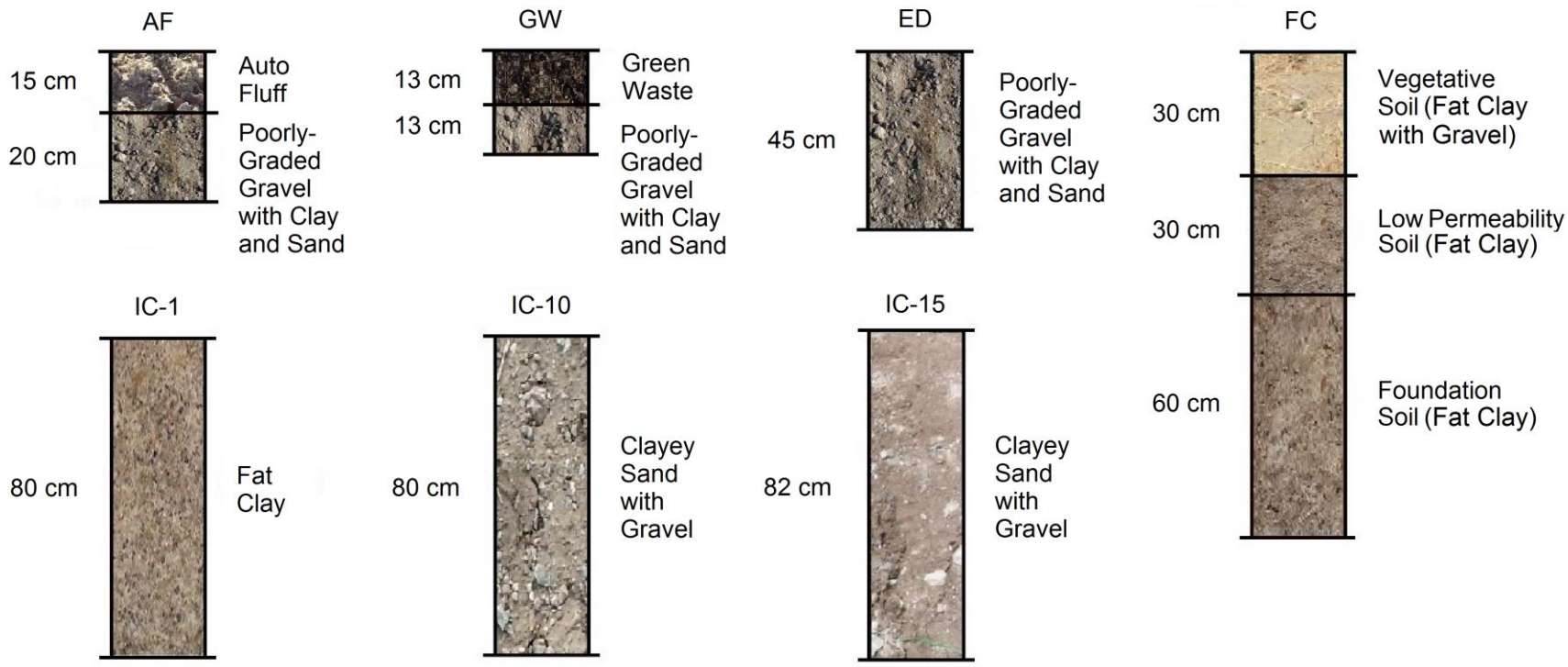

Figure 30 – Vertical Profiles of the Cover Systems for the Seven Test Locations

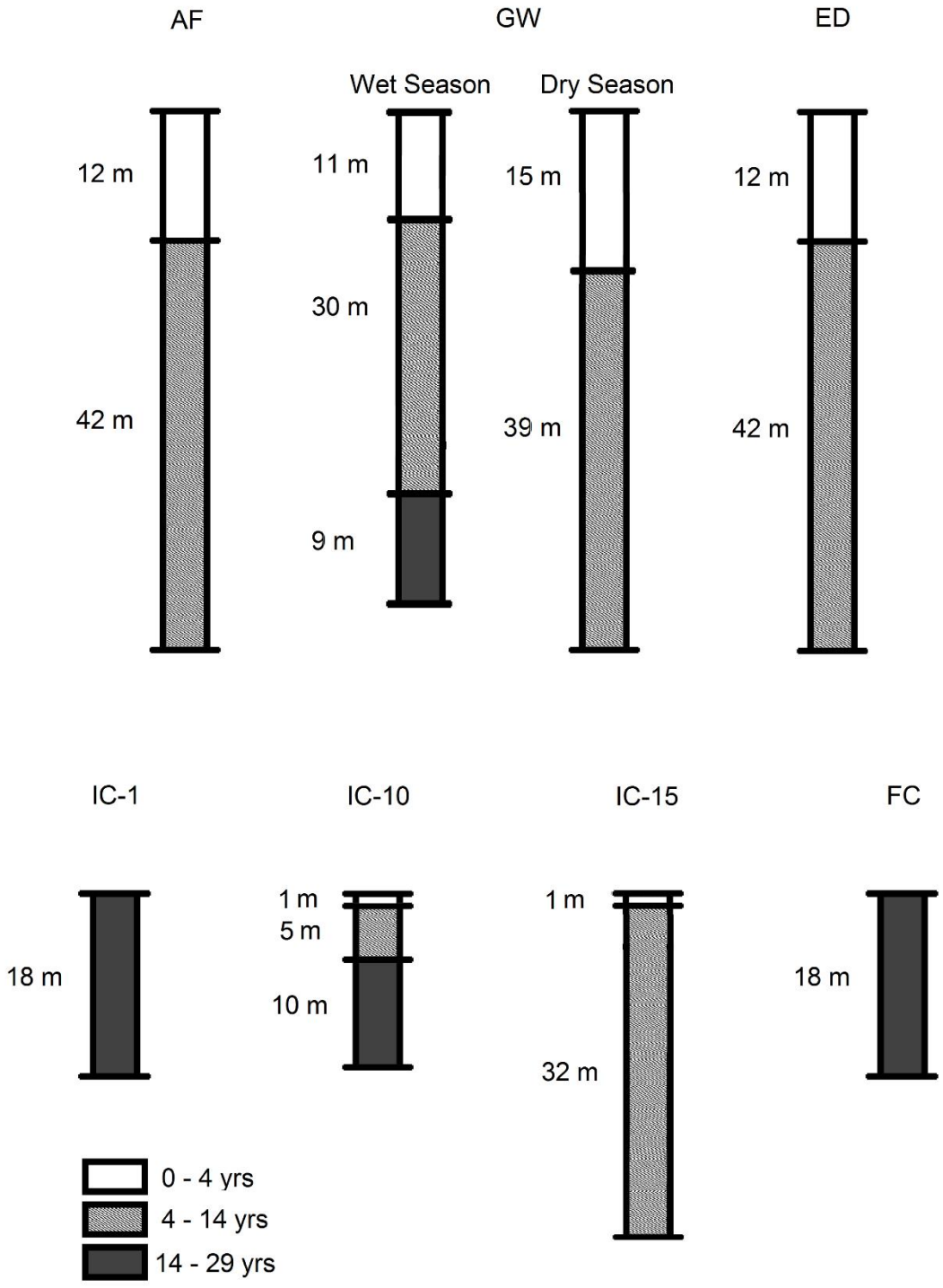

Figure 31 – Vertical Profiles of the Subsurface Waste for the Seven Locations

Table 21 - Material Type, Cover Thickness, and USCS Classification of the Landfill Covers

Location	Cover Type	Material	Group Symbol	Group Name	Cover Thickness
AF	Daily	Auto Fluff	N/A	N/A	15 cm auto fluff and 20 cm soil
GW	Daily	Green Waste	N/A	N/A	13 cm green waste and 13 cm soil
ED	Daily	Soil	GP-GC	Poorly-graded gravel with clay and sand	45 cm
IC-1	Intermediate	Soil	CH	Fat clay	80 cm
IC-10	Intermediate	Soil	SC	Clayey sand with gravel	80 cm
IC-15	Intermediate	Soil	SC	Clayey sand with gravel	82 cm
FC	Final	Soil	CH	Fat clay with gravel	30 cm vegetative soil layer, 30 cm low permeability soil layer, and 60 cm foundation soil layer

Table 22 - Geotechnical Properties of the Landfill Covers

Location	G_s	Wet Season						Dry Season					
		Moist Density (kg/m^3)	Dry Density (kg/m^3)	*w* (%)	*S* (%)	*n*	*e*	Moist Density (kg/m^3)	Dry Density (kg/m^3)	*w* (%)	*S* (%)	*n*	*e*
AF	1.48	597	519	15	12	0.65	1.85	519	460	13	9	0.69	2.22
GW	1.42	ND	ND	129	ND	ND	ND	280	266	6	2	0.81	4.35
ED	2.66	1764	1605	9	38	0.4	0.66	2052	1893	8	55	0.29	0.41
IC-1	2.77	1179	966	21	32	0.65	1.87	1246	1191	5	10	0.57	1.33
IC-10	2.65	1349	1143	18	36	0.57	1.32	1243	1200	4	8	0.55	1.21
IC-15	2.62	1589	1337	19	51	0.49	0.96	1437	1412	2	5	0.46	0.86
FC	2.67	1284	1033	24	41	0.61	1.58	1137	1076	6	10	0.6	1.48

ND – Not determined; Gs – Specific Gravity; n – Porosity; w – Moisture Content; S – Degree of Saturation

Table 23 – USCS Particle Size Distribution of the Landfill Soil Covers

Location	Gravel (%)	Sand (%)	Fine (%)
ED	54.3	39.7	6.0
IC-1	0.0	0.4	99.6
IC-10	25.6	38.4	36.0
IC-15	22.6	51.5	25.9
FC	17.8	9.6	72.6

4.3 Surface Flux of F-gases

Gas flux was determined for the field tests using methodology described in Section 3.2.2. For seven cover types, results are presented individually for each constituent and separately for wet and dry seasons. The bar charts (Figures 32 to 45) presented have four bars for each cover type on the x-axis and flux values on a logarithmic scale on the y-axis. The four bars for each cover type from left to right represents Chambers A, B, C, and D. For the wet season results, cover types including GW, IC-1, IC-10, IC-15 and FC-1 have only two bars for Chamber A and B. The flux values that did not meet the 0.9 R^2 threshold were denoted using a diamond symbol whereas the flux values with significant number of below detection limit measurements were denoted using an x symbol. The negative flux values were denoted using a triangle symbol. The results from the static flux chamber tests for seven cover types for the wet and dry season are presented in Figures 32 to 45 and in Tables 24 and 25.

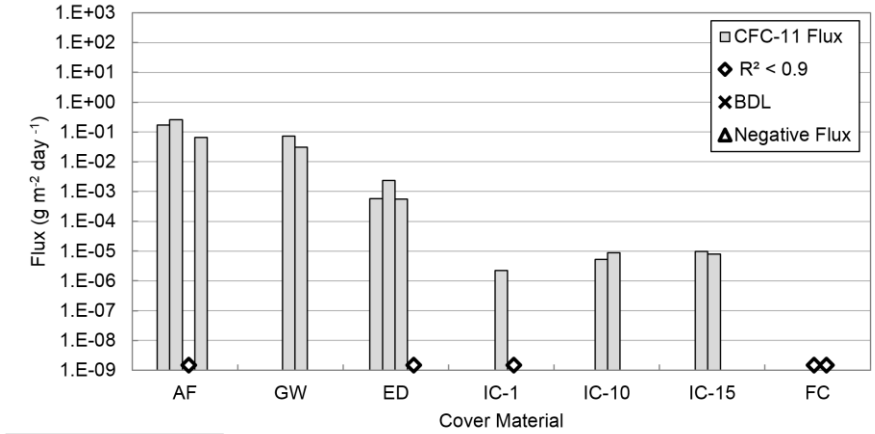

CFC-11 (Wet Season)

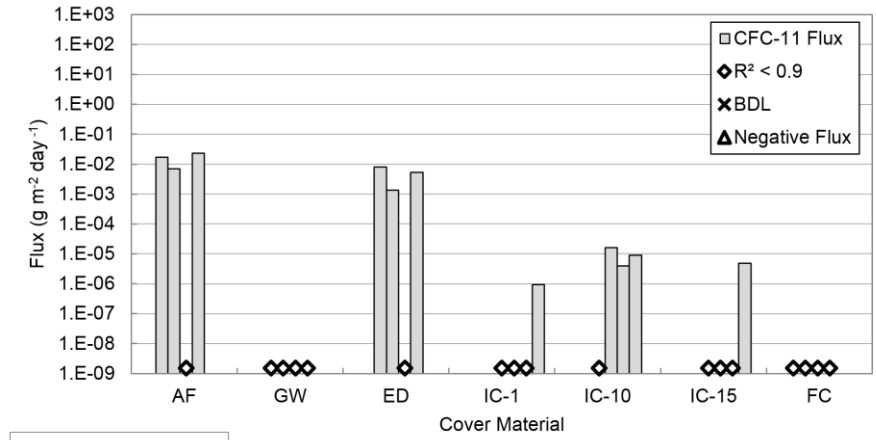

CFC-11 (Dry Season)

Figure 32 – Surface Flux Results for CFC-11 for the Wet and Dry Season

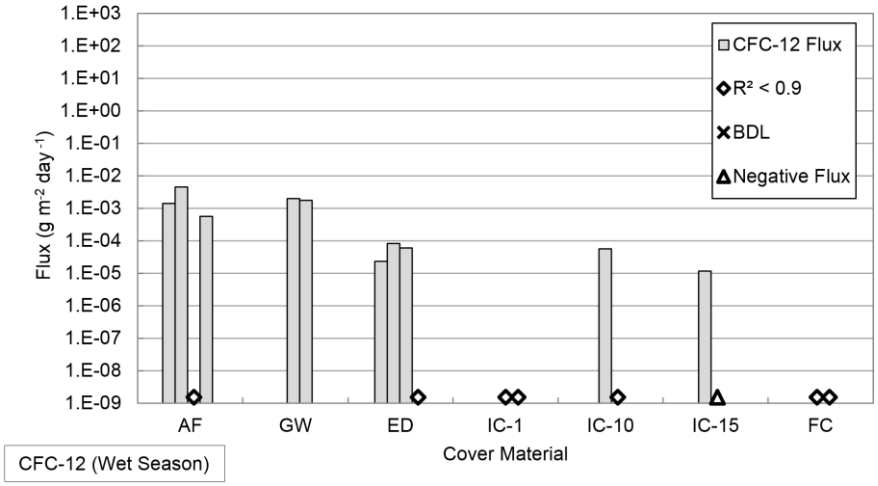

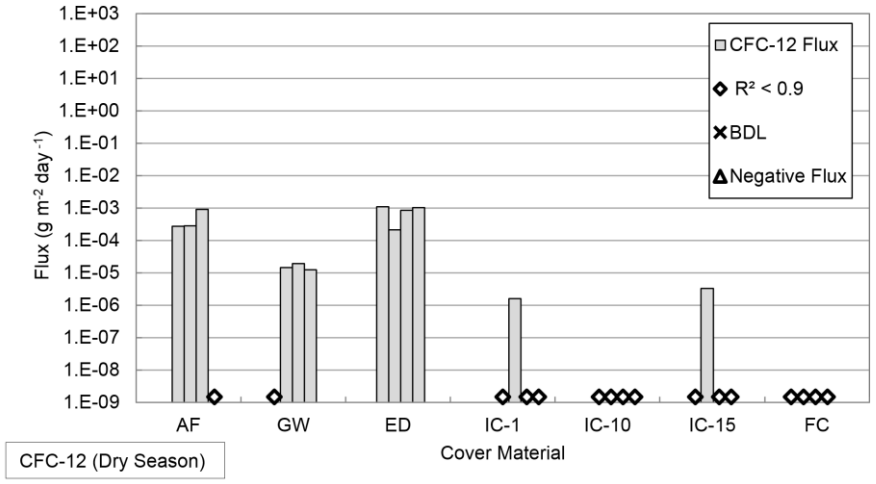

Figure 33 – Surface Flux Results for CFC-12 for the Wet and Dry Season

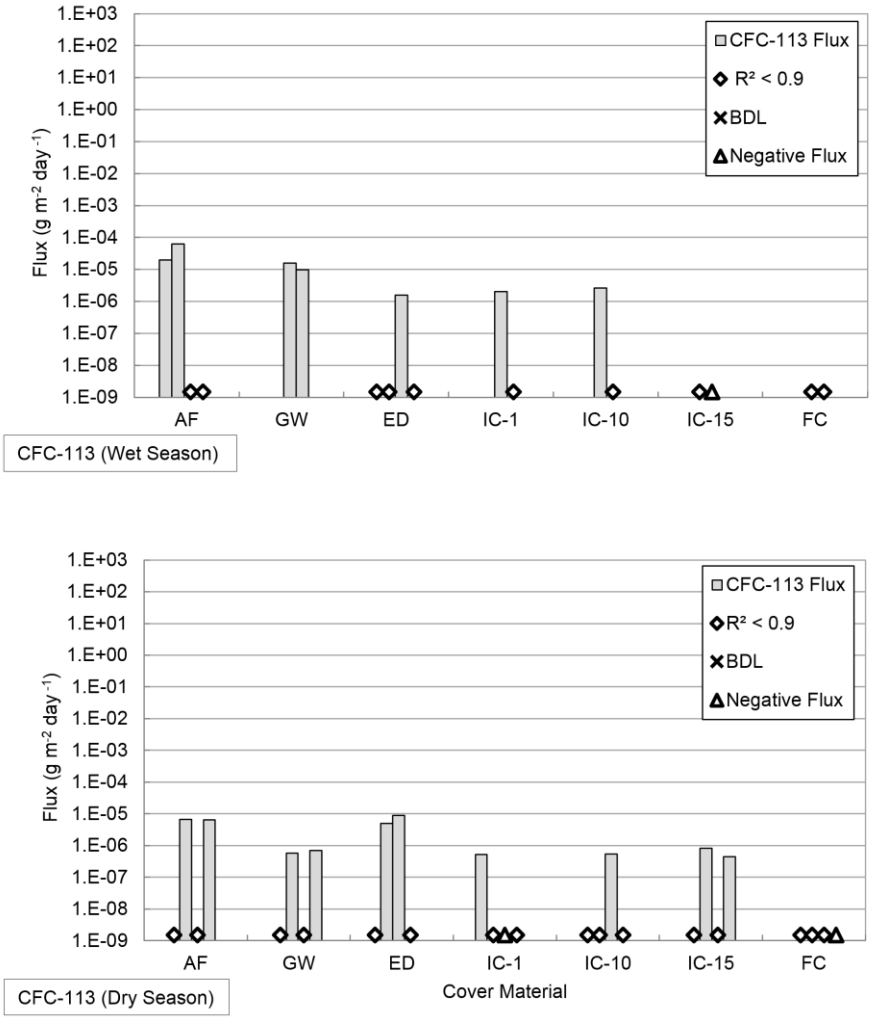

Figure 34 – Surface Flux Results for CFC-113 for the Wet and Dry Season

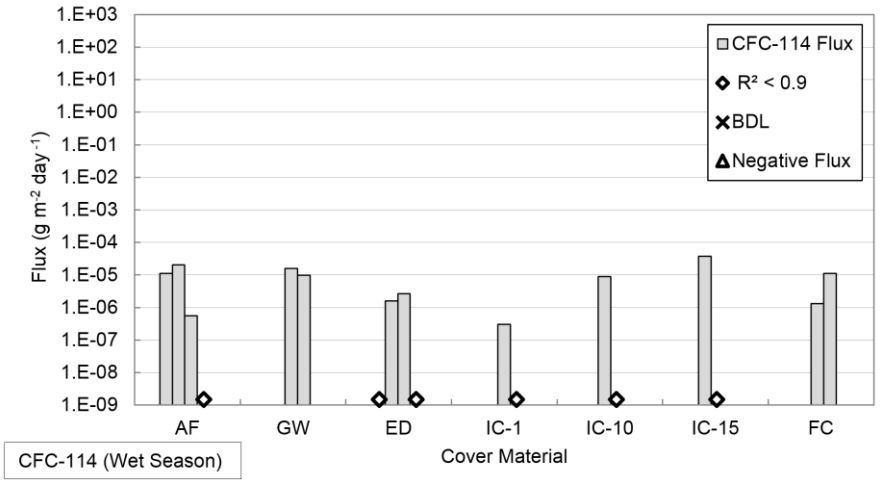

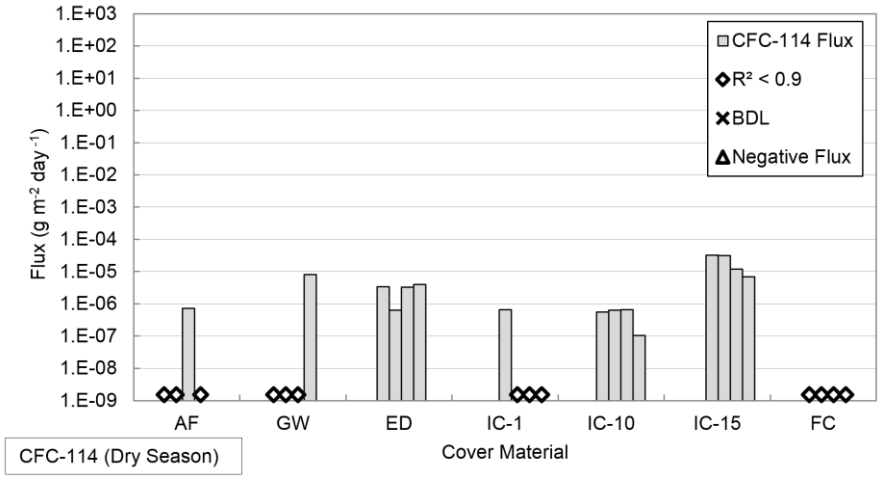

Figure 35 – Surface Flux Results for CFC-114 for the Wet and Dry Season

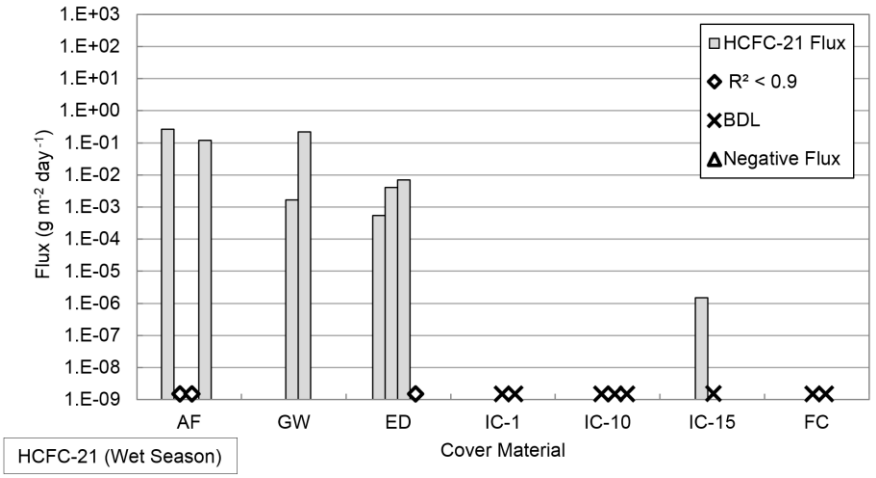

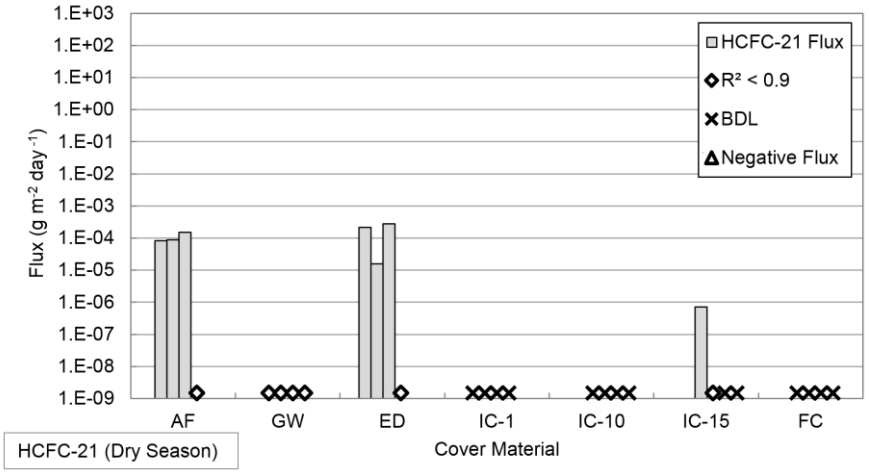

Figure 36 – Surface Flux Results for HCFC-21 for the Wet and Dry Season

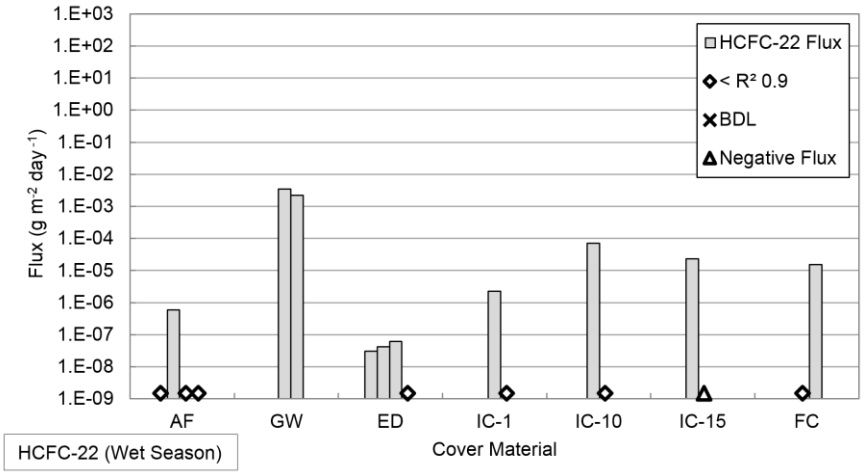

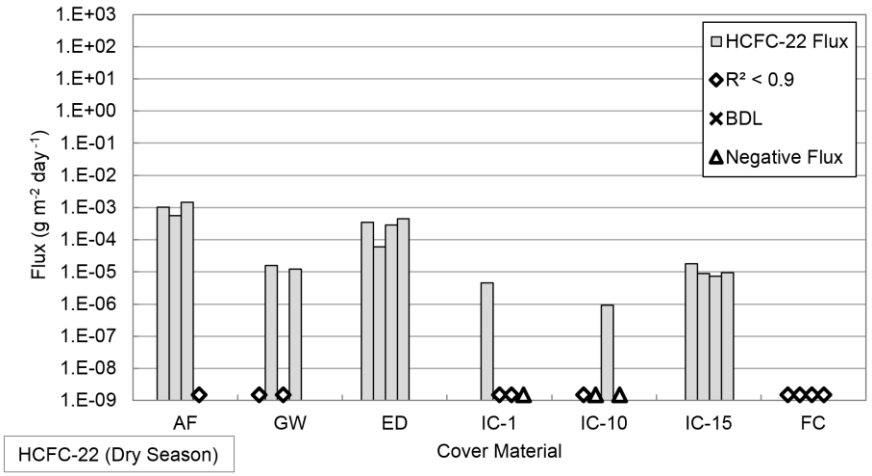

Figure 37 – Surface Flux Results for HCFC-22 for the Wet and Dry Season

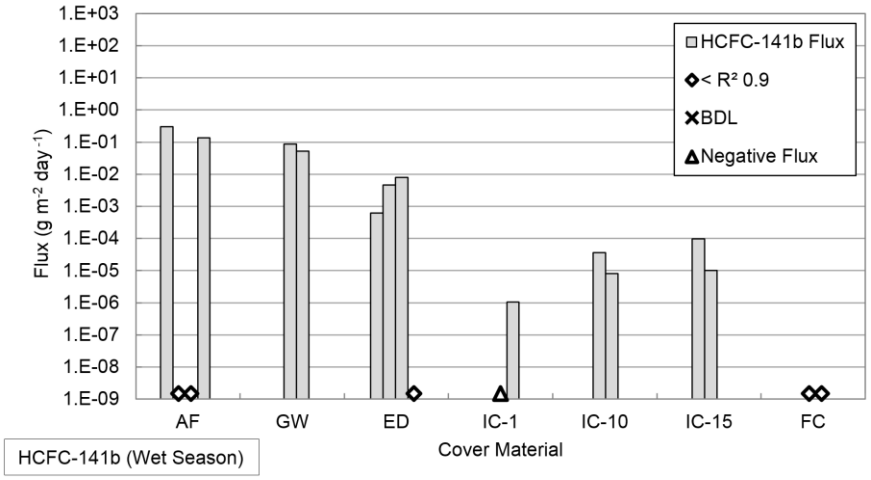

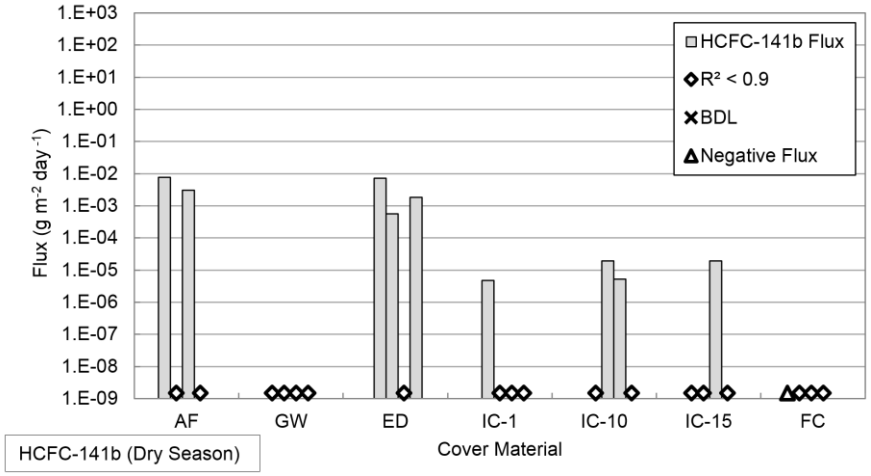

Figure 38 – Surface Flux Results for HCFC-141b for the Wet and Dry Season

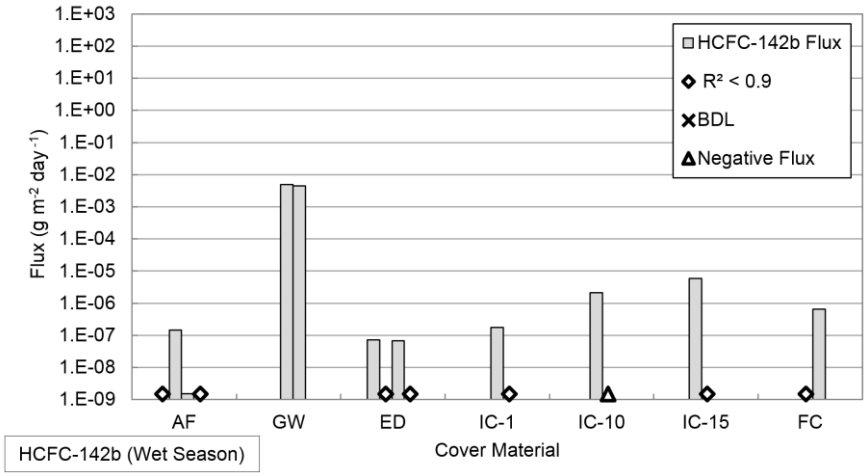

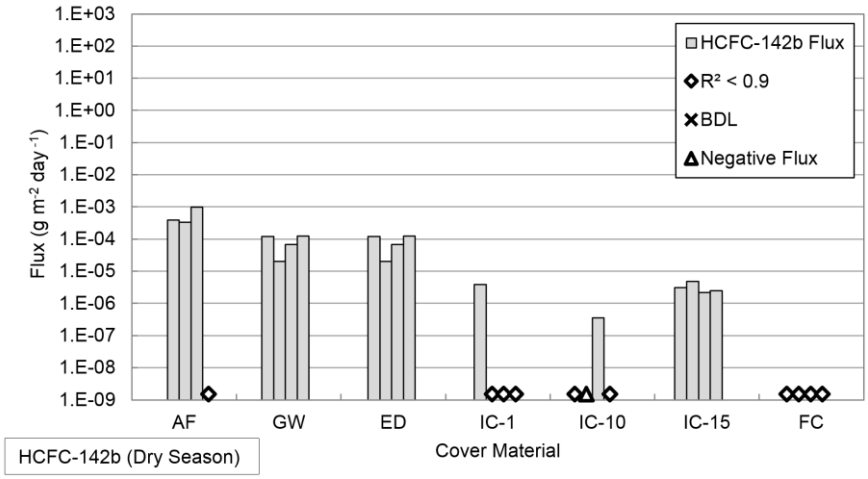

Figure 39 – Surface Flux Results for HCFC-142b for the Wet and Dry Season

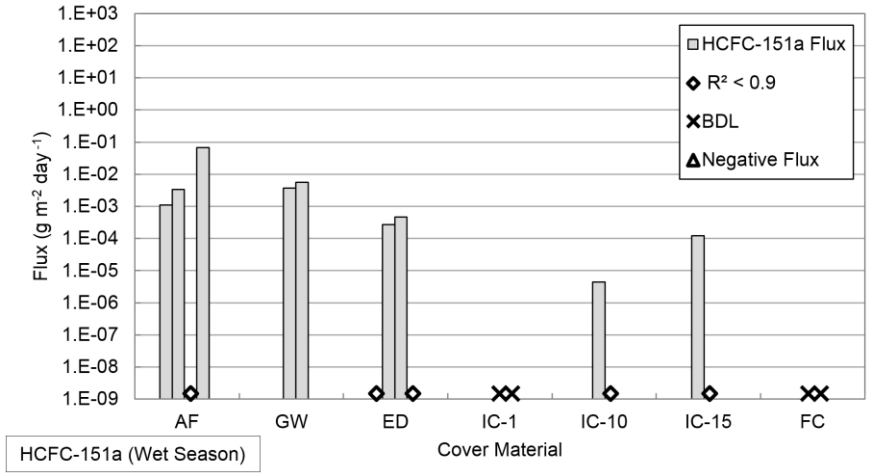

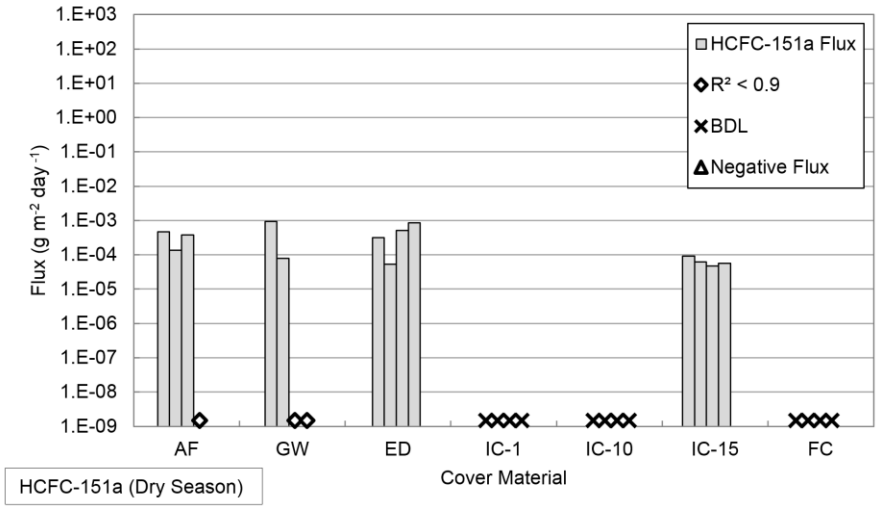

Figure 40 Surface Flux – Surface Flux Results for HCFC-151a for the Wet and Dry Season

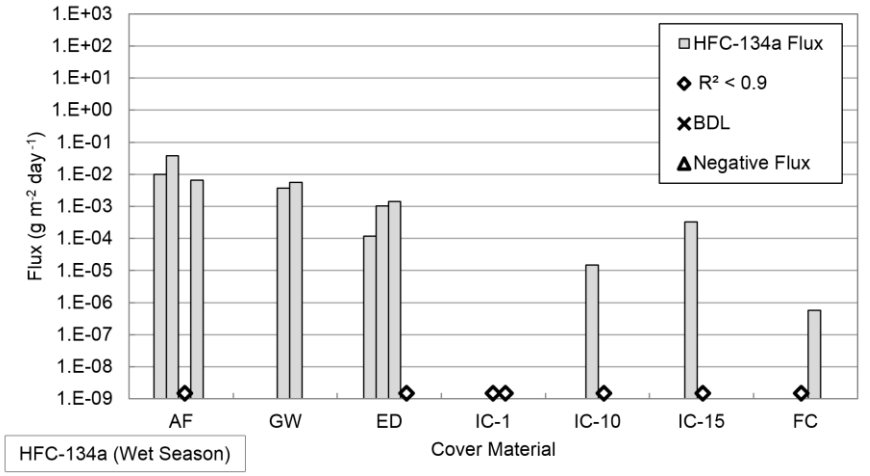

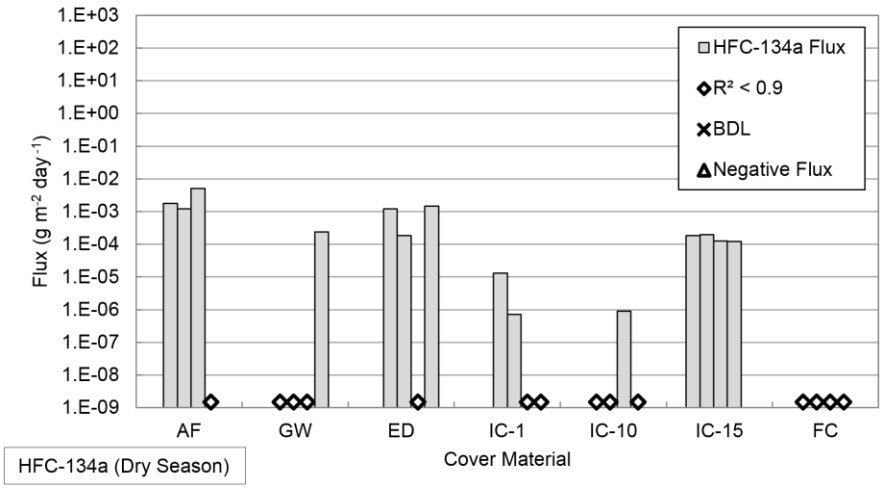

Figure 41 – Surface Flux Results for HFC-134a for the Wet and Dry Season

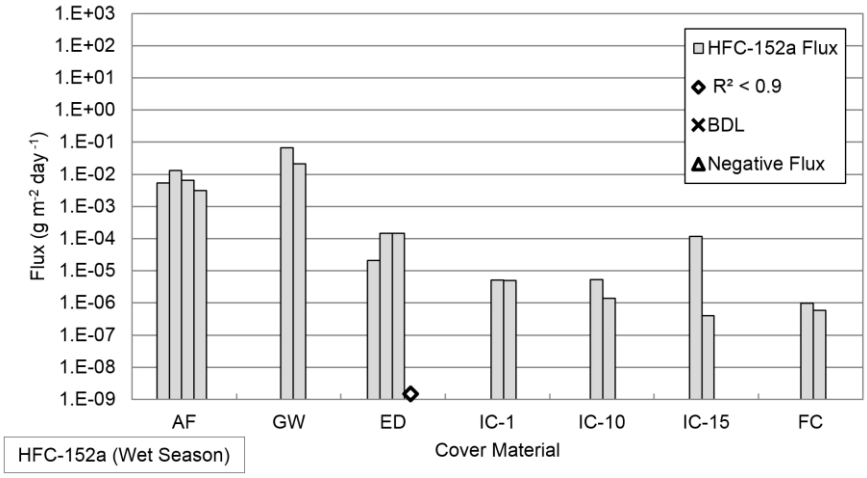

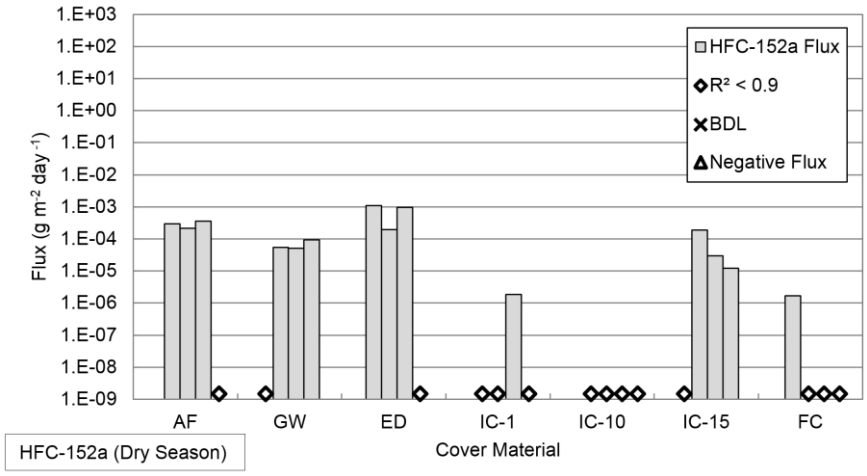

Figure 42 – Surface Flux Results for HFC-152a for the Wet and Dry Season

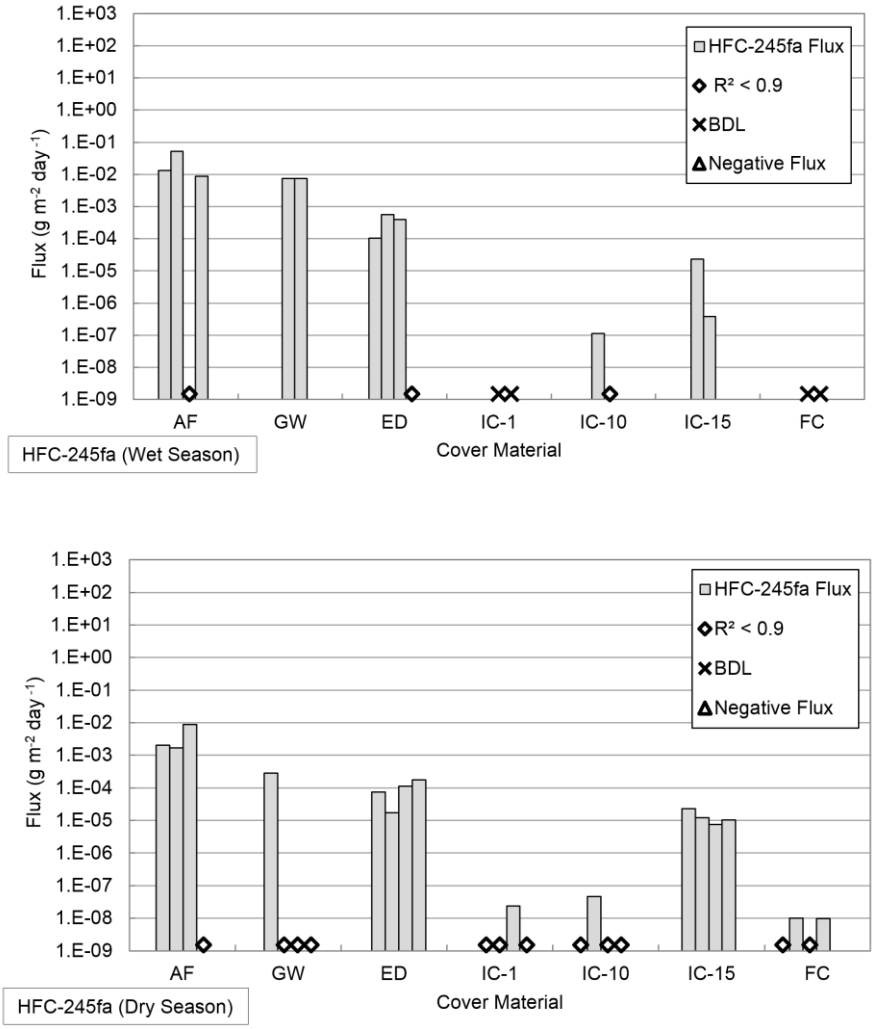

Figure 43 – Surface Flux Results for HFC-245fa for the Wet and Dry Season

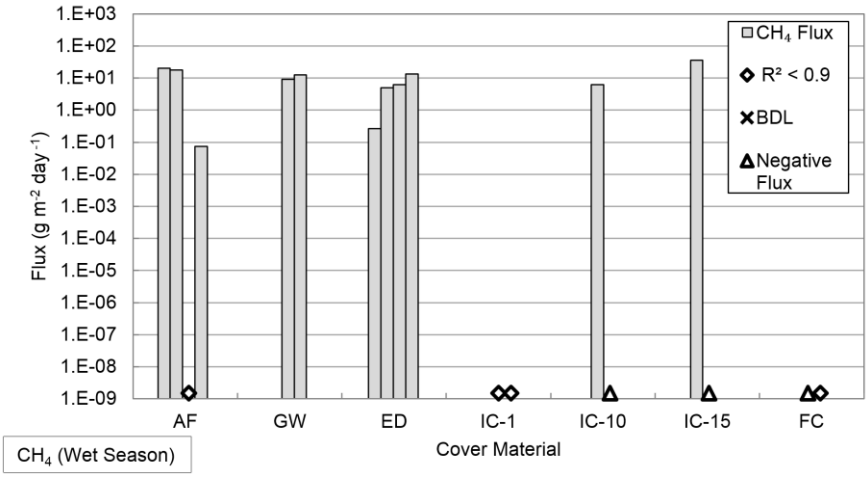

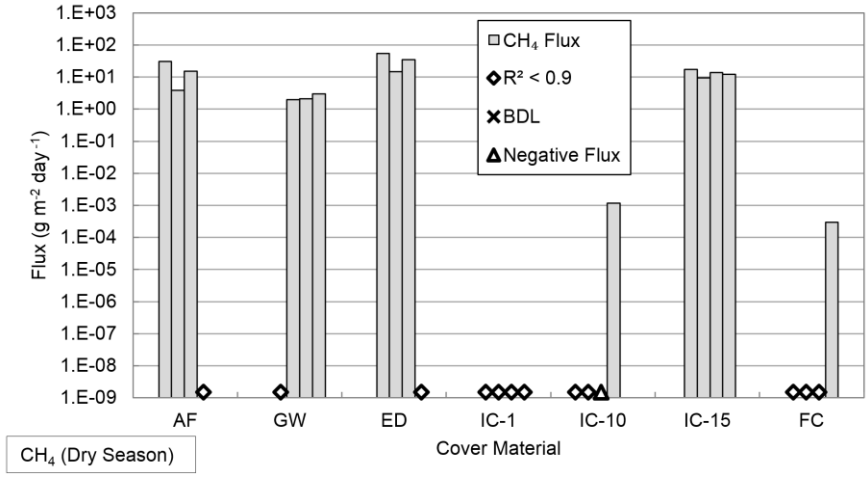

Figure 44 – Surface Flux Results for Methane for the Wet and Dry Season

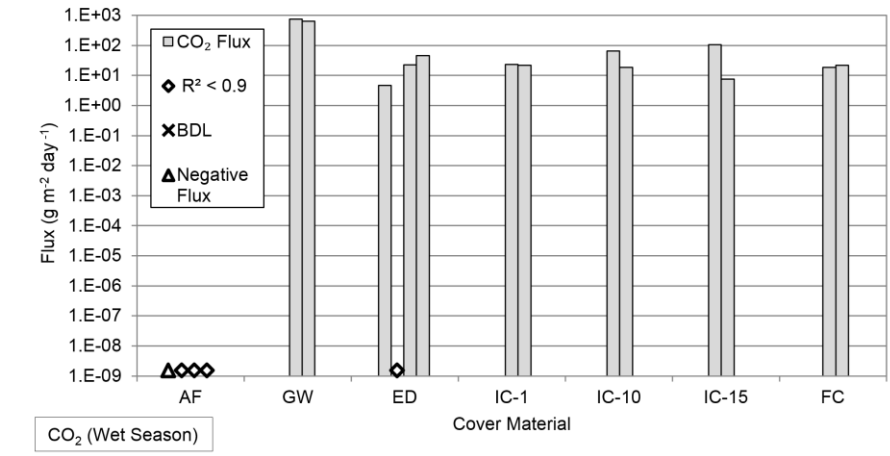

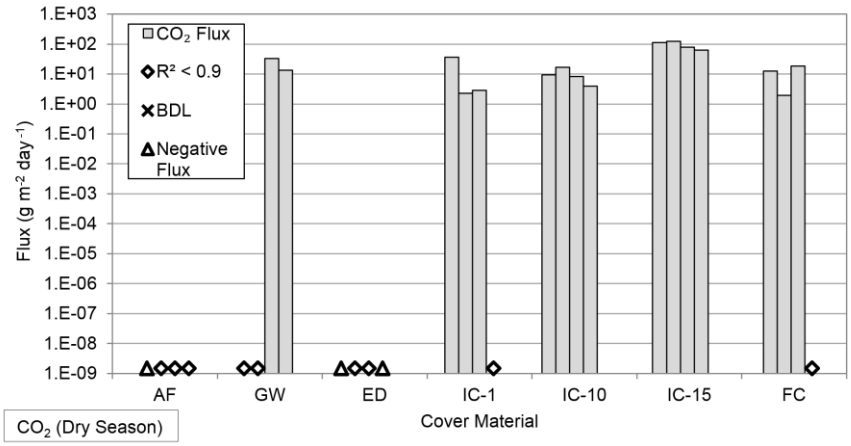

Figure 45 – Surface Flux Results for Carbon Dioxide for the Wet and Dry Season

Table 24 – Minimum and Maximum Flux Values (g m^{-2} day^{-1}) of the Twelve F-gases, Methane, and Carbon Dioxide for the Wet Season

Location	CFC-11		CFC-12		CFC-113		CFC-114		HCFC-21		HCFC-22	
	Min	Max	Min	Max	Min	Max	Min	Max	Min	Max	Min	Max
AF	6.66E-02	2.57E-01	5.54E-04	4.48E-03	1.95E-05	6.31E-05	5.59E-07	2.07E-05	1.20E-01	2.63E-01	5.92E-07	5.92E-07
GW	3.12E-02	7.36E-02	1.74E-03	1.95E-03	9.67E-06	1.57E-05	5.59E-05	1.10E-04	1.65E-03	2.22E-01	2.23E-03	3.43E-03
ED	5.50E-04	2.34E-03	2.32E-05	8.26E-05	1.57E-06	1.57E-06	1.59E-06	2.68E-06	5.42E-04	7.08E-03	3.09E-08	6.09E-08
IC-1	2.27E-06	2.27E-06	I	I	2.06E-06	2.06E-06	3.05E-07	3.05E-07	I	I	2.26E-06	2.26E-06
IC-10	5.19E-06	8.93E-06	5.67E-05	5.67E-05	2.59E-06	2.59E-06	8.99E-06	8.99E-06	I	I	7.07E-05	7.07E-05
IC-15	7.93E-06	9.92E-06	-3.41E-06	1.16E-05	-5.22E-07	-5.22E-07	3.72E-05	3.72E-05	1.47E-06	1.47E-06	-1.60E-06	2.30E-05
FC-1	I	I	I	I	I	I	1.30E-06	1.11E-05	I	I	1.55E-05	1.55E-05

I – Inconclusive flux values due to poor R^2 fit or significant number of below detection limit readings.

Location	HCFC-141b		HCFC-142b		HCFC-151a		HFC-134a		HFC-152a		HFC-245fa	
	Min	Max	Min	Max	Min	Max	Min	Max	Min	Max	Min	Max
AF	1.36E-01	2.99E-01	1.50E-08	1.46E-07	1.53E-05	3.40E-03	6.46E-03	3.79E-02	3.15E-03	1.31E-02	8.73E-03	5.21E-02
GW	5.22E-02	8.70E-02	4.54E-03	4.93E-03	3.73E-03	5.67E-03	7.08E-03	7.13E-03	2.09E-02	6.76E-02	7.44E-03	7.55E-03
ED	6.16E-04	8.04E-03	6.67E-08	7.30E-08	2.71E-04	4.67E-04	1.17E-04	1.42E-03	2.06E-05	1.48E-04	1.05E-04	5.71E-04
IC-1	-5.59E-06	1.04E-06	1.78E-07	1.78E-07	I	I	I	I	4.92E-06	5.06E-06	I	I
IC-10	7.99E-06	3.65E-05	-3.50E-07	2.13E-06	4.47E-06	4.47E-06	1.48E-05	1.48E-05	1.40E-06	5.24E-06	1.14E-07	1.14E-07
IC-15	1.02E-05	9.80E-05	5.90E-06	5.90E-06	1.22E-04	1.22E-04	3.29E-04	3.29E-04	4.00E-07	1.18E-04	3.75E-07	2.31E-05
FC-1	I	I	6.60E-07	6.60E-07	I	I	5.69E-07	5.69E-07	5.89E-07	9.79E-07	I	I

I – Inconclusive flux values due to poor R^2 fit or significant number of below detection limit readings.

Location	Methane		Carbon Dioxide	
	Min	Max	Min	Max
AF	7.41E-02	2.00E+01	-2.36E+01	-2.36E+01
GW	9.16E+00	1.26E+01	6.31E+02	7.47E+02
ED	2.68E-01	1.32E+01	4.60E+00	4.54E+01
IC-1	I	I	2.16E+01	2.30E+01
IC-10	-1.94E-02	6.29E+00	1.85E+01	6.40E+01
IC-15	-9.65E-03	3.60E+01	7.43E+00	1.07E+02
FC-1	-1.07E-03	-1.07E-03	1.86E+01	2.18E+01

I – Inconclusive flux values due to poor R^2 fit or significant number of below detection limit readings.

Table 25 - Minimum and Maximum Flux Values (g m^{-2} day^{-1}) of the Twelve F-gases, Methane, and Carbon Dioxide for the Dry Season

Location	CFC-11		CFC-12		CFC-113		CFC-114		HCFC-21		HCFC-22	
	Min	Max	Min	Max	Min	Max	Min	Max	Min	Max	Min	Max
AF	7.10E-03	3.42E-02	2.76E-04	9.14E-04	6.37E-06	6.63E-06	7.15E-07	7.15E-07	8.41E-05	1.54E-04	5.54E-04	1.46E-03
GW	2.71E-04	2.71E-04	1.24E-05	1.95E-05	5.79E-07	6.91E-07	8.07E-06	8.07E-06	I	I	1.22E-05	1.58E-05
ED	1.35E-03	8.13E-03	2.14E-04	1.12E-03	4.94E-06	9.05E-06	6.34E-07	4.03E-06	1.59E-05	2.75E-04	5.94E-05	4.48E-04
IC-1	9.47E-07	9.47E-07	1.63E-06	1.63E-06	-5.96E-07	5.31E-07	6.56E-07	6.56E-07	I	I	-1.07E-07	4.50E-06
IC-10	3.91E-06	1.57E-05	I	I	5.46E-07	5.46E-07	1.06E-07	6.56E-07	I	I	-2.30E-06	9.22E-07
IC-15	4.81E-06	4.81E-06	3.27E-06	3.27E-06	4.46E-07	8.29E-07	6.85E-06	3.23E-05	7.21E-07	7.21E-07	7.23E-06	1.80E-05
FC-1	I	I	I	I	-6.81E-08	-6.81E-08	I	I	I	I	I	I

I – Inconclusive flux values due to poor R^2 fit or significant number of below detection limit readings.

Location	HCFC-141b		HCFC-142b		HCFC-151a		HFC-134a		HFC-152a		HFC-245fa	
	Min	Max	Min	Max	Min	Max	Min	Max	Min	Max	Min	Max
AF	3.09E-03	7.58E-03	3.32E-04	9.68E-04	1.36E-04	4.62E-04	1.21E-03	5.07E-03	2.18E-04	3.56E-04	1.68E-03	8.77E-03
GW	I	I	I	I	7.80E-05	9.40E-04	2.34E-04	2.34E-04	5.04E-05	9.44E-05	2.83E-04	2.83E-04
ED	5.68E-04	7.22E-03	2.01E-05	1.23E-04	5.32E-05	8.62E-04	1.85E-04	1.47E-03	1.94E-04	1.27E-03	1.72E-05	1.78E-04
IC-1	4.79E-06	4.79E-06	3.84E-06	3.84E-06	I	I	7.19E-07	1.31E-05	1.83E-06	1.83E-06	2.35E-08	2.35E-08
IC-10	5.19E-06	2.07E-05	-7.04E-08	3.57E-07	I	I	9.06E-07	9.06E-07	I	I	3.68E-08	4.51E-08
IC-15	1.93E-05	1.93E-05	2.19E-06	4.78E-06	4.74E-05	9.29E-05	1.24E-04	1.95E-04	1.22E-05	1.86E-04	7.56E-06	2.30E-05
FC-1	-5.01E-07	-5.01E-07	I	I	I	I	I	I	1.70E-06	1.70E-06	9.74E-09	9.89E-09

I – Inconclusive flux values due to poor R^2 fit or significant number of below detection limit readings.

Location	Methane		Carbon Dioxide	
	Min	Max	Min	Max
AF	3.82E+00	3.05E+01	-1.54E+00	-1.54E+00
GW	1.96E+00	2.99E+00	1.32E+01	3.27E+01
ED	1.47E+01	5.38E+01	-1.96E+01	-2.55E-01
IC-1	I	I	2.29E+00	3.69E+01
IC-10	-6.06E-03	1.17E-03	3.90E+00	1.63E+01
IC-15	9.33E+00	1.73E+01	6.21E+01	1.25E+02
FC-1	2.94E-04	2.94E-04	1.95E+00	1.85E+01

I – Inconclusive flux values due to poor R^2 fit or significant number of below detection limit readings.

Minimum and maximum F-gas flux values are presented in Table 25 and Table 26 for the wet and dry season, respectively. The F-gas flux values for the daily covers (AF, GW, and ED) were in the 10^{-8} to 10^{-1} g m^{-2} day^{-1} range and 10^{-7} to 10^{-2} g m^{-2} day^{-1} range for the wet and dry season, respectively. The F-gas flux values for the intermediate covers (IC-1, IC-10, and IC-15) were in the -10^{-6} to 10^{-4} g m^{-2} day^{-1} range and -10^{-6} to 10^{-4} g m^{-2} day^{-1} range for the wet and dry season, respectively. The F-gas flux values for the final covers (FC) were in the 10^{-7} to 10^{-5} g m^{-2} day^{-1} range and -10^{-7} to 10^{-6} g m^{-2} day^{-1} range for the wet and dry season, respectively. F-gas fluxes for the final covers had the highest number of below detection limit cases as well as lower than R^2 threshold cases. Highest F-gas fluxes were measured from the AF location for the wet and dry season. Lowest F-gas fluxes were measured from the FC location for the wet and dry season.

Lower level of variation was observed for methane and carbon dioxide with flux values ranging over five orders of magnitude for the seven tested locations. The methane flux values for the daily covers were in the 10^{-2} to 10^{+1} g m^{-2} d^{-1} range and 1 to 10^{+1} g m^{-2} day^{-1} range for the wet and dry season, respectively. The carbon dioxide flux values for the daily covers were in the -10^{+1} to 10^{+2} g m^{-2} day^{-1} range and -10^{+1} to 10^{+1} g m^{-2} day^{-1} range for the wet and dry season, respectively. The methane flux values for the intermediate covers were in the -10^{-2} to 10^{+1} g m^{-2} d^{-1} range and -10^{-3} to 10^{+1} g m^{-2} day^{-1} range for the wet and dry season, respectively. The carbon dioxide flux values for the intermediate covers were in the 1 to 10^{+2} g m^{-2} day^{-1} range for both seasons. The methane fluxes for the final cover were -10^{-3} g m^{-2} day^{-1} and 10^{-4} g m^{-2} day^{-1} for the wet and dry season, respectively. The

carbon dioxide flux values for the final cover were in the 10^{+1} g m^{-2} d^{-1} range and 1 to 10^{+1} g m^{-2} day^{-1} range for the wet and dry season, respectively. Negative flux values were typically observed during the wet season and at the intermediate and final covers.

Of the F-gases detected and quantified, the highest fluxes were measured for CFC-11, HCFC-21, and HCFC-141b in the wet season (Figure 46) and for CFC-11, HCFC-141b, and HFC-134a in the dry season (Figure 47) across the seven cover locations. The lowest fluxes were measured for CFC-113 and CFC-114 for both the wet and dry season. All twelve F-gas constituents were present in all the three daily cover locations for the wet season and were present at two out three locations for the dry season at the daily cover locations. For the intermediate and final cover tests, the number of constituents detected typically decreased with older waste age.

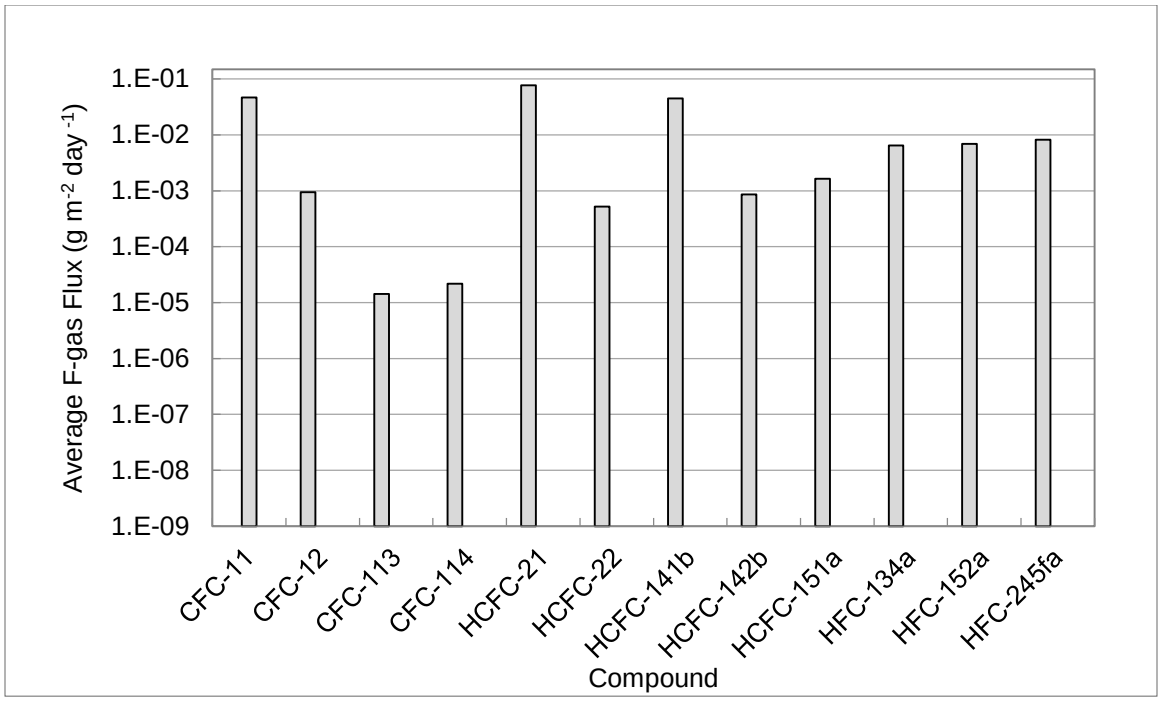

Figure 46 – Average Surface Flux over the Seven Locations for the Twelve F-gases for the Wet Season

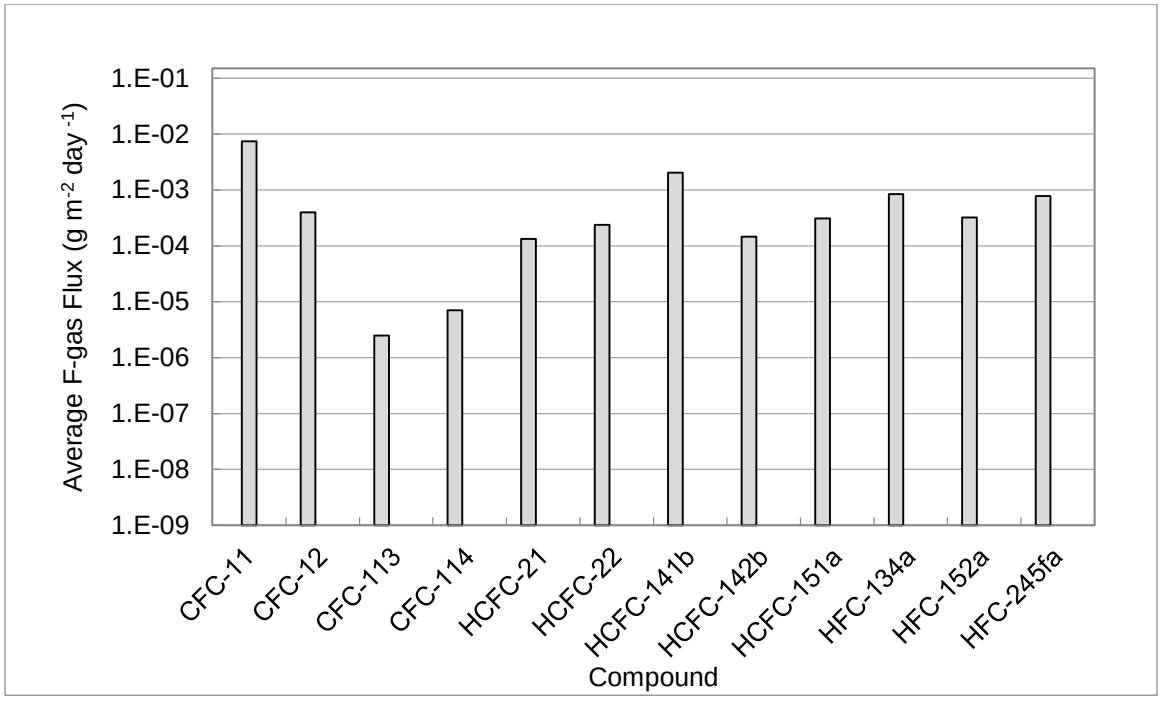

Figure 47 - Average Surface Flux over the Seven Locations for the Twelve F-gases for the Dry Season

The average F-gas fluxes decreased from daily, intermediate, to final cover similar to the results for methane fluxes presented in Abichou et al. (2006b). The average F-gas fluxes for the wet and dry season respective to daily, intermediate, and final covers are presented in Figure 48. The decrease in emissions from daily, to intermediate, to final cover systems can be attributed to several factors: difference in cover material, cover thickness, waste height, and waste age. First, the intermediate and final cover locations had much thicker covers in comparison to the daily cover locations. Second, age of the underlying waste present at the daily cover locations in comparison to the intermediate and final cover locations was much younger. The daily cover locations also had fresh waste placed 1 to 8 days old prior to the measurements. Also, the hydraulic conductivity of the covers decreased from daily to intermediate to final covers. Lastly, the waste height at the daily cover location was much higher in comparison to the intermediate and final cover locations. The high flux values at the daily cover locations was attributed to this combination of conditions.

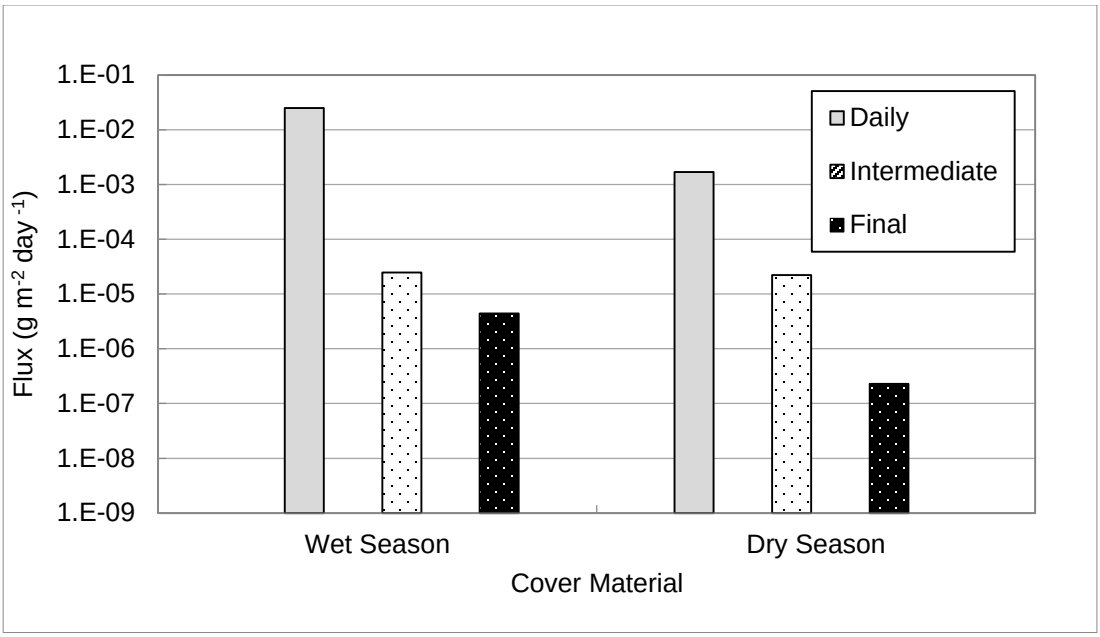

Figure 48 – Average F-gas Surface Flux for Daily, Intermediate, and Final Covers for the Wet and Dry Season

The F-gas fluxes typically decreased from AF, to GW, to ED for the daily cover locations. The average F-gas fluxes for the wet and dry season are presented in Figure 49. The tests for the daily covers were conducted at the same cell (Cell 12) with similar waste age, waste height, and cover thickness indicating that the differences in emissions were likely due to difference in cover material. The highest F-gas flux values were measured from the auto fluff cover and the lowest F-gas flux values were typically measured from the extended-daily cover during the wet season and from green waste during the dry season. As the porosity of the cover material increased, an increase in F-gas flux values was observed.

In addition, presence of F-gas in auto shredder residue has been reported in previous studies conducted by Scheutz et al. (2007c, 2011a, 2011b). The F-

gas present in the auto fluff is likely contributed to high emissions of the F-gases from the auto fluff cover. Further investigation would be necessary to assess whether the auto fluff used for daily cover at PHL contained F-gas blowing agents.

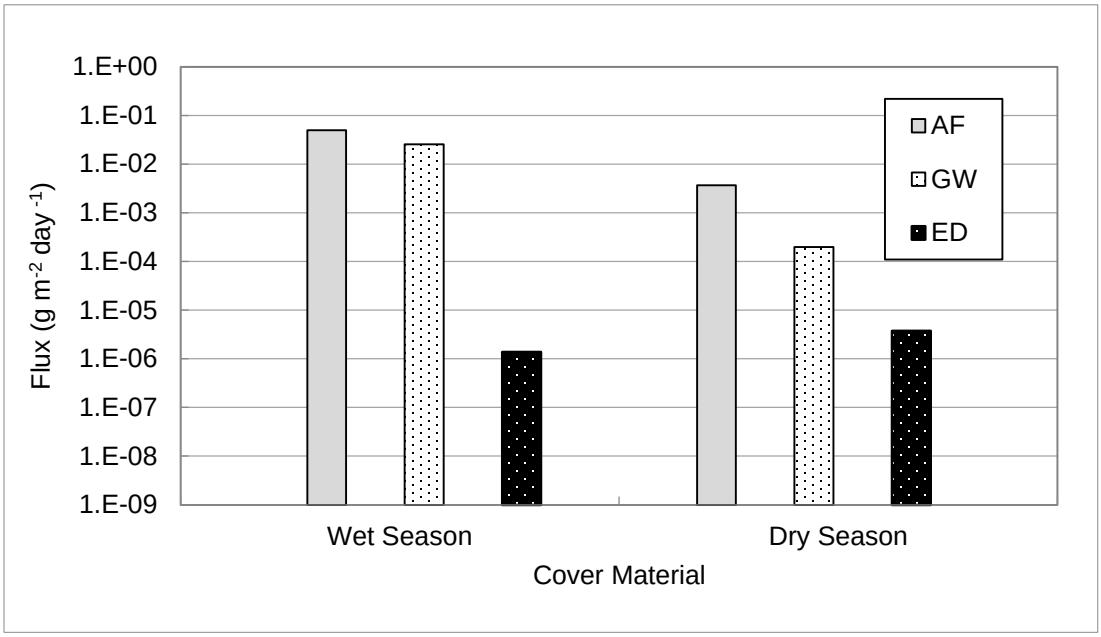

Figure 49 - Average F-gas Surface Flux for AF, GW, and ED for the Wet and Dry Season

F-gas fluxes for the intermediate covers decreased from IC-15, to IC-10, to IC-1. The average F-gas fluxes for IC-1, IC-10, and IC-15 for the wet and dry season are presented in Figure 50. The three locations not only were similar in cover thicknesses (all three locations approximately 80 cm), but also had soil cover systems. Thus, the decreasing trend was likely due to difference in waste age and waste height. Highest F-gas flux values were measured from the location with the highest waste height and youngest waste (IC-15) whereas lowest F-gas flux values were from the location with the lowest waste height and oldest waste (IC-1) among intermediate cover locations. The results indicated that the F-gas fluxes typically

decreased with increasing waste age and with decreasing waste height. In addition, as the fine soil fraction of the soil increased in the soil cover system, the emission rate typically decreased.

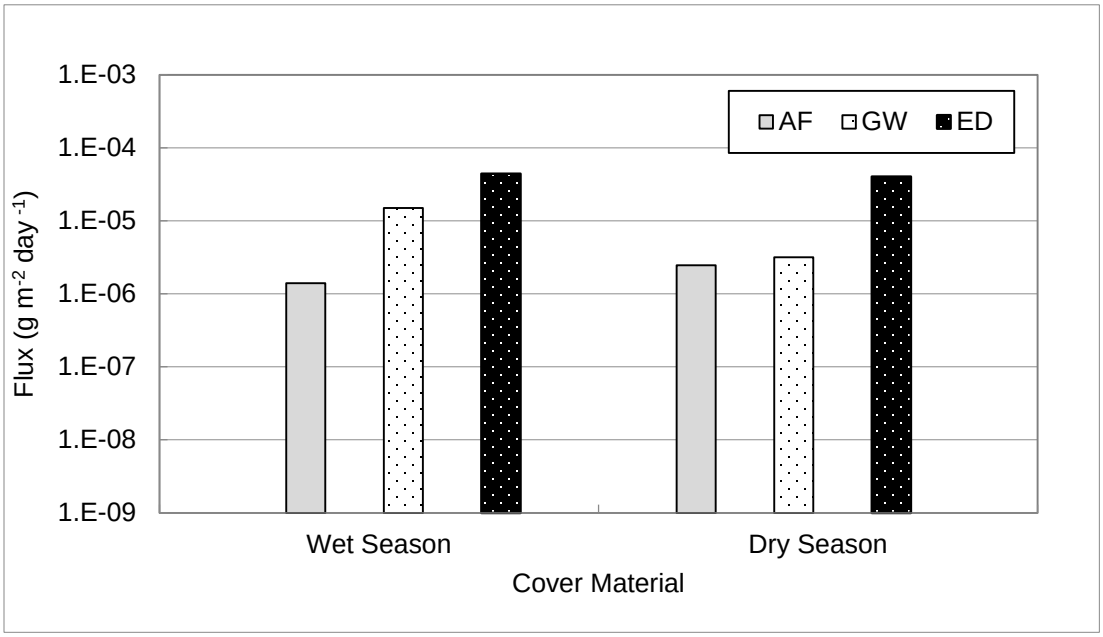

Figure 50 - Average F-gas Surface Flux for IC-1, IC-10, and IC-15 for the Wet and Dry Season

The level of variation observed for the F-gas fluxes between the seven cover types/locations and between the two seasons was significant (Tables 25 and 26). This high level of variation was likely introduced due to precipitation during the wet season. The measured water content of the cover system had considerably larger range (9 to 129%) during the wet season in comparison to the measured water content during the dry season (12 to 51%). This is likely indicating that presence of water can severely impact the gas emission rates and also cause heterogeneity in the available pore space in the cover system, since the aqueous

diffusion is considerably slower in comparison to gaseous diffusion as presented in Whalen et al. (1990).

The average F-gas flux between the seven locations varied up to four orders of magnitude. However, the differences in F-gas flux between the two seasons were considerably less (up to two orders of magnitude in variation). Greater variations were observed between the seven test locations indicating that physical factors such as cover thickness, cover material, waste age, and waste height had greater influence on F-gas emissions than environmental factors such as precipitation, temperature, barometric pressure, or cover moisture conditions.

4.4 F-gas Destruction Efficiency

The destruction efficiencies of the flare system for the twelve F-gases and methane were calculated based on the inlet and outlet concentration of the flare system as outlined in Section 3.4.2. The inlet F-gas concentrations ranged from 10^3 to 10^6 pptv. Highest F-gas concentration was measured for HFC-134a while the lowest F-gas concentration was measured for CFC-113. The destruction efficiencies for the twelve F-gases and methane are presented in Table 26. The destruction efficiencies were greater than 99% for all twelve F-gases and methane. Destruction efficiencies of more than 90% were reported in literature for CFCs and HCFCs for landfills with similar landfill gas collection and combustion systems as those used in California (Environment Canada 1999, 2000a, 2000b, 2000c, 2002, 2005).

Table 26 – Destruction Efficiency of the Flare System at PHL for the Twelve F-gases and Methane

Compounds	Average Inlet Concentration (pptv)	Average Outlet Concentration (pptv)		Destruction Efficiency (%)
		Actual	With Air Dilution Correction	
CFC-11	6.69E+04	1.18E+01	7.64E+01	99.89%
CFC-12	1.21E+06	9.94E+02	6.43E+03	99.47%
CFC-113	3.15E+03	0.00E+00	0.00E+00	100.00%
CFC-114	1.08E+05	3.95E+01	2.56E+02	99.76%
HCFC-21	2.74E+04	5.00E+00	3.24E+01	99.88%
HCFC-22	1.94E+06	5.00E+00	3.24E+01	99.99%
HCFC-141b	8.28E+05	5.00E+00	3.24E+01	99.99%
HCFC-142b	1.23E+05	5.00E+00	3.24E+01	99.97%
HCFC-151a	1.34E+05	5.00E+00	3.24E+01	99.98%
HFC-134a	2.16E+06	6.88E+01	4.45E+02	99.98%
HFC-152a	1.21E+06	5.00E+00	3.24E+01	99.99%
HFC-245fa	2.60E+04	5.00E+00	3.24E+01	99.88%
CH_4	4.39E+11	7.47E+06	4.84E+07	99.99%

Chapter 5: Engineering Significance

5.1 Introduction

An emission inventory of the twelve F-gases, methane, and carbon dioxide was performed to estimate overall emission for PHL using the flux values calculated in Chapter 4 to understand the contributions of F-gas emissions from the landfill to overall California emissions. The field-based emission values were scaled up to facility level fugitive emission values using landfill area containing waste and the area fractions of the three cover types (daily, intermediate, and final) present at the site. The facility level fugitive emission values were then converted to carbon dioxide equivalent (CO_2E) emission values using GWP. The scaled up F-gas emission and methane emission values were compared to determine contribution of high GWP gases on facility-wide GHG emissions of the landfill. In addition, the scaled up methane emission values were compared to methane emission values from IPCC-First Order Decay (IPCC-FOD) model reported on EPA Facility Level GHG Emission Data website and waste-in-place (WIP) – landfill gas correlation equation presented in Spokas et al. (2015) to compare field-based emission values to model- and correlation-based emission values.

5.2 Scaling-Up Surface Area Fluxes to a Facility-Level Fugitive Emissions

The surface emission measurement values from the field investigation were scaled up to facility-wide fugitive emission values using the waste containing surface area and the daily, intermediate, and final cover distribution at the landfill. The surface area of the landfill containing waste (approximately 600,000 m^2) was

obtained from site record provided on Facility Level GHG Emission Data from EPA (USEPA 2014e). The distribution of the daily, intermediate, and final covers was determined using topographic survey records for the site (Table 27).

Table 27 – Potrero Hills Landfill Waste Containing Surface Area and Landfill Cover Distribution

Cover Type		%
Daily	AF	1
	GW	1
	ED	1
Intermediate	IC-1	28
	IC-10	28
	IC-15	28
Final	FC	13

The scaled up emission values were calculated using both minimum and maximum surface flux values of the twelve F-gases, methane, and carbon dioxide to obtain a range of the facility-wide emissions. The scaled up emission values were then converted to a CO_2E using the GWP values presented in Section 2.4. The facility-wide emissions were calculated using both wet season and dry season surface flux values to take account of effect of seasonal variations. The facility-wide emissions for wet season and dry season were calculated based on 12-month season for comparison. In addition, facility-wide emissions based on 30-year weather data were calculated to estimate overall emissions during a 12-month calendar year (Wunderground 2015). Based on the 30-year weather data from a weather station near the Potreo Hills Landfill, the wet and dry season fraction in a 12-month calendar year was 58% and 42%, respectively. The weather fractions were then used to calculated annual emissions by prorating emissions data for the wet and dry season. The scaled up facility-wide emission values for the wet season

are presented in Tables 28 to 35 and Figures 51 to 55. The scaled up facility-wide emission values for the dry season are presented in Tables 36 to 43 and Figures 56 to 60. The scaled up facility-wide emission values for the prorated season are presented in Tables 44 to 51 and Figures 61 to 65.

Table 28 – Minimum and Maximum Fugitive Emissions for the Twelve F-gases, Methane, and Carbon Dioxide for the Wet Season

Compounds	Surface Emissions (CO_2E Tonnes/year)			
	Minimum	%	Maximum	%
CFC-11	1.01E+03	14.54	3.40E+03	3.61
CFC-12	8.49E+01	1.23	1.88E+02	0.20
CFC-113	1.86E+00	0.03	2.49E+00	0.00
CFC-114	2.59E+01	0.37	2.97E+01	0.03
HCFC-21	3.95E+01	0.57	1.59E+02	0.17
HCFC-22	1.70E+01	0.25	2.43E+01	0.03
HCFC-141b	3.23E+02	4.67	6.80E+02	0.72
HCFC-142b	2.04E+01	0.29	2.24E+01	0.02
HCFC-151a	N/A	N/A	N/A	N/A
HFC-134a	5.70E+01	0.82	1.37E+02	0.15
HFC-152a	7.32E+00	0.11	2.55E+01	0.03
HFC-245fa	3.06E+01	0.44	1.14E+02	0.12
Total F-gases Emissions	1.61E+03	23.32	4.78E+03	5.07
CH_4	5.31E+02	7.67	7.53E+04	79.88
CO_2	4.78E+03	69.01	1.42E+04	15.04
Total Surface Emissions (F-gases + CH_4 + CO_2)	6.92E+03	100.00	9.42E+04	100.00

Table 29 – Minimum and Maximum Fugitive Emissions for the Twelve F-gases and Methane for the Wet Season (Without Carbon Dioxide)

Compounds	Surface Emissions (CO_2E Tonnes/year)			
	Minimum	%	Maximum	%
CFC-11	1.01E+03	46.92	3.40E+03	4.24
CFC-12	8.49E+01	3.96	1.88E+02	0.23
CFC-113	1.86E+00	0.09	2.49E+00	0.00
CFC-114	2.59E+01	1.21	2.97E+01	0.04
HCFC-21	3.95E+01	1.84	1.59E+02	0.20
HCFC-22	1.70E+01	0.79	2.43E+01	0.03
HCFC-141b	3.23E+02	15.06	6.80E+02	0.85
HCFC-142b	2.04E+01	0.95	2.24E+01	0.03
HCFC-151a	N/A	N/A	N/A	N/A
HFC-134a	5.70E+01	2.66	1.37E+02	0.17
HFC-152a	7.32E+00	0.34	2.55E+01	0.03
HFC-245fa	3.06E+01	1.42	1.14E+02	0.14
Total F-gases Emissions	1.61E+03	75.24	4.78E+03	5.97
CH_4	5.31E+02	24.76	7.53E+04	94.03
Total Surface Emissions (F-gases + CH_4)	2.14E+03	100.00	8.00E+04	100.00

Table 30 – Minimum Fugitive Emissions for the
F-gases, Methane, and Carbon Dioxide for the Wet Season

Cover Type	Total Fugitive Emissions (CO_2E Tonnes/year)		
	F-gases	CH_4	CO_2
AF	9.95E+02	4.54E+00	-5.16E+01
GW	5.13E+02	5.61E+02	1.38E+03
ED	7.89E+00	1.64E+01	1.01E+01
IC-1	1.58E+00	0.00E+00	1.32E+03
IC-10	5.15E+01	-3.33E+01	1.13E+03
IC-15	4.31E+01	-1.65E+01	4.55E+02
FC	1.15E+00	-8.51E-01	5.29E+02
Total	1.61E+03	5.31E+02	4.78E+03

Table 31 - Emission Fractions for Minimum Fugitive Emissions for the
F-gases, Methane, and Carbon Dioxide for the Wet Season

Cover Type	Total Fugitive Emissions Fraction (%)		
	F-gases	CH_4	CO_2
AF	14.4	0.1	-0.7
GW	7.4	8.1	19.9
ED	0.1	0.2	0.1
IC-1	0.0	0.0	19.1
IC-10	0.7	-0.5	16.4
IC-15	0.6	-0.2	6.6
FC	0.0	0.0	7.6
Total	23.3	7.7	69.0

Table 32 - Emission Fractions for Minimum Fugitive Emissions for the
F-gases and Methane for the Wet Season (Without Carbon Dioxide)

Cover Type	Scaled-up Fraction (%)	
	F-gases	CH_4
AF	46.4	0.2
GW	23.9	26.1
ED	0.4	0.8
IC-1	0.1	0.0
IC-10	2.4	-1.6
IC-15	2.0	-0.8
FC	0.1	0.0
Total	75.2	24.8

Table 33 – Maximum Fugitive Emissions and Emission Fractions for the F-gases, Methane, and Carbon Dioxide for the Wet Season

Cover Type	Total Fugitive Emissions (CO_2E Tonnes/year)		
	F-gases	CH_4	CO_2
AF	3.51E+03	1.22E+03	-5.16E+01
GW	1.10E+03	7.71E+02	1.63E+03
ED	4.64E+01	8.08E+02	9.93E+01
IC-1	1.90E+00	0.00E+00	1.41E+03
IC-10	5.43E+01	1.08E+04	3.92E+03
IC-15	6.21E+01	6.17E+04	6.55E+03
FC	3.54E+00	-8.51E-01	6.20E+02
Total	4.78E+03	7.53E+04	1.42E+04

Table 34 - Emission Fractions for Maximum Fugitive Emissions for the F-gases, Methane, and Carbon Dioxide for the Wet Season

Cover Type	Total Fugitive Emissions Fraction (%)		
	F-gases	CH_4	CO_2
AF	3.7	1.3	-0.1
GW	1.2	0.8	1.7
ED	0.0	0.9	0.1
IC-1	0.0	0.0	1.5
IC-10	0.1	11.4	4.2
IC-15	0.1	65.5	7.0
FC	0.0	0.0	0.7
Total	5.1	79.9	15.0

Table 35 - Emission Fractions for Maximum Fugitive Emissions for the F-gases and Methane for the Wet Season (Without Carbon Dioxide)

Cover Type	Scaled-up Fraction (%)	
	F-gases	CH_4
AF	4.4	1.5
GW	1.4	1.0
ED	0.1	1.0
IC-1	0.0	0.0
IC-10	0.1	13.5
IC-15	0.1	77.1
FC	0.0	0.0
Total	6.0	94.0

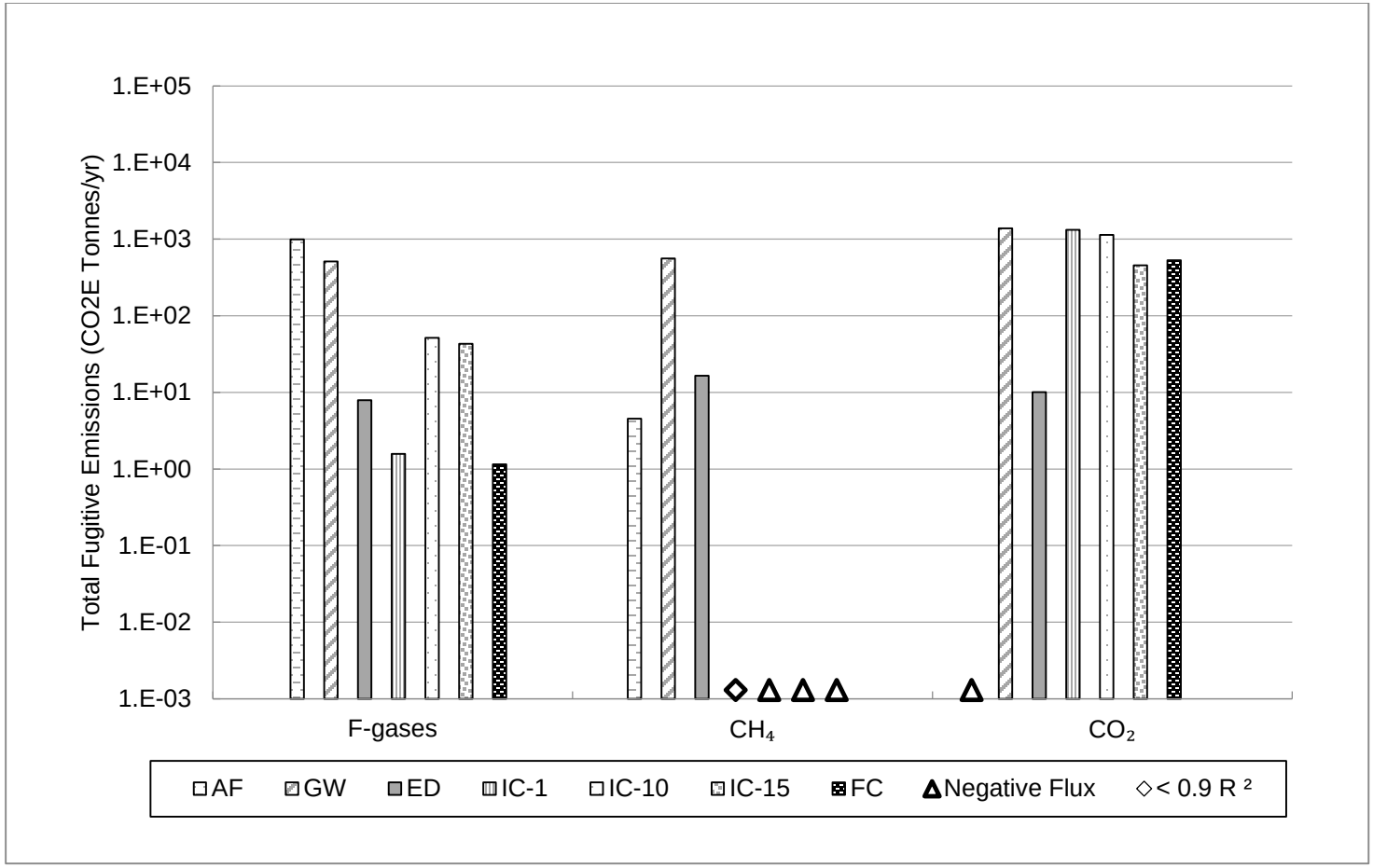

Figure 51 – Minimum Fugitive Emissions for
the F-gases, Methane, and Carbon Dioxide for the Wet Season

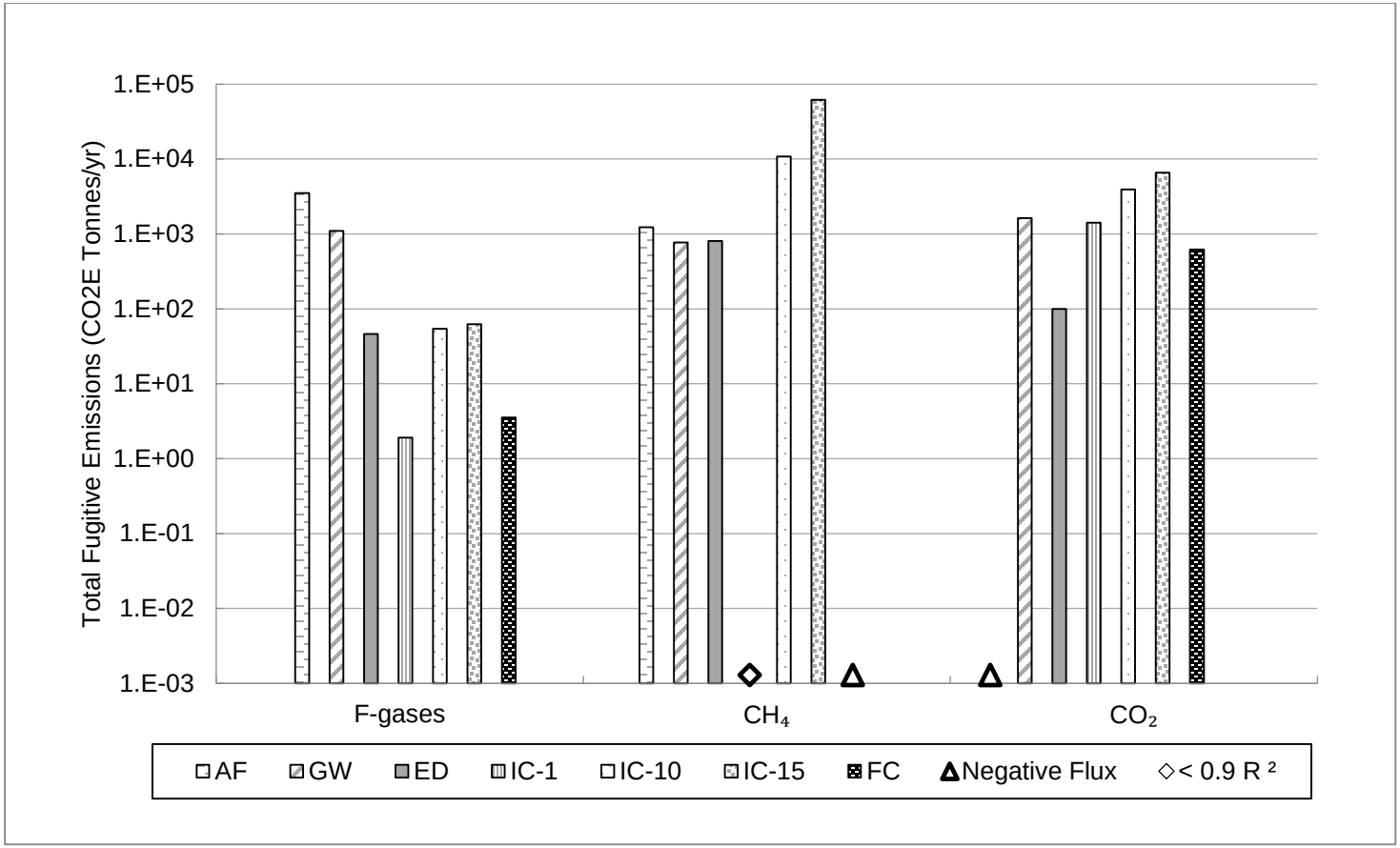

Figure 52 - Maximum Fugitive Emissions for
the F-gases, Methane, and Carbon Dioxide for the Wet Season

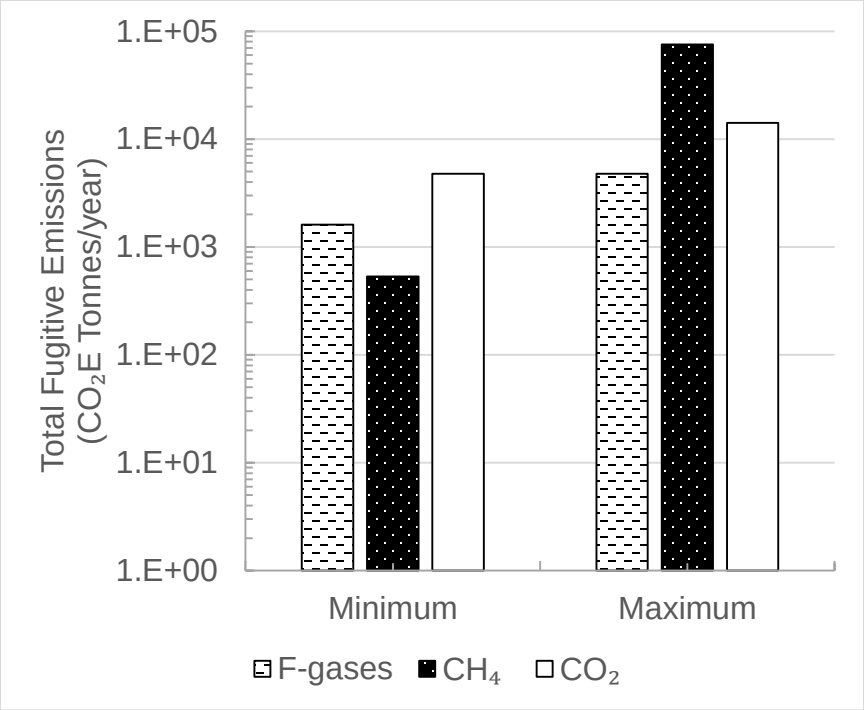

Figure 53 - Minimum and Maximum Fugitive Emissions for the F-gases, Methane, and Carbon Dioxide for the Wet Season

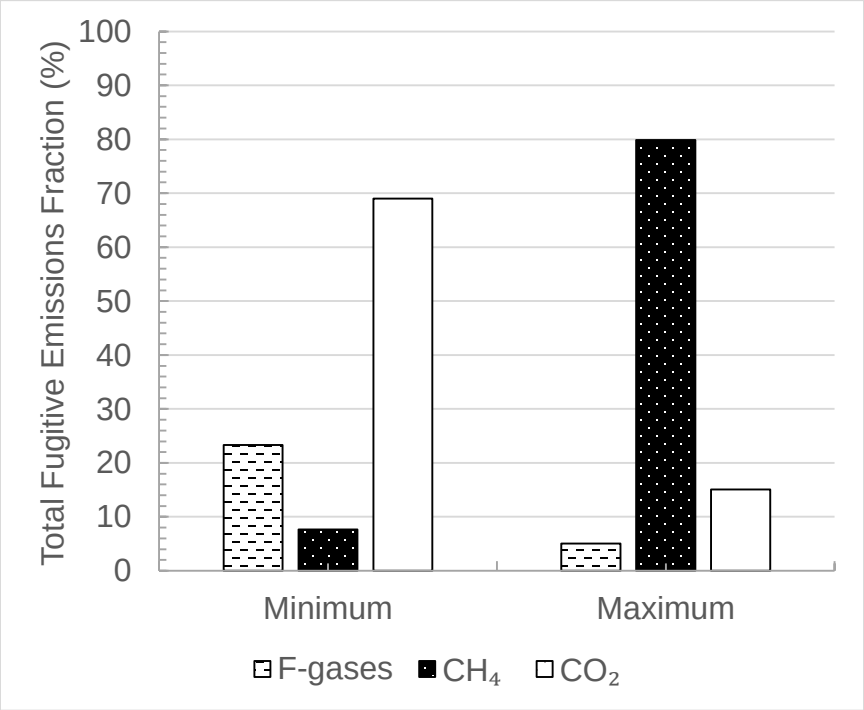

Figure 54 – Emission Fractions for the F-gases, Methane, and Carbon Dioxide for the Wet Season

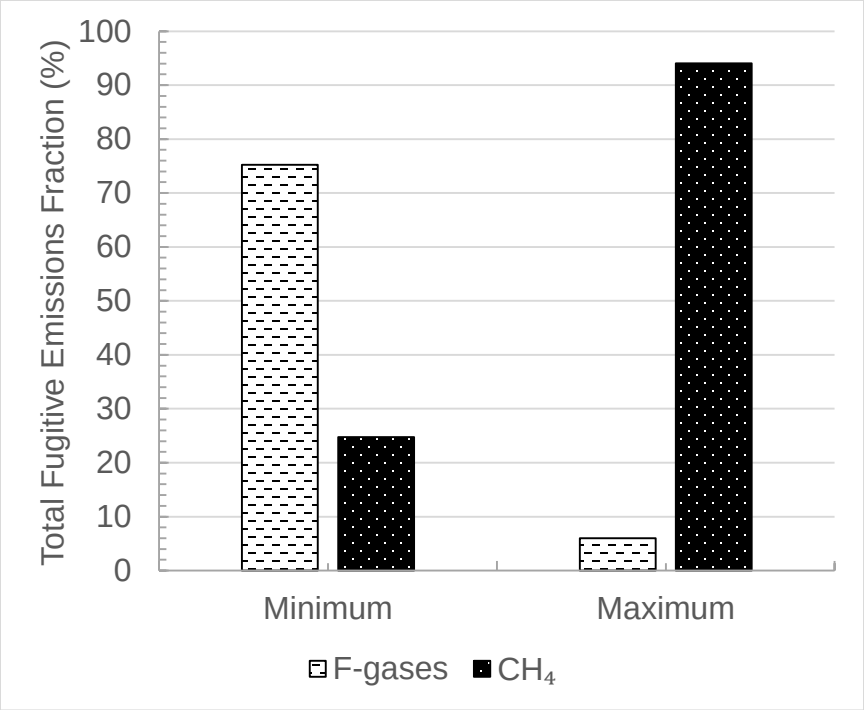

Figure 55 –Emission Fractions for the F-gases and Methane for the Wet Season (Without Carbon Dioxide)

Table 36 - Minimum and Maximum Fugitive Emissions for the Twelve F-gases, Methane, and Carbon Dioxide for the Dry Season

Compounds	Surface Emissions (CO_2E Tonnes/year)			
	Minimum	%	Maximum	%
CFC-11	9.15E+01	0.42	4.40E+02	0.93
CFC-12	1.43E+01	0.07	4.88E+01	0.10
CFC-113	2.81E-01	0.00	8.76E-01	0.00
CFC-114	4.18E+00	0.02	1.79E+01	0.04
HCFC-21	3.89E-02	0.00	1.45E-01	0.00
HCFC-22	2.93E+00	0.01	9.92E+00	0.02
HCFC-141b	7.64E+00	0.04	2.74E+01	0.06
HCFC-142b	2.25E+00	0.01	5.81E+00	0.01
HCFC-151a	N/A	N/A	N/A	N/A
HFC-134a	1.26E+01	0.06	3.09E+01	0.07
HFC-152a	2.65E-01	0.00	2.12E+00	0.00
HFC-245fa	4.11E+00	0.02	1.85E+01	0.04
Total F-gases Emissions	1.40E+02	0.65	6.03E+02	1.28
CH_4	1.72E+04	79.81	3.50E+04	74.28
CO_2	4.22E+03	19.54	1.15E+04	24.44
Total Surface Emissions (F-gases + CH_4 + CO_2)	2.16E+04	100.00	4.71E+04	100.00

Table 37 – Minimum and Maximum Fugitive Emissions for the Twelve F-gases and Methane for the Dry Season (Without Carbon Dioxide)

Compounds	Surface Emissions (CO_2E Tonnes/year)			
	Minimum	%	Maximum	%
CFC-11	9.15E+01	0.53	4.40E+02	1.24
CFC-12	1.43E+01	0.08	4.88E+01	0.14
CFC-113	2.81E-01	0.00	8.76E-01	0.00
CFC-114	4.18E+00	0.02	1.79E+01	0.05
HCFC-21	3.89E-02	0.00	1.45E-01	0.00
HCFC-22	2.93E+00	0.02	9.92E+00	0.03
HCFC-141b	7.64E+00	0.04	2.74E+01	0.08
HCFC-142b	2.25E+00	0.01	5.81E+00	0.02
HCFC-151a	N/A	N/A	N/A	N/A
HFC-134a	1.26E+01	0.07	3.09E+01	0.09
HFC-152a	2.65E-01	0.00	2.12E+00	0.01
HFC-245fa	4.11E+00	0.02	1.85E+01	0.05
Total F-gases Emissions	1.40E+02	0.81	6.03E+02	1.69
CH_4	1.72E+04	99.19	3.50E+04	98.31
Total Surface Emissions (F-gases + CH_4)	1.74E+04	100.00	3.56E+04	100.00

Table 38 – Minimum Fugitive Emissions and Emission Fractions for the F-gases, Methane, and Carbon Dioxide for the Dry Season

Cover Type	Total Fugitive Emissions (CO_2E Tonnes/year)		
	F-gas	CH_4	CO_2
AF	9.36E+01	2.34E+02	-3.36E+00
GW	4.37E+00	1.20E+02	2.89E+01
ED	2.04E+01	8.98E+02	-4.29E+01
IC-1	2.17E+00	0.00E+00	1.40E+02
IC-10	1.42E+00	-1.04E+01	2.38E+02
IC-15	1.81E+01	1.60E+04	3.80E+03
FC	-1.55E-02	2.34E-01	5.55E+01
Total	1.40E+02	1.72E+04	4.22E+03

Table 39 - Emission Fractions for Minimum Fugitive Emissions for the F-gases, Methane, and Carbon Dioxide for the Dry Season

Cover Type	Total Fugitive Emissions Fraction (%)		
	F-gas	CH_4	CO_2
AF	0.4	1.1	0.0
GW	0.0	0.6	0.1
ED	0.1	4.2	-0.2
IC-1	0.0	0.0	0.7
IC-10	0.0	0.0	1.1
IC-15	0.1	74.1	17.6
FC	0.0	0.0	0.3
Total	0.6	79.8	19.5

Table 40 –Emission Fractions for Minimum Fugitive Emissions for the F-gases and Methane for the Dry Season (Without Carbon Dioxide)

Cover Type	Scaled-up Fraction (%)	
	F-gases	CH_4
AF	0.5	1.3
GW	0.0	0.7
ED	0.1	5.2
IC-1	0.0	0.0
IC-10	0.0	-0.1
IC-15	0.1	92.0
FC	0.0	0.0
Total	0.8	99.2

Table 41 – Maximum Fugitive Emissions for the F-gases, Methane, and Carbon Dioxide for the Dry Season

Cover Type	Total Fugitive Emissions (CO_2E Tonnes/year)		
	F-gas	CH_4	CO_2
AF	4.21E+02	1.87E+03	-3.36E+00
GW	4.55E+00	1.83E+02	7.14E+01
ED	1.27E+02	3.29E+03	-5.57E-01
IC-1	3.92E+00	0.00E+00	2.26E+03
IC-10	6.23E+00	2.00E+00	1.00E+03
IC-15	4.03E+01	2.97E+04	7.67E+03
FC	-1.55E-02	2.34E-01	5.25E+02
Total	6.03E+02	3.50E+04	1.15E+04

Table 42 - Emission Fractions for Maximum Fugitive Emissions for the F-gases, Methane, and Carbon Dioxide for the Dry Season

Cover Type	Total Fugitive Emissions Fraction (%)		
	F-gas	CH_4	CO_2
AF	0.9	4.0	0.0
GW	0.0	0.4	0.2
ED	0.3	7.0	0.0
IC-1	0.0	0.0	4.8
IC-10	0.0	0.0	2.1
IC-15	0.1	62.9	16.3
FC	0.0	0.0	1.1
Total	1.3	74.3	24.4

Table 43 - Emission Fractions for Maximum Fugitive Emissions for the F-gases and Methane for the Dry Season (Without Carbon Dioxide)

Cover Type	Scaled-up Fraction (%)	
	F-gases	CH_4
AF	1.2	5.2
GW	0.0	0.5
ED	0.4	9.2
IC-1	0.0	0.0
IC-10	0.0	0.0
IC-15	0.1	83.3
FC	0.0	0.0
Total	1.7	98.3

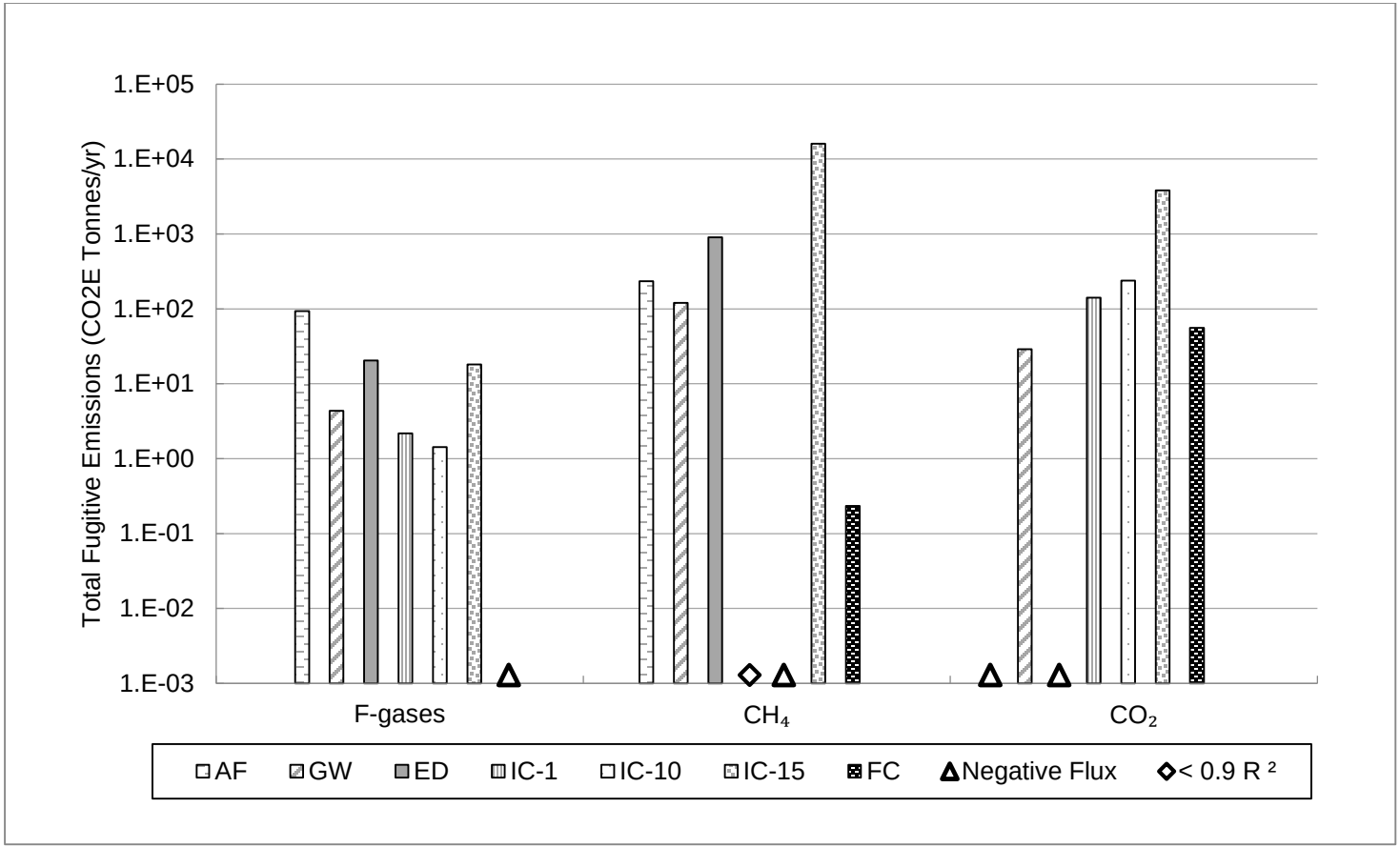

Figure 56 - Minimum Fugitive Emissions for
the F-gases, Methane, and Carbon Dioxide for the Dry Season

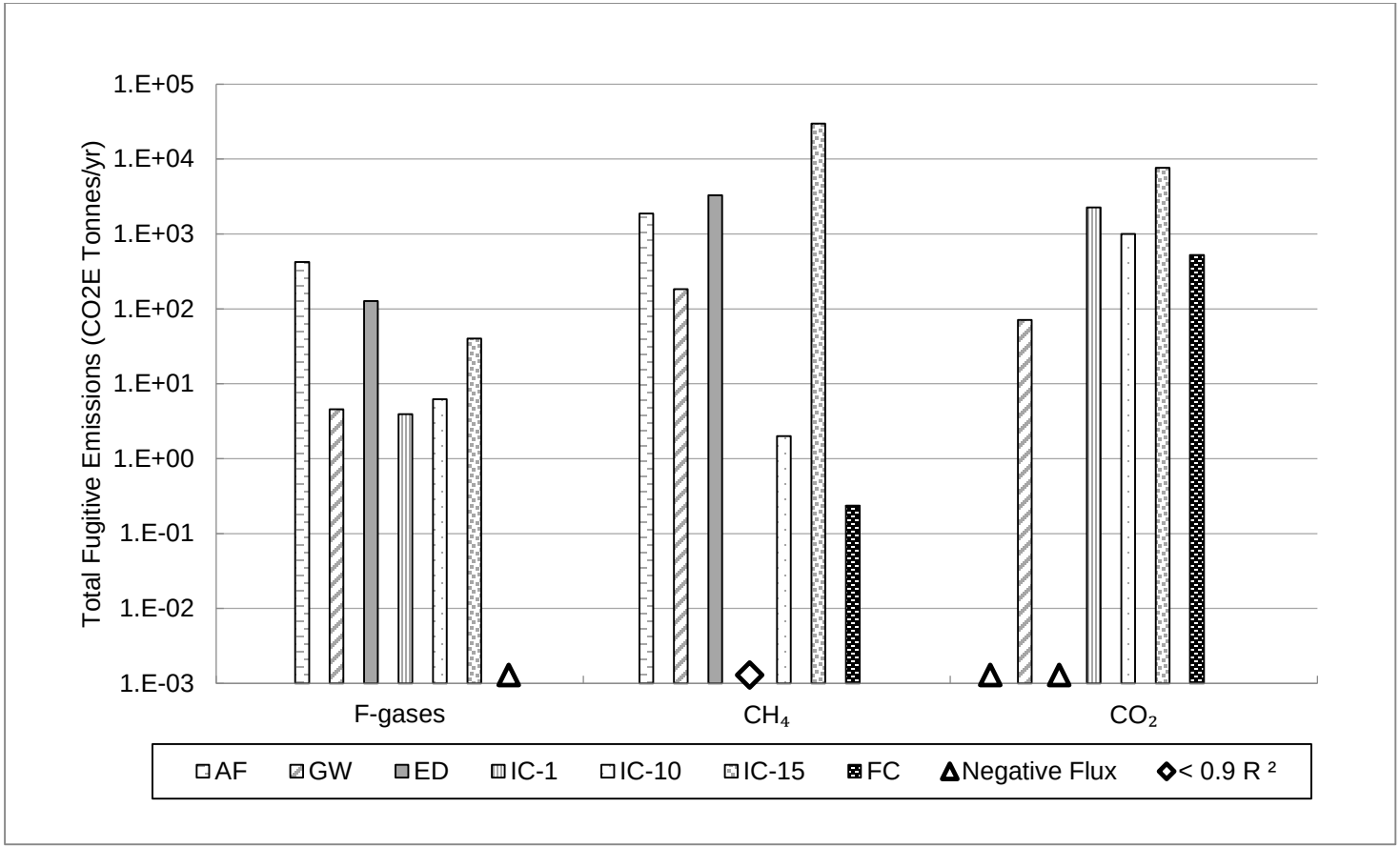

Figure 57 - Maximum Fugitive Emissions for
the F-gases, Methane, and Carbon Dioxide for the Dry Season

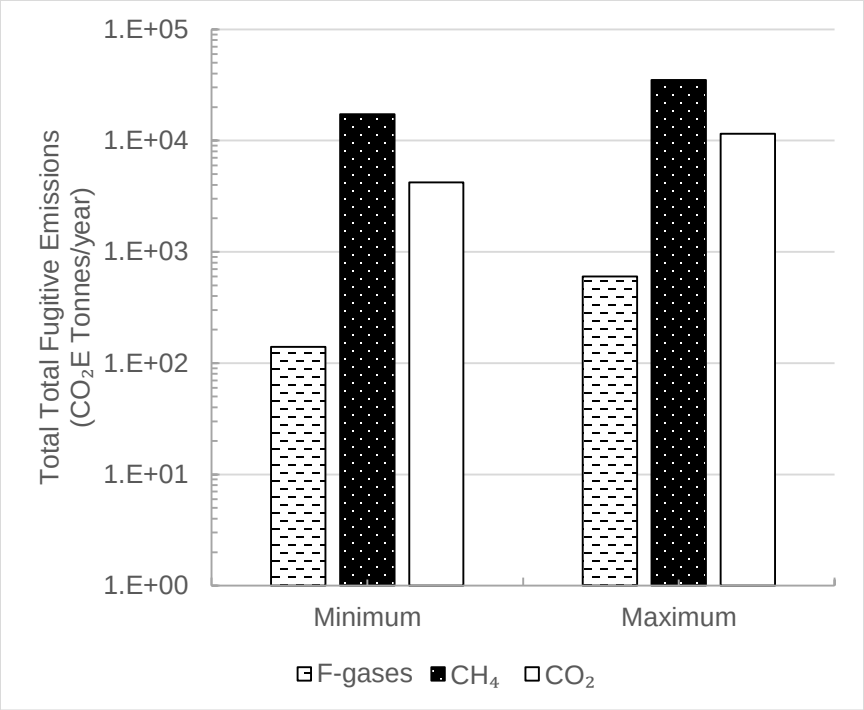

Figure 58 - Minimum and Maximum Fugitive Emissions for the F-gases, Methane, and Carbon Dioxide for the Dry Season

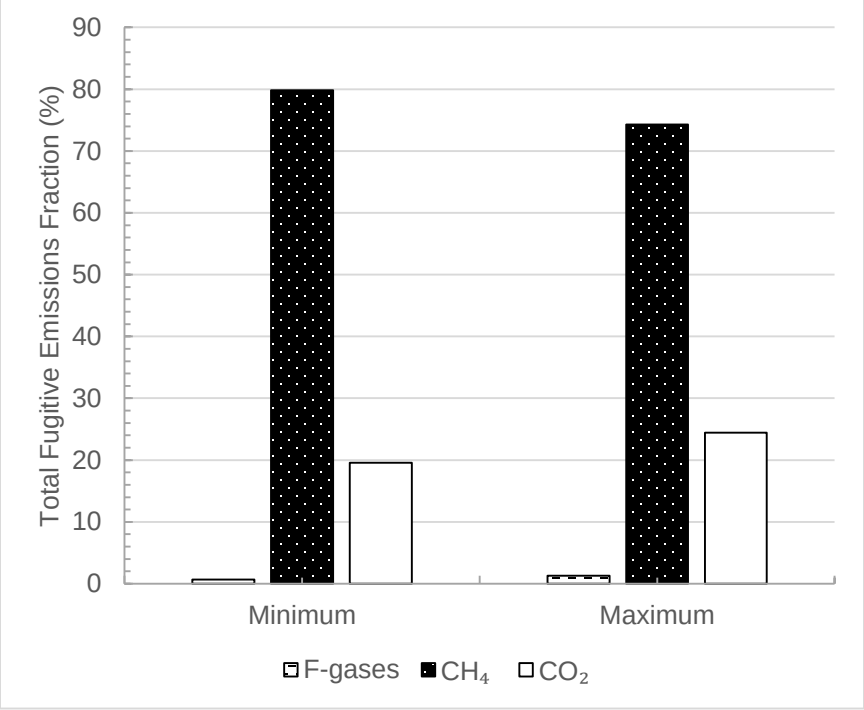

Figure 59 - Emission Fractions for the F-gases, Methane, and Carbon Dioxide for the Dry Season

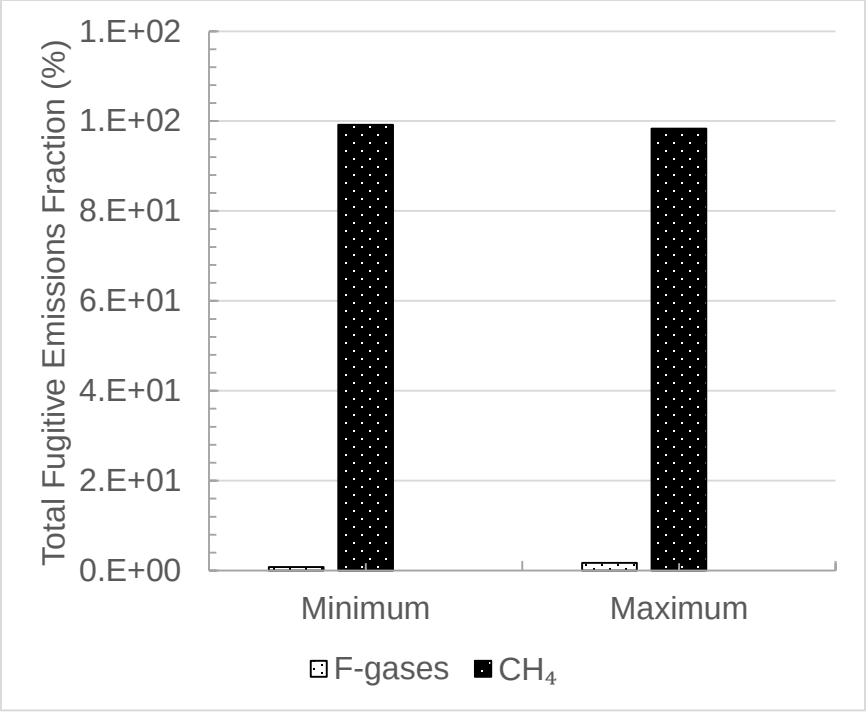

Figure 60 - Emission Fractions for the F-gases and Methane for the Dry Season (Without Carbon Dioxide)

Table 44 - Minimum and Maximum Fugitive Emissions for the Twelve F-gases, Methane, and Carbon Dioxide for the Prorated Season

Compounds	Surface Emissions (CO_2E Tonnes/year)			
	Minimum	%	Maximum	%
CFC-11	6.23E+02	4.77	2.16E+03	2.90
CFC-12	5.53E+01	0.42	1.30E+02	0.17
CFC-113	1.20E+00	0.01	1.81E+00	0.00
CFC-114	1.68E+01	0.13	2.47E+01	0.03
HCFC-21	2.30E+01	0.18	9.25E+01	0.12
HCFC-22	1.11E+01	0.09	1.83E+01	0.02
HCFC-141b	1.91E+02	1.46	4.07E+02	0.55
HCFC-142b	1.28E+01	0.10	1.54E+01	0.02
HCFC-151a	N/A	N/A	N/A	N/A
HFC-134a	3.84E+01	0.29	9.27E+01	0.12
HFC-152a	4.36E+00	0.03	1.57E+01	0.02
HFC-245fa	1.95E+01	0.15	7.41E+01	0.10
Total F-gases Emissions	9.96E+02	7.62	3.03E+03	4.07
CH_4	7.53E+03	57.62	5.84E+04	78.40
CO_2	4.54E+03	34.75	1.31E+04	17.54
Total Surface Emissions (F-gases + CH_4 + CO_2)	1.31E+04	100.00	7.45E+04	100.00

Table 45 – Minimum and Maximum Fugitive Emissions for the Twelve F-gases and Methane for the Prorated Season (Without Carbon Dioxide)

Compounds	Surface Emissions (CO_2E Tonnes/year)			
	Minimum	%	Maximum	%
CFC-11	6.23E+02	7.30	2.16E+03	3.51
CFC-12	5.53E+01	0.65	1.30E+02	0.21
CFC-113	1.20E+00	0.01	1.81E+00	0.00
CFC-114	1.68E+01	0.20	2.47E+01	0.04
HCFC-21	2.30E+01	0.27	9.25E+01	0.15
HCFC-22	1.11E+01	0.13	1.83E+01	0.03
HCFC-141b	1.91E+02	2.24	4.07E+02	0.66
HCFC-142b	1.28E+01	0.15	1.54E+01	0.03
HCFC-151a	N/A	N/A	N/A	N/A
HFC-134a	3.84E+01	0.45	9.27E+01	0.15
HFC-152a	4.36E+00	0.05	1.57E+01	0.03
HFC-245fa	1.95E+01	0.23	7.41E+01	0.12
Total F-gases Emissions	9.96E+02	11.68	3.03E+03	4.93
CH_4	7.53E+03	88.32	5.84E+04	95.07
Total Surface Emissions (F-gases + CH_4)	8.53E+03	100.00	6.14E+04	100.00

Table 46 - Minimum Fugitive Emissions for the
F-gases, Methane, and Carbon Dioxide for the Prorated Season

Cover Type	Scaled-up Emissions (CO_2E Tonnes/year)		
	F-gases	CH_4	CO_2
AF	6.17E+02	1.01E+02	-3.13E+01
GW	3.00E+02	3.76E+02	8.12E+02
ED	1.31E+01	3.87E+02	-1.22E+01
IC-1	1.83E+00	0.00E+00	8.26E+02
IC-10	3.05E+01	-2.37E+01	7.57E+02
IC-15	3.26E+01	6.71E+03	1.86E+03
FC	6.61E-01	-3.95E-01	3.30E+02
Total	9.95E+02	7.55E+03	4.54E+03

Table 47 - Emission Fractions for Minimum Fugitive Emissions for the
F-gases, Methane, and Carbon Dioxide for the Prorated Season

Cover Type	Scaled-up Fraction (%)		
	F-gases	CH_4	CO_2
AF	4.7	0.8	-0.2
GW	2.3	2.9	6.2
ED	0.1	3.0	-0.1
IC-1	0.0	0.0	6.3
IC-10	0.2	-0.2	5.8
IC-15	0.2	51.3	14.2
FC	0.0	0.0	2.5
Total	7.6	57.7	34.7

Table 48 - Emission Fractions for Minimum Fugitive Emissions for the
F-gases and Methane for the Prorated Season (Without Carbon Dioxide)

Cover Type	Scaled-up Fraction (%)	
	F-gases	CH_4
AF	7.2	1.2
GW	3.5	4.4
ED	0.2	4.5
IC-1	0.0	0.0
IC-10	0.4	-0.3
IC-15	0.4	78.5
FC	0.0	0.0
Total	11.7	88.3

Table 49 - Maximum Fugitive Emissions for the
F-gases, Methane, and Carbon Dioxide for the Prorated Season

Cover Type	Scaled-up Emissions (CO_2E Tonnes/year)		
	F-gases	CH_4	CO_2
AF	2.21E+03	1.49E+03	-3.13E+01
GW	6.41E+02	5.24E+02	9.77E+02
ED	8.02E+01	1.85E+03	5.73E+01
IC-1	2.75E+00	0.00E+00	1.76E+03
IC-10	3.41E+01	6.25E+03	2.69E+03
IC-15	5.29E+01	4.82E+04	7.02E+03
FC	2.05E+00	-3.95E-01	5.80E+02
Total	3.03E+03	5.84E+04	1.31E+04

Table 50 – Emission Fractions for Maximum Fugitive Emissions for the
F-gases, Methane, and Carbon Dioxide for the Prorated Season

Cover Type	Scaled-up Fraction (%)		
	F-gases	CH_4	CO_2
AF	3.0	2.0	0.0
GW	0.9	0.7	1.3
ED	0.1	2.5	0.1
IC-1	0.0	0.0	2.4
IC-10	0.0	8.4	3.6
IC-15	0.1	64.8	9.4
FC	0.0	0.0	0.8
Total	4.1	78.4	17.5

Table 51 - Emission Fractions for Maximum Fugitive Emissions for the
F-gases and Methane for the Prorated Season (Without Carbon Dioxide)

Cover Type	Scaled-up Fraction (%)	
	F-gases	CH_4
AF	3.6	2.4
GW	1.0	0.9
ED	0.1	3.0
IC-1	0.0	0.0
IC-10	0.1	10.2
IC-15	0.1	78.6
FC	0.0	0.0
Total	4.9	95.1

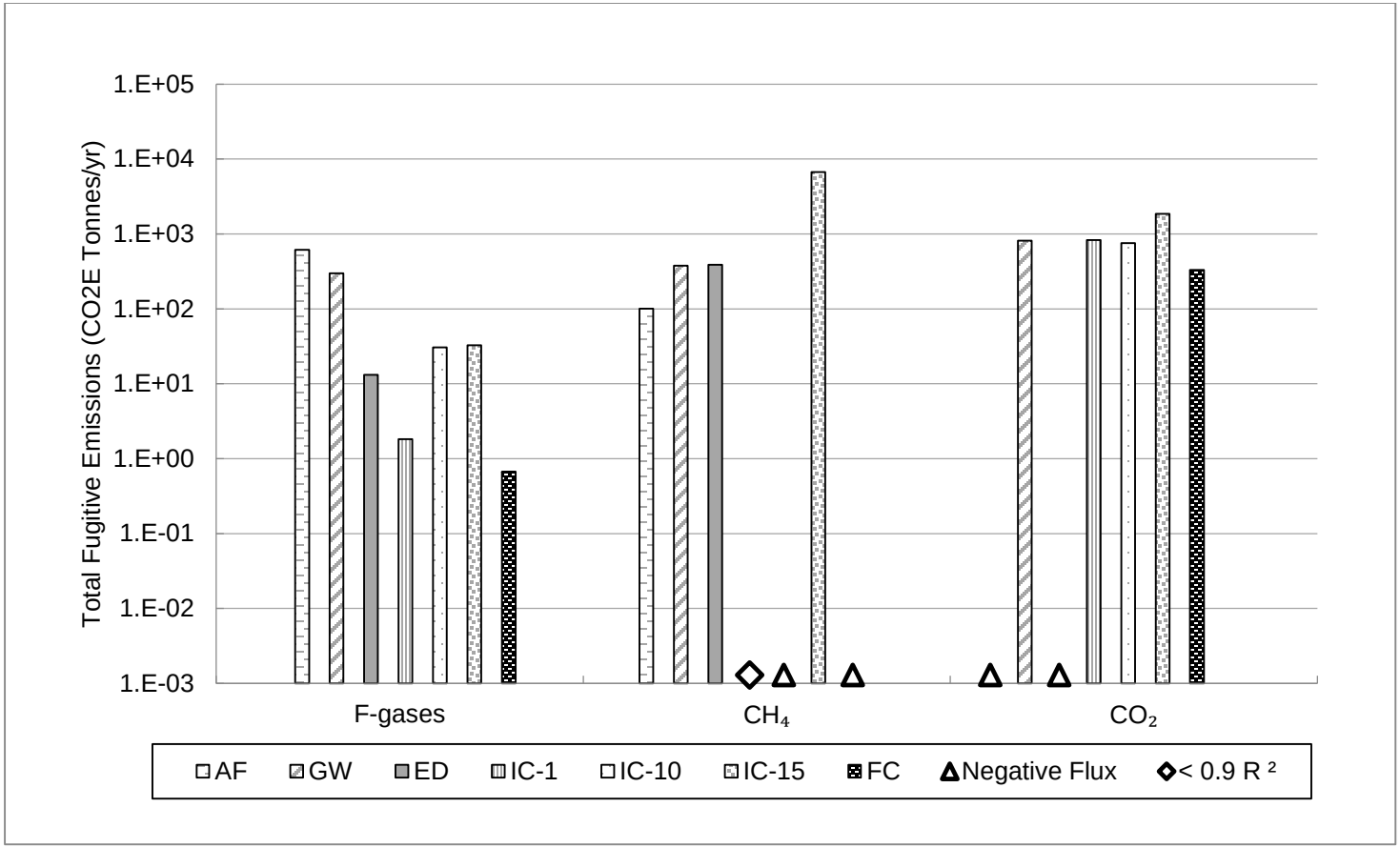

Figure 61 - Minimum Fugitive Emissions for the
F-gases, Methane, and Carbon Dioxide for the Prorated Season

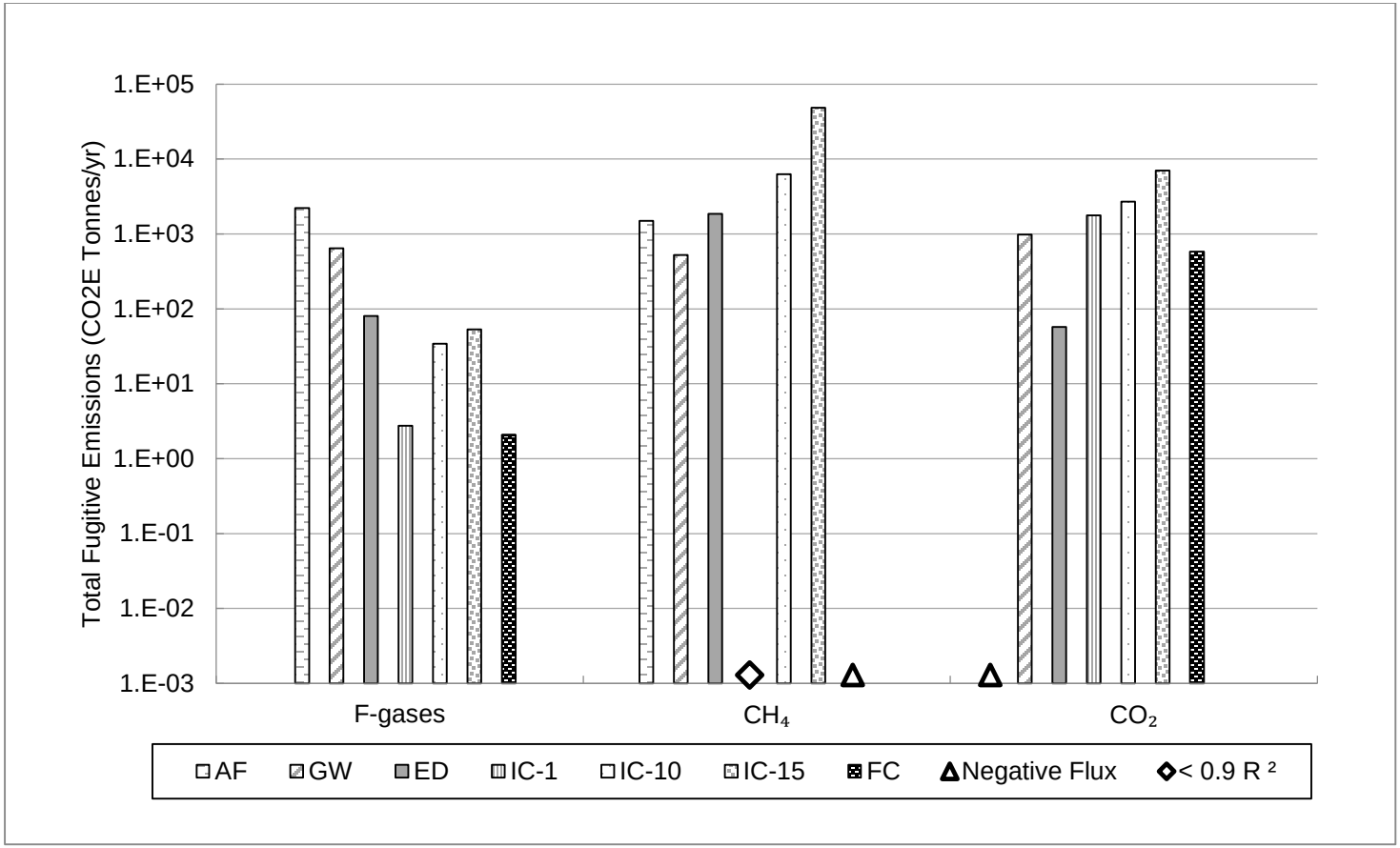

Figure 62 - Maximum Fugitive Emissions for the
F-gases, Methane, and Carbon Dioxide for the Prorated Season

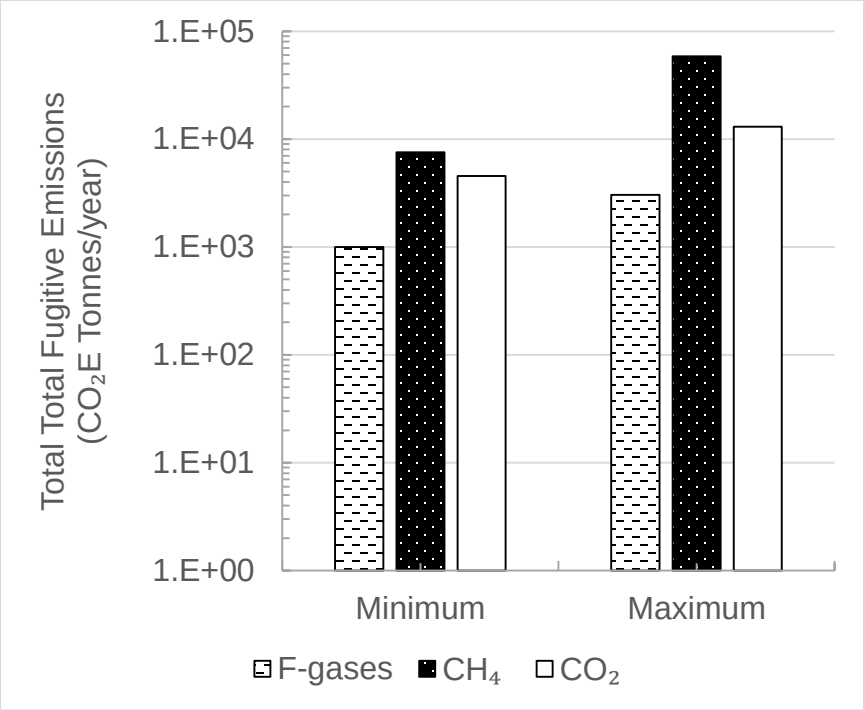

Figure 63 - Minimum and Maximum Fugitive Emissions for the F-gases, Methane, and Carbon Dioxide for the Prorated Season

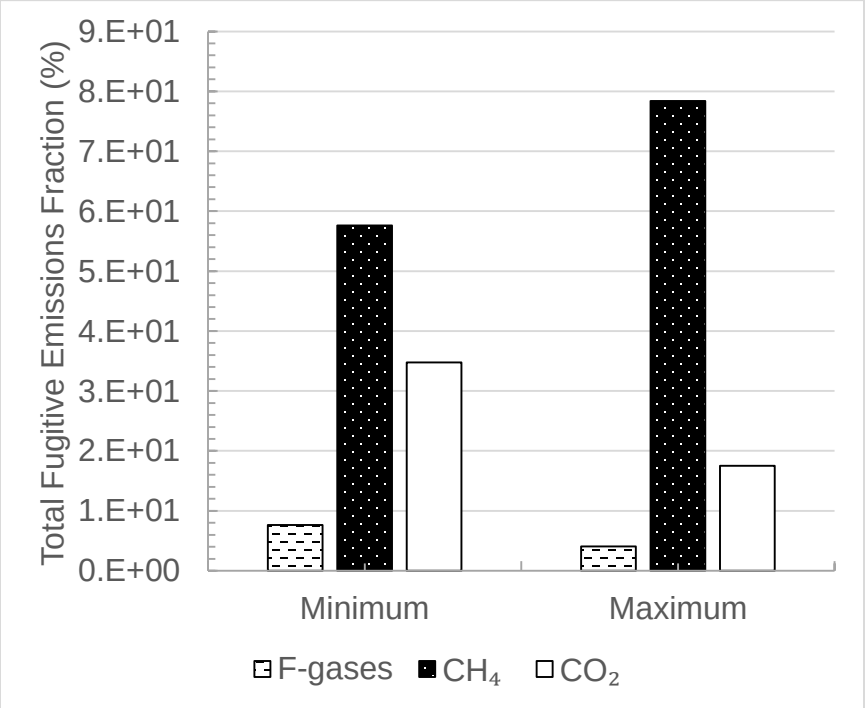

Figure 64 - Emission Fractions for the F-gases, Methane, and Carbon Dioxide for the Prorated Season

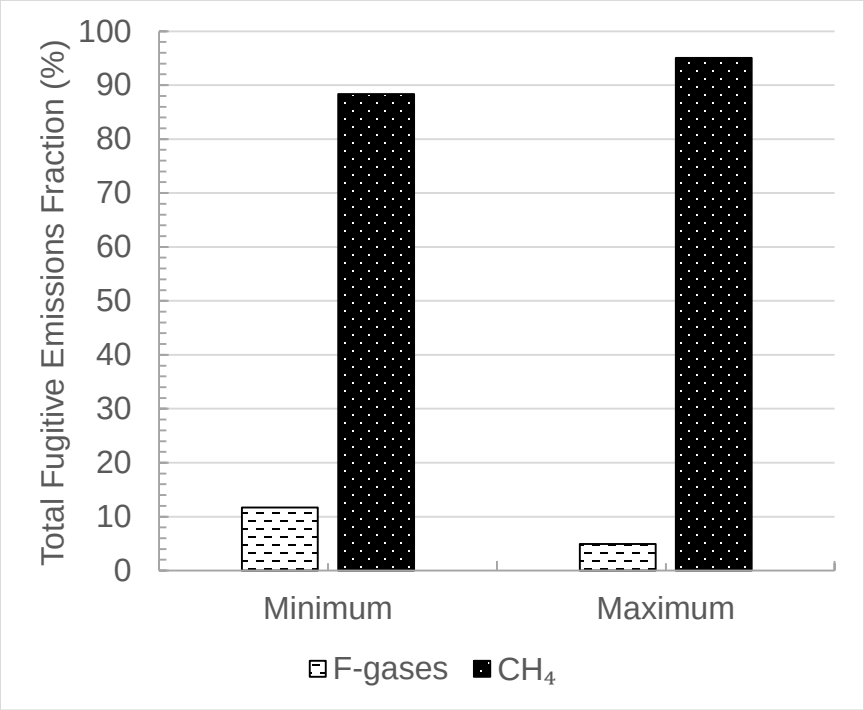

Figure 65 - Emission Fractions for the F-gases and Methane for the Prorated Season (Without Carbon Dioxide)

The total fugitive emission rates from the site ranged from 6,900 to 94,000 CO_2E tonnes per year during the wet season conditions, from 21,000 to 47,000 CO_2E tonnes per year for the dry season conditions, and from 13,000 to 75,000 CO_2E tonnes per year during the prorated season (representing weighted average of 58% wet season emission rate and 42% dry season emission rate in a 12-month calendar year). The total fugitive F-gas emission rates ranged from 1,600 to 4,800 CO_2E tonnes per year during the wet season condition, from 140 to 600 CO_2E tonnes per year during the dry season condition, and from 1,000 to 3,000 CO_2E tonnes per year during the prorated season. The total fugitive methane emission rates ranged from 530 to 75,000 CO_2E tonnes per year during the wet season condition, 17,000 to 35,000 CO_2E tonnes per year during the dry season condition, and from 7,500 to 58,000 CO_2E tonnes per year during the prorated season. The total fugitive carbon dioxide emission rates ranged from 5,000 to 14,000 CO_2E tonnes per year during the wet season condition, 4,200 to 12,000 CO_2E tonnes per year during the dry season condition, and from 4,500 to 13,000 CO_2E tonnes per year during the prorated season.

Between the F-gases, methane, and carbon dioxide, methane typically had the highest emission fraction (on CO_2E basis) whereas the F-gases had the lowest emission fractions. During the wet season, the methane fraction varied highly ranging from 8% to 80%. During the dry season, the methane fraction ranged from 74 to 80%.

Among the seven locations, the highest methane emissions were associated with measurement at IC-15. The high methane emissions were likely due to presence of large amount of waste (i.e. high waste height) and large surface area at the cell. In addition, among the intermediate cover locations, IC-15 had the youngest average waste age (approximately 7.2 years) while the majority of the waste present at IC-1 and IC-10 were considerably older age waste (approximately average waste age of 22 and 14 years, respectively). Thus, it is likely that the presence of younger waste age, high surface area coverage, and high waste height had caused high methane emissions from the Cell 15 location.

Whereas only the 1% of the landfill cover consisted of AF cover, high percentage of F-gas emissions (ranging from 62% to 73% and 67% to 70% for the wet and dry season, respectively) were attributed to AF cover. The high F-gas emissions from the auto fluff cover system were likely due to presence of high residual F-gas blowing agents within the auto fluff material as indicated in Scheutz et al. (2007c, 2011b). In addition, the open structure of the auto fluff likely also contributed to higher F-gas emissions due to high permeability of the material. The above results indicate that the auto fluff daily cover can lead to significant F-gas emissions in a landfill environment.

Between the wet and dry season, larger variance (i.e. larger difference between minimum and maximum emission rate) was observed during the wet season, whereas considerably smaller variance (i.e. smaller difference between

minimum and maximum emission rate) were observed during the dry season. This can likely be attributed to combination of difference in gas-phase and aqueous diffusion rate and heterogeneity in water-filled void spaces introduced by precipitation during the wet season. Since the gas flow through the cover system was not disturbed by presence of water during the dry season, the variability in emission rates were considerably smaller as indicated by small range between minimum and maximum emission rates and similar bar graph trends or identical increase and decrease across all constituents for both minimum and maximum emission values.

5.3 Comparison with the Model Based Emission Value

The scaled up emission values were compared to the greenhouse gas emission value available for Potrero Hills Landfill on EPA Facility-level Greenhouse Gas Emission Database (USEPA 2014e). The emissions reported to the EPA must follow the emission calculation guideline in 40 CFR Part 98, Subpart HH "Mandatory Greenhouse Gas Reporting: Municipal Solid Waste Landfills", which requires the use of IPCC-FOD model to estimate emissions of greenhouse gas from landfills (IPCC 2006). Since the emission calculation guideline specified in 40 CFR part 98, Subpart HH does not include potent greenhouses gases such as F-gases, only the field derived methane emission values were compared to the emission values available from EPA for the site. The model incorporates FOD landfill gas generation model, landfill gas collection and destruction efficiency, and methane oxidation factor to estimate site-specific fugitive emission rate. The

methane emission rate comparison is presented in Table 52 and Figure 66. In comparison to emission value calculated using the FOD model reported in EPA (USEPA 2014e) and calculated using the WIP-LFG correlation equation, the scaled up emission values were one to three orders of magnitude lower.

Table 52 – Fugitive Methane Emission Value Comparisons

Description	Methane Emissions (CO_2E Tonne/year)
Minimum (Wet Season)	531
Maximum (Wet Season)	75,264
Minimum (Dry Season)	17,234
Maximum (Dry Season)	35,006
Minimum (Prorated season)	7,532
Maximum (Prorated season)	58,389
IPCC-FOD Model (2014)	283,668
WIP - LFG Correlation Equation (Spokas et al. 2015)	257,967

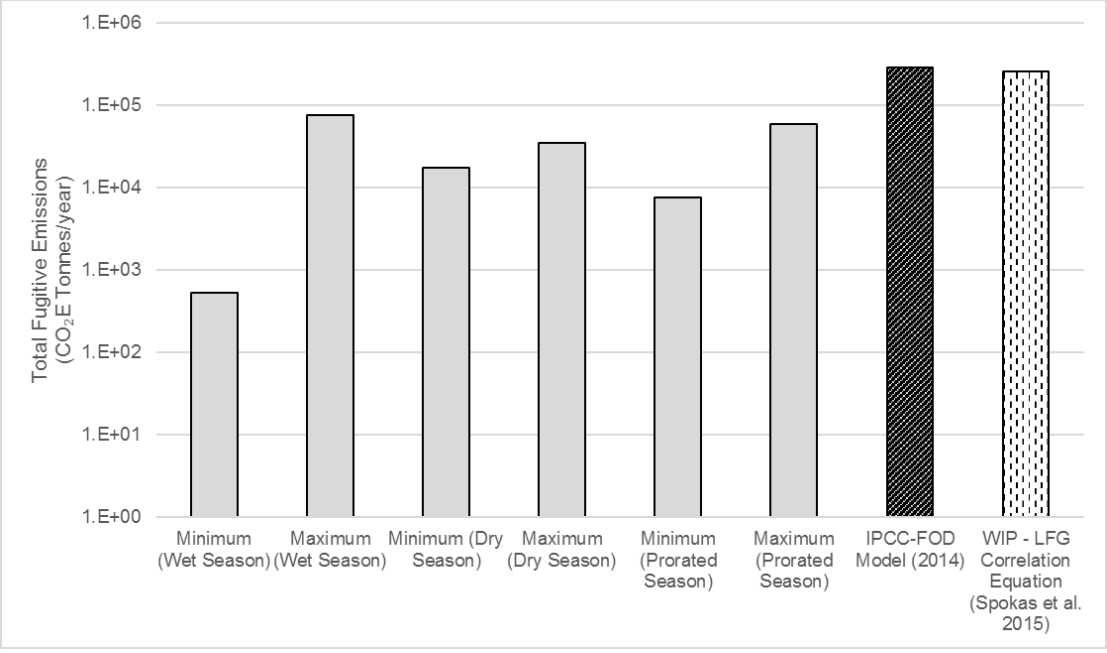

Figure 66 – Total Fugitive Methane Emissions Comparisons

Chapter 6: Summary and Conclusions

Due to historical usage of F-gas BAs in insulation foams, high volume of F-gas containing insulation foams are expected in landfills. Emissions of F-gases to the atmosphere are a concern due to their GWPs as well as due to high ODPs of certain class of F-gases. Very limited field data for landfill emissions of F-gases is available in literature.

A field investigation coupled with laboratory analysis was conducted to assess emissions of chlorinated and fluorinated hydrocarbons (i.e., F-gases) from a landfill in California. The following twelve F-gases were quantified during this investigation: CFC-11, CFC-12, CFC-113, CFC-114, HCFC-21, HCFC-22, HCFC-141b, HCFC-142b, HCFC-151a, HFC-134a, HFC-152a, and HFC-245fa. The field testing program was conducted at a landfill located in Suisun, CA. The surface flux for the twelve F-gases, methane, and carbon dioxide was determined using static large scale flux chamber with a 1 m x 1 m area. Various types of cover systems ranging from daily, intermediate, to final cover system were tested. The tests were conducted over both wet and dry season to evaluate effect of seasonal variation on landfill surface emissions. The seven locations tested at the site had varying waste height, waste age, and cover material present at each location. In addition, destruction efficiencies for the twelve F-gases were measured based on the inlet and outlet concentration of the on-site flare system. This study characterized not only the effect of seasonal variation, but also the effect of cover type, waste height,

and waste age on F-gases emissions, which has not been previously reported in literature.

Based on the F-gas, methane, and carbon dioxide surface fluxes measured during the wet and dry seasons, the following conclusions were drawn:

1. The F-gas flux values for the daily covers (AF, GW, and ED) were in the 10^{-8} to 10^{-1} g m^{-2} day^{-1} range and 10^{-7} to 10^{-2} g m^{-2} day^{-1} range for the wet and dry season, respectively.
2. The F-gas flux values for the intermediate covers (IC-1, IC-10, and IC-15) were in the -10^{-6} to 10^{-4} g m^{-2} day^{-1} range and -10^{-6} to 10^{-4} g m^{-2} day^{-1} range for the wet and dry season, respectively.
3. The F-gas flux values for the final covers (FC) were in the 10^{-7} to 10^{-5} g m^{-2} day^{-1} range and -10^{-7} to 10^{-6} g m^{-2} day^{-1} range for the wet and dry season, respectively. F-gas fluxes for the final covers had the highest number of below detection limit cases as well as lower than R^2 threshold cases.
4. The highest fluxes were measured for CFC-11, HCFC-21, and HCFC-141b in the wet season and for CFC-11, HCFC-141b, and HFC-134a in the dry season across the seven cover locations.
5. The lowest fluxes were measured for CFC-113 and CFC-114 for both wet and dry seasons.
6. The average F-gas flux decreased from daily, intermediate, to final cover for both wet and dry season.

7. The highest F-gas flux rates were measured from the auto fluff cover for both seasons. The F-gas present in the auto fluff likely contributed to high emissions of the F-gases from the auto fluff cover.
8. Among the intermediate covers, the highest F-gas flux values were measured from the location with the highest waste height and the youngest waste (IC-15), whereas the lowest F-gas flux values were from the location with the lowest waste height and the oldest waste (IC-1). The test results indicate that the F-gas fluxes typically decrease with increasing waste age and with decreasing waste height.
9. The level of variation observed for the F-gas fluxes between the seven cover types and between the two seasons were different. The average F-gas flux between the seven locations varied up to four orders of magnitude. However, the differences in F-gas flux between the two seasons were considerably less (up to two orders of magnitude in variation). Greater variations were observed between the seven test locations indicating that physical factors such as cover thickness, cover material, waste age, and waste height had greater influence on F-gas emissions than environmental factors such as precipitation temperature, barometric pressure, or precipitation.

Based on the destruction efficiencies of the F-gas, the following conclusions were drawn:

1. The inlet F-gas concentrations (i.e., raw gas) ranged from 10^3 to 10^6 pptv.

2. The highest F-gas concentration was measured for HFC-134a while the lowest F-gas concentration was measured for CFC-113.
3. The destruction efficiencies of the flare system for the twelve F-gases were above 99.5% for all gases.

Based on the facility-wide emissions calculations for twelve F-gases, methane, and carbon dioxide, following conclusions were drawn:

1. The total fugitive emission rates from the site ranged from 6,900 to 94,000 CO_2E tonnes per year during the wet season condition, from 21,000 to 47,000 CO_2E tonnes per year during the dry season condition, and from 13,000 to 75,000 CO_2E tonnes per year during the prorated season.
2. The total fugitive F-gas emission rates ranged from 1,600 to 4,800 CO_2E tonnes per year during the wet season condition, from 140 to 600 CO_2E tonnes per year during the dry season condition, and from 1,000 to 3,000 CO_2E tonnes per year during the prorated season.
3. The total fugitive methane emission rates ranged from 530 to 75,000 CO_2E tonnes per during the wet season condition, 17,000 to 35,000 CO_2 tonnes per year during the dry season condition, and from 7,500 to 58,000 CO_2E tonnes per year during the prorated season.
4. The total fugitive carbon dioxide emission rates ranged from 5,000 to 14,000 CO_2E tonnes per year during the wet season condition, 4,200 to 12,000 CO_2E tonnes per year during the dry season condition, and from 4,500 to 13,000 CO_2E tonnes per year during the prorated season.

5. In comparison to emission values calculated using the IPCC-FOD model (IPCC 2006) reported in EPA and calculated using the WIP-LFG correlation equation (Spokas et al. 2015), the scaled-up emission values were one to three orders of magnitude lower.

REFERENCES

Abichou, T., Chanton, J., Powelson, D., Fleiger, J., Escoriaza, S., Lei, Y., and Stern, J., (2006a), “Methane Flux and Oxidation at Two Types of Intermediate Landfill Covers,” *Waste Management*, Vol. 26, 1305-1312.

Abichou, T., Chanton, J., and Powelson, D., (2006b), “Field Performance of Biocells, Biocovers, and Biofilters to Mitigate Greenhouse Gas Emissions from Landfills,” Final Report, Prepared for Florida Center for Solid and Hazardous Waste Management.

Abichou, T., Powelson, D., Chanton, J., Escoriaza, S., and Stern, J., (2006c), “Characterization of Methane Flux and Oxidation at a Solid Waste Landfill,” *Journal of Environmental Engineering*, Vol. 132(2), 1305-1312.

Advanced Global Atmospheric Gas Experiment (AGAGE), (2009), "A*LE/GAGE/AGAGE Data through September 2008*," *http://www.agage.eas.gatech.edu/data.htm*, Last Accessed March, 25, 2015.

Advanced Global Atmospheric Gas Experiment (AGAGE), (2014), "ALE/GAGE/AGAGE Data," *http://agage.eas.gatech.edu /data.html*, Last Accessed: April, 1, 2015.

Albanna, M., and Fernandes, L., (2009), "Effect of Temperature, Moisture Content, and Fertilizer Addition on Biological Oxidation in Landfill Cover Soils," *Waste Management 13*, 187-195.

Allen, M., Braithwaite, A., and Hills, C. H., (1997), "Trace Organic Compounds in Landfill Gas at Seven UK Waste Disposal Sites," *Environmental Science & Technology, Vol. 31*, 1054-1061.

ARCADIS U.S., Inc., (2012), "Quantifying Methane Abatement Efficiency at Three Municipal Solid Waste Landfills, Durham NC8: Final Report," Prepared for the USEPA, #RN990271.0007.

Ban-Weiss, A., Cao, L., Bala, G., and Caldeira, K., (2010), "Dependence of Climate Forcing and Response on the Altitude of Black Carbon Aerosols" *Springer Verlag*.

Barlaz, M., Green, R., Chanton, J., Goldsmith, C., and Hater, G., (2004), "Evaluation of a Biologically Active Cover for Mitigation of Landfill Gas Emissions," *Environ. Sci. Technol. 38*, 4891-4899.

Barletta, B., Meinardi, S., Simpson, I. J., Rowland, F. S., Chan, C. Y., Wang, X., Zou, S., Chan, L. Y., and Blake, D. R., (2006), "Ambient Halocarbon Mixing Ratios in 45 Chinese Cities," *Atmospheric Environment,* Vol. 40, 7706-7719.

Barletta, B., Nissenson, P., Meinardi, S., Dabdub, D., Rowland, F. S., VanCuren R. A., Pederson, J., Diskin, G. S., and Blake D. R., (2011), "HFC-152a and HFC-134a Emission Estimates and Characterization of CFCs, CFC Replacements, and other Halogenated Solvents Measured during the 2008 ARCTAS Campaign (CARB phase) over the South Coast Air Basin of California," *Atmospheric Chemistry and Physics, 11(6)*, 2655-2669.

Barletta B., Carreras-Sospedra, M., Cohan, A., Nissenson, P., Dabdub, D., Meinardi, S., Atlas, E., Lueb, R., Holloway, J., Ryerson, T., Pederson, J., VanCuren, R., and Blake, D., (2013), "Emission estimates of HCFCs and

HFCs in California from the 2010 CalNex study," *Geophysical Research: Atmospheres,* Vol. 118, 2019-2030.
Bender, M., and Conrad, R., (1994), "Kinetics of Methane Oxidation in Oxic Soils," *Chemosphere,* Vol. 26(1), 687-696.
Blaga, A. (1974). "Rigid Thermosetting Plastic Foams," A National Council Canada Division of Building Research.
Blake, N. J., Blake, D. R., Simpson, I., Meinardi, S., Swanson, A. L., Lopez, J. P., Katzenstein, A. S., Barletta, B., Shirai, T., Atlas, E., Sachse, G., Avery, M., Vay, S., Fuelberg, H. E., Kiley, C. M., Kita, K., and Rowland, F. S., (2003), "NMHCs and Halocarbons in Asian Continental Outflow during the Transport and Chemical Evolution over the Pacific (TRACE-P) Field Campaign: Comparison With PEM-West B," *Journal of Geophysical Research,* Vol. 108.
Boeckx, P. and Van Cleemput, O, (1996), "Methane Oxidation in a Neutral Landfill Cover Soil: Influence of Moisture Content, Temperature, and Nitrogen Turnover," *Journal of Environmental Quality,* Vol. 25(1), 178-183.
Boeckx, P., Cleemput, O. V., and Villaralvo, I. D. A., (1996), "Methane Emission from a Landfill and the Methane Oxidizing Capacity of its Covering Soil," *Soil Biology and Biochemistry,* Vol. 28(10), 1397-1405.
Bogner, J., and Spokas, K., (2010), "Chapter 11: Landfills," *Methane and Climate Change,* Earthscan Publishers, UK.
Bogner, J., Spokas, K., Burton, E., Sweeney, R., and Corona, V, (1995), "Landfills as Atmosperic Sources and Sinks," *Chemosphere*, Vol. 31(9), 4119-4130.
Bogner, J., Spokas, K. A., and Burton, E. A., (1997a), "Kinetics of Methane Oxidation in a Landfill Oxidation Experiment, and Modeling of Net Methane Emissions," *Environmental Scient & Technology*, Vol. 31, 2504-2514.
Bogner, J., Spokas, K., Niemann, M., Niemann, L., and Baker, J., (1997b), "Emissions of Non-Methane Organic Compounds at an Illinois (USA) Landfill Site: Preliminary Field Measurements," *Environmental Impact, Aftercare, and Remediation of Landfills*, 127-138.
Bogner, J., Scheutz, C., Chaton, J., Blake, D., Morcet, M., Aran, C., and Kjeldsen, P., (2003), "Field Measurement of Non-Methane Organic Compouund Emissions from Landfill Cover Soils," *Proceedings of the Ninth International Waste Management and Landfill Symposium*, Caligari, Italy.
Bogner, J., Scheutz, C., Chanton, J., Blake, D., Morcet, M., Aran, C., and Kjeldsen, P., (2004), “Field Measurements of Speciated Hazardous Air Pollutant Emissions from Landfill Cover Soils,” *Proceedings of the SWANA 27th International Landfill Gas Symposium*, Published by Solid Waste Association of North America, Silver Spring, MD.
Bogner, J., Pipatti, R., Hasimoto, S., Diaz, C., Mareckova, K., Diaz, L., Kjeldsen, P., Monni, S., Faaij, A., Gao, Q., Zhang, T., Ahmed, M. A., Sutamigardja, R. T. M. and Gregory, R., (2007), "Mitigation of Greenhouse Gas Emissions from Waste: Conclusions and Strategies" from the

Intergovernmental Panel on Climate Change (IPCC) Fourth Assessment Report: Working Group III (Mitigation)," *Waste Management Research*, Vol. 26, 11-32.

Bogner, J., Chanton, J., Blake, D., Abichou, T., and Powelson, D., (2010), "Effectiveness of Florida Landfill Biocover for Reduction of Methane and NMHC Emissions". *Environ. Science and Technology*, Vol. 44, 1197-1203.

Bogner, J., Spokas, K., and Chanton, J., (2011), "Seasonal Greenhouse Gas Emissions (Methane, Carbon Dioxide, Nitrouse Oxide) from Engineered Landfills: Daily, Intermediate, and Final California Landfill Cover Soils," *Journal of Environmental Quality,* Vol. 140, 1010-1020.

Börjesson, G. and Svensson, B. H., (1997), "Seasonal and Diurnal Methane Emissions from a Landfill and their Regulation by Methane Oxidation," *Waste Management and Research,* Vol. 15, 33-54.

Börjesson, G., Chanton, J., and Svensson, B., (2001), "Methane Oxidation in Two Swedish Landfill Covers Measured with Carbon-13 to Carbon-12 Isotope Ratios," *Journal of Environmental Quality,* Vol. 30(2), 369-376.

Brookes, B. I. and Young, P. J., (1983), "The Development of Sampling and Gas Chromatography-Mass Spectrometry Analytical Procedures to Identify and Determine the Minor Organic Components of Landfill Gas," *Talanta,* Vol. 30(9), 665-676.

Building Research Establishment (BRE), (2002), "Test Report: Cutting of fridges: Estimating CFC releases & recommended best practice. Test report number 208329," United Kingdom: Building Research Establishment.

Building Science Corporation (BSC), (2007). "Guide to Insulating Sheathing," *http://www.buildingscience.com/documents/guides-and-manuals/gm-guideinsulating-*, Last Accessed March 2nd, 2013.

Cal Recycle, (1991), "Appliance Recycling Guide," Retrieved from Cal Recycle: http://www.calrecycle.ca.gov/Publications/Documents/Special%5C50094022.pdf

Cal Recycle, (2006), "Targeted Statewide Waste Characterization Study: Detailed Characterization of Construction and Demolition Waste," California Environmental Protection Agency Integrated Waste Management Board.

Cal Recycle, (2008), "California 2008 Statewide Waste Characterization Study - Report, Submitted to California Environmental Protection Agency," California Environmental Protection Agency Integrated Waste Management Board.

Cal Recycle, (2009). "Interview with Greg Dick of the California Integrated Waste Management Board, Construction and Demolition Waste Volumes and Practices Discussed," California Environmental Protection Agency Integrated Waste Management Board.

Cal Recycle, (2014), "Annual California Waste Disposal: Total Instate Waste Disposal: 1995-2013," *http://www.calrecycle.ca.gov/ LGCentral/Reports/ ReportViewer.aspx?ReportName=ReportEDRSAnnualWaste*, Last Accessed June 4th, 2015.

Caleb Management Services, (2004), "Determination of Comparative HCFC and the Emission Profiles for the Foam and Refrigeration Sector until 2015," Bristol, UK.

Caleb Management Services, (2011), "Developing a California Inventory for Ozone Depleting Substances (ODS) and Hydrofluorocarbon (HFC) Foam Banks and Emissions from Foams," Bristol, UK.

California Air Resources Board, (2008), "Draft Concept Paper Foam Recovery and Destruction Program," *http://www.arb.ca.gov /cc/hgwpss/meetings/ 021508/Foam_Recovery_ Destruction*, Last Accessed August, 10, 2015.

California Air Resources Board, (2011), "California Waste Disposal and ADC/AIC Amounts Supporting Data."

California Waste Management Board, (1988), "Landfill Gas Characterization," State of California, Sacremento, CA.

Cecchi, F., Pavan, P., Musacco, A., Mata-Alvarez, J., and Vallini, G., (1993), "Digesting the Organic Fraction of Municipal Solid Waste: Moving from Mesophilic (37°C) to Thermophilic (55°C) Conditions," *Waste Manage. Res.,* Vol. 11, 403-414.

Christophersen, M., Kjeldsen, P., Holst, H., and Chanton, J, (2001), "Lateral Gas Transport in Soil Adjacent to an Old Landfill: Factors Governing Emissions and Methane Oxidation," *Waste Management & Research,* Vol. 19(6), 595-612.

Cianciarelli, D. and Borgeau, S., (2002), “Characterization of Emissions from a 1 MWe Reciprocating Engine Fired with Landfill Gas,” *Environment Canada,* Report ERMD 2001-03.

Colman, J. J., Swanson, A. L., Meinardi, S., Sive, B. C., Blake, D. R., and Rowland, F. S., (2001), "Landfill Methane Emission Measured by Enclosure and Atmospheric Tracer Methods," *Journal of Geophysical Research, American Geophysical Union,* Vol. 101(D11), 16711-16719.

Crawford, R. and Throne, J. (2002), "Rotational Molding Technology," William Andrew Publishing, Norwich, NY;

Czepiel, P. M., Mosher, B., Crill, P. M., and Harris, R. C., (1996), "Quantifying the Effect of Oxidation on Landfill Methane Emissions," *Journal of Geophysical Research,* Vol. 101(D11), 16, 721-729.

Czepiel, P. M., Shorter, J. H., Mosher, B., Allwine, E., McManus, J. B., Harriss, R. C., Kolb, C. E., and Lamb, B. K., (2003), "The Influence of Atmospheric Pressure on Landfill Methane Emissions," *Waste Management,* Vol. 23(7), 593-598.

Daniel, J. S., Velders, G. J. M., (2007), "Halocarbons Scenarios, Ozone Depletion Potentials, and Global Warming Potentials. Scientific Assessment of Ozone Depletion 2006."

Deipser, A. and Stegmann, R, (1994), “The Origin and Fate of Volatile Trace Components in Municipal Solid Waste Landfills,” *Waste Management & Researc*h, Vol. 12(2), 129-139.

Dent, C. G., Scott, P., and Baldwin, G., (1986), "Study of Landfill Gas Composition at Three UK Domestic Waste Disposal Sites," *Proceedings of Energy from Landfill Gas Conference,* 130-149.

Department of Toxic Substances Control (DTSC), (2002), "Draft Report California's Automobile Shredder Waste Initiative," *http://www.dtsc.ca.gov /HazardousWaste/upload/HWMP_ REP_ASW_draft.pdf*, Last Accessed February 15, 2015.

Department of Toxic Substances Control (DTSC), (2007), "Changes to the Appliance Recycling Program, Fact Sheet 2007" *http://www.dtsc.ca.gov /HazardousWaste/Mercury/Certified_ Appliance_Recycler.cfm*, Last Accessed February 11, 2015.

Derwent, R. G., Simmonds, P. G., Greally, B.R., O'doherty, S., McCulloch, A., Manning, A., Reimann, S., Folini, D., and Vollmer, M.K., (2007), "The phase-in and phase-out of European emissions of HCFC-141b and HCFC-142b under the Montreal Protocol: evidence from observations at Mace Head, Ireland and Jungfraujoch, Switzerland from 1994 to 2004," *Atmos. Environ.,* Vol. 41, 757-767.

Devore, J., (2008), "Probability and Statistics, Seventh Edition," Thompson Brooks/Cole, Belmont, CA.

Dieckmann, J. and Magid, H, (1999), "Global Comparative Analysis of HFC and Alternative Technologies for Refrigeration, Air Conditioning, Foam, Solvent, Aerosol Propellant, and Fire Protection Applications," *http://unfccc.int/files/methods_and_science/other_ methodological_issues /interactions_with_ozone_layer/application/pdf/adlittle.pdf*, Last Accessed January 29th, 2015.

Dunham, Michael, (2009), "Interview with Michael Dunham from JACO Environmental Inc."

Duranceau, C. and Spangenberger, J., (2011), "All Auto Shredding: Evaluation of Automotive Shredder Residue Generated by Shredding Only Vehicles. Report from the Argonne National Laboratory," http://www.ipd.anl.gov /anlpubs/2011/09/70931.pdf, Last Accessed February 18th, 2015.

Elkins, J. W. (1999), "Chlorofluorocarbons (CFCs)," In *The Chapman & Hall Encyclopedia of Environmental Science*, 78-80, Kluwer Academic.

Environment Canada, (1999), "Characterization of Emissions from a 812 kWe Reciprocating Engine Fired with Landfill Gas. Meloche Landfill, Kirkland, Québec," *Environment Canada,* Report ERMD 99-05*.*

Environment Canada, (2000a), "Characterization of Emissions from a Power Boiler Fired with Landfill Gas. Report ERMD 99-07".

Environment Canada, (2000b), "Characterization of Emissions from an Enclosed Flare. Trail Road Landfill, Ottawa-Carleton, Ontario," *Environment Canada,* Report ERMD 2000-02."

Environment Canada, (2000c), "Characterization of Emissions from a 1 MWe Reciprocating Engine Fired with Landfill Gas. BFI Usine de Triage Lachenaie Ltée Lachenaie, Québec. Report ERMD 2001-03."

Environment Canada, (2000d), "Characterization of Emissions from a 925 kWe Reciprocating Engine Fired with Landfill Gas. Waterloo Regional Landfill, Waterloo, Ontario," *Environment Canada,* Report ERMD 2000-04*.*

Environment Canada, (2002), "Characterization of Emissions from a 1 MWe Reciprocating Engine Fired with Landfill Gas. BFI Usine de Triage Lachenaie Ltée Lachenaie, Québec. Report ERMD 2001-03."

Environment Canada, (2005), "Characterization of Emissions from a 26 kWe Micro Turbine Fired with Landfill Gas. Shepard Landfill, Calgary, Alberta," *Environment Canada,* Report ERMD 2004-02.

Fabian, P., Borchers, B., Kruger, C., Lal, S., (1985), "The Vertical-Distribution of CFC-114 in the Atmosphere," *Geophysical Research,* Vol. 90, 13,091-13,093.

Farquhar, G. J., and Rovers, F. A., (1973), "Gas production during refuse decomposition," *Water, Air, Soil Pollution,* Vol. 2(4), 483-495.

Fenhann, J., (2000), "Industrial non-energy, non-CO2 greenhouse gas emissions," *Techn Forecasting Soc Change,* Vol. 63, 313-334.

Figueroa, R. A., (1993), "Methane Oxidation in Landfill Top Soils," *Proceedings of the 4th International Landfill Symposium,* Vol. 1, 701-716.

Forster, P., Solomon, S., Qin, D., Manning, M., Chen, Z., Marquis, M., Averyt, M., Tignor, M., and Miller, H., (2007), "Changes in Atmospheric Constituents in Radiative Forcing In: Climate Change 2007: The Physical Science Basis Contribution of Working Group I to the IPCC,".

Fredenslund, A. M., Scheutz, C., and Kjeldsen, P., (2005), "Disposal of Refrigerators - Freezers in the US: State of the Practice 2. Determination of Content of Blowing Agent in Pre- and Post-Shredded Foam and Modeling," *Environment & Resources DTU*, 1-26.

Godwin, D. S., Van Pelt, M. M., and Peterson, K., (2003), "Modeling Emissions of High Global Warming Potential Gases," *http://www.epa.gov/ttnchie1 /conference/ei12/green/godwin.pdf*, Last Accessed February 4th, 2015.

Google Earth, (2015), Potrero Landfill. Retrieved June 16, 2015.

Greer, A. and Cianciarelli, D., (2005), "Characterization of Emissions from a 26 kWe Micro Turbine Fired with Landfill Gas at Shepard Landfill: Calgary, Alberta," *Environment Canada,* Report ERMD 2004-02.

Hanson, J. L., Yesiller, N., and Kendall, L. A., (2005), "Integrated Temperature and Gas Analysis at a Municipal Solid Waste Landfill," *Proceedings of the 16th International Conference on Soil Mechanics and Geotechnical Engineering, Geotechnology in Harmony with the Global Environment,* Vol. 4, 2265-2268.

Hanson, J. L., Yesiller, N., Howard, K. A., Liu, W. L., and Cooper, S. P., (2006), "Effects of Placement Conditions on Decomposition of Municipal Solid Wastes in Cold Regions," *Current Practices in Cold Regions Engineering - Proceedings of the 13th International Conference on Cold Regions Engineering,* 1-11.

Hanson, J. L., Yesiller, N., Von Stockhausen, S. A., and Wong, W. W., (2010), "Compaction Characteristics of Municipal Solid Waste," *Journal of Geotechnical and Geoenvironmental Engineering*, 1095-1102.

Harper, M. (2000), "Sorbent Trapping of Volatile Organic Compound from Air". *Journal of Chromatography*, 129-151.

Hartman, B., (2013), "How to Collect Reliable Soil-Gas Data for Upward Risk Assessments," *http://www.handpmg.com/articles/ lustline44-flux-chambers-part,* Last Accessed March 4th, 2015.

Hartz, K. E., Klink, R. E., and Ham, R. K., (1982), "Temperature Effects: Methane Generation from Landfill Samples," *Journal of the Environmental. Engineering Division,* Vol. 108 (4), 629-638.

Haynes, W. M. and Lide, D. R., (2015), *CRC Handbook of Chemistry and Physics: A Ready-Reference Book of Chemical and Physical Data*, CRC Press, Boca Raton, FL.

Heinmayer, A. and McNamara, N., (2011), "Comparing the Closed Static Versus the Closed Dynamic Chamber Flux Methodology: Implications for Soil Respiration Studies". *Plant Soil*, 145-151.

Hodson, E. L., Martin, D., and Prinn, R. G. (2010), "The Municipal Solid Waste Landfill as a Source of Ozone-Depleting Substances in the United States and United Kingdom," *Atmospheric Chemistry and Physics*, 1988-1910.

Hofstetter Gastechnik, A. G., (2014), "Production of LFG, Conditions for gas, production, Quality, Quantity, Gas Yield and Energy Value," Retrieved Feb 25, 2015, from http://www.slideshare.net/HOFSTGAS/1-production-of-landfill-gas

Holtz, R., Kovacs, W, and Sheahan, T., (2010), *An Introduction to Geotechnical Engineering*, 2nd Ed., Prentice Hall, New York, NY.

Houghton, J. T., G. J. Jenkins, and J. J. Ephraums, (1990), "Climate Change. The IPCC Scientific Assessment," Cambridge, United Kingdom.

Houi, D., Paul, E., and Couturier, C., (1997), "Heat and mass transfer in landfills and biogas recovery," *Proc., 6th Int. Waste Management and Landfill Symposuim*, 101-108.

Intergovernmental Panel on Climate Change (IPCC), (2001), "Climate Change 2001: The Scientific Basis." *http://www.ipcc.ch/ ipccreports/tar/wg1/*, Last Accessed August 4th, 2015.

Intergovernmental Panel on Climate Change (IPCC), (2005), "Special Report on Safeguarding the Ozone Layer and the Global Climate System: Issues Related to Hydrofluorocarbons and Perfluorocarbons, prepared by Working Group I and III of the IPCC and TEAP,." *https://www.ipcc.ch/pdf /special-reports/sroc/sroc_full.pdf*, Last Accessed June 4th, 2015.

Intergovernmental Panel on Climate Change (IPCC), (2006), "IPCC Guidelines for National Greenhouse Gas Inventories," *http://www.ipcc-nggip.iges.or.jp /public/2006gl/*, Last Accessed May 2nd, 2015.

Intergovernmental Panel on Climate Change (IPCC), (2007), "The Physical Science Basis. Contribution of Working Group I to the Fourth Assessment Report of IPCC," *https://www.ipcc.ch/publications_and_data /ar4/wg1/en/contents.html*, Last Accessed March 20th, 2015.

Intergovernmental Panel on Climate Change (IPCC), (2013), "Working Group I Contribution to the IPCC Fifth Assessment Report Climate Change 2013: The Physical Science Basis," *https://www.ipcc.ch/report/ar5/wg1/*, Last Accessed February 2nd, 2015.

Jacobson, M., (2012), "Air Pollution and Global Warming: History, Science, and Solutions," Cambridge University Press.
Jones, H. A. and Nedwell, D. B., (1993), "Methane Emission and Methane Oxidation in Landfill Cover Soil," *FEMS Microbiology Ecology,* Vol. 102, 185-195.
Khalil, M. A. K. and Rasmussen, R. A., (1986), "The Release of Trichlorofluoromethane from Rigid Polyurethane Foams," *Journal of the Air Pollution Control Association,* Vol. 36(2), 159-163.
Khalil, M. A. K. and Rasmussen, R. A., (1987), "The Residence Time of Trichlorofluoromethane in Polyurethane Foams: Variability, Trends, and Effects of Ambient Temperature," *Chemosphere,* Vol. 16(4), 759-775.
Kjeldsen, P., (2010), "Construction and Demolition Waste - a Source to Ozone Depletion and Global Warming?" *Proceeding of the Global Waste Management Symposium.*
Kjeldsen, P. and Jensen, M. H., (2001), "Release of CFC-11 from Disposal of Polyurethane from Waste," *Environmental Science and Technology,* Vol. 35, 3055-3063.
Lamothe, D. and Edgers, L., (1994), "The Effects of Environmental Parameters on the Laboratory Compression of Refuse," *Proceedings of the 17th International Madison Waste Conference.* Department of Engineering Professional.
Landrock, A., (1996), "Handbook of Plastic Foams: Types, Properties," Noyes Publications. Print, New Jersey.
Lang R. J., Herrera, T. A., Chang, D. P. Y., Tchobanoglous, G., and Spicher, R. G., (1989), "Summary Report: Movement of Gases in Municipal Solid Waste Landfills," Davis, CA: Department of Civil Engineering, University of California-Davis.
Liptak, B. G., (2003), *Instrument Engineers Handbook: Process of Measurement and Analysis*, 4th Edition, CRC Press.
Livingston, G. P. and Hutchinson, G. L., (1995), "Enclosure-Based Measurement of Trace Gas Exchange: Applications and Sources of Error." *Biogenic Trace Gases: Measuring Emissions from Soil and Water.* Matson, P.A. and Harriss, R.C. Eds. Blackwell Scientific Publications: Oxford, 14–51.
Maione, M., Arduini, J., Rinaldi, M., Mangani, F., and Capaccioni, B., (2005), "Emission of Non CO_2 Greenhouse Gases from Landfills of Different Age Located in Central Italy," *Environmental Sciences,* 167-176.
Marshack, J., (2012), "California Waste Classification Workshop," California Environmental Protection Agency.
Martin, L. and Kerfoot, B., (1988), "Soil-Gas Surveying Techniques," *Environmental Science & Technology,* Vol. *22*, 741.
Mata-Alvarez, J. and Martinez-Viturtia, A., (1986), "Laboratory Simulation of Municipal Solid Waste Fermentation with Leachate Recycle," *Journal of Chemical Technology and Biotechnology,* Vol. 36 (12), 547-556.
McFarland, M., (1992), "Investigations of the Environmental Acceptability of Fluorocarbon Alternative to Chlorofluorocarbons," *Proc. Natl. Acad. Sci.* Vol. 89, 807-811.

McCulloch, A., (1999)., "CFC and Halon Replacements in the Environment," *Journal of Fluorine Chemistry*, 163-173.
McCulloch, A., (2007), "Personal Communication," Deparment of Chemistry, University of Bristol.
McCulloch, A. and Midgley, P., (1998), "Estimated Historic Emissions of Fluorocarbons from the European Union," *Atmos. Environ.,* Vol. 32, 1571-1580.
McCulloch, A., Ashford, P., and Midgley, P., (2001)., "Historic Emissions of Fluorotrichloromethane based on a Market Survey," *Atmos. Environ.,* Vol. 35, 4387-97.
McCulloch, A., ,Midgley, P. M., and Ashford, P., (2003), "Release of Refrigerant Gases to the Atmosphere," *Atmost. Environ.,* Vol. 37, 889-902.
Merz, R. C., (1964), "Investigation to Determine the Quantity and Quality of Gases Produced During Refuse Decomposition," Final Report to the California Water Quality Control Board, University of Southern California, (#99-10).
Midgley, T., and Henne, A., (1930), "Organic Fluorides as Refrigerants," *Industrial and Engineering Chemistry, 22*, 542-547.
Moakley, J., Weller, M., and Zelic, M., (2010), "Alternative Methods to Landfilling Auto Shredding Residue in Compliance with the Strict Environmental Quota by the European Union," *http://www.wpi.edu/Pubs/E-project/Available/E-project-051110-050238/unrestricted/Final_Report.pdf*, Last Accessed February 5th, 2015.
Mosher, B. W., Czepiel, P. C., Shorter, J., Allwine, E., Harriss, R. C., Kolb, C., and Lamb, B., (1996), “Mitigation of Methane Emissions at Landfill Sites in New England, USA,” *Energy Conversion and Management*, Vol. 37(6), 1093-1098.
Moon, S., Nam, K., Kim, J. Y., Hwan, S. K., and Chung, M., (2008), "Effectiveness of Compacted Soil Liner as a Gas Barrier Layer in the Landfill Final Cover," System. *Waste Management,* Vol. 28, 1909-1914.
National Aeronautics and Space Administration (NASA), (2014), "Upper Atmosphere," *http://www.nasa.gov/mission_pages/sunearth /multimedia/mos-upper-atmosphere_prt.htm*, Last Accessed July 2nd, 2013.
National Aeronautics and Space Administration (NASA), (2015), "Ozone," *http://earthobservatory.nasa.gov/ Features/Ozone/ozone_2.php*, Last Accessed February 2nd, 2013.
National Oceanic and Atmospheric Administration (NOAA), (2014), "Trends in Atmospheric Carbon Dioxide," *http://www.esrl.noaa.gov/ gmd/ccgg/trends/global.html*, Last Accessed February, 2nd 2014.
National Oceanic and Atmospheric Administration (NOAA), (2015), "Hydrochlorofluorocarbon Measurements in the Chlorofluorocarbon Alternatives Measurement Project," *http://www.esrl.noaa. gov/gmd/hats /flask/hcfc.html*, Last Accessed March 20th, 2014.
Park, J. W. and Shin, H. C., (2001), "Surface Emission of Landfill Gas from Solid Waste Landfill," *Atmospheric Environment,* Vol. 35(20), 3445-3451.

Payne, W. V. and O'Neal, D. L., (1998), "Two-Phase Flow of Two HFC Refrigerant Mixtures Through Short-Tube Orifices," U.S. Environmental Protection Agency.

Peach, M. J. and Carr, W. G., (1986), "Air Sampling and Analysis for Gases and Vapors," *http://www.cdc.gov/niosh/pdfs/86-102-c.pdf*, Last Accessed March 2nd, 2014.

Peel, M. C., Finlayson, B. L. and McMahon, T. A., (2007), "Updated World Map of the Koppen-Geiger Climate Classification," *Hydrol. Earth Syst. Sci.,* Vol. 11, 1633-1644.

Pellizzari, E. G., (1984), "Evaluation of Sampling Methods of Gaseous Atmospheric Samples," U.S. Environmental Protection Agency.

Perkins, R., Cusco, L., Howley, J., Laesecke, A., Sigrun, M., and Ramires, M., (2001), "Thermal Conductivities of Alternatives to CFC-11 for Foam Insulation," *Chemical Engineer*, Data 46.

Qian, X., Koerner, R. M., and Gray, D. H., (2002), "Geotechnical Aspects of Landfill Design and Construction," Prentice Hall, Upper Saddle River, NJ.

Prather, M. J., (1996), "Theory, GWPs, for Methane and Carbon Monoxide, and Runaway Growth," *Geophys, Res. Lett,* Vol. 23 (19), 2597-2600.

Prather, M. J., (2002), "Lifetimes of atmospheric species: Integrating environmental impacts," *Geophys. Res. Lett.,* Vol. 29 (22), 2063.

Ramaswamy, J. N., (1970), "*Nutritional Effects on Acid and Gas Production in Sanitary Landfills,"* Ph.D. Thesis Department of Civil Engineering, West Virginia University.

Rees, J. F., (1980a), "Optimization of Methane Production and Refuse Decomposition in Landfills by Temperature Control," *Journal of Chemical Technology and Biotechnology*, Vol. 30(8), 458-465.

Rees, J. F., (1980b), "The Fate of Carbon Compounds in the Landfill Disposal of Organic Matter," *Journal of Chemical Technology and Biotechnology*, Vol. 30(4), 161-175.

Reinhart, D. R., Cooper, D. C., and Walker, B. L, (1992), “Flux Chamber Design and 175 Operation for the Measurement of Municipal Solid Waste Landfill Gas Emission Rates,” *Journal of the Air & Waste Management Association*, Vol. 42(8), 1067-1070.

Rettenberger, G. and Stegmann, R., (1996), "Landfill Gas Components," In Christensen, T., Cossu, R., and Stegmann, R., *Landfilling of Waste: Biogas*, 51-58, E & FN Spoon, London, UK.

Scheutz, C., (2005), "Attenuation of Methane and Trace Organics in Landfill Soil Covers," *Diss. Environment & Resources,* Technical University of Denmark.

Scheutz, C. and Kjeldsen, P., (2003a), "Capacity for Biodegradation of CFCs and HCFCs in a Methane Oxidative Counter-Gradient Laboratory System Simulating Landfill Soil Covers," *Environ. Sci. Technol.,* Vol. 37, 5143-5149.

Scheutz, C. and Kjeldsen, P., (2003b), "*Determination of the Fraction of Blowing Agents Released from Refrigerator/Freezer Foam Decomissioning the Product,"* Technical University of Denmark.

Scheutz, C., and Kjeldsen, P., (2004), "Environmental Factors Influencing Attenuation of Methane and Hydrochlorofluorocarbons in Landfill Cover Soils," *Journal of Environmental Quality,* Vol. 33(1), 72-79.

Scheutz, C., Bogner, J., Morcet, M., and Kjeldsen, P., (2003a), "Attenuation of Alternative Blowing Agents in Landfills," Final Report, Prepared for the Appliance Research Consortium by the Environment Resources, Technical University of Denmark.

Scheutz, C., Bogner, J., Morcet, M., and Kjeldsen, P., (2003b), "Aerobic Degradation of Non-Methane Organic Compounds in Landfill Cover Soils," *Proceedings of Ninth International Waste Management and Landfill Symposium,* 1-10, Cagiliari, Italy.

Scheutz, C., Bogner, J., Chanton, J., Blake, D., Morcet, M., Kjeldsen, P., (2003c), "Comparative Oxidation and Net Emissions of Methane and Selected Non-Methane Organic Compounds in Landfill Cover Soils," *Environmental Science & Technology,* Vol. 37, 5150-5158.

Scheutz, C., Mosbæk, H., and Kjeldsen, P, (2004), "Attenuation of Methane and Volatile Organic Compounds in Landfill Soil Coavers," *Journal of Environmental Quality,* Vol. 33(1), 61-71.

Scheutz, C., Fredenslund, A.M., Tant, M., and Kjeldsen, P., (2007a), "Release of Fluorocarbons from Insulation Foam in Home Appliances during Shredding," *Journal of the Air & Waste Management Association,* Vol. 57, 1452-1460.

Scheutz, C., Dote, Y., Fredenslund, A. M., Mosbæk, H., and Kjeldsen, P., (2007b), "Attenuation of Fluorocarbons Released from Foam Insulation in Landfills," *Environmental Science & Technology,* Vol. 41, 7714-7722.

Scheutz, C., Fredenslund, A. M., Lemming, G., and Kjeldsen, P., (2007c), "Investigation of Emissions from the AV Miljo Landfill-1. Gas Quantity, Quality, and Attenuation Properties," *Institute of Environment and Resources,* Technical University of Denmark.

Scheutz, C., Bogner, J., Chanton, J. P., Blake, D., Morcet, M., Aran, C., and Kjeldsen, P., (2008), “Atmospheric Emissions and Attenuation of Non-Methane Organic Compounds in Cover Soils at a French Landfill,” *Waste Management*, Vol. 28, 1892-1908.

Scheutz, C., Fredenslund, M., Nedenskov, J., and Kjeldsen, P., (2011a), "Release and Fate of Fluorocarbons in a Shredder Residue Landfill Cell: 1 Laboratory Experiments," *Waste Management,* Vol. 30, 2153-2162.

Scheutz, C., Fredenslund, M., Nedenskov, J., and Kjeldsen, P., (2011b), "Release and Fate of Fluorocarbons in a Shredder Residue Landfill Cell: 2 Field Investigations," *Waste Management,* Vol. 30, 2163-2169.

Schroer, D., Hudack, M., and Soderquist, M., (2011), "Rigid Polymeric Foam Boardstock Techical Assessment," The Dow Chemical Company.

SCS Engineers, (2008), "Current MSW Industry Position and State-of-the-Practice on LFG Collection Efficiency, Methane Oxidation, and Carbon Sequestration in Landfills," Report prepared for Solid Waste Industry for Climate Solutions by SCS Engineers.

Shackelford, C. D., (2005), "Environmental Issues in Geotechnical Engineering," *Proceedings of the 16th Conference on Soil Mechanics and Geotechnical Engineering*, 95-122.

Shine, K., (2009), "The Global Warming Potential - the Need for an Interdisciplinary Retrial," *Clim. Change,* Vol. 96, 467-472.

Singh, S. N., Randall, D., Karremans, M., and Biesmans, G., (1998), "Long Term Performance of Rigid Foams Blown with Non-CFC Blowing Agents," *Journal of Cellular Plastics,* Vol. 34(4), 349-360.

Sivertsen, K., (2007), "Polymer Foams," *http://www.core.org.cn/NR/rdonlyres/BC5A6FD8-4841-4031-8795-5153AA5E3DAF/0/polymer_foams.pdf*, Last Accessed July 1st, 2014.

Spokas, K. A., Bogner, J., Chanton, J. P., Morcet, M., Aran, C., Graff, C., Moreeau-Le Golvan, Y., and Hebe, I., (2006), "Methane Mass Balance at Three Landfill Sites: What is the Efficiency of Capture by Gas Collection Systems?" *Waste Management*, Vol. 26(5), 516-525.

Spokas, K. A., and Bogner, J., (2011), "Limits and Dynamics of Methane Oxidation in Landfill Cover Soils," *Waste Management,* Vol. 31, 823-832.

Spokas, K. A., Bogner J., Corcoran, M., and Walker, S., (2015), "From California Dreaming to California Data: Challenging Historic Models for Landfill CH_4 Emissions," *Elementa: Science of the Anthropocene,* 1-16.

Spokas, K. A., Bogner, J., and Chanton, J. A., (2011), "A Process-Based Inventory Model for Landfill CH_4 Emissions Inclusive of Soil Microclimate and Seasonal Methane Oxidation," *Journal of Geophysical Research - Biogeosciences,* Vol. 116, 1-19.

Spokas, K. B., (2012), "From California Dreaming to California Data: Challenging Historic Models for Landfill Methane Emissions," *Elementa: Science of the Athropocene*.

Stein, V. B. and Hettiaratchi, J. P. A., (2001), "Methane Oxidation in Three Alberta Soils: Influence of Soil Parameters and Methane Flux Rates," *Environmental Technology,* Vol. 22(1), 101-111.

Stern, J. C., Chanton, J., Abichou, T., Powelson, D., Yuan, L., Escoriza, S., and Bogner, J., (2007), "Use of a Biologically Active Cover to Reduce Landfill Methane Emissions and Enhance Methane Oxidation," *Waste Management,* Vol. 27(9), 1248-1258.

Streese-Kleeberg , J. and Stegmann, R., (2008), "Biofiltration of Landfill Gas Methane with Active Ventilation," *Proceedings of the Global Waste Management Symposium*.

Sturrock, G. A., Etheridge, D. M., Trudinger, C. M., Fraser, P. J., and Smith, A. M., (2002), "Atmospheric Histories of Halocarbons from Analysis of Antarctic Firn Air: Major Montreal Protocol Species," *J. Geophys. Res.,* Vol. 107, 4765-4778.

Sundararajan, T. and Malikarjuna, J. M., (2015), "Required Properties of Ideal Refrigerant," *http://nptel.ac.in/courses/112106133/Module_6/12_Required_Properties_of_Idea_Refrigerants.pdf*, :Last Accessed November 5th, 2013.

Tang, X., Madronich, S., Wallington, T., and Calamari, D., (1998), "Changes in Tropospheric Composition and Air Quality," *In Journal of Photo Chemistry and Photobiology,* Vol. 46, 83- 95.

Tchobanoglous G., Theisen, H., and Vigil, S., (1993), "Composition and Characteristics, Generation, Movement, and Control of Landfill Gases," In *Integrated Solid Waste Management,* McGraw-Hill, New York City, NY.

The National Institute for Occupational Safety and Health (NIOSH), (2013), *NIOSH Pocket Guide to Chemical Hazards*, *http://www.cdc.gov/niosh/npg/*, Last Accessed January 20th, 2013.

Throne, J. L., (2004), "Thermoplastic Foam Extrusion," Hans Gardner Publisher Print, Cincinnati, OH.

U.S. Bureau of the Census, (1997), "Construction Statistics Data User's Conference," U.S. Bureau of the Census.

U.S. Environmental Protection Agency (USEPA), (1993), "The Use of Alternative Materials for Daily Cover at Municipal Solid Waste Landfills," EPA Report # 68-C1-0018.

U.S. Environmental Protection Agency, (2004), "Identification of Time-Integrated Sampling and Measurement Techniques to Support Human Exposure Studies," *http://cfpub.epa.gov/si /si_public_record_report.cfm? dirEntryId=83797*, Last Accessed March 2nd, 2015.

U.S. Environmental Protection Agency (USEPA), (2005), "Guidance For Evaluating Landfill Gas Emissions From Closed or Abandoned Facilities," *http://nepis.epa.gov/Adobe/PDF /P1000BRN.PDF*, Last Accessed January 2nd, 2013.

U.S. Environmental Protection Agency (USEPA), (2009), "Definition of Volatile Organic Compounds (VOC)," *http://www.epa.gov/ttn/naaqs /ozone/ozonetech/def_voc.html*, Last Accessed February 5th, 2013.

U.S. Environmental Protection Agency (USEPA), (2010), "Ozone-Layer Protection - Regulatory Programs," *http://www.epa.gov /ozone/title6/phaseout/hcfcuses.html*, Last Acessed October 2nd, 2013.

U.S. Environmental Protection Agency (USEPA), (2011), "Summa Canister," *http://www.epa.gov/region6/6pd/rcra_c/ca/canister.html*, Last Accessed, March 4th, 2014.

U.S. Environmental Protection Agency (USEPA), (2012), "Part 258 - Criterial for Municipal Waste Landfill," Title 40 - Protection of Environment, *http://www.gpo.gov/fdsys/pkg/CFR-2012-title40-vol26/xml/CFR-2012-title40-vol26-part258.xml#seqnum258.21*, Last Accessed, June, 1st, 2013.

U.S. Environmental Protection Agency (USEPA), (2013), "Complying With The Section 608 Refrigerant Recycling Rule," Ozone Layer Protection - Regulatory Programs, *http://www.epa.gov/Ozone /title6/608/608fact.html*, Last Accessed, July 4th, 2013.

U.S. Environmental Protection Agency (USEPA), (2014a), "Global Warming Potentials of ODS Substitutes, *http://www.epa.gov/ozone /geninfo/gwps.html*, Last Accessed August, 15th, 2013.

U.S. Environmental Protection Agency (USEPA), (2014b), "Guidance Note on Daily and Intermediate Cover at Landfills," *http://www.epa.ie/pubs*

/advice/waste/waste/EPA_Guidance_Note_On_Landfill_Daily_And_Intermediate_Cover_Final.pdf, Last Accessed June, 2nd, 2013.

U.S. Environmental Protection Agency (USEPA), (2014c), "The Phaseout of Ozone-Depleting Substances," Ozone Layer Depletion - Regulatory Programs, *http://www.epa.gov/ozone/title6/phaseout /classtwo.html*, Last Accessed March, 6th, 2013.

U.S. Environmental Protection Agency (USEPA), (2014d), "Municipal Solid Waste Generation, Recyling, and Disposal in the United States: Facts and Figures for 2011," *http://epa.gov/wastes/nonhaz /municipal/pubs /2012_msw_fs.pdf*, Last Accessed December, 4th, 2012.

U.S. Environmental Protection Agency (USEPA), (2014e), "Facility Level GHG Emissons Data," Greenhouse Gas Emissions Profile for Potrero Hills Landfill, *https://ghgdata.epa.gov/ghgp/service/html/ 2014?id=1007345&et=undefined*, Last Accessed January, 2013.

U.S. Environmental Protection Agency (USEPA), (2015), "Advancing Sustainable Materials Management: 2013 Fact Sheet," Retrieved from http://www.epa.gov/solidwaste/nonhaz/municipal/pubs/2013_advncng_smm_fs.pdf

United Nations Environment Program (UNEP), (2006), "Refrigerant blends containing HCFCs," *http://www.unep.org/ozonaction /Topics/ HCFCHelpCentre/RefrigerantblendscontainingHCFCs/tabid/52071/Default.aspx,* Last Accessed April 20th, 2014.

United Nations Environment Program (UNEP), (2011), "HFCs: A Critical Link in Protecting Climate and the Ozone Layer," *http://www.unep.org /dewa/Portals/67/pdf/HFC_report.pdf*, Last Accessed September, 5th, 2014.

United Nations Environment Program - Foams Technical Options Committee (UNEP-FTOC), (1998), "Report of the Flexible and Rigid Foams Technical Options Committee: Pursuant to Article (6) of the Montreal Protocol on Substances that Deplete the Ozone Layer Under the Auspices of the United Nations Environment Program," Keynote Publishing Company.

United Nations Environment Program -Technology and Economic Assessment Panel (UNEP-TEAP), (2002), "Montreal Protocol on Subtances that Deplete the Ozone Layer," *http://ozone.unep.org/en/Assessment_Panels /TEAP/Reports/MBTOC/MTOC2002.pdf*, Last Accessed May 4th, 2013.

United Nations Environment Program -Technology and Economic Assessment Panel (UNEP-TEAP), (2003), "Report of the Technology and Economic Assessment Panel, HCFC Task Force Report," Nairobi, Kenya.

United Nations Environment Program -Technology and Economic Assessment Panel (UNEP-TEAP), (2005), "Report of the Task Force on Foam End of Life Issues: Volume 3," *http://ozone.unep.org/ Assessment_Panels/TEAP/ Reports/TEAP_Reports/TEAP-May-2005-Vol-2-Forms-End-of-Life.pdf*, Last Accessed February 5th, 2014.

Vollhardt, K., Peter, C., Schore, N., (1999), "Organic Chemistry: Structure and Function," W.H. Freeman, New york, NY.

Weather Underground, (2015), "Travis Air Force Base, CA, Weather Almanac," *http://www.wunderground.com*, Last Accessed December 1st, 2014.

Whalen, S. C., Reeburgh, W. S., and Sandbeck, K. A., (1990), "Rapid Methane Oxidation in a Landfill Cover Soil," *Applied and Environmental Microbiology*, Vol. 56(11), 3405-3411.

World Meterological Organization (WMO), (2010), "Scientific Assessment of Ozone Depletion: Global Ozone Research and Monitoring Project - Report No. 52," Geneva, Switzerland.

Xu, L., Amen, J., Lin, X., and Welding, K., (2014), "The Impact of Changes in Barometric Pressure on Landfill Methane Emission," *Global Biogeochem. Cycles,* Vol. 28, 679–695.

Yesiller, N. and Shackelford, C. D., (2011), “Geoenvironmental Engineering: Chapter 13,” *Geotechnical Engineering Handbook* Das, B.M.. Ed. J Ross Publishing: Ft. Lauderdale, Florida, 1-61.

Yesiller, N., Hanson, J. L., and Liu, W. L., (2005), "Heat Generation in Municipal Solid Waste Landfills," *Journal of Geotechnical and Geoenvironmental Engineering,* ASCE, Vol. 131(11), 1330-1344.

Yesiller, N, Hanson, J. L., Oettle, N. K., and Liu, W. L., (2008), “Thermal Analysis of Cover Systems in Municipal Solid Waste Landfills,” *Journal of Geotechnical and Geoenvironmental Engineering*, Vol. 134(11), 1655-1664.

Young, A., (1992), "The Effect of Fluctuations in Atmospheric Pressure on Landfill Gas Migration and Composition," *Water, Air and Soil Pollution,* Vol. 64, 601-616.

Young, P. J. and Heasman, L. A., (1985), “An Assessment of the Odor and Toxicity of the Trace Components of Landfill Gas,” *Proceedings of the 8th International Landfill Gas Symposium,* GRCDA, April, San Antonio, Texas, 93-114.

Zhang, F., Wang, X., Yi, Z., Li, L., Chan, C., Chan, L., and Blake, D. R., (2006), "Preliminary Investigation on Levels and Trends of Atmospheric Chlorodifuoromethane (HCFC-22) in the Pearl River Delta," *Huanjing Kexue Xuebao,* Vol. 26, 987-991.

APPENDICES

Appendix A - Raw Concentration Data from Field Testing Program

Wet Season - AF

CFC-11

A		B		C		D	
Time (min)	Conc. (pptv)	Time (min)	Conc. (pptv)	Time (min)	Conc. (pptv)	Time (min)	Conc. (pptv)
0	201887	0	153063	0	41938	0	35732
7	967563	30	4612384	30	202331	60	1929439
15	1636933	60	7828218	60	183463	120	2749987
30	1947464	90	9507629				
60	3950839	120	11083241				

CFC-12

A		B		C		D	
Time (min)	Conc. (pptv)	Time (min)	Conc. (pptv)	Time (min)	Conc. (pptv)	Time (min)	Conc. (pptv)
0	2329	0	2056	0	945	0	808
7	9193	30	46957	30	2264	60	18088
15	14838	60	85168	60	2183	120	26460
30	18265	90	135887				
60	36245	120	222226				

CFC-113

A		B		C		D	
Time (min)	Conc. (pptv)	Time (min)	Conc. (pptv)	Time (min)	Conc. (pptv)	Time (min)	Conc. (pptv)
0	90	0	91	0	77	0	79
7	154	30	473	30	92	60	241
15	222	60	823	60	94	120	272
30	225	90	1328				
60	402	120	2071				

Wet Season – AF (cont'd)

CFC-114

A		B		C		D	
Time (min)	Conc. (pptv)	Time (min)	Conc. (pptv)	Time (min)	Conc. (pptv)	Time (min)	Conc. (pptv)
0	27	0	30	0	25	0	26
7	45	30	188	30	29	60	56
15	72	60	308	60	34	120	28
30	56	90	475				
60	90	120	752				

HCFC-21

A		B		C		D	
Time (min)	Conc. (pptv)	Time (min)	Conc. (pptv)	Time (min)	Conc. (pptv)	Time (min)	Conc. (pptv)
0	319956	0	286935	0	91577	0	89190
7	2043162	30	8696919	30	454177	60	4755989
15	3413338	60	10905399	60	423207	120	6593457
30	4155155	90	12366675				
60	7915480	120	13901683				

HCFC-22

A		B		C		D	
Time (min)	Conc. (pptv)	Time (min)	Conc. (pptv)	Time (min)	Conc. (pptv)	Time (min)	Conc. (pptv)
0	4	0	4	0	4	0	5
7	9	30	13	30	6	60	6
15	6	60	15	60	7	120	5
30	5	90	32				
60	11	120	44				

Wet Season – AF (cont'd)

HCFC-141b

A		B		C		D	
Time (min)	Conc. (pptv)	Time (min)	Conc. (pptv)	Time (min)	Conc. (pptv)	Time (min)	Conc. (pptv)
0	319956	0	286935	0	91577	0	89190
7	2043162	30	8696919	30	454177	60	4755989
15	3413338	60	10905399	60	423207	120	6593457
30	4155155	90	12366675				
60	7915480	120	13901683				

HCFC-142b

A		B		C		D	
Time (min)	Conc. (pptv)	Time (min)	Conc. (pptv)	Time (min)	Conc. (pptv)	Time (min)	Conc. (pptv)
0	3	0	3	0	4	0	4
7	3	30	5	30	4	60	4
15	5	60	5	60	4	120	4
30	3	90	9				
60	3	120	11				

HCFC-151a

A		B		C		D	
Time (min)	Conc. (pptv)	Time (min)	Conc. (pptv)	Time (min)	Conc. (pptv)	Time (min)	Conc. (pptv)
0	2724	0	2819	0	1150	0	312
7	7729	30	58794	30	1365	60	1111
15	11989	60	102612	60	1413	120	1352
30	12649	90	159051				
60	17701	120	247040				

Wet Season – AF (cont'd)

HFC-134a

A		B		C		D	
Time (min)	Conc. (pptv)	Time (min)	Conc. (pptv)	Time (min)	Conc. (pptv)	Time (min)	Conc. (pptv)
0	17709	0	15263	0	4716	0	3476
7	80406	30	465796	30	21320	60	227485
15	135616	60	838768	60	21359	120	358330
30	160804	90	1354625				
60	308598	120	2227388				

HFC-152a

A		B		C		D	
Time (min)	Conc. (pptv)	Time (min)	Conc. (pptv)	Time (min)	Conc. (pptv)	Time (min)	Conc. (pptv)
0	9663	0	8436	0	2495	0	2323
7	47355	30	261558	30	12833	60	176257
15	84875	60	466920	60	12481	120	269432
30	112066	90	735287				
60	242925	120	1192654				

HFC-245fa

A		B		C		D	
Time (min)	Conc. (pptv)	Time (min)	Conc. (pptv)	Time (min)	Conc. (pptv)	Time (min)	Conc. (pptv)
0	14635	0	15535	0	4104	0	4139
7	69175	30	501705	30	20356	60	251248
15	124752	60	896964	60	20191	120	369082
30	147305	90	1428695				
60	308302	120	2329404				

Wet Season – AF (cont'd)

CH_4

A		B		C		D	
Time (min)	Conc. (ppmv)	Time (min)	Conc. (pptmv)	Time (min)	Conc. (ppmv)	Time (min)	Conc. (ppmv)
0	264	0	165	0	78.8	0	32.3
7	795	30	2927	30	83.1	60	47.8
15	1126	60	4698	60	80.4	120	58.1
30	1211	90	5772				
60	970	120	6764				

CO_2

A		B		C		D	
Time (min)	Conc. (ppmv)	Time (min)	Conc. (pptmv)	Time (min)	Conc. (ppmv)	Time (min)	Conc. (ppmv)
0	492	0	494	0	471	0	436
7	236	30	29	30	304	60	19
15	119	60	24	60	270	120	24
30	47	90	34				
60	16	120	26				

Wet Season – GW (cont'd)

CFC-11

A		B		C		D	
Time (min)	Conc. (pptv)	Time (min)	Conc. (pptv)	Time (min)	Conc. (pptv)	Time (min)	Conc. (pptv)
0	297787	0	35413	0	38431	0	9643
7	693623	30	176435	60	1750144	120	196171
15	1190657	60	503943				
30	1729279	90	951640				
60	2487881	120	850521				
120	3766054	150	771810				

Wet Season – GW (cont'd)

CFC-12

A		B		C		D	
Time (min)	Conc. (pptv)	Time (min)	Conc. (pptv)	Time (min)	Conc. (pptv)	Time (min)	Conc. (pptv)
0	12276	0	3101	0	2985	0	1018
7	25338	30	11481	60	116110	120	8846
15	40590	60	33272				
30	57617	90	60819				
60	83197	120	54152				
120	116277	150	46996				

CFC-113

A		B		C		D	
Time (min)	Conc. (pptv)	Time (min)	Conc. (pptv)	Time (min)	Conc. (pptv)	Time (min)	Conc. (pptv)
0	211	0	140	0	122	0	116
7	236	30	186	60	347	120	213
15	283	60	240				
30	310	90	355				
60	440	120	266				
120	737	150	263				

CFC-114

A		B		C		D	
Time (min)	Conc. (pptv)	Time (min)	Conc. (pptv)	Time (min)	Conc. (pptv)	Time (min)	Conc. (pptv)
0	429	0	164	0	117	0	27
7	673	30	456	60	4797	120	153
15	1050	60	1412				
30	1367	90	2761				
60	2061	120	2478				
120	2498	150	2286				

Wet Season – GW (cont'd)

HCFC-21

A		B		C		D	
Time (min)	Conc. (pptv)	Time (min)	Conc. (pptv)	Time (min)	Conc. (pptv)	Time (min)	Conc. (pptv)
0	6293	0	1693	0	1600	0	289
7	11960	30	8467	60	55800	120	21267
15	19547	60	23027				
30	30613	90	40027				
60	48160	120	35893				
120	107893	150	35107				

HCFC-22

A		B		C		D	
Time (min)	Conc. (pptv)	Time (min)	Conc. (pptv)	Time (min)	Conc. (pptv)	Time (min)	Conc. (pptv)
0	25524	0	5547	0	6469	0	1279
7	55237	30	26036	60	257826	120	25497
15	89007	60	72926				
30	128081	90	133539				
60	198476	120	126273				
120	278395	150	118225				

HCFC-141b

A		B		C		D	
Time (min)	Conc. (pptv)	Time (min)	Conc. (pptv)	Time (min)	Conc. (pptv)	Time (min)	Conc. (pptv)
0	396264	0	77161	0	90311	0	18005
7	917365	30	372787	60	2942488	120	941693
15	1513447	60	1048238				
30	2180991	90	1867458				
60	3467255	120	1629769				
120	5135285	150	1602206				

Wet Season – GW (cont'd)

HCFC-142b

A		B		C		D	
Time (min)	Conc. (pptv)	Time (min)	Conc. (pptv)	Time (min)	Conc. (pptv)	Time (min)	Conc. (pptv)
0	32161	0	7248	0	11619	0	1744
7	69196	30	33181	60	414704	120	35079
15	111419	60	100935				
30	157950	90	188615				
60	247457	120	166124				
120	344600	150	157695				

HCFC-151a

A		B		C		D	
Time (min)	Conc. (pptv)	Time (min)	Conc. (pptv)	Time (min)	Conc. (pptv)	Time (min)	Conc. (pptv)
0	23580	0	11033	0	8487	0	1527
7	48993	30	57393	60	294287	120	139433
15	81880	60	162913				
30	124200	90	286007				
60	197587	120	256993				
120	308765	150	246280				

HFC-134a

A		B		C		D	
Time (min)	Conc. (pptv)	Time (min)	Conc. (pptv)	Time (min)	Conc. (pptv)	Time (min)	Conc. (pptv)
0	47546	0	12851	0	8545	0	2015
7	102675	30	53132	60	329113	120	39176
15	168262	60	159463				
30	241469	90	292890				
60	350231	120	256595				
120	495840	150	229415				

Wet Season – GW (cont'd)

HFC-152a

A		B		C		D	
Time (min)	Conc. (pptv)	Time (min)	Conc. (pptv)	Time (min)	Conc. (pptv)	Time (min)	Conc. (pptv)
0	597538	0	76232	0	64363	0	20663
7	1374109	30	333434	60	2749460	120	551614
15	2267899	60	927967				
30	3277651	90	1630805				
60	5215291	120	1568010				
120	7104602	150	1495601				

HFC-245fa

A		B		C		D	
Time (min)	Conc. (pptv)	Time (min)	Conc. (pptv)	Time (min)	Conc. (pptv)	Time (min)	Conc. (pptv)
0	31674	0	8817	0	6378	0	1398
7	75890	30	42530	60	267300	120	58275
15	127301	60	127818				
30	182486	90	234709				
60	276118	120	196622				
120	388806	150	184231				

CH_4

A		B		C		D	
Time (min)	Conc. (ppmv)	Time (min)	Conc. (pptmv)	Time (min)	Conc. (ppmv)	Time (min)	Conc. (ppmv)
0	189	0	162	0	98.6	0	53.1
7	503	30	1190	60	1876.0	120	373.0
15	809	60	2160				
30	1241	90	3532				
60	2007	120	4326				
120	2157	150	3587				

Wet Season – GW (cont'd)

CO_2

A		B		C		D	
Time (min)	Conc. (ppmv)	Time (min)	Conc. (pptmv)	Time (min)	Conc. (ppmv)	Time (min)	Conc. (ppmv)
0	5267	0	3394	0	3051	0	7678
7	19943	30	25897	60	20350	120	9052
15	30118	60	42410				
30	44756	90	72534				
60	91230	120	94770				
120	109976	150	91987				

Wet Season – ED

CFC-11

A		B		C		D	
Time (min)	Conc. (pptv)	Time (min)	Conc. (pptv)	Time (min)	Conc. (pptv)	Time (min)	Conc. (pptv)
0	3398	0	5672	0	647	0	1980
7	3972	30	30000	30	6456	60	39471
15	5386	60	54344	60	11629	120	10943
30	10055	90	79830				
60	14150	120	93999				

CFC-12

A		B		C		D	
Time (min)	Conc. (pptv)	Time (min)	Conc. (pptv)	Time (min)	Conc. (pptv)	Time (min)	Conc. (pptv)
0	498	0	598	0	484	0	514
7	498	30	1625	30	1218	60	3816
15	564	60	2628	60	1843	120	767
30	797	90	3628				
60	974	120	4141				

CFC-113

A		B		C		D	
Time (min)	Conc. (pptv)	Time (min)	Conc. (pptv)	Time (min)	Conc. (pptv)	Time (min)	Conc. (pptv)
0	69	0	75	0	70	0	74
7	63	30	69	30	85	60	289
15	64	60	71	60	93	120	62
30	77	90	79				

60	73	120	79				

Wet Season – ED (cont'd)

CFC-114

A		B		C		D	
Time (min)	Conc. (pptv)	Time (min)	Conc. (pptv)	Time (min)	Conc. (pptv)	Time (min)	Conc. (pptv)
0	17	0	20	0	18	0	18
7	15	30	35	30	43	60	122
15	16	60	50	60	61	120	25
30	17	90	63				
60	18	120	68				

HCFC-21

A		B		C		D	
Time (min)	Conc. (pptv)	Time (min)	Conc. (pptv)	Time (min)	Conc. (pptv)	Time (min)	Conc. (pptv)
0	7773	0	15034	0	7730	0	9751
7	8054	30	69412	30	106558	60	396209
15	9764	60	125037	60	196229	120	97487
30	15910	90	186933				
60	20985	120	219875				

HCFC-22

A		B		C		D	
Time (min)	Conc. (pptv)	Time (min)	Conc. (pptv)	Time (min)	Conc. (pptv)	Time (min)	Conc. (pptv)
0	3	0	4	0	4	0	5
7	4	30	4	30	5	60	5
15	4	60	5	60	6	120	2
30	4	90	6				
60	5	120	4				

Wet Season – ED (cont'd)

HCFC-141b

A		B		C		D	
Time (min)	Conc. (pptv)	Time (min)	Conc. (pptv)	Time (min)	Conc. (pptv)	Time (min)	Conc. (pptv)
0	7773	0	15034	0	7730	0	9751
7	8054	30	69412	30	106558	60	396209
15	9764	60	125037	60	196229	120	97487
30	15910	90	186933				
60	20985	120	219875				

HCFC-142b

A		B		C		D	
Time (min)	Conc. (pptv)	Time (min)	Conc. (pptv)	Time (min)	Conc. (pptv)	Time (min)	Conc. (pptv)
0	3	0	4	0	4	0	3
7	3	30	3	30	4	60	16
15	3	60	3	60	5	120	3
30	4	90	4				
60	4	120	4				

HCFC-151a

A		B		C		D	
Time (min)	Conc. (pptv)	Time (min)	Conc. (pptv)	Time (min)	Conc. (pptv)	Time (min)	Conc. (pptv)
0	882	0	748	0	677	0	702
7	807	30	5173	30	8900	60	36024
15	828	60	9763	60	16186	120	7627
30	973	90	14768				
60	1032	120	17783				

HFC-134a

A		B		C		D	
Time (min)	Conc. (pptv)	Time (min)	Conc. (pptv)	Time (min)	Conc. (pptv)	Time (min)	Conc. (pptv)
0	978	0	1866	0	1454	0	880
7	1150	30	17520	30	21560	60	63571
15	1551	60	32374	60	39631	120	13702
30	2682	90	46901				
60	3932	120	54726				

Wet Season – ED (cont'd)

HFC-152a

A		B		C		D	
Time (min)	Conc. (pptv)	Time (min)	Conc. (pptv)	Time (min)	Conc. (pptv)	Time (min)	Conc. (pptv)
0	442	0	875	0	441	0	437
7	470	30	3898	30	3659	60	14645
15	580	60	6991	60	6581	120	3109
30	900	90	10316				
60	1239	120	12170				

HFC-245fa

A		B		C		D	
Time (min)	Conc. (pptv)	Time (min)	Conc. (pptv)	Time (min)	Conc. (pptv)	Time (min)	Conc. (pptv)
0	324	0	957	0	272	0	329
7	465	30	7254	30	4508	60	20094
15	720	60	13510	60	8371	120	5036
30	1512	90	19663				
60	2347	120	23099				

CH_4

A		B		C		D	
Time (min)	Conc. (ppmv)	Time (min)	Conc. (ppmv)	Time (min)	Conc. (ppmv)	Time (min)	Conc. (ppmv)
0	46	0	48	0	53.5	0	38.6
7	51	30	542	30	632.8	60	2605.0
15	57	60	1036	60	1110.0	120	4469.0
30	59	90	1359				
60	65	120	1725				

Wet Season – ED (cont'd)

CO_2

A		B		C		D	
Time (min)	Conc. (ppmv)	Time (min)	Conc. (ppmv)	Time (min)	Conc. (ppmv)	Time (min)	Conc. (ppmv)
0	492	0	658	0	540	0	470
7	537	30	628	30	1337	60	3692
15	586	60	757	60	1927	120	6026
30	695	90	856				
60	773	120	902				

Wet Season – IC-1

CFC-11

A		B		C		D	
Time (min)	Conc. (pptv)	Time (min)	Conc. (pptv)	Time (min)	Conc. (pptv)	Time (min)	Conc. (pptv)
0	234	0	222	0	247	0	207
7	248	30	323	60	252	120	297
15	254	60	267				
30	243	90	291				
60	288	120	280				
120	332	150	300				

CFC-12

A		B		C		D	
Time (min)	Conc. (pptv)	Time (min)	Conc. (pptv)	Time (min)	Conc. (pptv)	Time (min)	Conc. (pptv)
0	509	0	453	0	528	0	453
7	479	30	628	60	534	120	618
15	495	60	512				
30	473	90	514				
60	493	120	496				
120	509	150	525				

Wet Season – IC-1 (cont'd)

CFC-113

A		B		C		D	
Time (min)	Conc. (pptv)	Time (min)	Conc. (pptv)	Time (min)	Conc. (pptv)	Time (min)	Conc. (pptv)
0	63	0	64	0	75	0	64
7	68	30	94	60	75	120	92
15	71	60	72				
30	66	90	81				
60	69	120	70				
120	71	150	78				

CFC-114

A		B		C		D	
Time (min)	Conc. (pptv)	Time (min)	Conc. (pptv)	Time (min)	Conc. (pptv)	Time (min)	Conc. (pptv)
0	15	0	14	0	15	0	15
7	16	30	20	60	18	120	17
15	19	60	17				
30	17	90	17				
60	21	120	17				
120	26	150	19				

HCFC-21

A		B		C		D	
Time (min)	Conc. (pptv)	Time (min)	Conc. (pptv)	Time (min)	Conc. (pptv)	Time (min)	Conc. (pptv)
0	-888	0	-888	0	-888	0	-888
7	-888	30	-888	60	-888	120	-888
15	-888	60	-888				
30	-888	90	-888				
60	-888	120	-888				
120	-888	150	-888				

Wet Season – IC-1 (cont'd)

HCFC-22

A		B		C		D	
Time (min)	Conc. (pptv)	Time (min)	Conc. (pptv)	Time (min)	Conc. (pptv)	Time (min)	Conc. (pptv)
0	217	0	222	0	263	0	223
7	228	30	306	60	253	120	301
15	236	60	247				
30	227	90	244				
60	225	120	229				
120	225	150	242				

HCFC-141b

A		B		C		D	
Time (min)	Conc. (pptv)	Time (min)	Conc. (pptv)	Time (min)	Conc. (pptv)	Time (min)	Conc. (pptv)
0	72	0	44	0	32	0	23
7	47	30	70	60	44	120	61
15	37	60	68				
30	31	90	80				
60	35	120	90				
120	45	150	116				

HCFC-142b

A		B		C		D	
Time (min)	Conc. (pptv)	Time (min)	Conc. (pptv)	Time (min)	Conc. (pptv)	Time (min)	Conc. (pptv)
0	24	0	22	0	23	0	22
7	22	30	29	60	32	120	44
15	24	60	26				
30	25	90	26				
60	28	120	26				
120	33	150	29				

HCFC-151a

A		B		C		D	
Time (min)	Conc. (pptv)	Time (min)	Conc. (pptv)	Time (min)	Conc. (pptv)	Time (min)	Conc. (pptv)
0	-888	0	-888	0	-888	0	-888
7	-888	30	-888	60	-888	120	-888
15	-888	60	-888				
30	-888	90	-888				
60	-888	120	-888				
120	-888	150	-888				

Wet Season – IC-1 (cont'd)

HFC-134a

A		B		C		D	
Time (min)	Conc. (pptv)	Time (min)	Conc. (pptv)	Time (min)	Conc. (pptv)	Time (min)	Conc. (pptv)
0	62	0	63	0	77	0	76
7	70	30	86	60	87	120	93
15	70	60	82				
30	69	90	86				
60	70	120	82				
120	73	150	88				

HFC-152a

A		B		C		D	
Time (min)	Conc. (pptv)	Time (min)	Conc. (pptv)	Time (min)	Conc. (pptv)	Time (min)	Conc. (pptv)
0	33	0	24	0	20	0	16
7	72	30	171	60	28	120	28
15	104	60	242				
30	156	90	345				
60	272	120	416				
120	483	150	583				

HFC-245fa

A		B		C		D	
Time (min)	Conc. (pptv)	Time (min)	Conc. (pptv)	Time (min)	Conc. (pptv)	Time (min)	Conc. (pptv)
0	3	0	2	0	-888	0	-888
7	1	30	1	60	-888	120	-888
15	-888	60	2				
30	-888	90	-888				
60	1	120	-888				
120	-888	150	-888				

Wet Season – IC-1 (cont'd)

CH_4

A		B		C		D	
Time (min)	Conc. (ppmv)	Time (min)	Conc. (ppmv)	Time (min)	Conc. (ppmv)	Time (min)	Conc. (ppmv)
0	2	0	4	0	2.3	0	2.1
7	2	30	4	60	2.3	120	2.1
15	2	60	4				
30	2	90	3				
60	2	120	3				
120	2	150	3				

CO_2

A		B		C		D	
Time (min)	Conc. (ppmv)	Time (min)	Conc. (ppmv)	Time (min)	Conc. (ppmv)	Time (min)	Conc. (ppmv)
0	517	0	471	0	433	0	418
7	766	30	1309	60	1441	120	1041
15	983	60	2063				
30	1469	90	2716				
60	2271	120	3412				
120	3560	150	3859				

Wet Season – IC-10

CFC-11

A		B		C		D	
Time (min)	Conc. (pptv)	Time (min)	Conc. (pptv)	Time (min)	Conc. (pptv)	Time (min)	Conc. (pptv)
0	222	0	272	0	260	0	228
7	235	30	388	60	545	120	737
15	266	60	470				
30	282	90	567				
60	321	120	670				
120	448	150	736				

Wet Season – IC-10 (cont'd)

CFC-12

A		B		C		D	
Time (min)	Conc. (pptv)	Time (min)	Conc. (pptv)	Time (min)	Conc. (pptv)	Time (min)	Conc. (pptv)
0	515	0	742	0	483	0	487
7	629	30	535	60	783	120	535
15	862	60	505				
30	1152	90	507				
60	1737	120	520				
120	3232	150	528				

CFC-113

A		B		C		D	
Time (min)	Conc. (pptv)	Time (min)	Conc. (pptv)	Time (min)	Conc. (pptv)	Time (min)	Conc. (pptv)
0	64	0	106	0	72	0	65
7	70	30	77	60	78	120	71
15	74	60	73				
30	74	90	73				
60	77	120	73				
120	86	150	73				

CFC-114

A		B		C		D	
Time (min)	Conc. (pptv)	Time (min)	Conc. (pptv)	Time (min)	Conc. (pptv)	Time (min)	Conc. (pptv)
0	19	0	26	0	16	0	19
7	33	30	20	60	45	120	21
15	54	60	21				
30	87	90	22				
60	151	120	26				
120	324	150	26				

Wet Season – IC-10 (cont'd)

HCFC-21

A		B		C		D	
Time (min)	Conc. (pptv)	Time (min)	Conc. (pptv)	Time (min)	Conc. (pptv)	Time (min)	Conc. (pptv)
0	-888	0	-888	0	-888	0	-888
7	-888	30	-888	60	-888	120	-888
15	-888	60	-888				
30	-888	90	-888				
60	23	120	-888				
120	30	150	-888				

HCFC-22

A		B		C		D	
Time (min)	Conc. (pptv)	Time (min)	Conc. (pptv)	Time (min)	Conc. (pptv)	Time (min)	Conc. (pptv)
0	259	0	421	0	276	0	264
7	520	30	296	60	341	120	274
15	860	60	278				
30	1380	90	283				
60	2416	120	280				
120	5014	150	286				

HCFC-141b

A		B		C		D	
Time (min)	Conc. (pptv)	Time (min)	Conc. (pptv)	Time (min)	Conc. (pptv)	Time (min)	Conc. (pptv)
0	57	0	117	0	82	0	65
7	144	30	220	60	455	120	609
15	272	60	315				
30	485	90	419				
60	865	120	531				
120	1869	150	595				

Wet Season – IC-10 (cont'd)

HCFC-142b

A		B		C		D	
Time (min)	Conc. (pptv)	Time (min)	Conc. (pptv)	Time (min)	Conc. (pptv)	Time (min)	Conc. (pptv)
0	24	0	35	0	25	0	24
7	27	30	28	60	35	120	27
15	41	60	25				
30	51	90	25				
60	75	120	26				
120	147	150	27				

HCFC-151a

A		B		C		D	
Time (min)	Conc. (pptv)	Time (min)	Conc. (pptv)	Time (min)	Conc. (pptv)	Time (min)	Conc. (pptv)
0	0	0	0	0	0	0	0
7	0	30	23	60	27	120	27
15	36	60	24				
30	72	90	26				
60	150	120	22				
120	305	150	21				

HFC-134a

A		B		C		D	
Time (min)	Conc. (pptv)	Time (min)	Conc. (pptv)	Time (min)	Conc. (pptv)	Time (min)	Conc. (pptv)
0	107	0	274	0	131	0	129
7	155	30	211	60	223	120	163
15	220	60	212				
30	305	90	209				
60	478	120	218				
120	956	150	219				

HFC-152a

A		B		C		D	
Time (min)	Conc. (pptv)	Time (min)	Conc. (pptv)	Time (min)	Conc. (pptv)	Time (min)	Conc. (pptv)
0	22	0	35	0	24	0	25
7	59	30	62	60	47	120	384
15	93	60	98				
30	154	90	134				
60	250	120	165				
120	489	150	179				

Wet Season – IC-10 (cont'd)

HFC-245fa

A		B		C		D	
Time (min)	Conc. (pptv)	Time (min)	Conc. (pptv)	Time (min)	Conc. (pptv)	Time (min)	Conc. (pptv)
0	1	0	7	0	5	0	4
7	1	30	6	60	8	120	10
15	2	60	6				
30	3	90	8				
60	3	120	8				
120	6	150	9				

CH_4

A		B		C		D	
Time (min)	Conc. (ppmv)	Time (min)	Conc. (ppmv)	Time (min)	Conc. (ppmv)	Time (min)	Conc. (ppmv)
0	32	0	27	0	18.0	0	17.7
7	188	30	25	60	14.4	120	11.5
15	397	60	23				
30	751	90	21				
60	1331	120	20				
120	2298	150	18				

CO_2

A		B		C		D	
Time (min)	Conc. (ppmv)	Time (min)	Conc. (ppmv)	Time (min)	Conc. (ppmv)	Time (min)	Conc. (ppmv)
0	520	0	451	0	577	0	431
7	1080	30	1240	60	2917	120	2861
15	1694	60	1983				
30	2728	90	2592				
60	4889	120	3120				
120	8927	150	3429				

Wet Season – IC-15

CFC-11

A		B		C		D	
Time (min)	Conc. (pptv)	Time (min)	Conc. (pptv)	Time (min)	Conc. (pptv)	Time (min)	Conc. (pptv)
0	280	0	360	0	240	0	497
7	325	30	406	60	575	120	669
15	355	60	444				
30	368	90	617				
60	529	120	614				
120	703	150	780				

CFC-12

A		B		C		D	
Time (min)	Conc. (pptv)	Time (min)	Conc. (pptv)	Time (min)	Conc. (pptv)	Time (min)	Conc. (pptv)
0	507	0	538	0	508	0	555
7	560	30	515	60	963	120	623
15	578	60	457				
30	933	90	550				
60	699	120	489				
120	760	150	554				

CFC-113

A		B		C		D	
Time (min)	Conc. (pptv)	Time (min)	Conc. (pptv)	Time (min)	Conc. (pptv)	Time (min)	Conc. (pptv)
0	71	0	72	0	71	0	74
7	80	30	70	60	78	120	80
15	80	60	64				
30	73	90	77				
60	77	120	66				
120	72	150	78				

Wet Season – IC-15 (cont'd)

CFC-114

A		B		C		D	
Time (min)	Conc. (pptv)	Time (min)	Conc. (pptv)	Time (min)	Conc. (pptv)	Time (min)	Conc. (pptv)
0	24	0	19	0	27	0	24
7	113	30	19	60	570	120	283
15	213	60	15				
30	196	90	19				
60	772	120	17				
120	1262	150	21				

HCFC-21

A		B		C		D	F
Time (min)	Conc. (pptv)	Time (min)	Conc. (pptv)	Time (min)	Conc. (pptv)	Time (min)	Conc. (pptv)
0	10	0	-888	0	-888	0	-888
7	10	30	-888	60	-888	120	-888
15	10	60	-888				
30	29	90	-888				
60	33	120	-888				
120	93	150	-888				

HCFC-22

A		B		C		D	
Time (min)	Conc. (pptv)	Time (min)	Conc. (pptv)	Time (min)	Conc. (pptv)	Time (min)	Conc. (pptv)
0	275	0	314	0	288	0	356
7	398	30	302	60	1776	120	360
15	527	60	261				
30	1142	90	314				
60	1196	120	283				
120	1868	150	300				

HCFC-141b

A		B		C		D	
Time (min)	Conc. (pptv)	Time (min)	Conc. (pptv)	Time (min)	Conc. (pptv)	Time (min)	Conc. (pptv)
0	147	0	138	0	98	0	376
7	440	30	247	60	3847	120	1252
15	790	60	336				
30	1234	90	555				
60	2691	120	582				
120	4999	150	773				

Wet Season – IC-15 (cont'd)

HCFC-142b

A		B		C		D	
Time (min)	Conc. (pptv)	Time (min)	Conc. (pptv)	Time (min)	Conc. (pptv)	Time (min)	Conc. (pptv)
0	34	0	32	0	33	0	65
7	57	30	36	60	464	120	283
15	85	60	30				
30	138	90	40				
60	230	120	34				
120	375	150	42				

HCFC-151a

A		B		C		D	
Time (min)	Conc. (pptv)	Time (min)	Conc. (pptv)	Time (min)	Conc. (pptv)	Time (min)	Conc. (pptv)
0	55	0	-888	0	86	0	59
7	522	30	34	60	6349	120	231
15	1089	60	-888				
30	2135	90	37				
60	4286	120	-888				
120	8641	150	40				

HFC-134a

A		B		C		D	
Time (min)	Conc. (pptv)	Time (min)	Conc. (pptv)	Time (min)	Conc. (pptv)	Time (min)	Conc. (pptv)
0	244	0	202	0	488	0	740
7	1361	30	242	60	20328	120	2377
15	2593	60	242				
30	285	90	300				
60	10039	120	271				
120	14566	150	322				

Wet Season – IC-15 (cont'd)

HFC-152a

A		B		C		D	
Time (min)	Conc. (pptv)	Time (min)	Conc. (pptv)	Time (min)	Conc. (pptv)	Time (min)	Conc. (pptv)
0	83	0	23	0	159	0	110
7	639	30	32	60	6613	120	6135
15	1385	60	37				
30	264	90	53				
60	4527	120	53				
120	4865	150	68				

HFC-245fa

A		B		C		D	
Time (min)	Conc. (pptv)	Time (min)	Conc. (pptv)	Time (min)	Conc. (pptv)	Time (min)	Conc. (pptv)
0	15	0	10	0	20	0	60
7	80	30	13	60	1241	120	1041
15	155	60	17				
30	3	90	24				
60	580	120	24				
120	980	150	30				

CH_4

A		B		C		D	
Time (min)	Conc. (ppmv)	Time (min)	Conc. (ppmv)	Time (min)	Conc. (ppmv)	Time (min)	Conc. (ppmv)
0	120	0	15	0	302.0	0	18.0
7	975	30	14	60	11539.7	120	267.9
15	1946	60	13				
30	3397	90	12				
60	34595	120	12				
120	517700	150	11				

Wet Season – IC-15 (cont'd)

CO_2

A		B		C		D	
Time (min)	Conc. (ppmv)	Time (min)	Conc. (ppmv)	Time (min)	Conc. (ppmv)	Time (min)	Conc. (ppmv)
0	525	0	431	0	704	0	492
7	1427	30	767	60	17032	120	4255
15	2467	60	1018				
30	4187	90	1275				
60	7733	120	1462				
120	14718	150	1657				

Wet Season – FC

CFC-11

A		B		C		D	
Time (min)	Conc. (pptv)	Time (min)	Conc. (pptv)	Time (min)	Conc. (pptv)	Time (min)	Conc. (pptv)
0	254	0	225	0	212	0	289
7	269	30	252	60	243	120	237
15	232	60	246				
30	244	90	251				
60	263	120	235				
120	245	150	247				

CFC-12

A		B		C		D	
Time (min)	Conc. (pptv)	Time (min)	Conc. (pptv)	Time (min)	Conc. (pptv)	Time (min)	Conc. (pptv)
0	534	0	463	0	445	0	615
7	562	30	541	60	532	120	564
15	480	60	545				
30	517	90	572				
60	531	120	565				
120	485	150	607				

Wet Season – FC (cont'd)

CFC-113

A		B		C		D	
Time (min)	Conc. (pptv)	Time (min)	Conc. (pptv)	Time (min)	Conc. (pptv)	Time (min)	Conc. (pptv)
0	75	0	66	0	67	0	91
7	82	30	74	60	73	120	69
15	71	60	73				
30	75	90	75				
60	77	120	69				
120	71	150	74				

CFC-114

A		B		C		D	
Time (min)	Conc. (pptv)	Time (min)	Conc. (pptv)	Time (min)	Conc. (pptv)	Time (min)	Conc. (pptv)
0	16	0	16	0	14	0	19
7	19	30	117	60	19	120	98
15	20	60	217				
30	28	90	316				
60	42	120	384				
120	59	150	487				

HCFC-21

A		B		C		D	
Time (min)	Conc. (pptv)	Time (min)	Conc. (pptv)	Time (min)	Conc. (pptv)	Time (min)	Conc. (pptv)
0	-888	0	-888	0	-888	0	-888
7	-888	30	-888	60	-888	120	-888
15	-888	60	-888				
30	-888	90	-888				
60	-888	120	-888				
120	-888	150	-888				

Wet Season – FC (cont'd)

HCFC-22

A		B		C		D	
Time (min)	Conc. (pptv)	Time (min)	Conc. (pptv)	Time (min)	Conc. (pptv)	Time (min)	Conc. (pptv)
0	260	0	233	0	219	0	281
7	278	30	576	60	269	120	234
15	237	60	841				
30	248	90	1145				
60	253	120	1286				
120	227	150	1550				

HCFC-141b

A		B		C		D	
Time (min)	Conc. (pptv)	Time (min)	Conc. (pptv)	Time (min)	Conc. (pptv)	Time (min)	Conc. (pptv)
0	45	0	39	0	26	0	35
7	90	30	42	60	31	120	49
15	34	60	39				
30	34	90	41				
60	39	120	38				
120	40	150	41				

HCFC-142b

A		B		C		D	
Time (min)	Conc. (pptv)	Time (min)	Conc. (pptv)	Time (min)	Conc. (pptv)	Time (min)	Conc. (pptv)
0	22	0	22	0	21	0	23
7	29	30	32	60	22	120	54
15	21	60	43				
30	22	90	52				
60	25	120	59				
120	23	150	70				

Wet Season – FC (cont'd)

HCFC-151a

A		B		C		D	
Time (min)	Conc. (pptv)	Time (min)	Conc. (pptv)	Time (min)	Conc. (pptv)	Time (min)	Conc. (pptv)
0	-888	0	-888	0	-888	0	-888
7	-888	30	-888	60	-888	120	-888
15	-888	60	-888				
30	-888	90	-888				
60	-888	120	-888				
120	-888	150	-888				

HFC-134a

A		B		C		D	
Time (min)	Conc. (pptv)	Time (min)	Conc. (pptv)	Time (min)	Conc. (pptv)	Time (min)	Conc. (pptv)
0	76	0	76	0	68	0	74
7	81	30	80	60	74	120	86
15	69	60	92				
30	78	90	100				
60	79	120	104				
120	74	150	116				

HFC-152a

A		B		C		D	
Time (min)	Conc. (pptv)	Time (min)	Conc. (pptv)	Time (min)	Conc. (pptv)	Time (min)	Conc. (pptv)
0	18	0	17	0	16	0	21
7	30	30	32	60	30	120	85
15	30	60	44				
30	41	90	60				
60	67	120	66				
120	106	150	83				

Wet Season – FC (cont'd)

HFC-245fa

A		B		C		D	
Time (min)	Conc. (pptv)	Time (min)	Conc. (pptv)	Time (min)	Conc. (pptv)	Time (min)	Conc. (pptv)
0	-888	0	-888	0	-888	0	-888
7	3	30	-888	60	-888	120	1
15	-888	60	1				
30	-888	90	1				
60	-888	120	-888				
120	1	150	1				

CH_4

A		B		C		D	
Time (min)	Conc. (ppmv)	Time (min)	Conc. (ppmv)	Time (min)	Conc. (ppmv)	Time (min)	Conc. (ppmv)
0	2	0	2	0	1.9	0	2.0
7	2	30	2	60	1.9	120	1.2
15	2	60	2				
30	2	90	2				
60	2	120	2				
120	2	150	2				

CO_2

A		B		C		D	
Time (min)	Conc. (ppmv)	Time (min)	Conc. (ppmv)	Time (min)	Conc. (ppmv)	Time (min)	Conc. (ppmv)
0	411	0	396	0	414	0	404
7	557	30	1140	60	785	120	3656
15	720	60	1880				
30	1019	90	2577				
60	1629	120	3276				
120	2872	150	3939				

Dry Season – AF

CFC-11

A		B		C		D	
Time (min)	Conc. (pptv)	Time (min)	Conc. (pptv)	Time (min)	Conc. (pptv)	Time (min)	Conc. (pptv)
0	31494	0	35352	0	21198	0	24592
7	137555	30	156788	30	260805	60	244505
15	125029	60	189541	60	729689	120	1004622
30	218634	90	295675				
60	418887	120	334388				

CFC-12

A		B		C		D	
Time (min)	Conc. (pptv)	Time (min)	Conc. (pptv)	Time (min)	Conc. (pptv)	Time (min)	Conc. (pptv)
0	996	0	807	0	931	0	846
7	3009	30	4392	30	13552	60	15803
15	3744	60	7513	60	22428	120	17215
30	5286	90	7144				
60	8127	120	8899				

CFC-113

A		B		C		D	
Time (min)	Conc. (pptv)	Time (min)	Conc. (pptv)	Time (min)	Conc. (pptv)	Time (min)	Conc. (pptv)
0	98	0	88	0	85	0	97
7	110	30	153	30	250	60	174
15	109	60	189	60	268	120	295
30	114	90	165				
60	99	120	294				

Dry Season – AF (cont'd)

CFC-114

A		B		C		D	
Time (min)	Conc. (pptv)	Time (min)	Conc. (pptv)	Time (min)	Conc. (pptv)	Time (min)	Conc. (pptv)
0	23	0	22	0	20	0	21
7	29	30	23	30	29	60	45
15	28	60	46	60	32	120	37
30	34	90	26				
60	38	120	32				

HCFC-21

A		B		C		D	
Time (min)	Conc. (pptv)	Time (min)	Conc. (pptv)	Time (min)	Conc. (pptv)	Time (min)	Conc. (pptv)
0	233	0	154	0	118	0	119
7	972	30	1679	30	3265	60	4143
15	1469	60	2601	60	4368	120	4557
30	1981	90	2424				
60	2798	120	2608				

HCFC-22

A		B		C		D	
Time (min)	Conc. (pptv)	Time (min)	Conc. (pptv)	Time (min)	Conc. (pptv)	Time (min)	Conc. (pptv)
0	2015	0	1283	0	1075	0	1458
7	10698	30	13113	30	26268	60	61982
15	14700	60	19568	60	48979	120	72109
30	22659	90	18981				
60	38549	120	24687				

HCFC-141b

A		B		C		D	
Time (min)	Conc. (pptv)	Time (min)	Conc. (pptv)	Time (min)	Conc. (pptv)	Time (min)	Conc. (pptv)
0	33493	0	44347	0	9567	0	33667
7	80988	30	532731	30	41235	60	26969
15	65318	60	26616	60	84706	120	39045
30	114625	90	745643				
60	231121	120	741540				

Dry Season – AF (cont'd)

HCFC-142b

A		B		C		D	
Time (min)	Conc. (pptv)	Time (min)	Conc. (pptv)	Time (min)	Conc. (pptv)	Time (min)	Conc. (pptv)
0	835	0	570	0	587	0	397
7	4894	30	8833	30	17713	60	18301
15	6349	60	10191	60	27977	120	17656
30	8887	90	15819				
60	13376	120	13649				

HCFC-151a

A		B		C		D	
Time (min)	Conc. (pptv)	Time (min)	Conc. (pptv)	Time (min)	Conc. (pptv)	Time (min)	Conc. (pptv)
0	1396	0	740	0	712	0	614
7	5174	30	3942	30	10885	60	9332
15	7421	60	5443	60	13730	120	10341
30	9929	90	4781				
60	13227	120	5042				

HFC-134a

A		B		C		D	
Time (min)	Conc. (pptv)	Time (min)	Conc. (pptv)	Time (min)	Conc. (pptv)	Time (min)	Conc. (pptv)
0	4130	0	2666	0	3078	0	1974
7	17556	30	35924	30	57862	60	56552
15	21830	60	38179	60	144240	120	61142
30	31396	90	63434				
60	58678	120	73712				

HFC-152a

A		B		C		D	
Time (min)	Conc. (pptv)	Time (min)	Conc. (pptv)	Time (min)	Conc. (pptv)	Time (min)	Conc. (pptv)
0	7064	0	1294	0	852	0	2167
7	11511	30	7066	30	10238	60	10731
15	10668	60	10700	60	16157	120	10185
30	12515	90	8388				
60	21593	120	10363				

Dry Season – AF (cont'd)

HFC-245fa

A		B		C		D	
Time (min)	Conc. (pptv)	Time (min)	Conc. (pptv)	Time (min)	Conc. (pptv)	Time (min)	Conc. (pptv)
0	2451	0	1901	0	2944	0	1368
7	14948	30	29512	30	111433	60	109574
15	19683	60	53910	60	188883	120	106854
30	28411	90	56318				
60	50143	120	77880				

CH_4

A		B		C		D	
Time (min)	Conc. (ppmv)	Time (min)	Conc. (ppmv)	Time (min)	Conc. (ppmv)	Time (min)	Conc. (ppmv)
0	320	0	79	0	100.8	0	1653.0
7	902	30	643	30	1818.0	60	1099.0
15	1692	60	989	60	2773.0	120	2110.0
30	1866	90	1277				
60	2285	120	1462				

CO_2

A		B		C		D	
Time (min)	Conc. (ppmv)	Time (min)	Conc. (ppmv)	Time (min)	Conc. (ppmv)	Time (min)	Conc. (ppmv)
0	492	0	436	0	420	0	427
7	484	30	189	30	178	60	106
15	454	60	143	60	141	120	83
30	422	90	130				
60	394	120	117				

Dry Season – GW (cont'd)

CFC-11

A		B		C		D	
Time (min)	Conc. (pptv)	Time (min)	Conc. (pptv)	Time (min)	Conc. (pptv)	Time (min)	Conc. (pptv)
0	6882	0	4166	0	1643	0	1725
7	80141	30	28361	30	17890	60	9817
15	9598	60	7026	60	12682	120	12969
30	20551	90	34390				
60	32345	120	37490				

Dry Season – GW (cont'd)

CFC-12

A		B		C		D	
Time (min)	Conc. (pptv)	Time (min)	Conc. (pptv)	Time (min)	Conc. (pptv)	Time (min)	Conc. (pptv)
0	842	0	599	0	614	0	605
7	12798	30	769	30	949	60	956
15	1280	60	951	60	1073	120	1189
30	1965	90	867				
60	2011	120	813				

CFC-113

A		B		C		D	
Time (min)	Conc. (pptv)	Time (min)	Conc. (pptv)	Time (min)	Conc. (pptv)	Time (min)	Conc. (pptv)
0	103	0	76	0	140	0	84
7	75	30	81	30	86	60	97
15	74	60	84	60	143	120	105
30	255	90	90				
60	137	120	133				

CFC-114

A		B		C		D	
Time (min)	Conc. (pptv)	Time (min)	Conc. (pptv)	Time (min)	Conc. (pptv)	Time (min)	Conc. (pptv)
0	37	0	19	0	27	0	27
7	39	30	18	30	233	60	211
15	20	60	23	60	244	120	296
30	31	90	23				
60	24	120	25				

HCFC-21

A		B		C		D	
Time (min)	Conc. (pptv)	Time (min)	Conc. (pptv)	Time (min)	Conc. (pptv)	Time (min)	Conc. (pptv)
0	250	0	46	0	66	0	89
7	2860	30	951	30	1000	60	1002
15	3558	60	1171	60	1032	120	1043
30	4578	90	1215				
60	5160	120	1132				

Dry Season – GW (cont'd)

HCFC-22

A		B		C		D	
Time (min)	Conc. (pptv)	Time (min)	Conc. (pptv)	Time (min)	Conc. (pptv)	Time (min)	Conc. (pptv)
0	695	0	359	0	418	0	447
7	5610	30	697	30	818	60	987
15	2431	60	891	60	862	120	1249
30	4199	90	843				
60	4528	120	738				

HCFC-141b

A		B		C		D	
Time (min)	Conc. (pptv)	Time (min)	Conc. (pptv)	Time (min)	Conc. (pptv)	Time (min)	Conc. (pptv)
0	24400	0	5500	0	2497	0	3984
7	34663	30	25671	30	20590	60	15375
15	5503	60	1019	60	11030	120	15096
30	12240	90	27920				
60	17090	120	21270				

HCFC-142b

A		B		C		D	
Time (min)	Conc. (pptv)	Time (min)	Conc. (pptv)	Time (min)	Conc. (pptv)	Time (min)	Conc. (pptv)
0	209	0	80	0	55	0	60
7	1740	30	203	30	331	60	437
15	704	60	188	60	291	120	476
30	1049	90	294				
60	1064	120	298				

HCFC-151a

A		B		C		D	
Time (min)	Conc. (pptv)	Time (min)	Conc. (pptv)	Time (min)	Conc. (pptv)	Time (min)	Conc. (pptv)
0	1253	0	202	0	584	0	896
7	7547	30	2344	30	3447	60	6683
15	14417	60	2954	60	3664	120	6515
30	18302	90	3016				
60	20811	120	2865				

Dry Season – GW (cont'd)

HFC-134a

A		B		C		D	
Time (min)	Conc. (pptv)	Time (min)	Conc. (pptv)	Time (min)	Conc. (pptv)	Time (min)	Conc. (pptv)
0	900	0	573	0	830	0	1198
7	16366	30	3934	30	6077	60	9975
15	2609	60	2691	60	6887	120	14276
30	5328	90	4551				
60	5929	120	4674				

HFC-152a

A		B		C		D	
Time (min)	Conc. (pptv)	Time (min)	Conc. (pptv)	Time (min)	Conc. (pptv)	Time (min)	Conc. (pptv)
0	802	0	423	0	548	0	1011
7	22671	30	2038	30	2259	60	6520
15	3688	60	2847	60	2722	120	9148
30	6107	90	2613				
60	6360	120	2746				

HFC-245fa

A		B		C		D	
Time (min)	Conc. (pptv)	Time (min)	Conc. (pptv)	Time (min)	Conc. (pptv)	Time (min)	Conc. (pptv)
0	427	0	187	0	58	0	72
7	1276	30	171	30	620	60	577
15	2212	60	240	60	412	120	504
30	3548	90	271				
60	3582	120	233				

CH_4

A		B		C		D	
Time (min)	Conc. (ppmv)	Time (min)	Conc. (ppmv)	Time (min)	Conc. (ppmv)	Time (min)	Conc. (ppmv)
0	62	0	33	0	64.2	0	78.5
7	7417	30	254	30	353.3	60	903.8
15	375	60	389	60	439.4	120	1140.0
30	372	90	282				
60	548	120	245				

Dry Season – GW (cont'd)

CO_2

A		B		C		D	
Time (min)	Conc. (ppmv)	Time (min)	Conc. (ppmv)	Time (min)	Conc. (ppmv)	Time (min)	Conc. (ppmv)
0	673	0	531	0	530	0	517
7	28	30	5163	30	2186	60	1758
15	4659	60	6319	60	2643	120	2225
30	4807	90	6484				
60	7197	120	6176				

Dry Season – ED

CFC-11

A		B		C		D	
Time (min)	Conc. (pptv)	Time (min)	Conc. (pptv)	Time (min)	Conc. (pptv)	Time (min)	Conc. (pptv)
0	3331	0	1298	0	3406	0	8415
7	13150	30	17973	30	136632	60	87956
15	23008	60	27718	60	115861	120	220818
30	84268	90	27497				
60	32536	120	27063				

CFC-12

A		B		C		D	
Time (min)	Conc. (pptv)	Time (min)	Conc. (pptv)	Time (min)	Conc. (pptv)	Time (min)	Conc. (pptv)
0	895	0	664	0	934	0	1562
7	3785	30	4504	30	15867	60	25411
15	6258	60	6938	60	21365	120	48706
30	13727	90	7810				
60	1094	120	7335				

CFC-113

A		B		C		D	
Time (min)	Conc. (pptv)	Time (min)	Conc. (pptv)	Time (min)	Conc. (pptv)	Time (min)	Conc. (pptv)
0	83	0	77	0	79	0	88
7	91	30	95	30	95	60	195
15	92	60	94	60	154	120	355
30	82	90	98				
60	113	120	97				

Dry Season – ED (cont'd)

CFC-114

A		B		C		D	
Time (min)	Conc. (pptv)	Time (min)	Conc. (pptv)	Time (min)	Conc. (pptv)	Time (min)	Conc. (pptv)
0	23	0	19	0	24	0	21
7	31	30	24	30	63	60	93
15	33	60	32	60	79	120	151
30	49	90	32				
60	19	120	31				

HCFC-21

A		B		C		D	
Time (min)	Conc. (pptv)	Time (min)	Conc. (pptv)	Time (min)	Conc. (pptv)	Time (min)	Conc. (pptv)
0	129	0	43	0	99	0	137
7	1152	30	433	30	4107	60	7711
15	1981	60	721	60	7696	120	12184
30	3131	90	805				
60	2838	120	900				

HCFC-22

A		B		C		D	
Time (min)	Conc. (pptv)	Time (min)	Conc. (pptv)	Time (min)	Conc. (pptv)	Time (min)	Conc. (pptv)
0	500	0	338	0	527	0	1034
7	1643	30	1656	30	7028	60	14301
15	2633	60	2549	60	10073	120	29680
30	6129	90	3127				
60	2000	120	2937				

HCFC-141b

A		B		C		D	
Time (min)	Conc. (pptv)	Time (min)	Conc. (pptv)	Time (min)	Conc. (pptv)	Time (min)	Conc. (pptv)
0	3192	0	1357	0	2372	0	11227
7	2918	30	9494	30	47112	60	34721
15	4806	60	14443	60	18887	120	97356
30	36853	90	8395				
60	167738	120	8513				

Dry Season – ED (cont'd)

HCFC-142b

A		B		C		D	
Time (min)	Conc. (pptv)	Time (min)	Conc. (pptv)	Time (min)	Conc. (pptv)	Time (min)	Conc. (pptv)
0	144	0	61	0	111	0	977
7	478	30	448	30	1490	60	4207
15	801	60	715	60	2042	120	7729
30	1814	90	870				
60	806	120	797				

HCFC-151a

A		B		C		D	
Time (min)	Conc. (pptv)	Time (min)	Conc. (pptv)	Time (min)	Conc. (pptv)	Time (min)	Conc. (pptv)
0	541	0	185	0	484	0	813
7	2920	30	1863	30	9880	60	37381
15	5356	60	2990	60	18158	120	58572
30	8273	90	3401				
60	11626	120	3766				

HFC-134a

A		B		C		D	
Time (min)	Conc. (pptv)	Time (min)	Conc. (pptv)	Time (min)	Conc. (pptv)	Time (min)	Conc. (pptv)
0	1018	0	503	0	1031	0	3116
7	4053	30	4605	30	20798	60	40339
15	6944	60	7100	60	25618	120	82969
30	17436	90	7832				
60	3065	120	7458				

HFC-152a

A		B		C		D	
Time (min)	Conc. (pptv)	Time (min)	Conc. (pptv)	Time (min)	Conc. (pptv)	Time (min)	Conc. (pptv)
0	1595	0	542	0	1434	0	12368
7	5783	30	6388	30	32968	60	56319
15	9650	60	9885	60	43023	120	118833
30	24065	90	12568				
60	2583	120	11921				

Dry Season – ED (cont'd)

HFC-245fa

A		B		C		D	
Time (min)	Conc. (pptv)	Time (min)	Conc. (pptv)	Time (min)	Conc. (pptv)	Time (min)	Conc. (pptv)
0	140	0	79	0	102	0	748
7	392	30	389	30	1760	60	4150
15	678	60	590	60	2518	120	8083
30	1353	90	769				
60	1665	120	756				

CH_4

A		B		C		D	
Time (min)	Conc. (ppmv)	Time (min)	Conc. (ppmv)	Time (min)	Conc. (ppmv)	Time (min)	Conc. (ppmv)
0	174	0	78	0	11.2	0	107.6
7	1389	30	1779	30	4169.0	60	7416.0
15	2599	60	3498	60	6205.0	120	43921.0
30	4840	90	3616				
60	297	120	3931				

CO_2

A		B		C		D	
Time (min)	Conc. (ppmv)	Time (min)	Conc. (ppmv)	Time (min)	Conc. (ppmv)	Time (min)	Conc. (ppmv)
0	434	0	407	0	435	0	43
7	239	30	43	30	54	60	20
15	124	60	25	60	27	120	11
30	51	90	27				
60	3301	120	33				

Dry Season – IC-1

CFC-11

A		B		C		D	
Time (min)	Conc. (pptv)	Time (min)	Conc. (pptv)	Time (min)	Conc. (pptv)	Time (min)	Conc. (pptv)
0	243	0	238	0	239	0	237
7	239	30	263	30	233	60	247
15	291	60	240	60	258	120	276
30	0	90	259				
60	0	120	235				

Dry Season – IC-1 (cont'd)

CFC-12

A		B		C		D	
Time (min)	Conc. (pptv)	Time (min)	Conc. (pptv)	Time (min)	Conc. (pptv)	Time (min)	Conc. (pptv)
0	538	0	532	0	542	0	551
7	536	30	554	30	533	60	574
15	559	60	557	60	614	120	558
30	0	90	593				
60	0	120	544				

CFC-113

A		B		C		D	
Time (min)	Conc. (pptv)	Time (min)	Conc. (pptv)	Time (min)	Conc. (pptv)	Time (min)	Conc. (pptv)
0	74	0	79	0	74	0	94
7	75	30	84	30	73	60	81
15	76	60	85	60	87	120	76
30	0	90	84				
60	0	120	75				

CFC-114

A		B		C		D	
Time (min)	Conc. (pptv)	Time (min)	Conc. (pptv)	Time (min)	Conc. (pptv)	Time (min)	Conc. (pptv)
0	16	0	16	0	16	0	17
7	17	30	18	30	16	60	17
15	19	60	17	60	24	120	17
30	0	90	18				
60	0	120	17				

HCFC-21

A		B		C		D	
Time (min)	Conc. (pptv)	Time (min)	Conc. (pptv)	Time (min)	Conc. (pptv)	Time (min)	Conc. (pptv)
0	-888	0	-888	0	-888	0	-888
7	-888	30	-888	30	-888	60	-888
15	-888	60	-888	60	-888	120	-888
30		90	-888				
60		120	-888				

Dry Season – IC-1 (cont'd)

HCFC-22

A		B		C		D	
Time (min)	Conc. (pptv)	Time (min)	Conc. (pptv)	Time (min)	Conc. (pptv)	Time (min)	Conc. (pptv)
0	229	0	240	0	249	0	280
7	255	30	230	30	247	60	278
15	266	60	267	60	302	120	273
30		90	295				
60		120	246				

HCFC-141b

A		B		C		D	
Time (min)	Conc. (pptv)	Time (min)	Conc. (pptv)	Time (min)	Conc. (pptv)	Time (min)	Conc. (pptv)
0	24	0	24	0	24	0	23
7	41	30	58	30	23	60	24
15	53	60	47	60	39	120	37
30	0	90	65				
60	0	120	57				

HCFC-142b

A		B		C		D	
Time (min)	Conc. (pptv)	Time (min)	Conc. (pptv)	Time (min)	Conc. (pptv)	Time (min)	Conc. (pptv)
0	24	0	27	0	24	0	24
7	39	30	26	30	24	60	27
15	51	60	27	60	35	120	25
30		90	31				
60		120	24				

HCFC-151a

A		B		C		D	
Time (min)	Conc. (pptv)	Time (min)	Conc. (pptv)	Time (min)	Conc. (pptv)	Time (min)	Conc. (pptv)
0	-888	0	70	0	-888	0	-888
7	-888	30	-888	30	-888	60	-888
15	-888	60	-888	60	-888	120	-888
30		90	-888				
60		120	-888				

Dry Season – IC-1 (cont'd)

HFC-134a

A		B		C		D	
Time (min)	Conc. (pptv)	Time (min)	Conc. (pptv)	Time (min)	Conc. (pptv)	Time (min)	Conc. (pptv)
0	78	0	83	0	85	0	86
7	137	30	91	30	84	60	92
15	169	60	107	60	99	120	88
30	0	90	116				
60	0	120	119				

HFC-152a

A		B		C		D	
Time (min)	Conc. (pptv)	Time (min)	Conc. (pptv)	Time (min)	Conc. (pptv)	Time (min)	Conc. (pptv)
0	24	0	18	0	21	0	37
7	88	30	53	30	38	60	51
15	66	60	48	60	100	120	41
30		90	31				
60		120	27				

HFC-245fa

A		B		C		D	
Time (min)	Conc. (pptv)	Time (min)	Conc. (pptv)	Time (min)	Conc. (pptv)	Time (min)	Conc. (pptv)
0	0.50	0.00	1.10	0.00	0.60	0.00	0.60
7	1.00	30.00	0.70	30.00	0.80	60.00	0.60
15	0.80	60.00	0.80	60.00	1.10	120.00	0.70
30	0.00	90.00	1.00				
60	0.00	120.00	-888.00				

CH_4

A		B		C		D	
Time (min)	Conc. (ppmv)	Time (min)	Conc. (ppmv)	Time (min)	Conc. (ppmv)	Time (min)	Conc. (ppmv)
0	2	0	2	0	1.9	0	2.6
7	6	30	2	30	1.9	60	3.2
15	4	60	3	60	3.7	120	1.9
30		90	2				
60		120	2				

Dry Season – IC-1 (cont'd)

CO_2

A		B		C		D	
Time (min)	Conc. (ppmv)	Time (min)	Conc. (ppmv)	Time (min)	Conc. (ppmv)	Time (min)	Conc. (ppmv)
0	410	0	378	0	381	0	393
7	760	30	504	30	520	60	485
15	1003	60	556	60	569	120	498
30		90	600				
60		120	614				

Dry Season – IC-10 (cont'd)

CFC-11

A		B		C		D	
Time (min)	Conc. (pptv)	Time (min)	Conc. (pptv)	Time (min)	Conc. (pptv)	Time (min)	Conc. (pptv)
0	258	0	252	0	251	0	259
7	318	30	374	30	273	60	479
15	274	60	512	60	331	120	646
30	320	90	751				
60	356	120	682				

CFC-12

A		B		C		D	
Time (min)	Conc. (pptv)	Time (min)	Conc. (pptv)	Time (min)	Conc. (pptv)	Time (min)	Conc. (pptv)
0	540	0	535	0	532	0	545
7	570	30	550	30	531	60	553
15	547	60	537	60	548	120	538
30	568	90	597				
60	538	120	629				

CFC-113

A		B		C		D	
Time (min)	Conc. (pptv)	Time (min)	Conc. (pptv)	Time (min)	Conc. (pptv)	Time (min)	Conc. (pptv)
0	79	0	79	0	77	0	82
7	82	30	87	30	80	60	88
15	77	60	88	60	93	120	99
30	80	90	146				
60	88	120	100				

Dry Season – IC-10 (cont'd)

CFC-114

A		B		C		D	
Time (min)	Conc. (pptv)	Time (min)	Conc. (pptv)	Time (min)	Conc. (pptv)	Time (min)	Conc. (pptv)
0	16	0	16	0	17	0	17
7	17	30	19	30	22	60	20
15	17	60	23	60	28	120	21
30	19	90	29				
60	26	120	38				

HCFC-21

A		B		C		D	
Time (min)	Conc. (pptv)	Time (min)	Conc. (pptv)	Time (min)	Conc. (pptv)	Time (min)	Conc. (pptv)
0	-888	0	-888	0	-888	0	-888
7	-888	30	-888	30	-888	60	-888
15	-888	60	-888	60	-888	120	-888
30	-888	90	-888				
60	-888	120	-888				

HCFC-22

A		B		C		D	
Time (min)	Conc. (pptv)	Time (min)	Conc. (pptv)	Time (min)	Conc. (pptv)	Time (min)	Conc. (pptv)
0	248	0	304	0	257	0	256
7	243	30	249	30	264	60	250
15	255	60	228	60	287	120	247
30	286	90	257				
60	283	120	253				

HCFC-141b

A		B		C		D	
Time (min)	Conc. (pptv)	Time (min)	Conc. (pptv)	Time (min)	Conc. (pptv)	Time (min)	Conc. (pptv)
0	171	0	114	0	102	0	119
7	239	30	350	30	143	60	360
15	196	60	620	60	227	120	409
30	238	90	954				
60	256	120	972				

Dry Season – IC-10 (cont'd)

HCFC-142b

A		B		C		D	
Time (min)	Conc. (pptv)	Time (min)	Conc. (pptv)	Time (min)	Conc. (pptv)	Time (min)	Conc. (pptv)
0	30	0	33	0	28	0	36
7	30	30	32	30	34	60	35
15	31	60	31	60	38	120	35
30	38	90	38				
60	37	120	40				

HCFC-151a

A		B		C		D	
Time (min)	Conc. (pptv)	Time (min)	Conc. (pptv)	Time (min)	Conc. (pptv)	Time (min)	Conc. (pptv)
0	-888	0	-888	0	-888	0	-888
7	-888	30	-888	30	-888	60	-888
15	-888	60	-888	60	-888	120	-888
30	-888	90	-888				
60	-888	120	-888				

HFC-134a

A		B		C		D	
Time (min)	Conc. (pptv)	Time (min)	Conc. (pptv)	Time (min)	Conc. (pptv)	Time (min)	Conc. (pptv)
0	147	0	154	0	136	0	143
7	143	30	143	30	143	60	146
15	144	60	151	60	161	120	146
30	161	90	168				
60	167	120	176				

HFC-152a

A		B		C		D	
Time (min)	Conc. (pptv)	Time (min)	Conc. (pptv)	Time (min)	Conc. (pptv)	Time (min)	Conc. (pptv)
0	84	0	164	0	72	0	85
7	94	30	71	30	73	60	85
15	73	60	70	60	86	120	82
30	83	90	77				
60	86	120	72				

Dry Season – IC-10 (cont'd)

HFC-245fa

A		B		C		D	
Time (min)	Conc. (pptv)	Time (min)	Conc. (pptv)	Time (min)	Conc. (pptv)	Time (min)	Conc. (pptv)
0	2	0	1	0	1	0	2
7	2	30	2	30	2	60	3
15	2	60	3	60	2	120	3
30	2	90	3				
60	2	120	3				

CH_4

A		B		C		D	
Time (min)	Conc. (ppmv)	Time (min)	Conc. (pptv)	Time (min)	Conc. (pptv)	Time (min)	Conc. (pptv)
0	7	0	4	0	7.6	0	4.1
7	6	30	4	30	6.9	60	4.4
15	5	60	4	60	6.6	120	4.6
30	5	90	4				
60	5	120	4				

CO_2

A		B		C		D	
Time (min)	Conc. (ppmv)	Time (min)	Conc. (ppmv)	Time (min)	Conc. (ppmv)	Time (min)	Conc. (ppmv)
0	412	0	411	0	410	0	409
7	509	30	1037	30	714	60	704
15	599	60	1586	60	931	120	925
30	768	90	2085				
60	1043	120	2538				

Dry Season – IC-15

CFC-11

A		B		C		D	
Time (min)	Conc. (ppmv)	Time (min)	Conc. (ppmv)	Time (min)	Conc. (ppmv)	Time (min)	Conc. (ppmv)
0	3091	0	357	0	276	0	285
7	1846	30	1205	30	292	60	413
15	1799	60	1064	60	388	120	476
30	2788	90	1195				
60	1705	120	2065				

Dry Season – IC-15 (cont'd)

CFC-12

A		B		C		D	
Time (min)	Conc. (pptv)	Time (min)	Conc. (pptv)	Time (min)	Conc. (pptv)	Time (min)	Conc. (pptv)
0	609	0	558	0	607	0	537
7	564	30	598	30	567	60	561
15	579	60	629	60	571	120	546
30	681	90	670				
60	726	120	828				

CFC-113

A		B		C		D	
Time (min)	Conc. (pptv)	Time (min)	Conc. (pptv)	Time (min)	Conc. (pptv)	Time (min)	Conc. (pptv)
0	88	0	78	0	82	0	80
7	85	30	89	30	81	60	85
15	85	60	92	60	81	120	93
30	90	90	97				
60	88	120	124				

CFC-114

A		B		C		D	
Time (min)	Conc. (pptv)	Time (min)	Conc. (pptv)	Time (min)	Conc. (pptv)	Time (min)	Conc. (pptv)
0	21	0	18	0	19	0	22
7	61	30	269	30	145	60	169
15	104	60	443	60	217	120	241
30	245	90	647				
60	277	120	1075				

HCFC-21

A		B		C		D	
Time (min)	Conc. (pptv)	Time (min)	Conc. (pptv)	Time (min)	Conc. (pptv)	Time (min)	Conc. (pptv)
0	5	0	5	0	-888	0	-888
7	5	30	16	30	-888	60	25
15	19	60	24	60	18	120	39
30	23	90	33				
60	25	120	44				

Dry Season – IC-15 (cont'd)

HCFC-22

A		B		C		D	
Time (min)	Conc. (pptv)	Time (min)	Conc. (pptv)	Time (min)	Conc. (pptv)	Time (min)	Conc. (pptv)
0	380	0	263	0	301	0	259
7	419	30	447	30	358	60	571
15	506	60	570	60	539	120	863
30	743	90	687				
60	893	120	308				

HCFC-141b

A		B		C		D	
Time (min)	Conc. (pptv)	Time (min)	Conc. (pptv)	Time (min)	Conc. (pptv)	Time (min)	Conc. (pptv)
0	2689	0	110	0	98	0	27
7	819	30	1128	30	322	60	790
15	802	60	957	60	568	120	593
30	1434	90	856				
60	2309	120	3563				

HCFC-142b

A		B		C		D	
Time (min)	Conc. (pptv)	Time (min)	Conc. (pptv)	Time (min)	Conc. (pptv)	Time (min)	Conc. (pptv)
0	147	0	28	0	25	0	31
7	157	30	111	30	73	60	131
15	167	60	143	60	87	120	166
30	253	90	190				
60	204	120	311				

HCFC-151a

A		B		C		D	
Time (min)	Conc. (pptv)	Time (min)	Conc. (pptv)	Time (min)	Conc. (pptv)	Time (min)	Conc. (pptv)
0	160	0	66	0	72	0	50
7	507	30	989	30	870	60	2092
15	890	60	2005	60	1708	120	3793
30	1630	90	2986				
60	1893	120	4114				

Dry Season – IC-15 (cont'd)

HFC-134a

A		B		C		D	
Time (min)	Conc. (pptv)	Time (min)	Conc. (pptv)	Time (min)	Conc. (pptv)	Time (min)	Conc. (pptv)
0	1575	0	269	0	240	0	176
7	2167	30	2899	30	2136	60	3939
15	2818	60	5287	60	3710	120	6780
30	3909	90	7470				
60	4324	120	10916				

HFC-152a

A		B		C		D	
Time (min)	Conc. (pptv)	Time (min)	Conc. (pptv)	Time (min)	Conc. (pptv)	Time (min)	Conc. (pptv)
0	3439	0	308	0	170	0	111
7	4054	30	3950	30	889	60	563
15	4216	60	7623	60	1438	120	1120
30	4308	90	11041				
60	4162	120	15906				

HFC-245fa

A		B		C		D	
Time (min)	Conc. (pptv)	Time (min)	Conc. (pptv)	Time (min)	Conc. (pptv)	Time (min)	Conc. (pptv)
0	127	0	21	0	8	0	8
7	158	30	154	30	95	60	257
15	199	60	271	60	168	120	427
30	348	90	387				
60	272	120	523				

CH_4

A		B		C		D	
Time (min)	Conc. (ppmv)	Time (min)	Conc. (ppmv)	Time (min)	Conc. (ppmv)	Time (min)	Conc. (ppmv)
0	100	0	42	0	23.5	0	41.4
7	558	30	1135	30	1325.0	60	2332.0
15	1073	60	2265	60	2446.0	120	4186.0
30	1520	90	3080				
60	1407	120	3013				

Dry Season – IC-15 (cont'd)

CO_2

A		B		C		D	
Time (min)	Conc. (ppmv)	Time (min)	Conc. (ppmv)	Time (min)	Conc. (ppmv)	Time (min)	Conc. (ppmv)
0	531	0	488	0	480	0	459
7	1386	30	4535	30	3236	60	5172
15	2274	60	8311	60	5633	120	8161
30	3888	90	12244				
60	4042	120	15931				

Dry Season – FC (cont'd)

CFC-11

A		B		C		D	
Time (min)	Conc. (pptv)	Time (min)	Conc. (pptv)	Time (min)	Conc. (pptv)	Time (min)	Conc. (pptv)
0	245	0	250	0	235	0	237
7	234	30	235	30	243	60	234
15	234	60	236	60	240	120	238
30	231	90	236				
60	247	120	236				

CFC-12

A		B		C		D	
Time (min)	Conc. (pptv)	Time (min)	Conc. (pptv)	Time (min)	Conc. (pptv)	Time (min)	Conc. (pptv)
0	542	0	549	0	533	0	535
7	532	30	537	30	594	60	551
15	535	60	547	60	572	120	550
30	544	90	542				
60	541	120	538				

CFC-113

A		B		C		D	
Time (min)	Conc. (pptv)	Time (min)	Conc. (pptv)	Time (min)	Conc. (pptv)	Time (min)	Conc. (pptv)
0	79	0	79	0	78	0	82
7	81	30	81	30	83	60	81
15	80	60	81	60	83	120	80
30	74	90	80				
60	74	120	79				

Dry Season – FC (cont'd)

CFC-114

A		B		C		D	
Time (min)	Conc. (pptv)	Time (min)	Conc. (pptv)	Time (min)	Conc. (pptv)	Time (min)	Conc. (pptv)
0	17	0	16	0	18	0	19
7	17	30	16	30	40	60	61
15	17	60	16	60	31	120	44
30	20	90	16				
60	17	120	16				

HCFC-21

A		B		C		D	
Time (min)	Conc. (pptv)	Time (min)	Conc. (pptv)	Time (min)	Conc. (pptv)	Time (min)	Conc. (pptv)
0	-888	0	-888	0	-888	0	-888
7	-888	30	-888	30	-888	60	-888
15	-888	60	-888	60	-888	120	-888
30	-888	90	-888				
60	-888	120	-888				

HCFC-22

A		B		C		D	
Time (min)	Conc. (pptv)	Time (min)	Conc. (pptv)	Time (min)	Conc. (pptv)	Time (min)	Conc. (pptv)
0	233	0	233	0	240	0	256
7	234	30	234	30	516	60	292
15	232	60	229	60	404	120	293
30	237	90	240				
60	234	120	237				

HCFC-141b

A		B		C		D	
Time (min)	Conc. (pptv)	Time (min)	Conc. (pptv)	Time (min)	Conc. (pptv)	Time (min)	Conc. (pptv)
0	27	0	23	0	23	0	24
7	25	30	27	30	271	60	28
15	24	60	24	60	31	120	27
30	23	90	31				
60	24	120	26				

Dry Season – FC (cont'd)

HCFC-142b

A		B		C		D	
Time (min)	Conc. (pptv)	Time (min)	Conc. (pptv)	Time (min)	Conc. (pptv)	Time (min)	Conc. (pptv)
0	24	0	24	0	23	0	24
7	24	30	24	30	42	60	44
15	30	60	26	60	35	120	38
30	32	90	24				
60	28	120	24				

HCFC-151a

A		B		C		D	
Time (min)	Conc. (pptv)	Time (min)	Conc. (pptv)	Time (min)	Conc. (pptv)	Time (min)	Conc. (pptv)
0	-888	0	-888	0	-888	0	-888
7	-888	30	-888	30	-888	60	-888
15	-888	60	-888	60	-888	120	-888
30	-888	90	-888				
60	-888	120	-888				

HFC-134a

A		B		C		D	
Time (min)	Conc. (pptv)	Time (min)	Conc. (pptv)	Time (min)	Conc. (pptv)	Time (min)	Conc. (pptv)
0	79	0	82	0	80	0	83
7	83	30	84	30	90	60	85
15	80	60	81	60	85	120	82
30	84	90	84				
60	81	120	82				

HFC-152a

A		B		C		D	
Time (min)	Conc. (pptv)	Time (min)	Conc. (pptv)	Time (min)	Conc. (pptv)	Time (min)	Conc. (pptv)
0	15	0	27	0	35	0	36
7	27	30	35	30	39	60	41
15	33	60	32	60	35	120	35
30	30	90	109				
60	28	120	32				

Dry Season – FC (cont'd)

HFC-245fa

A		B		C		D	
Time (min)	Conc. (pptv)	Time (min)	Conc. (pptv)	Time (min)	Conc. (pptv)	Time (min)	Conc. (pptv)
0	-888	0	5.00E-01	0	5.00E-01	0	4.00E-01
7	0	30	1	30	0	60	1
15	1	60	1	60	1	120	1
30	1	90	1				
60	1	120	1				

CH_4

A		B		C		D	
Time (min)	Conc. (ppmv)	Time (min)	Conc. (ppmv)	Time (min)	Conc. (ppmv)	Time (min)	Conc. (ppmv)
0	1.87E+00	0	1.88E+00	0	2.03E+00	0	1.89E+00
7	2	30	2	30	2.8	60	1.9
15	2	60	2	60	2.5	120	2.0
30	2	90	2				
60	2	120	2				

CO_2

A		B		C		D	
Time (min)	Conc. (ppmv)	Time (min)	Conc. (ppmv)	Time (min)	Conc. (ppmv)	Time (min)	Conc. (ppmv)
0	414	0	394	0	444	0	422
7	579	30	491	30	1379	60	1395
15	707	60	558	60	1670	120	1461
30	830	90	597				
60	965	120	642				

Appendix B - R^2 Linear Regression Analysis of the Concentration versus Time Dataset

The values in the dataset represent the fraction of the data accepted respective to number of points removed for varying R^2 threshold.

Cover Type	R^2=0.90				
	No point Removed	Last Point Removed	Last 2 Points Removed	Last 3 Points Removed	Fraction above threshold
AF	0.719	0	0.125	0	0.844
ED	0.719	0.063	0.031	0	0.813
GW	0.469	0.156	0.375	0	1
IC-1	0.308	0	0	0.115	0.423
IC-10	0.567	0	0	0.067	0.633
IC-15	0.467	0	0.033	0.2	0.7
FC	0.417	0	0	0	0.417

Cover Type	R^2=0.85				
	No point Removed	Last Point Removed	Last 2 Points Removed	Last 3 Points Removed	Fraction above threshold
AF	0.719	0	0.188	0	0.906
ED	0.781	0.063	0	0	0.844
GW	0.531	0.438	0.031	0	1
IC-1	0.308	0	0	0.115	0.423
IC-10	0.6	0	0	0.033	0.633
IC-15	0.5	0	0.1	0.133	0.733
FC	0.417	0	0	0.042	0.458

Cover Type	R^2=0.80				
	No point Removed	Last Point Removed	Last 2 Points Removed	Last 3 Points Removed	Fraction above threshold
AF	0.813	0.031	0.094	0.000	0.938
ED	0.781	0.063	0.000	0.000	0.844
GW	0.656	0.313	0.031	0.000	1.000
IC-1	0.346	0.000	0.000	0.154	0.500
IC-10	0.633	0.000	0.033	0.100	0.767
IC-15	0.567	0.000	0.033	0.167	0.767
FC	0.423	0.000	0.000	0.038	0.462

Appendix B - R^2 Linear Regression Analysis of the Concentration versus Time Dataset (cont'd)

Cover Type	R^2=0.75				
	No point Removed	Last Point Removed	Last 2 Points Removed	Last 3 Points Removed	Fraction above threshold
AF	0.813	0.063	0.094	0.000	0.969
ED	0.781	0.063	0.000	0.000	0.844
GW	0.813	0.156	0.031	0.000	1.000
IC-1	0.346	0.000	0.115	0.077	0.538
IC-10	0.633	0.000	0.033	0.133	0.800
IC-15	0.600	0.000	0.067	0.133	0.800
FC	0.423	0.000	0.000	0.038	0.462

Cover Type	R^2=0.70				
	No point Removed	Last Point Removed	Last 2 Points Removed	Last 3 Points Removed	Fraction above threshold
AF	0.844	0.063	0.063	0.000	0.969
ED	0.813	0.063	0.000	0.000	0.875
GW	0.906	0.063	0.031	0.000	1.000
IC-1	0.346	0.000	0.115	0.115	0.577
IC-10	0.633	0.000	0.033	0.167	0.833
IC-15	0.600	0.000	0.067	0.200	0.867
FC	0.423	0.000	0.000	0.038	0.462

Cover Type	R^2=0.65				
	No point Removed	Last Point Removed	Last 2 Points Removed	Last 3 Points Removed	Fraction above threshold
AF	0.844	0.063	0.063	0.000	0.969
ED	0.813	0.063	0.000	0.000	0.875
GW	0.906	0.094	0.000	0.000	1.000
IC-1	0.346	0.000	0.115	0.115	0.577
IC-10	0.633	0.000	0.033	0.167	0.833
IC-15	0.600	0.000	0.067	0.200	0.867
FC	0.423	0.000	0.038	0.042	0.503